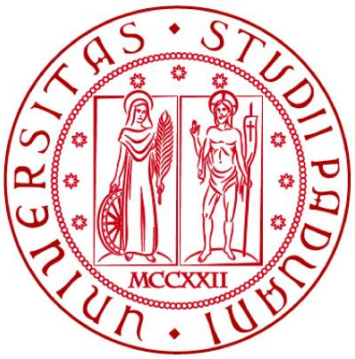

UNIVERSITÀ DEGLI STUDI DI PADOVA

DIPARTIMENTO DI INGEGNERIA INDUSTRIALE

Corso di Laurea Magistrale in Ingegneria Energetica

Tesi di Laurea Magistrale

Off-design performance model of Organic Rankine Cycle systems

Relatore: *Prof. Andrea Lazzaretto*

Correlatore: *Ing. Sergio Rech*

Controrelatore: *Prof. Massimo Masi*

Laureando: NICOLÒ MAZZI

ANNO ACCADEMICO 2013/2014

ABSTRACT

In this work an off-design dynamic model of an organic Rankine cycle system is presented. Organic Rankine cycle systems are waste heat recovery systems, where both hot and cold source are usually fluctuating and unforeseeable; therefore the system frequently works in strong off-design conditions. The aim of the work is to develop a dynamic model for each component involved in the system, creating a library of ready-to-use components exploitable also in future for different studies and simulations. In order to consider realistic mass and thermal inertias of the system, shell-and-tube heat exchangers have been considered since they are widely used in ORC applications. The dynamic model has been implemented in Matlab Simulink code. The developed model is applied to a realistic waste heat recovery application from industrial processes, analyzing system response to variation of temperature and mass flow rate of heat sources.

In questa tesi un modello di off-deisign dinamico di un ciclo Rankine organico è presentato. I cicli Rankine a fluido organico sono sistemi per il recupero di calore di scarto, dove sia la sorgente calda sia la sorgente fredda sono spesso variabili nel tempo e non prevedibili; dunque lavorano spesso in forti condizioni di off-design. L'obiettivo del lavoro è sviluppare un modello dinamico per ogni singolo componente del sistema, creando una libreria di componenti pronti all'uso, utilizzabile anche in futuro per diverse simulazioni e diversi studi. Al fine di considerare inerzie termiche e di massa realistiche, scambiatori shell-and-tube sono stati considerati, poiché sono largamente utilizzati in applicazioni ORC. Il modello dinamico è stato implementato in ambiente Matlab Simulink. Il modello sviluppato è utilizzato per simulare un'applicazione di recupero di calore di scarto da processi industriali, analizzando la risposta del sistema a variazioni di portata e temperature delle sorgenti termiche.

CONTENT

INTRODUCTION

The “20-20-20” targets fixed by European Communities in 2007 are key objectives for global warming mitigation. Requirements to comply are, a 20% reduction of greenhouse gases emission comparing to 1990 values, a 20% of energy produced by renewable sources and a 20% increase of energy efficiency. In this context the interest in organic Rankine cycle applications is growing, both from companies and academic world. ORC (organic Rankine cycle) systems allow exploiting heat sources at low-medium temperature, such as geothermal sources or waste heat from engines and industrial processes, for electric energy production. Conventional fluids as air and water are not efficient and cost effective in exploiting low temperature sources and usage of non-conventional fluids allows performing more efficient cycles. Fluid choice and design optimization are two topics very analyzed in literature, such as Toffolo et al. [1], Guo et al. [2] and Wang et al. [3] for working fluid selection and Toffolo et al. [1], Pierobon et al. [4], Branchini et al. [5], Wang et al. [6] et Sun et al. [7] for optimal design strategy. Nevertheless, since ORC plants are waste heat recovery systems, both hot and cold source are usually fluctuating and unforeseeable and the system frequently works in strong off-design conditions. Performance analysis of organic Rankine cycles systems at off-design conditions, at the moment, is not a topic covered exhaustively in literature. Calise et al. [1] have analyzed off-design behavior of a superheated regenerative organic Rankine cycles by mean of a steady state model. Quolin et al. [2], Xie et al. [3], Zhang et al [4] and Vaja [5] have proposed dynamic models of ORC systems but all studies refer to non-regenerative cycles performed using pipe-in-pipe exchangers and do not seem to match the real applications. The aim of this work is to develop a dynamic model which could really represent a real ORC plant, indeed shell-and-tube heat exchangers and internal regeneration has been considered. The idea is to develop a dynamic model of each component involved in the system, thus creating a modular system. Matlab Simulink code has been selected for model implementation, resulting the most suitable for the purpose.

1. ORC SYSTEMS OVERVIEW

Introduction

The aim of this chapter is to provide a brief overview of organic Rankine cycle systems. Main important characteristics of ORC plants are presented, highlighting differences with conventional steam cycles. In the second part of the chapter most important field of applications of organic Rankine cycles are reported. Several techno-economical surveys are available in literature, such as works presented by Quolin et al [13],Vèlez et al. [14] and Campana et al. [15].

1.1 Comparison with conventional Steam cycles

Organic Rankine cycle arrangement is very similar to steam cycles, as they both perform Rankine cycle. A typical and general layout of an ORC system is presented in figure 1.1:

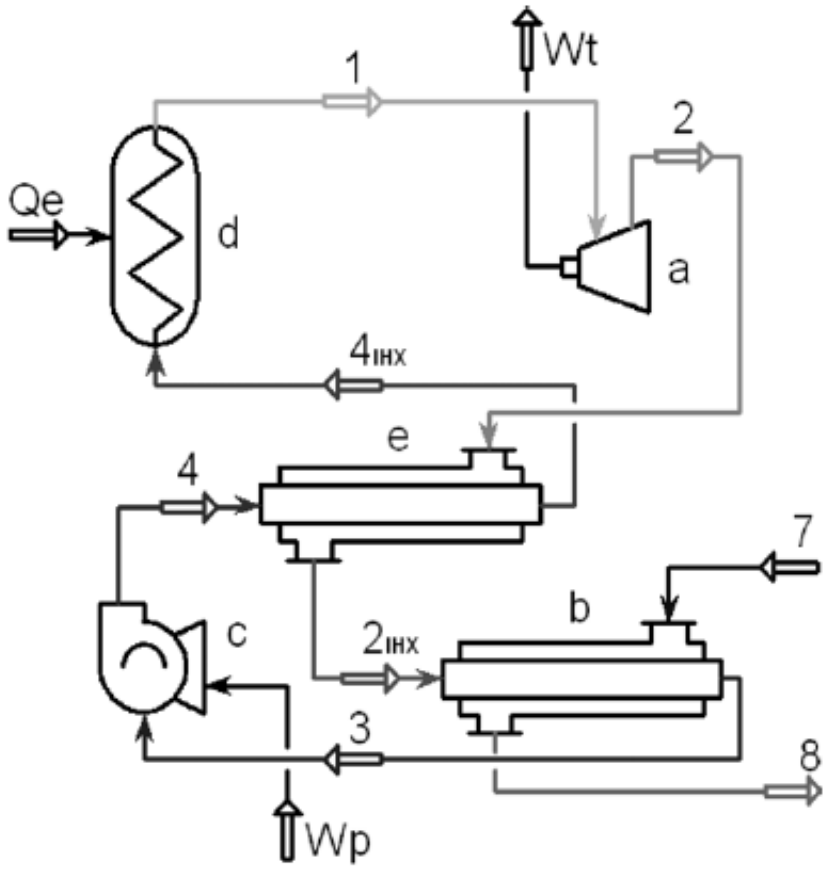

Figure 1.1 Schematic diagram of ORC system. (a) Turbine, (b) condenser, (c) pump, (d) evaporator, (e) regenerator [14]

Hot source is represented by mean of heat flux Qe and cold source by inlet and outlet flows of cooling fluid (usually air or water), respectively flows 7 and 8.

The most important difference between steam cycles and ORC systems is constituted by the different working fluid used to perform the cycle. Figure 2.1 shows the saturation curve of water and some organic fluids used in ORC applications in a temperature-entropy diagram:

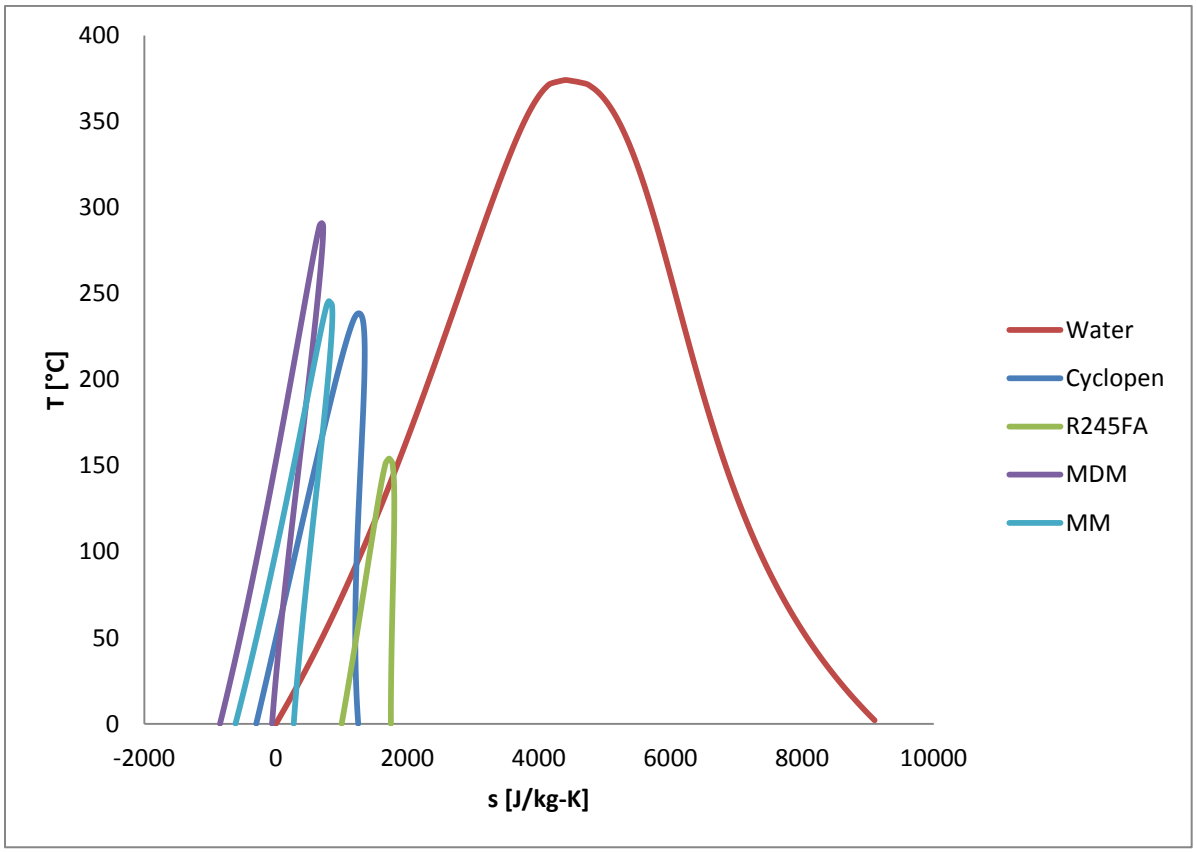

Figure 1.2 Saturation curve of water and various typical ORC working fluids

Two main important differences between organic fluids and water diagram are:

- Slope of saturated vapor curve is negative for water, while is positive or close to vertical for organic fluids.
- Entropy variation, for organic fluids, from saturated liquid and saturated vapor at a set temperature level is really smaller compared to water.

These peculiarities lead to many differences between organic Rankine cycles and steam cycles:

Steam plants require a superheated steam at turbine inlet in order to avoid the risk of having a too low steam quality in last expansion stages. On the contrary, the organic fluids remain superheated at turbine outlet due to a positive slope of saturated vapor curve; therefore for ORC plants the superheating is not strictly necessary. Nevertheless the organic fluid can be anyway superheated in order to enhance cycle performances.

- The possibility of chose from a large variety of fluids give the possibility create high efficiency cycles also for low temperature heat sources; where steam cycles result not well performing. In addition to that the lower vaporization enthalpy allows a better thermal coupling with the medium-low temperature hot source.

- In Steam plants the boiler is usually composed by an economizer, a hot recirculated drum and superheaters. In ORC systems there is the possibility to create once-trough boilers, making a more compact and less expensive component. [13]. This configuration is possible when the temperature of the hot source is lower than the maximal temperature that the fluid can reach without risk of deterioration. When that condition is not verified the evaporator can be split up into three exchangers: economizer, kettle evaporator and a superheater (if a superheated cycle is considered). In such way, the single exchanger can be in part bypassed by the hot fluid and thus controlling the maximum temperature reached by organic fluid.

- Enthalpy drop during expansion process is much lower compared to steam cycles. This peculiarity influences both turbine and pump component. For the same produced mechanical power, the organic Rankine cycles needs a higher value of circulation mass flow rate which implies higher consumption of the pump component [13]. Nevertheless the higher mass flow rate elaborated by turbine component usually avoids the necessity of partialization at turbine inlet.

- Evaporating pressures are usually of 60-70 bar for Steam plants, while rarely exceed 30 bar in ORC systems. This implies a less complex and expensive evaporator component in organic cycles.

- Condensing pressures in Steam plants are usually lower than 100 mbar, creating the necessity of introduce degasator component to extract incondensable gases. For refrigerant fluids the condensing pressure is higher than atmospheric pressure; avoiding the risk of entrance of incondensable gases. Fluids such as siloxanes and hydrocarbons usually have a condensing pressure lower than atmospheric one, but anyway they do not need introduction of degasser component.

- Condensing pressures in Steam plants are usually lower than 100 mbar, creating the necessity of introduce a degasser component to extract incondensable gases. For refrigerant fluids the condensing pressure is higher than atmospheric pressure; avoiding the risk of entrance of incondensable gases. Fluids such as siloxanes and hydrocarbons

usually have a condensing pressure lower than atmospheric one, but anyway they do not need usage of degasser component.

ORC systems are in general easier to manage, due to all differences listed. For small size plants, in addition to a higher efficiency in exploiting medium-low heat sources, ORCs are more competitive compared to conventional steam cycles.

2.2 Applications

In this section most important field of applications of organic Rankine cycles are presented.

Biomass plants

Biomass plants are one of the main markets for Organic Rankine Cycles systems. The heat source is represented by biomass combustion gases at very high temperature, so available also for Steam plants. Nevertheless biomass plants are usually limited up to sizes of 1-2 MWe [13], due to the difficulty in procurement large quantity of good quality and cheap biomass; steam cycle efficiency for this plant size is comparable with ORC plants. In addition, in order to avoid the necessity of licensed boiler operator supervision, usually heat from combustion gases is transferred to thermal oil; which cannot usually overcome 320°C of operating temperature. Moreover Biomass plants are often combined heat and power (CHP) plants and the possibility to utilize an operating fluid, such as octamethyltrisiloxane, which perform with good efficiency when condensing temperature is of around 100 °C makes ORC plants interesting for this application. The working principle of a biomass CHP ORC system is presented in figure 1.3:

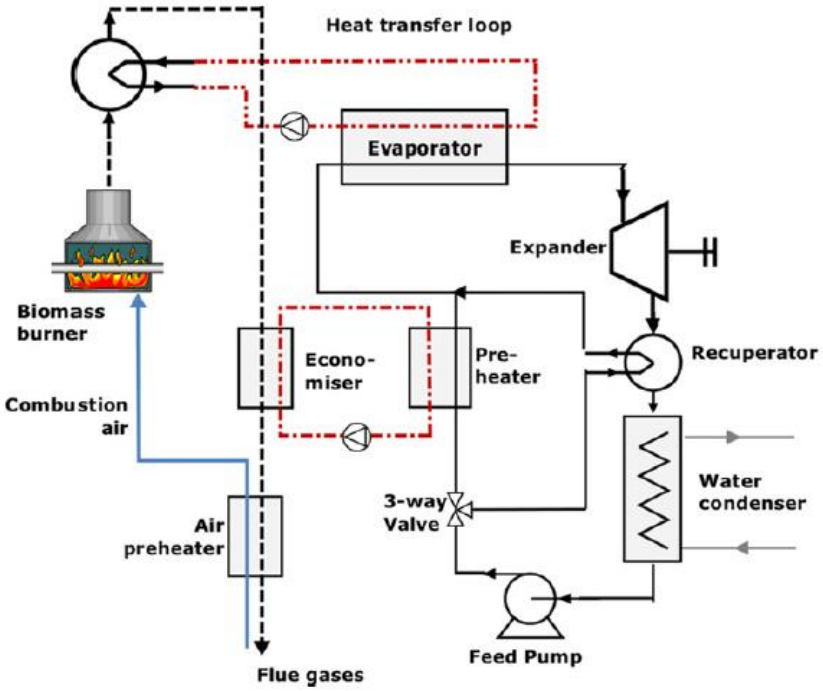

Figure 1.3 Working principle of a biomass CHP ORC plant. [13]

Geothermal applications

Geothermal heat sources are available in a wide range of temperature, which usually does not overcome 300°C. Fluid with a low critical temperature, such as R134A and R245FA, well match the necessity to recover energy at very low temperature. The actual technological level fix at around 80 °C the lowest exploitable hot source temperature; under this temperature in fact geothermal plant are no more economical [13].

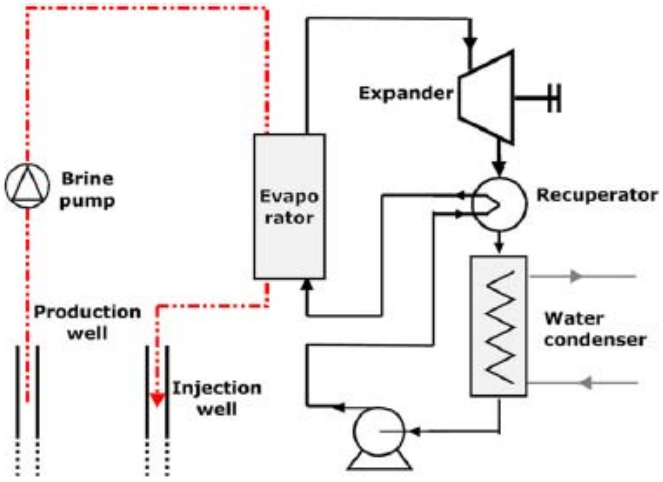

Figure 1.4 Working principle of a geothermal ORC plant. [13]

Waste heat recovery from internal combustion engines

Internal combustion engines (ICEs) convert fuel energy into mechanical power; they are used both for driving applications and electric power production. Nevertheless the converted energy is only around one third of the input fuel energy; the remaining part is waste heat. This heat is available at different temperatures; heat from the cooling circuit at around 80-100°C and exhaust gases at 400-900°C. The possibility of recover the waste heat by mean of an ORC system can increase the electric efficiency of the global system.

Waste heat recovery from industrial process, cement plants

A simplified scheme of an organic Rankine cycle system applied on a cement factory is presented in figure 1.5. Two different thermal sources are available for the ORC system, exhaust gases from rotary kiln at temperature of 300-450°C and gases from clinker cooling system at temperature of around 300°C [15]. Usually a diathermic oil loop is used to extract heat from gases and release it to organic fluid, performing a binary cycle.

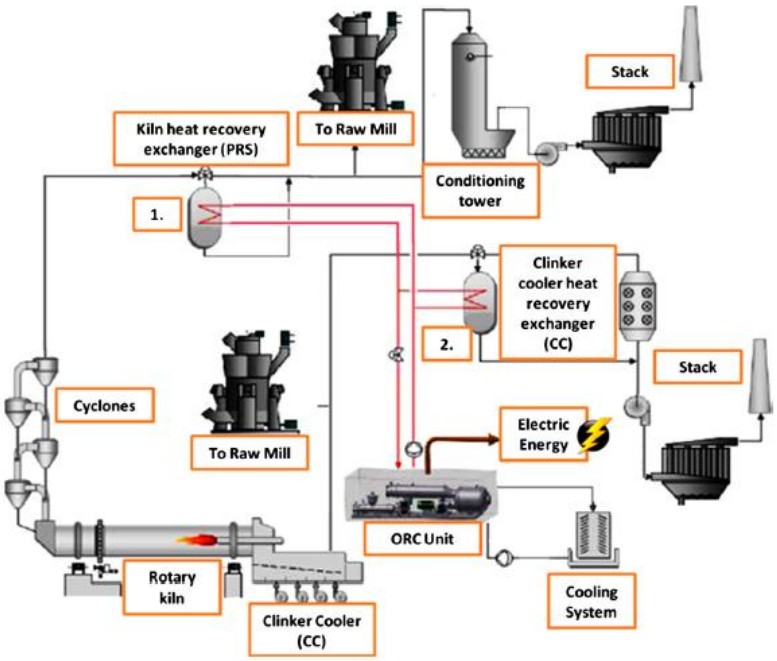

Figure 1.5 The working principle of a waste heat recovery ORC system applied to cement plants [15]

Waste heat recovery from industrial process, steel plants

Differently from cement plants, for steel plants many different processes and techniques are available and a very general analysis is not possible. Nevertheless usually the hot source is represented by hot gases that come out from Electric Arc Furnace and rolling mills. Several arrangements are possible; in figure 1.6 a simplified scheme of ORC application to steel factory is presented, highlighting typical temperature levels of available hot sources.

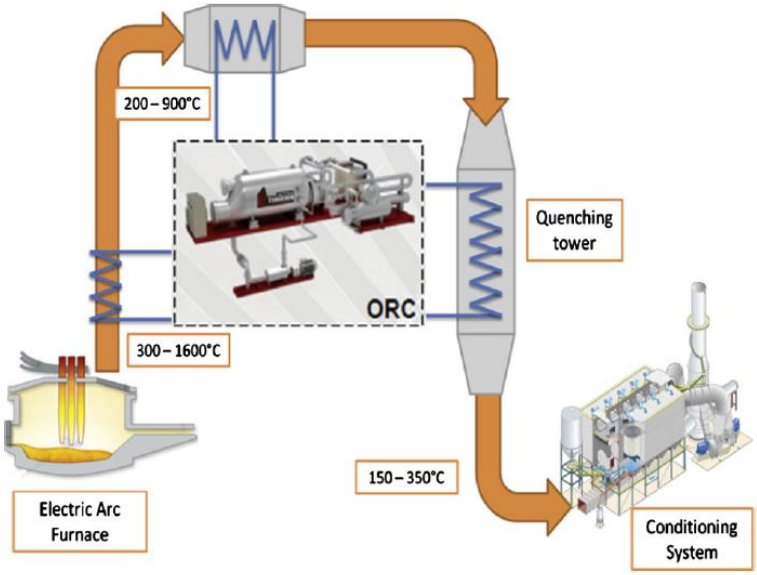

Figure 1.6 The working principle of a waste heat recovery ORC system applied to steel plants [15]

Waste heat recovery from industrial process, glass plants

Glass industry is diversified, depending on manufactured product. Here only flat glass production is analyzed. Hot exhaust gases come out from the furnace at a temperature of around 400-500°C. Due to chamber inversion process, which is performed every around 30 minutes, temperature of available heat source is usually not constant even in steady state operation of the furnace; rendering this application interesting for a dynamic analysis of ORC system performance in off-design conditions.

Conclusions

The presented brief overview shows potentiality of ORC systems in a wide range of applications and the contribution that this technology can provide to reach "20-20-20" targets in 2020. Even if the performed cycle is similar to steam cycles, the different working fluid strongly influences the arrangement and performances of the plant.

2. DESIGN MODEL

Introduction

In this chapter the design model of an ORC system is presented. The research of the optimum design point of an ORC system is a much analyzed topic in literature. Pierobon et al. [4] provide a multi-objective optimization method to design MW-size organic Rankine cycles, considering also shell-and-tube exchangers design. Chen et al. [16] propose a new design method to fully couple the ORC system with available heat sources while Branchini et al. [5] realize a comparative performance analysis for several ORC configurations. Although the research of the optimum ORC design point is not the aim of the work, the design model is a necessary step to perform the off-design model of the plant. In the first part of the chapter a model that allows to characterize the thermodynamic cycle and fixing the more important operating variables is presented. In the second part the procedure to design each component involved in the system is explained. For heat exchangers the design procedure allows defining all geometric parameters of a Shell&Tube heat exchanger; while for pump and turbine components the design model leads only to define parameters which are necessary for characterizing the off-design model of components.

Nomenclature

p	Pressure [bar]
T	Temperature [°C]
H	Enthalpy [kJ/kg]
s	Entropy [kJ/kg K]
x	Vapor mass fraction [-]
c_p	Specific heat at constant pressure [kJ/kg K]
$\dot{m}$	Mass flow rate [kg/s]
$\dot{V}$	Volumetric flow rate [m^3/s]
$\dot{q}$	Heat transfer rate [kW]
P	Power [kW]
K	Global heat transfer coefficient [kW/m^2 K] Stodola coefficient [m^2]
h	Heat transfer coefficient [kW/m^2 K]
f	Fouling factor [m^2 K/kW]
F_t	Temperature factor [-]
A	Surface [m^2]
OD	External tube diameter [m]
ID	Internal tube diameter [m]
L	Tube length [m]
$pitch$	Pitch distance [m]
B_C	Baffle cut [%]
b	Number of baffles [-]
$layout$	Tube layout [°]
N_{tt}	Number of tubes [-]
N_{ss}	Number of sealing strips [-]
y	Specific energy [kJ/kg]
w	Rotational speed [rad/s]

Greek symbols

ε	Heat transfer efficiency [-] Expansion ratio [-]
η	Efficiency [-]
χ	Overall efficiency [-]

Abbreviations and subscripts

1	Tube side fluid
2	Shell side fluid
hot	Hot source
$cold$	Cold Source
D	Design
E	Effective
IN	Inlet
OUT	Outlet
pp	Pitch point
ap	Approach point
t	Turbine
p	Pump
ev	Evaporation
$cond$	Condensation
is	Isentropic
max	Maximum
rec	Recover
ORC	Organic Rankine cycle
$conv$	Convective
ext	External
int	Internal
ml	Mean log
$wall$	Wall
cc	Countercurrent
$mecc$	Mechanical
el	Electrical
gen	Generator

2.1 Thermodynamic cycle design

In this section the design model of the thermodynamic cycle of an ORC system is presented. Thermodynamic cycle design is the first step in design process; indeed only after that cycle feature has been fixed, all components can be designed.

The first fundamental choices are the selection of the proper working fluid and the cycle configuration.

Fluid choice is strictly linked to the temperature level of both hot and cold source. In literature several fluids have been analyzed, although in commercial plants only few fluids are really used [13].

Cycle configuration directly influences performance and complexity of the plant; in this work only one configuration is considered: Superheated Regenerative Organic Rankine Cycle, as suggested by [4] and [5]. However the presented design procedure is quite general and can be easily adapted to all other possible configurations.

In thermodynamic cycle design, balance equations are applied in order to impose the conservation of both mass and energy. The design procedure starts from design specifications; which for these applications are usually represented by characteristics of hot and cold source:

- Mass flow rate of hot source fluid;
- Temperature of hot source fluid;
- Temperature of cold source fluid.

The scheme of component arrangement for the chosen configuration is shown in figure 2.1:

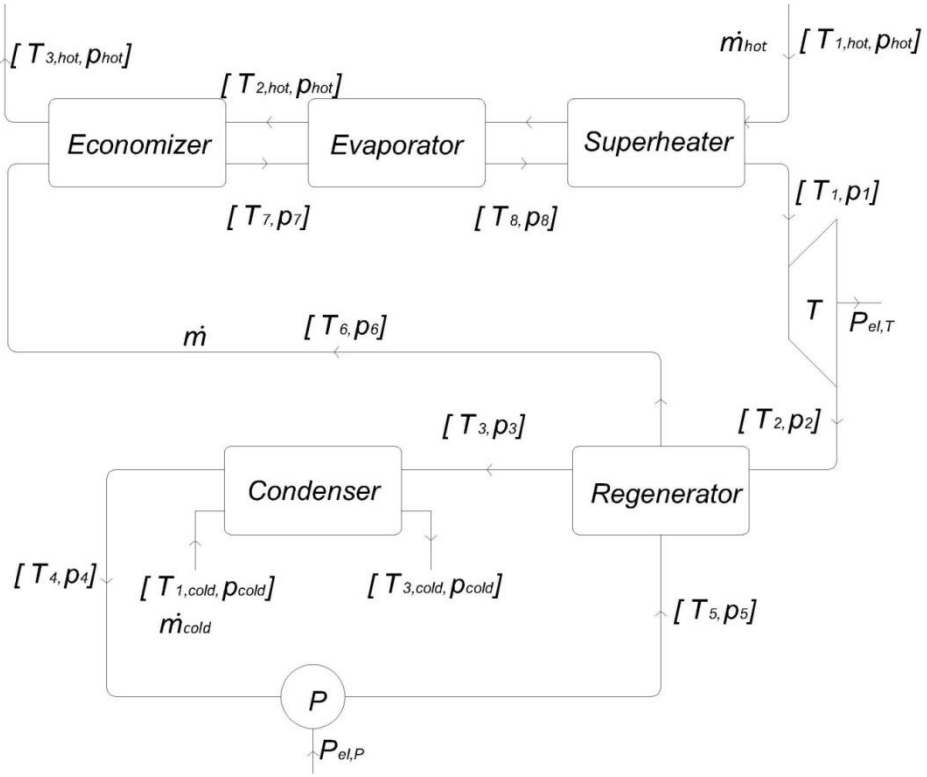

Figure 2.1 Components layout of a Superheated regenerative organic Rankine cycle

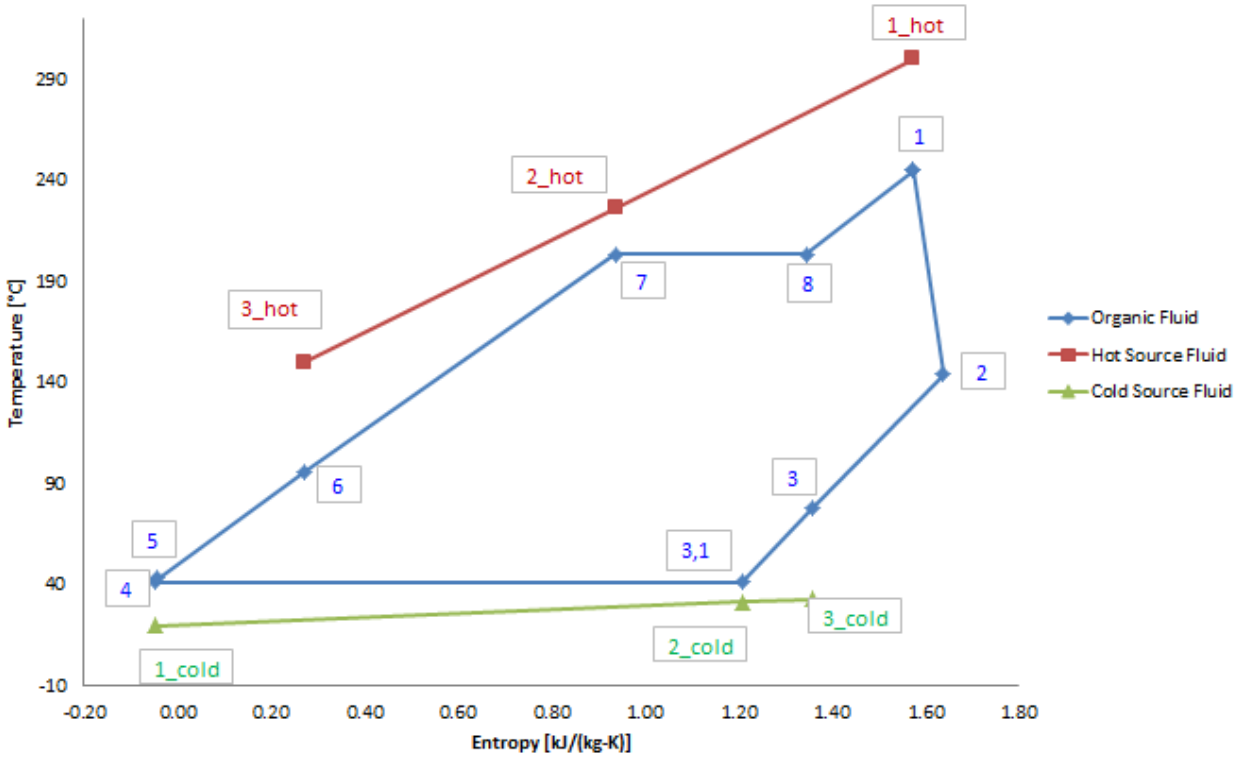

Figure 2.2 T-s diagram of a superheated regenerative organic Rankine cycle, including thermal coupling with hot and cold sources.

The first step is to design the specific cycle, defining the value of intensive variables (temperature and pressure) for all 8 state points that characterized the cycle. Organic fluid mass flow rate is computed subsequently; when thermal coupling with the hot source is imposed. The equations are subdivided in accordance with the component which they refer to. For chosen cycle configuration, 7 components are involved in the process:

- *Economizer;*
- *Evaporator;*
- *Superheater;*
- *Turbine;*
- *Regenerator;*
- *Condenser;*
- *Pump.*

Since 7 components are considered; at least 8 state points are necessary to well define the feature of thermodynamic cycle, as presented in figure 2.2. Nevertheless in the presented system of equations 9 state point are evaluated in order to consider saturated vapor phase during

condensation process (state point 3,1) which defines the pitch point temperature difference of thermal coupling with cold source.

For each component, conservation equations for both mass and energy are applied, in particular:

$$\sum \dot{m}_i = 0 \qquad 2.1$$

$$\sum \dot{m}_i H_i = 0 \qquad 2.2$$

In calculation procedure for the definition of specific cycle, the values of the intensive variables (H_i) expressed in equation 2.2 are computed. Subsequently considering thermal coupling with both hot and cold sources the value of extensive variables ($\dot{m}_i$) are evaluated by applying energy conservation equation.

Equations 2.1 is not directly performed in the thermodynamic cycle design model; nevertheless the mass conservation is anyway satisfied considering for each component the same inlet and outlet mass flow rate of the whole cycle $\dot{m}$.

Specific cycle can be evaluated by imposing the value of 8 independent variables:

- Approach point difference temperature ΔT_{ap}, the difference from hot source fluid inlet temperature $T_{IN,hot}$ and organic fluid temperature at turbine inlet T_1;
- Hot source pitch point difference ΔT_{pp1};
- Cold source pitch point difference ΔT_{pp2};
- Organic fluid evaporation pressure p_{ev};
- Organic fluid condensation pressure p_{cond};
- Exchange efficiency for regenerator component ε_{rigen};
- Turbine isentropic efficiency $\eta_{is,t}$;
- Pump isentropic efficiency $\eta_{is,t}$;

In addition design specifications provide the value of:

- Hot source fluid mass flow rate $\dot{m}_{hot}$;
- Hot source fluid pressure p_{hot} ;
- Hot source fluid inlet temperature $T_{IN,hot}$;
- Cold source fluid inlet temperature $T_{IN,cold}$.

Turbine

State point 1, turbine inlet, is evaluated after having imposed evaporating pressure and approach point difference temperature ΔT_{ap}. State point 2, turbine outlet, is computed by outlet enthalpy for an isentropic expansion process $H_{2,is}$ introducing irreversibility by mean of turbine isentropic

efficiency $\eta_{is,t}$. State equations lead to calculate the value of intensive variables of a state point by knowing two different intensive variables of the specific state. They are represented as a general function $f(v1, v2)$, providing the two intensive variables $v1$ and $v2$ which allow the calculation.

$$p_1 = p_{ev} \quad 2.3$$

$$p_2 = p_{cond} \quad 2.4$$

$$T_1 = T_{IN,hot} - \Delta T_{ap} \quad 2.5$$

$$[H_1, s_1] = f(T_1, p_1) \quad 2.6$$

$$H_{2,is} = f(p_2, s_1) \quad 2.7$$

$$H_2 = H_1 - \eta_{is,t}(H_1 - H_{2,is}) \quad 2.8$$

$$[T_2, c_{p,2}] = f(p_2,\ H_2) \quad 2.9$$

Pump

State point 4, pump inlet, is evaluated by imposing condensing pressure value and saturated liquid condition at pump inlet. As done for the turbine component, the outlet enthalpy is obtained calculating the outlet enthalpy for an isentropic transformation $H_{5,is}$ and introducing pump isentropic efficiency $\eta_{is,p}$.

$$p_4 = p_2 \quad 2.10$$

$$p_5 = p_1 \quad 2.11$$

$$[T_4, H_4, s_4] = f(p_4, x = 0) \quad 2.12$$

$$H_{5,is} = f(p_5, s_4) \quad 2.13$$

$$H_5 = H_4 + \frac{(H_{5,is} - H_4)}{\eta_{is,p}} \quad 2.14$$

$$[T_5, c_{p,5}] = f(p_5,\ H_5) \quad 2.15$$

Regenerator

Regenerator performance is established by the exchange efficiency ε_{rigen}. High value of exchange efficiency involves higher cycle efficiency but also an higher cost of the component. ε_{rigen} is defined as the ratio between the effective heat transferred ($\frac{\dot{q}}{\dot{m}}$) and the maximum specific heat that can be transferred ($\frac{\dot{q}_{max}}{\dot{m}}$) and. By knowing $\frac{\dot{q}}{\dot{m}}$ both state 3 and 6 intensive variables can be evaluated.

$$p_3 = p_2 \quad 2.16$$
$$p_6 = p_5 \quad 2.17$$
$$c_{p,min} = min(c_{p,2}, c_{p,5}) \quad 2.18$$
$$\frac{\dot{q}_{max}}{\dot{m}} = c_{p,min}\,(T_2 - T_5) \quad 2.19$$
$$c_{p,min} = min(c_{p,2}, c_{p,5}) \quad 2.20$$

$$\frac{\dot{q}_{max}}{\dot{m}} = c_{p,min}\,(T_2 - T_5) \quad 2.21$$
$$\frac{\dot{q}}{\dot{m}} = \frac{\dot{q}_{max}}{\dot{m}}\,\varepsilon_{rigen} \quad 2.22$$
$$H_3 = H_2 - \frac{\dot{q}}{\dot{m}} \quad 2.23$$
$$T_3 = f(p_3, H_3) \quad 2.24$$
$$H_6 = H_5 + \frac{\dot{q}}{\dot{m}} \quad 2.25$$
$$T_6 = f(p_6, H_6) \quad 2.26$$

Evaporator

Intensive variables of state points 7 and 8 are obtained by imposing saturation condition for liquid phase at economizer outlet and saturated vapor phase at superheater inlet.

$$p_7 = p_6 \quad 2.27$$
$$p_8 = p_7 \quad 2.28$$
$$[T_7, H_7] = f(p_7, x = 0) \quad 2.29$$
$$[T_8, H_8] = f(p_8, x = 1) \quad 2.30$$

Condenser

State point 3,1 is computed imposing condition of saturated vapor at condensing pressure.

$$p_{3,1} = p_3 \quad 2.31$$
$$\left[T_{3,1}, H_{3,1}\right] = f(p_{3,1}, x = 1) \quad 2.32$$

The choice of efficiency of turbine and pump components is strictly linked to the used technology and influence cycle performance (mainly turbine efficiency).

Evaporating and condensing pressures are key design parameters since they directly influence heat recovery efficiency, component size and so investment costs.

Thermal coupling with Hot Source

The design of thermodynamic cycle is strictly linked to available hot and cold sources, which represent design specifications for studied case. Key parameters are approach difference temperature ΔT_{ap} and pinch point difference temperatures ΔT_{pp1} and ΔT_{pp2}. Low value of such

parameters involves higher cycle performances as cycle can be performed at higher evaporating pressures and lower condensing pressure; increasing specific work elaborated by the cycle. Nevertheless it implies also lower mean difference temperature in all heat exchangers and therefore higher value of exchanger surfaces and higher investment costs. Approach and pinch point difference temperatures should be a compromise value between good efficiency and low investment cost of the designed plant. Cycle efficiency is not the only index to analyze the performances of the system; indeed also recovery efficiency is to consider. Recover efficiency (η_{rec}) is the ratio between the effective recovered heat and the maximum heat that could be recovered if hot temperature source flux would be cooled at the lowest acceptable temperature ($T_{3,hot,min}$). This value can be both ambient temperature or fixed design parameter. When the hot source is represented by combustion exhaust gases, for example, they cannot be cooled until ambient temperature, in order to avoid acid condensation. For ORC systems the index to maximize is not thermodynamic cycle efficiency but the product between cycle efficiency and recover efficiency, χ parameter.

By imposing hot source pinch point temperature ΔT_{pp1}, the value of temperature of hot fluid at economizer inlet $T_{2,hot}$ can be calculated. Since $T_{1,hot}$, $T_{2,hot}$, T_1, T_7 and mass flow rate of hot source $\dot{m}_{hot}$ are given by design specifications and thermodynamic cycle; by applying equation 2.2 to evaporator and superheater components, the circulating mass flow rate of organic fluid can be computed. By applying energy conservation to the overall evaporating process (economizer, evaporator and super-hater) both outlet temperature of hot source fluid and effective heat recovered can be evaluated.

$$T_{1,hot} = T_{IN,hot} \qquad 2.33$$

$$T_{2,hot} = T_7 + \Delta T_{pp1} \qquad 2.34$$

$$\dot{m} = \frac{\dot{m}_{hot}\bar{c}_{p,12,hot}\left(T_{1,hot} - T_{2,hot}\right)}{(H_1 - H_7)} \qquad 2.35$$

$$T_{3,hot} = T_{1,hot} - \frac{\dot{m}(H_1 - H_6)}{\dot{m}_{hot}\bar{c}_{p,13,hot}} \qquad 2.36$$

$$\bar{c}_{p,12,hot} = f\left(\frac{T_{1,hot+}T_{2,hot}}{2}, p_{hot}\right) \quad 2.37$$

$$\bar{c}_{p,13,hot} = f\left(\frac{T_{1,hot+}T_{3,hot}}{2}, p_{hot}\right) \quad 2.38$$

$$\bar{c}_{p,13,hot,min} = f\left(\frac{T_{1,hot+}T_{3,hot,min}}{2}, p_{hot}\right) \quad 2.39$$

$$\dot{Q}_{rec} = \dot{m}_{hot}\bar{c}_{p,13,hot}\left(T_{1,hot} - T_{3,hot}\right) \quad 2.40$$

$$\dot{Q}_{rec,max} = \dot{m}_{hot}\bar{c}_{p,hot}\left(T_{1,hot} - T_{3,hot,min}\right) \quad 2.41$$

$$\eta_{rec} = \frac{\dot{Q}_{rec}}{\dot{Q}_{rec,max}} \quad 2.42$$

Thermal coupling with Cold Source

By imposing cold source pinch point temperature ΔT_{pp2} the value of cold source mass flow rate is evaluated:

$$T_{1,cold} = T_{IN,cold} \quad 2.43$$

$$T_{2,cold} = T_{3,1} + \Delta T_{pp2} \quad 2.44$$

$$\dot{m}_{cold} = \frac{\dot{m}\left(H_{3,1} - H_4\right)}{\bar{c}_{p,12,cold}\left(T_{2,cold} - T_{1,cold}\right)} \quad 2.45$$

$$T_{3,cold} = T_{1,cold} + \frac{\dot{m}(H_3 - H_4)}{\dot{m}_{cold}\bar{c}_{p,13,cold}} \quad 2.46$$

$$\bar{c}_{p,12,cold} = f\left(\frac{T_{1,cold+}T_{2,cold}}{2}, p_{cold}\right) \quad 2.47$$

$$\bar{c}_{p,13,cold} = f\left(\frac{T_{1,cold+}T_{3,cold}}{2}, p_{cold}\right) \quad 2.48$$

Power Production

Since organic fluid mass flow rate $\dot{m}$ and specific cycle have been computed, mechanic power extracted by turbine shaft P_T and mechanic power at pump shaft P_P are evaluated by the product between $\dot{m}$ and organic fluid enthalpy drop. The ratio between net produced power ($P_T - P_P$) and heat recovered from hot source represents the efficiency of the ORC system.

$$P_T = \dot{m}(H_1 - H_2) \quad 2.49$$

$$P_P = \dot{m}(H_5 - H_4) \quad 2.50$$

$$\eta_{ORC} = \frac{P_T - P_P}{\dot{Q}_{rec}} \quad 2.51$$

$$\chi = \eta_{rec}\,\eta_{ORC} = \frac{P_T - P_P}{\dot{Q}_{rec,max}} \quad 2.52$$

Number of equations and variables involved in the presented model are summarized and listed:

N° of equations: 56
N° variables: 64
N° of fixed parameters: 6
N° of independent variables: 8

Fixed parameters refer to all that parameters which are imposed by design input data and cannot be changed by designer.
Independent variables refer to all variables whose values need to be fixed by designer in order to solve the presented system of equations. The number of independent variables is the difference between the number of variables and the number of equations.

Fixed parameters and independent variables of the presented model are listed in table 2.1.

Table 2.1 Variables and Parameters involved in Thermodynamic cycle design model

Variables and Parameters	
Fixed Parameters	***Independent variables***
$\dot{m}_{hot}$	p_{ev}
p_{hot}	p_{cond}
$T_{IN,hot}$	ε_{rigen}
$T_{3,hot,min}$	ΔT_{ap}
$T_{IN,cold}$	ΔT_{pp1}
p_{cold}	ΔT_{pp2}
	$\eta_{is,t}$
	$\eta_{is,p}$

2.2 Design model of Heat-exchanger without change of phase

In this section the heat exchanger with no change of phase design model is presented. Shell-and-tube exchangers are considered as suggest by [4] and [8]; since they are widely used in ORC applications. One fluid runs throughout a bundle of tubes; while second fluid flows externally to the bundle, guided by baffles.

Several configurations are available for these exchangers; nevertheless only three possible configurations are considered for the proposed model:

- One pass shell-side, one pass tube side (perfect countercurrent, *CC*);
- One pass shell-side, two passes tube side (*1-2*);
- Two pass shell-side, four passes tube side (*2-4*);

The design model implements the traditional design procedure for heat exchangers. The first step is configuration selection; the chosen configuration has to guarantee turbulent flow in both fluids and a sufficient high value of temperature factor F_t. The value of F_t indicates how much different is the selected configuration from a perfect countercurrent exchanger and can be calculated, for a specific configuration, by knowing inlet and outlet temperatures of both fluids (usually provided by design specifications for the component). By knowing F_t, the log mean temperature difference ΔT_{ml} is evaluated by the product between log mean temperature difference for perfect countercurrent configuration $\Delta T_{ml,cc}$ and F_t. This value represents the heat transfer driving force of the designed exchanger, inversely proportional to exchange surface needed to transfer the design heat flux. The preliminary global heat transfer coefficient K^D shall then be estimate by using typical heat transfer coefficient database [29] or by designer experience. K^D , ΔT_{ml} and the design transferred heat flux allow calculating the needed exchange surface. The designer has subsequently to impose the value of some geometrical parameters such as tube diameter, tube length and tube thickness, pitch distance, etc. When all geometry parameters are imposed, heat transfer coefficients for both fluids can be evaluated by applying heat transfer empirical correlations, available in literature [29]. The effective heat transfer coefficient of the exchanger K^E is compared with the estimated value K^D; if K^E is higher than K^D, the exchanger is able to satisfy design specifications and the design process is completed; otherwise the designer has to restart design procedure for a different value of K^D. Several configurations and different geometries can be chosen for the same design specifications; nevertheless the optimal design is the exchanger which leads to transfer all the designed heat flux, minimizing exchange surface and so investment cost.
In this model, for simplicity, pressure losses are neglected.

Balance equations

In steady state conditions no energy or mass storage is considered; simplifying balance equations. All following equations refers to a specific exchanger arrangement: hot fluid flowing throughout tubes and cold fluid in shell side. Nevertheless the presented equations are still valid also for opposite arrangement although some variables such as convective heat fluxes will be negative.

Inlet and outlet mass flow rate are imposed equal for both fluids; in order to satisfy continuity equations:

$$\dot{m}_{1,IN} = \dot{m}_{1,OUT} \quad 2.53$$

$$\dot{m}_{2,IN} = \dot{m}_{2,OUT} \quad 2.54$$

To meet energy conservation principle the thermal power received or released by fluids shall be equal to convective heat transferred by the heat exchanger.

$$\dot{m}_1 \bar{c}_{p,1}\left(T_{1,IN} - T_{1,OUT}\right) = \dot{q}_{CONV} \quad 2.55$$

$$\dot{m}_2 \bar{c}_{p,2}\left(T_{2,OUT} - T_{2,IN}\right) = \dot{q}_{CONV} \quad 2.56$$

Since the above mentioned assumption of neglecting pressure losses, momentum conservation equation is applied simply by equaling inlet and outlet pressures for both fluids.

$$p_{1,IN} = p_{1,OUT} \quad 2.57$$

$$p_{2,IN} = p_{2,OUT} \quad 2.58$$

State equations

State equations refer to all equations that allow calculating thermodynamic properties of a specific state point; they can be determinate by knowledge of two intensive variables such as temperature and pressure or pressure and enthalpy. These equations are performed in the presented model by mean of *Refprop* code, an engineering program that allows calculating several thermodynamic properties of a wide library of different fluids and mixtures. They are represented as a general function $f(v1, v2)$, providing the two involved intensive variables $v1$ and $v2$.

$$c_{p,1,IN} = f(T_{1,IN}, p_{1,IN}) \quad 2.59$$

$$c_{p,1,OUT} = f(T_{1,OUT}, p_{1,OUT}) \quad 2.60$$

$$c_{p,2,IN} = f(T_{2,IN}, p_{2,IN}) \quad 2.61$$

$$c_{p,2,OUT} = f(T_{2,OUT}, p_{2,OUT}) \quad 2.62$$

Additional equations

The convective heat transferred is equal to the product of estimated global heat transfer coefficient K^D, external surface A_{ext} and logarithmic mean difference temperature ΔT_{ml} .

$$\dot{q}_{CONV} = K^D A_{ext}\, \Delta T_{ml,cc}\, F_t \quad 2.63$$

The effective global heat transfer coefficient is computed by considering a series of 4 thermal resistances:

- Tube-side fluid convective resistance $\frac{A_{ext}}{h_{int}A_{int}}$
- Shell-side fluid convective resistance $\frac{1}{h_{ext}}$
- Shell-side and tube-side fouling resistances f_{ext} and $\frac{f_{int}\,A_{ext}}{A_{int}}$

$$K^E = \frac{1}{\frac{A_{ext}}{h_{int}A_{int}} + \frac{f_{int}\,A_{ext}}{A_{int}} + f_{ext} + \frac{1}{h_{ext}}} \quad 2.64$$

Internal and external exchange surfaces can be evaluated using equations 2.65 and 2.66:

$$A_{int} = \pi\ ID\ L\ N_{tt} \quad 2.65$$
$$A_{ext} = \pi\ OD\ L\ N_{tt} \quad 2.66$$

For heat transfer coefficients calculation, Delaware method correlations are adopted [29]. They are presented in Appendix 1, so in this section only parameters that allow the calculation of such coefficients are shown. Mean wall temperature is necessary to calculate transfer coefficients but at the same time mean wall temperature needs the values of heat transfer coefficients to be computed. This algebraic loop can be solved by mean of a simple iteration procedure.

$$h_{int} = f(\dot{m}_1, \overline{T_1}, \overline{p_1}, ID, L, N_{tt}, configuration) \quad 2.67$$
$$h_{ext} = f(\dot{m}_2, \overline{T_2}, \overline{p_2}, \overline{T}_{wall}, OD, L, pitch, b, B_C, N_{tt}, N_{ss}, layout, configuration) \quad 2.68$$
$$\overline{T}_{wall} = f(\alpha_{int}, f_{int}, A_{int}, \overline{T_1}) \quad 2.69$$

Logarithmic mean difference temperature ΔT_{ml} that drives the transfer of heat is the product of logarithmic mean difference temperature for perfect countercurrent configuration $\Delta T_{ml,cc}$ and temperature factor F_t. F_t is evaluated by applying empirical correlations for the chosen configuration; these correlations are presented in Appendix 1. In this section only parameters that allow F_t calculation are presented.

$$\Delta T_{ml,cc} = \frac{(T_{1,IN} - T_{2,OUT}) - (T_{1,OUT} - T_{2,IN})}{log[(T_{1,IN} - T_{2,OUT})/(T_{1,OUT} - T_{2,IN})]} \quad 2.70$$
$$F_t = f(T_{1,IN}, T_{1,OUT}, T_{2,IN}, T_{2,OUT}, configuration) \quad 2.71$$

Number of equations and variables involved the system of equations is:

N° of equations: 19

N° variables: 38

N° of fixed parameters: 7

N° of independent variables: 12

The number of variables is greater than the number of system equations, so 12 independent variables has to be imposed to solve the system. Significant parameters and variables involved in the model are listed in table 2.2:

Table 2.2 Variables and Parameters involved in heat exchanger design model

Variables and Parameters		
Fixed Parameters	***Independent variables***	***Output variables***
$\dot{m}_{1,IN}$	K_D	K_R
$\dot{m}_{2,IN}$	OD	N_{tt}
$p_{1,IN}$	ID	A_{ext}
$p_{2,IN}$	L	
$T_{1,IN}$	$pitch$	
$T_{1,OUT}$	b	
$T_{2,IN}$	B_C	
	N_{SS}	
	layout	
	configuration	
	f_{int}	
	f_{ext}	

In order to achieve heat exchanger design procedure, Excel datasheets have been created; performing the proposed system of equations. Excel is very useful for such application due to its possibility to integrate with *Refprom* add-in. By mean of *Refprom* add-in new *Excel* functions are available and allow calculating all thermodynamic properties included in *Refprop* code.

2.3 Design model of Heat-exchanger with change phase

When one of the two fluids needs to be evaporated or condensed a different heat-exchanger model is necessary. The change of phase occurs in the shell-side of heat exchanger, so outside a

tube bundle throughout which the second fluid flows. The design procedure is similar to previous model since only heat transfer equations change.

When a change of phase occurs the system become more complex to describe and some assumption are necessary to simplify the model. The shell-side fluid is considered to be in perfect equilibrium for both liquid and vapor phase; therefore fluid temperature inside shell is function of the shell-side pressure. Outlet flux is assumed to be in saturated conditions.

Log mean temperature difference is assumed to be exactly log mean temperature difference for countercurrent configuration (F_t=1), thus neglecting subcooled or superheated inlet fluid influence.

The tube side fluid is assumed not to change phase during the process and, as for previous model, pressure losses are neglected.

Balance equations

Balance equations are the same of previous model; the only difference is that energy balance equation for shell-side fluid cannot be expressed by mean of average specific heat since a change of phase occurs. To overcome this problem the fluid specific energy variation is expressed using enthalpy drop between inlet and outlet flows.

$$\dot{m}_{1,IN} = \dot{m}_{1,OUT} \quad (2.72)$$

$$\dot{m}_{2,IN} = \dot{m}_{2,OUT} \quad (2.73)$$

$$\dot{m}_1 \bar{c}_{p,1}\left(T_{1,IN} - T_{1,OUT}\right) = \dot{q}_{CONV} \quad (2.74)$$

$$\dot{m}_2\left(H_{2,OUT} - H_{2,IN}\right) = \dot{q}_{CONV} \quad (2.75)$$

$$p_{1,IN} = p_{1,OUT} \quad (2.76)$$

$$p_{2,IN} = p_{2,OUT} \quad (2.77)$$

State equations

For phase-changing fluid, due to model assumptions, outlet enthalpy and fluid temperature can be directly computed by shell-side pressure, imposing vapor quality value equal to 1 or 0. For tube-side fluid equations are unchanged.

$$c_{p,1,IN} = f(T_{1,IN}, p_{1,IN}) \quad (2.78)$$

$$c_{p,1,OUT} = f(T_{1,OUT}, p_{1,OUT}) \quad (2.79)$$

$$H_{2,IN} = f(T_{2,IN}, p_{2,IN}) \quad (2.80)$$

$$H_{2,OUT} = f(p_{2,OUT}, x = 1\ or\ 0) \quad (2.81)$$

$$T_2 = f(p_{2,OUT}, x = 1\ or\ 0) \quad (2.82)$$

Additional equations

$$\dot{q}_{CONV} = K^D A_{ext}\, \Delta T_{ml,cc} \quad 2.83$$

$$K^R = \frac{1}{\frac{A_{ext}}{\alpha_{int} A_{int}} + \frac{f_{int}\, A_{ext}}{A_{int}} + f_{ext} + \frac{1}{\alpha_{ext}}} \quad 2.84$$

$$A_{int} = \pi\, ID\, L\, N_{tt} \quad 2.85$$

$$A_{ext} = \pi\, OD\, L\, N_{tt} \quad 2.86$$

$$\alpha_{int} = f(\dot{m}_1, \overline{T_1}, \overline{p_1}, ID, L, N_{tt}, configuration) \quad 2.87$$

$$\alpha_{ext} = f(\dot{m}_2, \overline{p_2}, \overline{T}_{wall}, OD, L, pitch, N_{tt}, layout, configuration) \quad 2.88$$

$$\overline{T}_{wall} = f(\alpha_{int}, f_{int}, A_{int}, \overline{T_1}) \quad 2.89$$

$$\Delta T_{ml,cc} = \frac{(T_{1,IN} - T_2) - (T_{1,OUT-} T_2)}{log[(T_{1,IN} - T_2)/(T_{1,OUT-} T_2)]} \quad 2.90$$

N° of equations: 20

N° of fixed parameters: 6

N° variables: 29

N° of independent variables: 9

Fixed parameters, independent variables and output variables of the system are shown in the table 2.3:

Table 2.3 Variables and Parameters involved in heat exchanger with change phase design model

Variables and Parameters

Fixed Parameters
$\dot{m}_{1,IN}$
$\dot{m}_{2,IN}$
$p_{1,IN}$
p_2
$T_{2,IN}$
$H_{2,IN}$

Design variables
K^D
OD
ID
L
$pitch$
$layout$
$configuration$

Output variables
K^R
N_{tt}
A_{ext}
D_s

f_{int}
f_{ext}

2.4 Design model of Turbine

In this section the design model of turbine component is presented. It has the purpose of evaluate all parameters necessary to perform the off-design model of turbine component but not to define the effective geometry of the device.

Balance equations

$\dot{m}_{IN} = \dot{m}_D$ 2.91

$\dot{m}_{OUT} = \dot{m}_D$ 2.92

Energy conservation equation is applied imposing that the product of fluid specific energy variation and the processed mass flow rate $\dot{m}_D$ is equal to the mechanical power extracted at turbine shaft $P_{mecc,D}$, neglecting mechanical efficiency.

$\dot{m}_D(H_{IN,D} - H_{OUT,D}) = P_{mecc,D}$ *2.93*

State equations

State equations lead to calculate temperature, density and entropy of inlet flux in design conditions. Inlet entropy $s_{IN,D}$ is then used to evaluate outlet isentropic enthalpy in design conditions $H_{OUT,is,D}$.

$[T_{IN,D}, \rho_{IN,D}, s_{IN,D}] = f(p_{IN,D}, H_{IN,D})$ 2.94

$H_{OUT,is,D} = f(p_{OUT,D}, s_{IN,D})$ 2.95

Additional equations

K is a parameter that allows performing Stodola equation in dynamic model [12]; in particular it is proportional to inlet flow section and strongly influences the mass flow rate processed by the component. In the proposed model it is evaluated by imposing nominal inlet and outlet pressure ($p_{IN,D}$ and $p_{OUT,D}$), nominal inlet density $\rho_{IN,D}$ and nominal mass flow rate processed by the component $\dot{m}_D$.

$$K = \frac{\dot{m}_D}{\sqrt{\rho_{IN,D}\ p_{IN,D}\left[1-\left(\frac{1}{\varepsilon_D}\right)^2\right]}} \quad 2.96$$

$$\varepsilon_D = \frac{p_{IN,D}}{p_{OUT,D}} \quad 2.97$$

Turbine design isentropic efficiency takes into account effect of irreversibility of expansion process and allows calculating the effective fluid outlet enthalpy at design condition $H_{OUT,D}$.

$$\eta_{is,T,D} = \frac{H_{IN,D} - H_{OUT,D}}{H_{IN,D} - H_{OUT,is,D}} \quad 2.98$$

Reduced mass flow rate at design conditions $\dot{m}_{R,D}$ is computed since it represents an input parameter of off-design turbine model.

$$\dot{m}_{R,D} = \frac{\dot{m}_D \sqrt{T_{IN,D}}}{p_{IN,D}} \quad 2.99$$

$$P_{el,D} = P_{mecc,D}\,\eta_{GEN} \quad 2.100$$

N° of equations: 12
N° variables: 14
N° of fixed parameters: 4
N° of independent variables: 2

Table 2.4 Variables and Parameters involved in turbine design model

Variables and Parameters

Fixed Parameters
$\dot{m}_D$
$p_{IN,D}$
$p_{OUT,D}$
$H_{IN,D}$

Independent variables
$\eta_{is,D}$
η_{GEN}

Output variables
K
$\dot{m}_{R,D}$
$\eta_{is,D}$
η_{GEN}

2.5 Design model of Pump

Pump model is very similar to turbine model, due to the fact that only parameters necessary for the off-design model are here evaluated.

Balance equations

$$\dot{m}_{IN} = \dot{m}_D \qquad 2.101$$

$$\dot{m}_{OUT} = \dot{m}_D \qquad 2.102$$

$$\dot{m}_D\left(H_{OUT,D} - H_{IN,D}\right) = P_{mecc,D} \qquad 2.103$$

State equations

$$\left[\rho_{IN,D}, s_{IN,D}\right] = f\left(p_{IN,D}, H_{IN,D}\right) \qquad 2.104$$

$$H_{OUT,is,D} = f\left(p_{OUT,D}, s_{IN,D}\right) \qquad 2.105$$

Additional equations

Differently from turbine model the characteristic curve of the pump is function of inlet volumetric flow rate and specific energy processed by the pump [12]:

$$y_D = \frac{p_{OUT,D} - p_{IN,D}}{\rho_{IN,D}} \qquad 2.106$$

$$\dot{V}_D = \frac{\dot{m}_D}{\rho_{IN,D}} \qquad 2.107$$

$$\eta_{is,P,D} = \frac{H_{OUT,is,D} - H_{IN,D}}{H_{OUT,D} - H_{IN}, D} \qquad 2.108$$

$$P_{el,D} = P_{mec,D}\,\eta_{GEN} \qquad 2.109$$

Other two parameters need to be evaluated in order to complete design procedure:

- w_D, nominal rotational speed.
- $y_{0,D}$, which fixed the maximum pressure drop that the pump can provide at nominal speed.

N° of equations: 10

N° of variables: 14

N° of fixed parameters: 4

N° of independent variables: 4

Table 2.5 Variables and Parameters involved in pump design model

Variables and Parameters		
Fixed Parameters	***Independent variables***	***Output variables***
$\dot{m}_D$	$y_{0,D}$	$\dot{V}_D$
$p_{IN,D}$	w_D	y_D
$p_{OUT,D}$	$\eta_{is,P,D}$	y_0
$H_{IN,D}$	η_{GEN}	w_D
		$\eta_{is,D}$
		η_{GEN}

Conclusions

In this chapter design model of thermodynamic cycle and components involved in the process have been presented. The aim was to create general design models of each component, which could be used also for studying different systems configurations or different applications. For each component fixed parameter and independent variables that the designer has to impose in order to accomplish design procedure have been highlighted and listed.

3. OFF-DESIGN MODEL

Introduction

In this chapter the dynamic model of components is presented. The aim of the work is to create a dynamic model of different components involved in the superheated regenerative organic Rankine cycle system. The purpose is to develop models of the single components, which could be used to study, in future, different system configurations and different working fluids. Few studies in literature proposed dynamic models of ORC systems. Works of Quolin et al. [9], Vaja [12], Xie [10] et al., and Zhang et al. [11] propose dynamic models of non-regenerative ORC systems considering pipe-in-pipe heat exchangers. As suggest by Pierobon et al. [4] and Calise et al. [8] for practical applications of organic Rankine cycle systems shell-and-tube heat exchangers are used. In this work shell-and-tube heat exchangers dynamic model is proposed, in order to consider realistic volumes and thermal inertias of the system.

Nomenclature

p	Pressure [bar]
T	Temperature [°C]
H	Enthalpy [kJ/kg]
s	Entropy [kJ/kg K]
x	Vapor mass fraction [-]
c_p	Specific heat at constant pressure [kJ/kg K]
$\dot{m}$	Mass flow rate [kg/s]
$\dot{V}$	Volumetric flow rate [m^3/s]
$\dot{q}$	Heat transfer rate [kW]
P	Power [kW]
K	Global heat transfer coefficient [kW/m^2 K] Stodola coefficient [m^2]
h	Heat transfer coefficient [kW/m^2 K]
f	Fouling factor [m^2 K/kW]
F_t	Temperature factor [-]
A	Surface [m^2]
OD	External tube diameter [m]
ID	Internal tube diameter [m]
L	Tube length [m]
$pitch$	Pitch distance [m]
B_C	Baffle cut [%]
b	Number of baffles [-]
$layout$	Tube layout [°]
N_{tt}	Number of tubes [-]
N_{ss}	Number of sealing strips [-]
y	Specific energy [kJ/kg]
w	Rotational speed [rad/s]

Greek symbols

ε	Heat transfer efficiency [-] Expansion ratio [-]
η	Efficiency [-]
χ	Overall efficiency [-]

Abbreviations and subscripts

1	Tube side fluid
2	Shell side fluid
hot	Hot source
$cold$	Cold Source
D	Design
E	Effective
IN	Inlet
OUT	Outlet
pp	Pitch point
ap	Approach point
t	Turbine
p	Pump
ev	Evaporation
$cond$	Condensation
is	Isentropic
max	Maximum
rec	Recover
ORC	Organic Rankine cycle
$conv$	Convective
ext	External
int	Internal
ml	Mean log
$wall$	Wall
cc	Countercurrent
$mecc$	Mechanical
el	Electrical
gen	Generator
i	Unit i
t	time

3.1 Dynamic modeling

Before starting the presentation of off-design models of components, an important distinction between two different dynamic models is introduced: *Dynamic* models and *quasi steady-state* models.

Dynamic model is used to describe components in which a mass or energy storage occurs. For these components output variables are not only function of input variables but they depend also from the "history" of system. In fact the dynamic behavior of these devices is also determinate by

the evolution in time of so called "*state-variables*"; variables that are calculated by the model at previous time step of simulation. Accordingly to that is clear that the value of these "*state-variables*" at the beginning of the simulation is to define by the user in order to start the simulation. Heat-exchangers are included in this category.

Quasi steady-state model is used to describe components in which no energy or mass storage is considered. In that approach "*state-variables*" are not considered and consequently the value of output variables is directly determinate by the value of input variables. Nevertheless it does not mean that these devices do not have a dynamic behavior; but it is really faster compared to dynamic response of components with which they are connected to. These components can be modelled by mean of characteristic maps, derived from experimental studies and so treated using algebraic equations. Fluid machines such as pumps and turbines are included in this category.

Some assumptions have been introduced in order to simply system modelling:

- All components are considered perfectly adiabatic.
- Pressure drops for all components are neglected.

Component models have been then implemented using Matlab®/Simulink® software.
MATLAB®, the language of technical computing, is a programming environment for algorithm development, data analysis, visualization, and numeric computation. Simulink® is a graphical environment for simulation and Model-Based Design of multidomain dynamic and embedded systems.
Simulink is a data flow graphical programming language tool for modeling, simulating and analyzing dynamic systems. Its interface is a graphical block diagramming tool and a customizable set of block libraries. It does not include already models of devices such as turbines or exchangers as other engineering software but its block library includes sinks, sources, linear and nonlinear component and connectors which allow creating the desired model.

To realize the model another important feature is the evaluation of fluid thermodynamic properties during simulation process. These properties can be evaluated with simply correlations for ideal gases and incompressible fluids. Nevertheless when fluids and gases are considered real, *Refprop* database can be used. *Refprop* is a database that includes thermodynamic properties of many hydrocarbons and refrigerant fluids in a wide range of pressure and temperature. An interesting feature of *Refprop* is the possibility to execute it during *Matlab* or *Simulink* simulations by mean of a routine called *refprop.m*.

3.2 Dynamic model of heat exchanger with no phase change

In this section the dynamic model of heat exchangers is presented.

Several models have been proposed in literature to study exchangers' behavior.

Many *quasi steady-state models* are available, using for example ε-NTU charts or other empirical correlations. These models are really precise and furthermore ε-NTU charts are available for many possible exchangers configuration; nevertheless they cannot be used to describe dynamic behavior of the component.

Other studies propose two-dimensional or three-dimensional *dynamic model.* They result very accurate in studying also complex phenomena such as natural convection or bubbles formation outside tubes in evaporators. Nevertheless since the purpose of this work is to study the behavior of the whole system and not of the single component; these approaches seem not interesting for the scope and one-dimensional model has been chosen. In accordance to that assumption, properties of fluids are assumed to vary only in in function of time and flow direction (so only one direction). The entire exchanger volume is discretized in *units* limited by a fixed control volume and for each *unit* of fluid or pipe, mass and energy conservation equations are applied. The degree of discretization *nx* can be chosen by the designer; for high value of *nx* the model results more accurate but it requires a higher computational time to perform the simulation.

Differential equations involved in conservation laws are approximated using small finite time intervals (Δt) instead of time differential (δt). When Δt chosen is small, the error committed in the approximation is negligible; while the computational time increase. Vice versa for higher value of Δt the simulation results faster but the approximation error can become not negligible. The choice of Δt is an important parameter that influence also the stability of the model.

Some assumptions are necessary in order to simplify the exchanger model:

- Thermodynamic properties of both the metal pipe and the fluids are function of space (one-dimensional) and time;
- The conductive and radiative heat fluxes have been neglected, only convection heat flux is considered;
- The exchanger is assumed to be adiabatic, hence heat losses are neglected;
- Pressure losses are neglected for both fluids;
- Lumped thermal capacitance is assumed for both the metal pipe and the fluids;
- No mass storage is considered;
- Energy storage is considered in metal pipe and both fluids.

An example of a generic unit *i* of the heat exchanger at generic time *t* of simulation is shown in figure 3.1, highlighting the heat fluxes involved in the model.

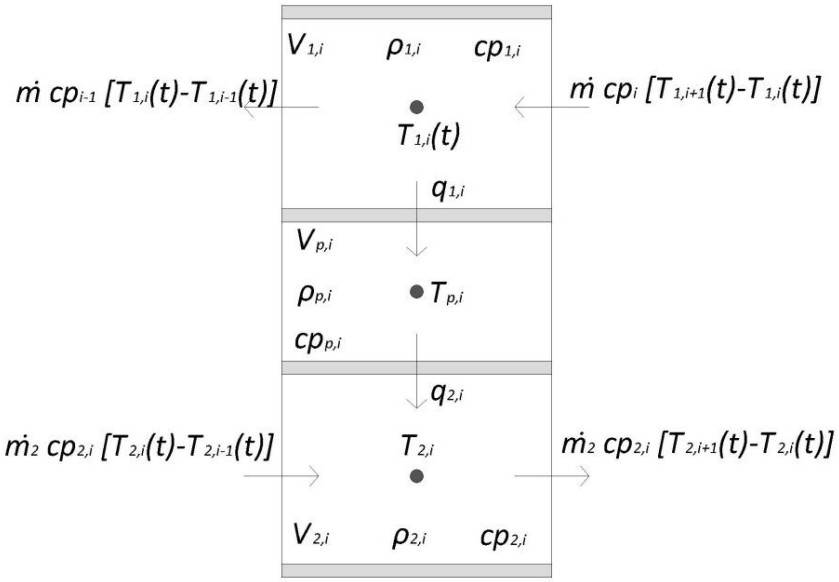

Figure 3.1Schematic representation of heat fluxes involved in energy balance for a generic discretized unit of the no-change phase heat exchanger

As for the design model three different possible configurations for heat exchangers without change of phase have been considered:

- One pass shell-side, one pass tube-side (perfect countercurrent)
- One pass shell-side, two passes tube-side (1-2)
- Two passes shell-side, four passes tube-side (2-4)

3.2.1 Perfect countercurrent

One pass shell-side, one pass tube-side model is here presented. Clearly it is the easiest configuration to model, due to the fact that shell-side fluid, tube-side fluid and pipe are discretized in the same number of units *nx*.
In figure 3.2 the arrangement of fluids and pipe units is shown.

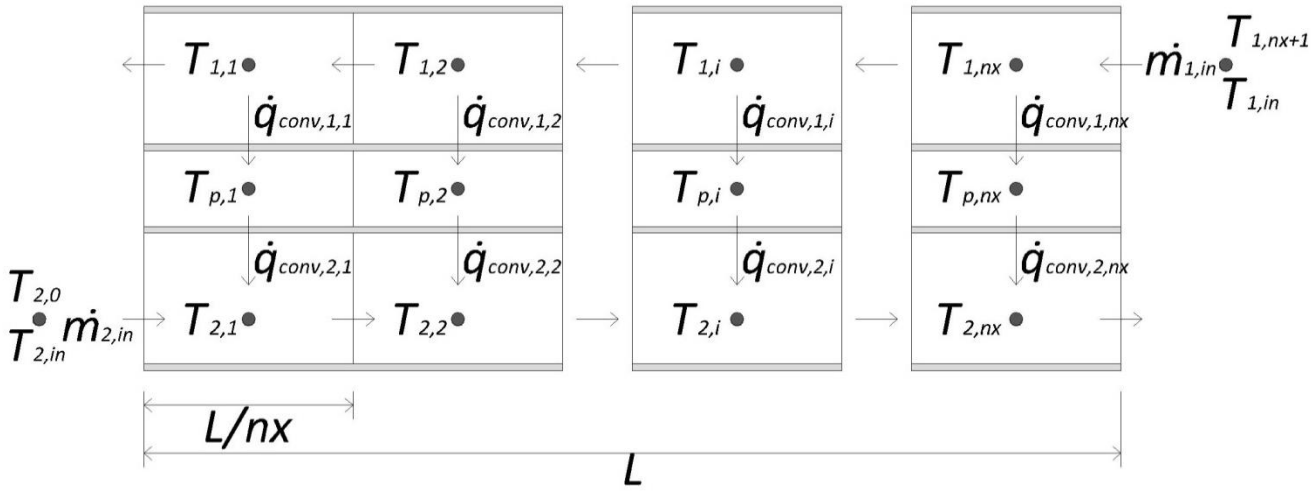

Figure 3.2 Discretization assumed for perfect countercurrent Shell&Tube heat exchanger, including convective heat fluxes involved.

All equations involved in the model are subdivided in balance equations, state equations and additional equations. At the end boundary equations are presented; they impose input and output variables of the heat exchanger model.

Mass Balance equations

Continuity equation is applied for both fluids, simply imposing that mass flow rate flowing a fluid unit is equal to mass flow rate that flows through the precedent (or the following, depends on the chosen units arrangement).

$\dot{m}_{1,i}^{t} = \dot{m}_{1,i+1}^{t}$ *i=1:nx* *3.1*

$\dot{m}_{2,i}^{t} = \dot{m}_{2,i-1}^{t}$ *i=1:nx* *3.2*

Energy balance equations

For both fluids energy conservation is guaranteed imposing that the difference between heat flow exchanged from a fluid *unit* with the precedent (or the following) *unit* and the convective heat flow exchanged with pipe is stored by the unit.

For pipe unit a similar approach is used since the difference between convective heat flows transferred with the two fluid units with which it interacts, is stored by mean of *unit* temperature variations.

$$\rho_{1,i}^{t}\, V_{1,i}\, c_{p,1,i}^{t}\, \frac{{T_{1,i}}^{t+\Delta t} - {T_{1,i}}^{t}}{\Delta t} = \dot{m}_{1,i}^{t}\, c_{p,1,i}^{t}\, \left(T_{1,i}^{t} - T_{1,i+1}^{t}\right) - \dot{q}_{CONV,1,i}^{t} \qquad i=1:nx \qquad 3.3$$

$$\rho_{2,i}^{t}\, V_{2,i}\, c_{p,2,i}^{t}\, \frac{{T_{2,i}}^{t+\Delta t} - {T_{2,i}}^{t}}{\Delta t} = \dot{q}_{CONV,2,i}^{t} - \dot{m}_{2,i}^{t}\, c_{p,2,i}^{t}\, \left(T_{2,i-1}^{t} - T_{2,i}^{t}\right) \qquad i=1:nx \qquad 3.4$$

$$\rho_{p}\, V_{p,i}\, c_{p,p}\, \frac{{T_{p,i}}^{t+\Delta t} - {T_{p,i}}^{t}}{\Delta t} = \dot{q}_{CONV,2,i}^{t} - \dot{q}_{CONV,1,i}^{t} \qquad i=1:nx \qquad 3.5$$

State equations

Specific heat and density of each fluid unit at time *t* can be computed by knowing fluid temperature and pressure of each *unit* at time *t* of simulation (using *Refprop*).

$$c_{p,1,i}^{t} = f(T_{1,i}^{t}, p_{1,i}^{t}) \qquad i=1:nx \qquad 3.6$$

$$c_{p,2,i}^{t} = f\left(T_{2,i}^{t}, p_{2,i}^{t}\right) \qquad i=1:nx \qquad 3.7$$

$$\rho_{1,i}^{t} = f(T_{1,i}^{t}, p_{1,i}^{t}) \qquad i=1:nx \qquad 3.8$$

$$\rho_{2,i}^{t} = f(T_{2,i}^{t}, p_{2,i}^{t}) \qquad i=1:nx \qquad 3.9$$

Additional equations

$$p_{1,i}^{t} = p_{1,i+1}^{t} \qquad i=1:nx \qquad 3.10$$

$$p_{2,i}^{t} = p_{2,i-1}^{t} \qquad i=1:nx \qquad 3.11$$

Convective heat flows are calculated considering the temperature difference and not the log mean temperature difference. This is acceptable due to the fact that a discretized approach is considered.

$$\dot{q}_{CONV,1,i}^{t} = h_{1,i}^{t}\, A_{1,i}\, \left(T_{p,i}^{t} - T_{1,i}^{t}\right) \qquad i=1:nx \qquad 3.12$$

$$\dot{q}_{CONV,2,i}^{t} = h_{2,i}^{t}\, A_{2,i}\, \left(T_{2,i}^{t} - T_{p,i}^{t}\right) \qquad i=1:nx \qquad 3.13$$

Volume and exchange area for each *unit* are calculated dividing the global volume or surface for the number of *units*:

$$A_{1,i} = (\pi\, ID\, L\, N_{tt})/nx \qquad i=1:nx \qquad 3.14$$

$$A_{2,i} = (\pi\, OD\, L\, N_{tt})/nx \qquad i=1:nx \qquad 3.15$$

$$V_{1,i} = \left(\frac{\pi\, ID^2}{4}\, N_{tt} L\right)/nx \qquad i=1:nx \qquad 3.16$$

$$V_{2,i} = \left(\frac{\pi\, D_s^2}{4}\, L\right)/nx - \left(\frac{\pi\, OD^2}{4}\, N_{tt} L\right)/nx \qquad i=1:nx \qquad 3.17$$

$$V_{p,i} = \left[\frac{\pi\, (OD^2 - ID^2)}{4}\, N_{tt} L\right]/nx \qquad i=1:nx \qquad 3.18$$

Heat transfer coefficients correlations are presented in Appendix 1, here only parameters necessary for the calculation are provided:

$$h_{1,i}^t = f(\dot{m}_{1,i}^t, T_{1,i}^t, p_{1,i}^t, T_{p,i}^t, ID, L, N_{tt}, conf) \qquad i=1:nx \qquad 3.19$$

$$h_{2,i}^t = f(\dot{m}_{2,i}^t, T_{2,i}^t, p_{2,i}^t, T_{p,i}^t, OD, L, pitch, b, B_C, N_{tt}, N_{ss}, layout, conf) \qquad i=1:nx \qquad 3.20$$

Boundary equations

Boundary equations lead to define input and output variables of the whole component. Equations refer to units arrangement presented in figure 3.2:

$$\dot{m}_{1,nx+1}^t = \dot{m}_{1,IN}^t \qquad 3.21$$

$$\dot{m}_{2,0}^t = \dot{m}_{2,IN}^t \qquad 3.22$$

$$\dot{m}_{1,OUT}^t = \dot{m}_{1,1}^t \qquad 3.23$$

$$\dot{m}_{2,OUT}^t = \dot{m}_{2,nx}^t \qquad 3.24$$

$$p_{1,nx+1}^t = p_{1,IN}^t \qquad 3.25$$

$$p_{2,0}^t = p_{2,IN}^t \qquad 3.26$$

$$p_{1,OUT}^t = p_{1,1}^t \qquad 3.27$$

$$p_{2,OUT}^t = p_{2,nx}^t \qquad 3.28$$

$$T_{1,nx+1}^t = T_{1,IN}^t \qquad 3.29$$

$$T_{2,0}^t = T_{2,IN}^t \qquad 3.30$$

$$T_{1,OUT}^t = T_{1,1}^t \qquad 3.31$$

$$T_{2,OUT}^t = T_{2,nx}^t \qquad 3.32$$

The number of equations and variables involved in the above system leads to calculate the number of independent variables to impose in order to solve the system.
The number of equations, variables and parameters are here listed:

N° of equations: 20*nx*+12
N° of fixed parameters: 15
N° variables: 23*nx*+18
N° of independent variables: 3*nx*+6
N° of input variables: 6
N° of state variables: 3*nx*

The system can be solved at time *t* by imposing the value of the 3*nx*+6 independent variables. The value of 6 independent variables is given by 6 input parameters at time *t:* inlet mass flow rate, pressure and temperature (or enthalpy) for both fluids.
Therefore 3*nx* independent variables still exceed the number of equations. Nevertheless the 3 temperature vectors $T_1^t|_{1,nx}, T_2^t|_{1,nx}, T_p^t\big|_{1,nx}$ are already known at time *t*; in fact they can be considered as output variables of simulation at previous time step *t-Δt*. The system results thus solvable since the number of equations and dependent variables are equal. Nevertheless, as the system is solvable only providing the value of the 3 temperature vectors at precedent step time; to start the simulation at *t=0* an initial solution of the 3*nx* "state-variables" is necessary.

Fixed parameters refer to parameters which do not vary during simulation, but they are imposed at the beginning of simulation. In particular they can be subdivided into two groups:

- Geometry parameters, which are the output of design model and define the geometry of the exchanger.
- Discretization parameters, *nx* and *Δt*, decided by the user at the beginning of simulation. They define the degree of discretization chosen for the model.

Fixed parameters, input, output and state variables are here listed.

Table 3.1 Variables and Parameters involved in countercurrent heat exchanger dynamic model

Variables and Parameters of simulation at instant t			
Fixed parameters	***Input variables***	***State variables***	***Output variables***
OD	$\dot{m}_{1,IN}^t$	$T_1^t\|_{1,nx}$	$\dot{m}_{1,OUT}^t$
ID	$p_{1,IN}^t$	$T_2^t\|_{1,nx}$	$p_{1,OUT}^t$

pitch
D_S
L
b
B_C
N_{tt}
N_{ss}
layout
configuration
ρ_p
$c_{p,p}$
nx
Δt

$T_{1,IN}^{t}$
$\dot{m}_{2,IN}^{t}$
$p_{2,IN}^{t}$
$T_{2,IN}^{t}$

$T_{p}^{t}\big\vert_{1,nx}$

$T_{1,OUT}^{t}$
$\dot{m}_{2,OUT}^{t}$
$p_{2,OUT}^{t}$
$T_{2,OUT}^{t}$
$T_{1}^{t+\Delta t}\big\vert_{1,nx}$
$T_{2}^{t+\Delta t}\big\vert_{1,nx}$
$T_{p}^{t+\Delta t}\big\vert_{1,nx}$

Since this component will have to be connected to other components, the causality diagram. In this diagram, arrows directions indicate if the variable should be an input or an output signal for the component. In particular the variables that are derived in time in a differential equation are constricted to be an output value of the component. In fact it would be impossible to impose with an input the result of an integral operation.

By applying the causality diagram to heat exchanger model, differential equations are used only in energy balance equations; so T_{IN} has to be a signal input and T_{OUT} a signal output.

Considering mass and momentum balances, due to assumptions, no differential equations are performed in the model so they can be input or output variables. Obviously if inlet mass flow rate is consider as input signal, outlet mass flow rate will be consider an output and vice versa. These variables are represented with a double direction arrow in the causality representation.

Figure 3.3 Causality diagram of heat exchanger dynamic model.

In the chosen representation, mass flow rate signals are marked in red, pressures in green and temperatures (or enthalpies) in blue; this distinction will be used also for other component causality diagrams.

3.2.2 One pass shell-side, two passes tube-side

The second configuration analyzed results more complex to model, due to the fact that fluid 1 and fluid 2 do not flows with the same number of passes throughout the exchanger. To overcome this problem the fluid 1 and pipe are discretized in 2*nx units*, while fluid 2 still in *nx units*. That solution asks that each *unit* of fluid 2 interacts with two *units* of pipe and fluid 2, thus simulating the two passes of fluid 1 in the exchanger.
The figure 3.4 is presented to clarify how fluid and pipe units are connected to each other to simulate the configuration.

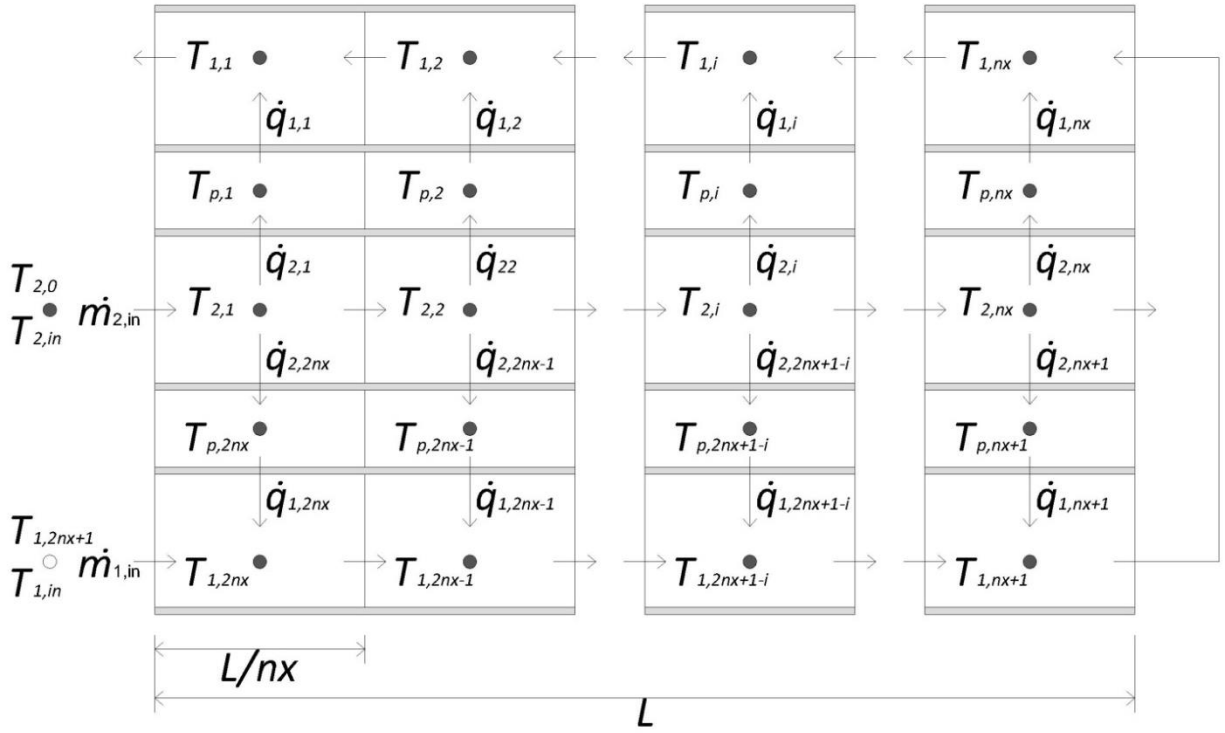

Figure 3.4 Discretization assumed for one pass shell-side, two passes tube-side heat exchanger, including convective heat fluxes involved.

Mass Balance equations

$$\dot{m}_{1,i}^{t} = \dot{m}_{1,i+1}^{t} \qquad i=1:2nx \qquad 3.33$$

$$\dot{m}_{2,i}^{t} = \dot{m}_{2,i-1}^{t} \qquad i=1:nx \qquad 3.34$$

Energy balance equations

$$\rho_{1,i}^{t}\, V_{1,i}\, c_{p,1,i}^{t}\, \frac{{T_{1,i}}^{t+\Delta t} - {T_{1,i}}^{t}}{\Delta t} = \dot{m}_{1,i}^{t}\, c_{p,1,i}^{t}\, \left(T_{1,i}^{t} - T_{1,i+1}^{t}\right) - \dot{q}_{CONV,1,i}^{t} \qquad i=1:2nx \qquad 3.35$$

$$\rho_{2,i}^{t}\, V_{2,i}\, c_{p,2,i}^{t}\, \frac{{T_{2,i}}^{t+\Delta t} - {T_{2,i}}^{t}}{\Delta t} = \left(\dot{q}_{CONV,2,i}^{t} + \dot{q}_{CONV,2,2nx+1-i}^{t}\right) - \dot{m}_{2,i}^{t}\, c_{p,2,i}^{t}\, \left(T_{2,i-1}^{t} - T_{2,i}^{t}\right) \qquad i=1:nx \qquad 3.36$$

$$\rho_{p}\, V_{p,i}\, c_{p,p}\, \frac{{T_{p,i}}^{t+\Delta t} - {T_{p,i}}^{t}}{\Delta t} = \dot{q}_{CONV,2,i}^{t} - \dot{q}_{CONV,1,i}^{t} \qquad i=1:2nx \qquad 3.37$$

State equations

$$c_{p,1,i}^{t} = f\left(T_{1,i}^{t}, p_{1,i}^{t}\right) \qquad i=1:2nx \qquad 3.38$$

$$c_{p,2,i}^{t} = f\left(T_{2,i}^{t}, p_{2,i}^{t}\right) \qquad i=1:nx \qquad 3.39$$

$$\rho_{1,i}^{t} = f\left(T_{1,i}^{t}, p_{1,i}^{t}\right) \qquad i=1:2nx \qquad 3.40$$

$$\rho_{2,i}^{t} = f\left(T_{2,i}^{t}, p_{2,i}^{t}\right) \qquad i=1:nx \qquad 3.41$$

Additional equations

$$p_{1,i}^{t} = p_{1,i+1}^{t} \qquad i=1:2nx \qquad 3.42$$

$$p_{2,i}^{t} = p_{2,i-1}^{t} \qquad i=1:nx \qquad 3.43$$

$$\dot{q}_{CONV,1,i}^{t} = h_{1,i}^{t} A_{1,i} \left(T_{p,i}^{t} - T_{1,i}^{t}\right) \qquad i=1:2nx \qquad 3.44$$

$$\dot{q}_{CONV,2,i}^{t} = \begin{cases} h_{2,i}^{t} A_{2,i} \left(T_{2,i}^{t} - T_{p,i}^{t}\right) & \text{for } i \le nx \\ h_{2,i}^{t} A_{2,2nx+1-i} \left(T_{2,2nx+1-i}^{t} - T_{p,i}^{t}\right) & \text{for } i > nx \end{cases} \qquad 3.45$$

$$A_{1,i} = (\pi\, ID\, L\, N_{tt})/nx \qquad i=1:2nx \qquad 3.46$$

$$A_{2,i} = (\pi\, OD\, L\, N_{tt})/nx \qquad i=1:nx \qquad 3.47$$

$$V_{1,i} = \left(\frac{\pi\, ID^2}{4}\, N_{tt} L\right)/2nx \qquad i=1:2nx \qquad 3.48$$

$$V_{2,i} = \left(\frac{\pi\, D_s^2}{4}\, L\right)/nx - \left(\frac{\pi\, OD^2}{4}\, N_{tt} L\right)/nx \qquad i=1:nx \qquad 3.49$$

$$V_{p,i} = \left[\frac{\pi\, (OD^2 - ID^2)}{4}\, N_{tt} L\right]/2nx \qquad i=1:2nx \qquad 3.50$$

$$h_{1,i}^{t} = f(\dot{m}_{1,i}^{t}, T_{1,i}^{t}, p_{1,i}^{t}, T_{p,i}^{t}, ID, L, N_{tt}, configuration) \qquad i=1:2nx \qquad 3.51$$

$$h_{2,i}^{t} = \begin{cases} f\left(\dot{m}_{2,i}^{t}, T_{2,i}^{t}, p_{2,i}^{t}, T_{p,i}^{t}, OD, L, pitch, b, B_C, N_{tt}, N_{ss}, layout, conf\right) & \text{for } i \le nx \\ f\left(\dot{m}_{2,2nx+1-i}^{t}, T_{2,2nx+1-i}^{t}, p_{2,2nx+1-i}^{t}, T_{p,i}^{t}, OD, L, pitch, b, B_C, N_{tt}, N_{ss}, lay, conf\right) & \text{for } i > nx \end{cases} \qquad 3.52$$

Boundary equations

$$\dot{m}_{1,2nx+1}^{t} = \dot{m}_{1,IN}^{t} \quad 3.53$$

$$\dot{m}_{2,0}^{t} = \dot{m}_{2,IN}^{t} \quad 3.54$$

$$\dot{m}_{1,OUT}^{t} = \dot{m}_{1,1}^{t} \quad 3.55$$

$$\dot{m}_{2,OUT}^{t} = \dot{m}_{2,nx}^{t} \quad 3.56$$

$$p_{1,2nx+1}^{t} = p_{1,IN}^{t} \quad 3.57$$

$$p_{2,0}^{t} = p_{2,IN}^{t} \quad 3.58$$

$$p_{1,OUT}^{t} = p_{1,1}^{t} \quad 3.59$$

$$p_{2,OUT}^{t} = p_{2,nx}^{t} \quad 3.60$$

$$T_{1,2nx+1}^{t} = T_{1,IN}^{t} \quad 3.61$$

$$T_{2,0}^{t} = T_{2,IN}^{t} \quad 3.62$$

$$T_{1,OUT}^{t} = T_{1,1}^{t} \quad 3.63$$

$$T_{2,OUT}^{t} = T_{2,nx}^{t} \quad 3.64$$

N° of equations: 32*nx*+12

N° of fixed parameters: 15

N° variables: 37*nx*+18

N° of independent variables: 5*nx*+6

N° of input variables: 6

N° of state variables: 5*nx*

Table 3.2 Variables and Parameters involved in 1-2n heat exchanger dynamic model

Variables and Parameters of simulation at instant t			
Fixed parameters	***Input variables***	***State variables***	***Output variables***
OD	$\dot{m}_{1,IN}^{t}$	$T_1^t\|_{1,2nx}$	$\dot{m}_{1,OUT}^{t}$
ID	$p_{1,IN}^{t}$	$T_2^t\|_{1,nx}$	$p_{1,OUT}^{t}$
pitch	$T_{1,IN}^{t}$	$T_p^t\|_{1,2nx}$	$T_{1,OUT}^{t}$
D_S	$\dot{m}_{2,IN}^{t}$		$\dot{m}_{2,OUT}^{t}$

L
b
B_C
N_{tt}
N_{ss}
layout
configuration
ρ_p
$c_{p,p}$
nx
Δt

$p_{2,IN}^t$
$T_{2,IN}^t$

$p_{2,OUT}^t$
$T_{2,OUT}^t$
$T_1^{t+\Delta t}\|_{1,2nx}$
$T_2^{t+\Delta t}\|_{1,nx}$
$T_p^{t+\Delta t}\|_{1,2nx}$

3.3 Dynamic model of Evaporator

In this section shell-and-tube evaporator model is presented. Differently from previous models here a change of phase of shell-side fluid occurs; in fact it enters the exchanger in liquid phase and it is extracted in saturated vapor condition. In this model fluid 2 is no more discretized in *nx* units, since it is considered to be all at the same temperature inside the exchanger.

Some assumptions are necessary in order to simplify the model:

- Thermodynamic properties of both the metal pipe and fluid 1 (hot fluid) are function of space (one-dimensional) and time;
- The conductive and radiative heat fluxes are neglected, only convection heat flux is considered for fluid 1 and nucleate boiling for fluid 2 (evaporating fluid);
- The exchanger is assumed to be adiabatic, hence heat losses are neglected;
- Pressure losses are neglected for both fluids;
- Fluid 2 is considered to be in perfect bi-phase equilibrium;
- Lumped thermal capacitance is assumed for pipe and the fluid 1;
- No mass storage is considered for fluid 1;
- Mass storage is considered for fluid 2;
- Energy storage is considered in metal pipe and both fluids.

Since the pipe is discretized in *nx* units also *nx* fictitious units of shell-side fluid are created; all at the same temperature. Fluid and pipe can now easily interface each other and calculate the *nx* heat fluxes exchanged as done in previous model. For shell side energy balance equations the *nx* heat fluxes are summed together in order to calculate the whole heat transferred from the pipe to evaporating fluid.
The figure 3.5 is presented to clarify how fluid and pipe *units* are connected to each other.

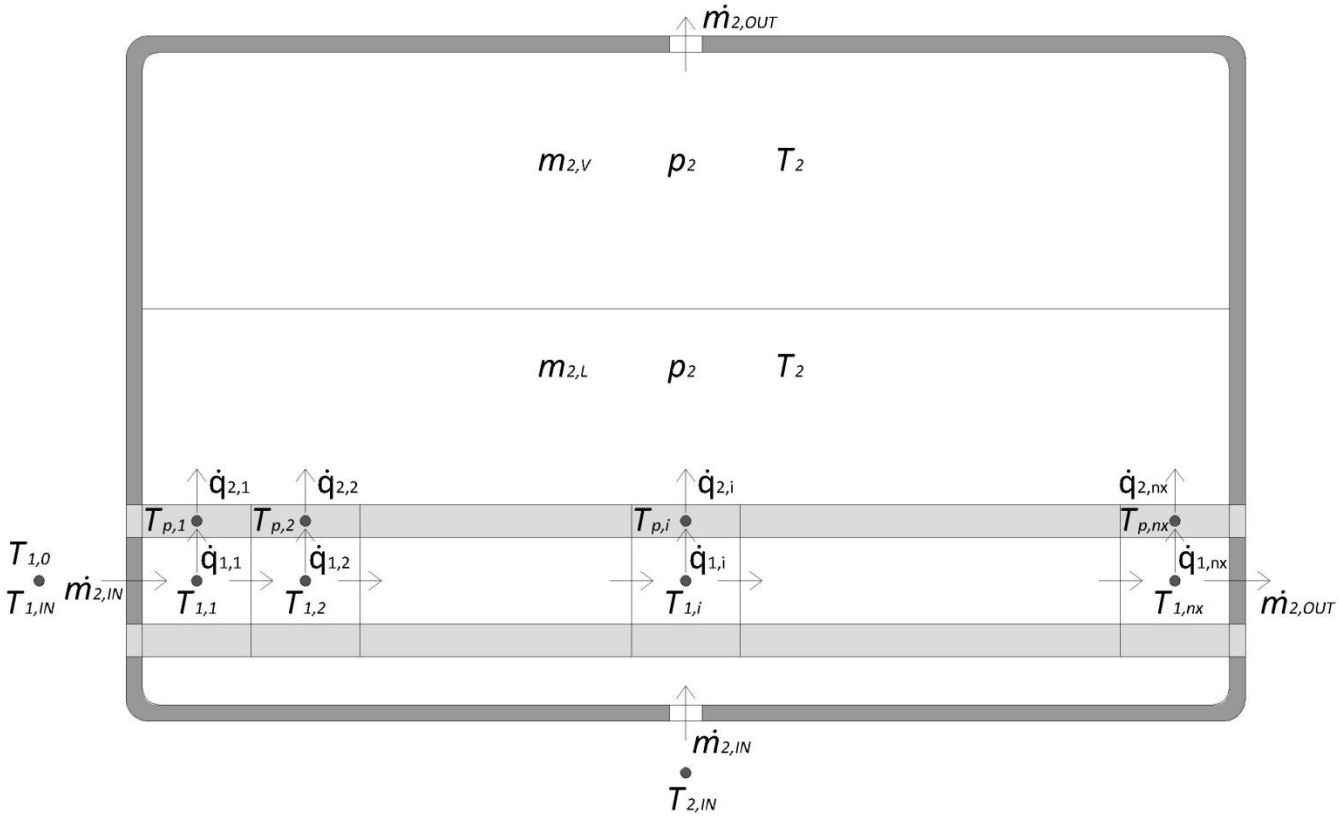

Figure 3.5 Discretization assumed for Shell&Tube evaporator, including convective heat fluxes involved.

Mass Balance equations

Mass balance of fluid 2 is performed by imposing that total mass at time $t+\Delta t$ is equal to the sum of total mass at time t and the integral of the difference of inlet and outlet mass flow rate for interval Δt.

$$\dot{m}_{1,i}^{t} = \dot{m}_{1,i-1}^{t} \qquad i=1:nx \qquad 3.65$$

$$m_{2,l}^{t+\Delta t} + m_{2,v}^{t+\Delta t} = m_{2,l}^{t} + m_{2,v}^{t} + \left(\dot{m}_{2,IN}^{t} - \dot{m}_{2,OUT}^{t}\right)\Delta t \qquad 3.66$$

Energy balance equations

Energy conservation for fluid 2 is obtained by imposing that total fluid internal energy at time $t+\Delta t$ is equal to the sum of total fluid internal energy at time t and the integral of inlet energy flow rate for time interval Δt.

$$\rho_{1,i}^{t}\, V_{1,i}\, c_{p,1,i}^{t}\, \frac{{T_{1,i}}^{t+\Delta t} - {T_{1,i}}^{t}}{\Delta t} = \dot{m}_{1,i}^{t}\, c_{p,1,i}^{t}\left(T_{1,i-1}^{t} - T_{1,i}^{t}\right) - \dot{q}_{CONV,1,i}^{t} \qquad i=1:nx \qquad 3.67$$

$$m_{2,l}^{t+\Delta t} u_{2,l}^{t+\Delta t} + m_{2,v}^{t+\Delta t} u_{2,v}^{t+\Delta t} = m_{2,l}^{t} u_{2,l}^{t} + m_{2,v}^{t} u_{2,v}^{t} + \left(\dot{m}_{2,IN}^{t} H_{2,IN}^{t} - \dot{m}_{2,OUT}^{t}\, H_{2,OUT}^{t} + \sum_{i=1}^{nx} \dot{q}_{CONV,2,i}^{t}\right)\Delta t \qquad 3.68$$

$$\rho_{p}\, V_{p,i}\, c_{p,p}\, \frac{{T_{p,i}}^{t+\Delta t} - {T_{p,i}}^{t}}{\Delta t} = \dot{q}_{CONV,1,i}^{t} - \dot{q}_{CONV,2,i}^{t} \qquad i=1:nx \qquad 3.69$$

Volume conservation

For shell-side fluid a further condition is imposed: the sum of liquid and vapor volumes of fluid 2 shall be equal to the global shell volume.

$$\frac{m_{2,l}^{t+\Delta t}}{\rho_{2,l}^{t+\Delta t}} + \frac{m_{2,v}^{t+\Delta t}}{\rho_{2,v}^{t+\Delta t}} = V_2 \qquad 3.70$$

State equations

$$c_{p,1,i}^{t} = f(T_{1,i}^{t}, p_{1,i}^{t}) \qquad i=1:nx \qquad 3.71$$

$$\rho_{1,i}^{t} = f(T_{1,i}^{t}, p_{1,i}^{t}) \qquad i=1:nx \qquad 3.72$$

For fluid 2 all thermodynamic properties can be determinate only from shell pressure, by imposing the value of vapor quality, due to the fact that perfect bi-phase equilibrium is considered.

$$u_{2,l}^{t} = f(p_2^t, x = 0) \qquad 3.73$$

$$u_{2,v}^{t} = f(p_2^t, x = 1) \qquad 3.74$$

$$T_{2,l}^{t} = f(p_2^t, x = 0) \qquad 3.75$$

$$H_{2,v}^{t} = f(p_2^t, x = 1) \qquad 3.76$$

$$\left(u_{2,l}^{t+\Delta t}, \rho_{2,l}^{t+\Delta t}\right) = f(p_2^{t+\Delta t}, x = 0) \qquad 3.77$$

$$\left(u_{2,v}^{t+\Delta t}, \rho_{2,v}^{t+\Delta t}\right) = f(p_2^{t+\Delta t}, x = 1) \qquad 3.78$$

Additional equations

$$p_{1,i}^{t} = p_{1,i-1}^{t} \qquad i=1:nx \qquad 3.79$$

$$\dot{q}_{CONV,1,i}^{t} = h_{1,i}^{t} A_{1,i} \left(T_{1,i}^{t} - T_{p,i}^{t}\right) \qquad i=1:nx \qquad 3.80$$

$$\dot{q}_{CONV,2,i}^{t} = h_{2,i}^{t} A_{2,i} \left(T_{p,i}^{t} - T_{2,l}^{t}\right) \qquad i=1:nx \qquad 3.81$$

$$A_{1,i} = (\pi\, ID\, L\, N_{tt})/nx \qquad i=1:nx \qquad 3.82$$

$$A_{2,i} = (\pi\, OD\, L\, N_{tt})/nx \qquad i=1:nx \qquad 3.83$$

$$V_{1,i} = \left(\frac{\pi\, ID^2}{4}\, N_{tt} L\right)/nx \qquad i=1:nx \qquad 3.84$$

$$V_2 = \left(\frac{\pi\, D_s^2}{4}\, L\right) - \left(\frac{\pi\, OD^2}{4}\, N_{tt} L\right) \qquad 3.85$$

$$V_{p,i} = \left[\frac{\pi\, (OD^2 - ID^2)}{4}\, N_{tt} L\right]/nx \qquad i=1:nx \qquad 3.86$$

$$h_{1,i}^{t} = f(\dot{m}_{1,i}^{t}, T_{1,i}^{t}, p_{1,i}^{t}, T_{p,i}^{t}, ID, L, N_{tt}, configuration) \qquad i=1:nx \qquad 3.87$$

$$h_{2,i}^{t} = f(T_{2,l,i}^{t}, T_{p,i}^{t}, OD, L, pitch, N_{tt}, layout, configuration) \qquad i=1:nx \qquad 3.88$$

Boundary conditions

$$\dot{m}_{1,0}^{t} = \dot{m}_{1,IN}^{t} \quad 3.89$$

$$\dot{m}_{1,OUT}^{t} = \dot{m}_{1,nx}^{t} \quad 3.90$$

$$p_{1,0}^{t} = p_{1,IN}^{t} \quad 3.91$$

$$p_{1,OUT}^{t} = p_{1,nx}^{t} \quad 3.92$$

$$p_{2,OUT}^{t} = p_{2}^{t} \quad 3.93$$

$$p_{2,IN}^{t} = p_{2}^{t} \quad 3.94$$

$$T_{1,0}^{t} = T_{1,IN}^{t} \quad 3.95$$

$$T_{1,OUT}^{t} = T_{1,nx}^{t} \quad 3.96$$

$$H_{2,OUT}^{t} = H_{2,v}^{t} \quad 3.97$$

N° of equations: 14*nx*+21

N° of fixed parameters: 12

N° variables: 16*nx*+30

N° of independent variables: 2*nx*+9

N° of input variables: 6

N° of state variables: 2*nx*+3

The system can be solved at time *t* by imposing the value of the 2*nx*+10 independent variables, nevertheless the value of 7 independent variables is given by the 7 inputs at time *t.*
2*nx*+3 independent variables still exceeds the number of equations; they are the temperature vectors of pipe and fluid *1* at time *t* and pressure, liquid mass and vapor mass of fluid *2* at time *t*.
The value of state variables at *t* is known by the simulation at time *t-Δt*. To start the simulation at *t=0* an initial solution of the state variables is necessary.
Variables and parameters involved in the system are here listed:

Table 3.3 Variables and Parameters involved in evaporator dynamic model

Variables and Parameters of simulation at instant t			
Fixed parameters	***Input variables***	***State variables***	***Output variables***
OD	$\dot{m}_{1,IN}^{t}$	$T_1^t\|_{1,nx}$	$\dot{m}_{1,OUT}^{t}$
ID	$p_{1,IN}^{t}$	$T_p^t\|_{1,nx}$	$p_{1,OUT}^{t}$
pitch	$T_{1,IN}^{t}$	$m_{2,l}^{t}$	$T_{1,OUT}^{t}$
D_S	$\dot{m}_{2,IN}^{t}$	$m_{2,v}^{t}$	$p_{2,IN}^{t}$
L	$\dot{m}_{2,OUT}^{t}$	p_2^t	$p_{2,OUT}^{t}$
N_{tt}	$H_{2,IN}^{t}$		$H_{2,OUT}^{t}$
layout			$T_1^{t+\Delta t}\|_{1,nx}$
configuration			$T_p^{t+\Delta t}\|_{1,nx}$
ρ_p			$m_{2,l}^{t+\Delta t}$
$c_{p,p}$			$m_{2,v}^{t+\Delta t}$
nx			$p_2^{t+\Delta t}$
Δt			

For tube side fluid (fluid 1) the causality diagram is exactly the same of exchanger model; since they are modelled with the same differential equations. The shell side fluid causality diagram is different since 2 also mass balance equations are involved differential equations. Inlet and outlet mass flow rate are integrated in order to calculate the fluid mass in the evaporator at following time step of simulation; so they are both input signals of the component. Inlet pressure of fluid 2 is an input signal since it cannot impose shell-side fluid pressure, which is determined by equilibrium of the two phases in the component.

Figure 3.6 **Causality diagram of evaporator dynamic model.**

3.5 Dynamic model of Condenser

In this section shell-and-tube condenser model is presented. Model configuration and assumptions are the same of Evaporator model, so for such model only the system of equation are presented. In Condenser component the shell-side fluid enters as superheated vapor and leaves the component in saturated liquid conditions.

Model configuration is shown in figure 3.7:

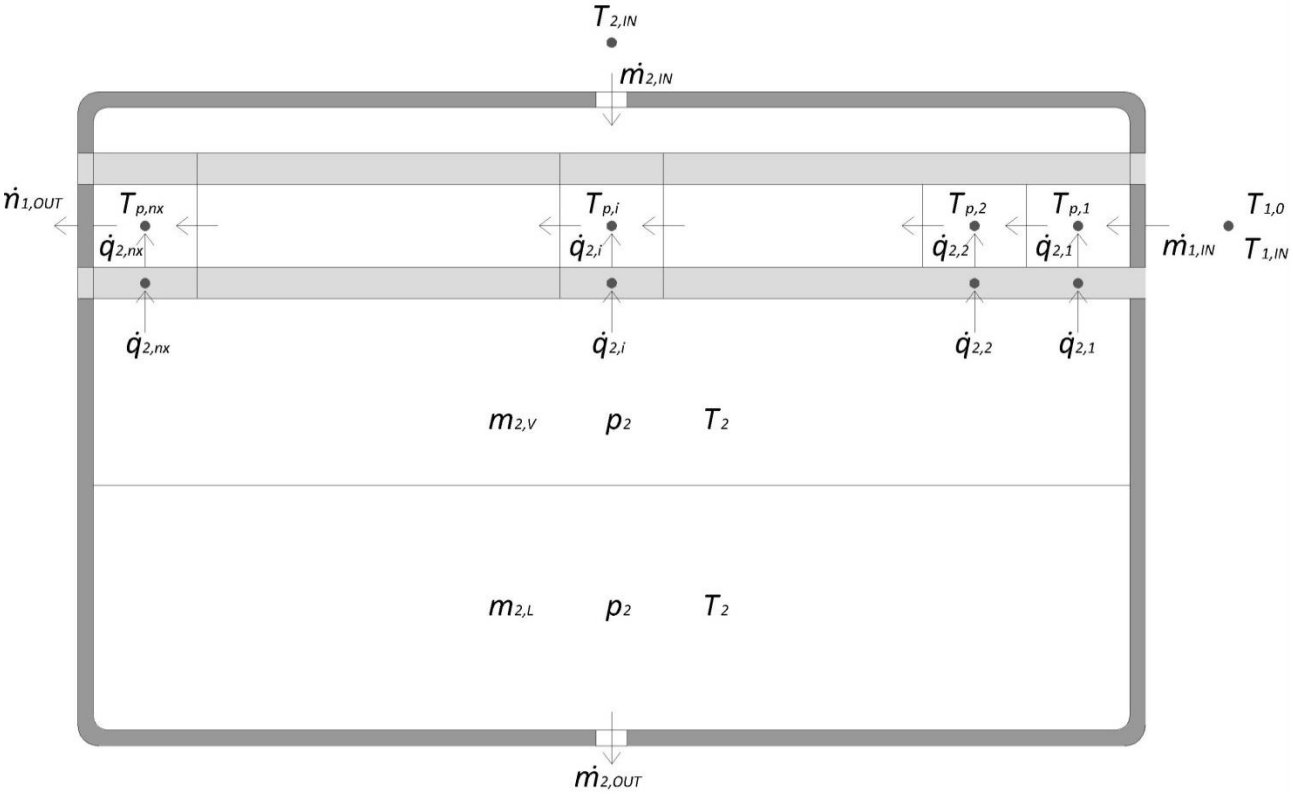

Figure 3.7 Discretization assumed for Shell&Tube condenser, including convective heat fluxes involved.

Mass Balance equations

$$\dot{m}_{1,i}^{t} = \dot{m}_{1,i-1}^{t} \qquad i=1:nx \quad 3.98$$

$$m_{2,l}^{t+\Delta t} + m_{2,v}^{t+\Delta t} = m_{2,l}^{t} + m_{2,v}^{t} + \left(\dot{m}_{2,IN}^{t} - \dot{m}_{2,OUT}^{t}\right)\Delta t \qquad i=1:nx \quad 3.99$$

Energy balance equations

$$\rho_{1,i}^{t}\, V_{1,i}\, c_{p,1,i}^{t}\, \frac{{T_{1,i}}^{t+\Delta t} - {T_{1,i}}^{t}}{\Delta t} = \dot{q}_{CONV,1,i}^{t} - \dot{m}_{1,i}^{t}\, c_{p,1,i}^{t}\, \left(T_{1,i-1}^{t} - T_{1,i}^{t}\right) \qquad i=1:nx \quad 3.100$$

$$m_{2,l}^{t+\Delta t} u_{2,l}^{t+\Delta t} + m_{2,v}^{t+\Delta t} u_{2,v}^{t+\Delta t} = m_{2,l}^{t} u_{2,l}^{t} + m_{2,v}^{t} u_{2,v}^{t} + \left(\dot{m}_{2,IN}^{t} H_{2,IN}^{t} - \dot{m}_{2,OUT}^{t}\, H_{2,OUT}^{t} - \sum_{i=1}^{nx} \dot{q}_{CONV,2,i}^{t} \right) \Delta t \qquad 3.101$$

$$\rho_{p}\, V_{p,i}\, c_{p,p}\, \frac{{T_{p,i}}^{t+\Delta t} - {T_{p,i}}^{t}}{\Delta t} = \dot{q}_{CONV,2,i}^{t} - \dot{q}_{CONV,1,i}^{t} \qquad i=1:nx \quad 3.102$$

Volume conservation

$$\frac{m_{2,l}^{t+\Delta t}}{\rho_{2,l}^{t+\Delta t}} + \frac{m_{2,v}^{t+\Delta t}}{\rho_{2,v}^{t+\Delta t}} = V_2 \qquad 3.103$$

State equations

$$c_{p,1,i}^{t} = f(T_{1,i}^{t}, p_{1,i}^{t}) \qquad i=1:nx \quad 3.104$$

$$\rho_{1,i}^{t} = f(T_{1,i}^{t}, p_{1,i}^{t}) \qquad i=1:nx \quad 3.105$$

$$u_{2,l}^{t} = f(p_2^{t}, x = 0) \qquad 3.106$$

$$u_{2,v}^{t} = f(p_2^{t}, x = 1) \qquad 3.107$$

$$T_{2,l}^{t} = f(p_2^{t}, x = 0) \qquad 3.108$$

$$H_{2,l}^{t} = f(p_2^{t}, x = 1) \qquad 3.109$$

$$\left(u_{2,l}^{t+\Delta t}, \rho_{2,l}^{t+\Delta t}\right) = f(p_2^{t+\Delta t}, x = 0) \qquad 3.110$$

$$\left(u_{2,v}^{t+\Delta t}, \rho_{2,v}^{t+\Delta t}\right) = f(p_2^{t+\Delta t}, x = 1) \qquad 3.111$$

Additional equations

$$p_{1,i}^{t} = p_{1,i-1}^{t} \qquad i=1:nx \quad 3.112$$

$$\dot{q}^t_{CONV,1,i} = h^t_{1,i} A_{1,i} \left(T^t_{1,i} - T^t_{p,i}\right) \quad i=1:nx \quad 3.113$$

$$\dot{q}^t_{CONV,2,i} = h^t_{2,i} A_{2,i} \left(T^t_{p,i} - T^t_{2,l}\right) \quad i=1:nx \quad 3.114$$

$$A_{1,i} = (\pi\, ID\, L\, N_{tt})/nx \quad i=1:nx \quad 3.115$$

$$A_{2,i} = (\pi\, OD\, L\, N_{tt})/nx \quad i=1:nx \quad 3.116$$

$$V_{1,i} = \left(\frac{\pi\, ID^2}{4}\, N_{tt} L\right)/nx \quad i=1:nx \quad 3.117$$

$$V_2 = \left(\frac{\pi\, D_s^2}{4}\, L\right) - \left(\frac{\pi\, OD^2}{4}\, N_{tt} L\right) \quad 3.118$$

$$V_{p,i} = \left[\frac{\pi\, (OD^2 - ID^2)}{4}\, N_{tt} L\right]/nx \quad i=1:nx \quad 3.119$$

$$h^t_{1,i} = f(\dot{m}^t_{1,i}, T^t_{1,i}, p^t_{1,i}, T^t_{p,i}, ID, L, N_{tt}, configuration) \quad i=1:nx \quad 3.120$$

$$h^t_{2,i} = f(T^t_{2,l,i}, T^t_{p,i}, OD, L, pitch, N_{tt}, layout, configuration) \quad i=1:nx \quad 3.121$$

Boundary equations

$$\dot{m}^t_{1,0} = \dot{m}^t_{1,IN} \quad 3.122$$

$$\dot{m}^t_{1,OUT} = \dot{m}^t_{1,nx} \quad 3.123$$

$$p^t_{1,0} = p^t_{1,IN} \quad 3.124$$

$$p^t_{1,OUT} = p^t_{1,nx} \quad 3.125$$

$$p^t_{2,OUT} = p^t_2 \quad 3.126$$

$$p^t_{2,IN} = p^t_2 \quad 3.127$$

$$T^t_{1,0} = T^t_{1,IN} \quad 3.128$$

$$T^t_{1,OUT} = T^t_{1,nx} \quad 3.129$$

$$H^t_{2,OUT} = H^t_{2,l} \quad 3.130$$

N° of equations: 14*nx*+21

N° of fixed parameters: 12

N° variables: 16*nx*+30

N° of independent variables: 2*nx*+9

N° of input variables: 6

N° of state variables: 2*nx*+3

Variables and parameters involved in the system are listed in table:

Table 3.4 Variables and Parameters involved in condenser dynamic model

Variables and Parameters of simulation at instant t			
Fixed parameters	***Input variables***	***State variables***	***Output variables***
OD	$\dot{m}_{1,IN}^{t}$	$T_1^t\vert_{1,nx}$	$\dot{m}_{1,OUT}^{t}$
ID	$p_{1,IN}^{t}$	$T_p^t\vert_{1,nx}$	$p_{1,OUT}^{t}$
pitch	$T_{1,IN}^{t}$	$m_{2,l}^{t}$	$T_{1,OUT}^{t}$
D_S	$\dot{m}_{2,IN}^{t}$	$m_{2,v}^{t}$	$p_{2,IN}^{t}$
L	$\dot{m}_{2,OUT}^{t}$	p_2^t	$p_{2,OUT}^{t}$
N_{tt}	$H_{2,IN}^{t}$		$H_{2,OUT}^{t}$
layout			$T_1^{t+\Delta t}\vert_{1,nx}$
configuration			$T_p^{t+\Delta t}\vert_{1,nx}$
ρ_p			$m_{2,l}^{t+\Delta t}$
$c_{p,p}$			$m_{2,v}^{t+\Delta t}$
nx			$p_2^{t+\Delta t}$
Δt			

The causality diagram is the same of Evaporator model, as the same differential equations characterized the two models.

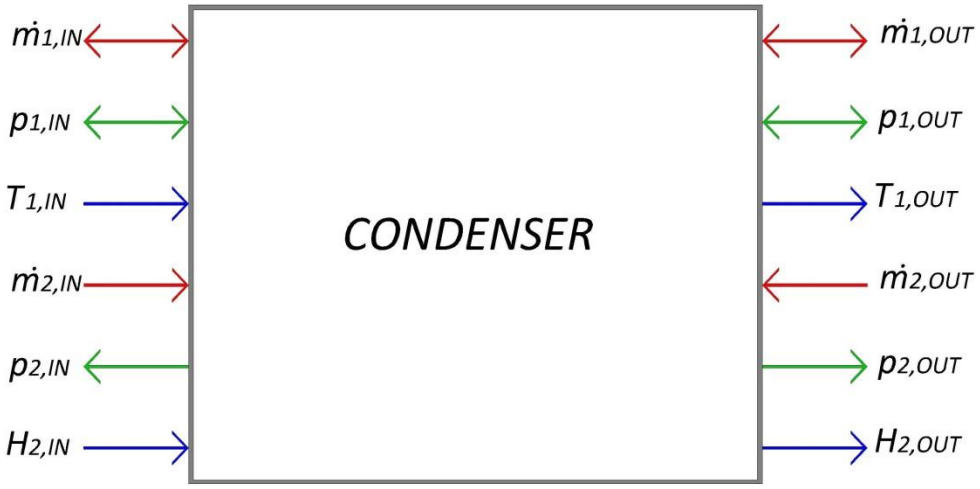

Figure 3.8 **Causality diagram of condenser dynamic model.**

3.6 Dynamic model of Turbine

Turbine model is here presented. As yet mentioned, for turbine and pump component, a quasi-steady state model has been used to describe the dynamic behavior. The dynamic response of these components is really faster compared to heat exchanger dynamics, thus resulting negligible.

Mass Balance equations

$$\dot{m}_{IN}^{t} = \dot{m}_{OUT}^{t} \qquad 3.131$$

Energy balance equations

For expander component, a variation of operating fluid energy flow is transferred to the shaft of the component as mechanical power. Fluid enthalpy drop is evaluated by inlet and outlet fluid pressure and expander isentropic efficiency.

$$\dot{m}_{IN}^{t}(H_{IN}^{t} - H_{OUT}^{t}) = P_{mec}^{t} \qquad 3.132$$

State equations

State equations leads to calculate inlet temperature, density and entropy from inlet pressure and enthalpy values. In particular inlet entropy s_{IN}^t is used to calculate the ideal value of outlet enthalpy $H_{OUT,is}^t$, when irreversibility is neglected. This represents the minimum value of outlet enthalpy that can be reached for the specific pressure drop.

$$[T_{IN}^t, \rho_{IN}^t, s_{IN}^t] = f(p_{IN}^t, H_{IN}^t) \quad 3.133$$

$$H_{OUT,is}^t = f(p_{OUT}^t, s_{IN}^t) \quad 3.134$$

Other Correlations

The elaborated mass flow rate is evaluated from input variables using "*Stodola*" equation [12]. The K parameter is provided by design model and it is proportional to flow inlet section of the component.

$$\dot{m}_{IN}^t = K \sqrt{\rho_{IN}^t \, p_{IN}^t \left[1 - \left(\frac{1}{\varepsilon^t}\right)^2\right]} \quad 3.135$$

$$\varepsilon^t = \frac{p_{IN}^t}{p_{OUT}^t} \quad 3.136$$

The outlet enthalpy is computed by mean of turbine isentropic efficiency $\eta_{is,T}^t$. It is defined as the ratio of effective enthalpy drop through the component and ideal enthalpy drop.

$$\eta_{is,T}^t = \frac{H_{IN}^t - H_{OUT}^t}{H_{IN}^t - H_{OUT,is}^t} \quad 3.137$$

$\eta_{is,T}^t$ at off-design conditions is calculated from the design value $\eta_{is,T,D}$ assuming a second degree dependence from the reduced mass flow rate $\dot{m}_R^t$; defined here below.

$$\eta_{is,T}^t = \eta_{is,T,D} \left[2\frac{\dot{m}_R^t}{\dot{m}_{R,D}} - \left(\frac{\dot{m}_R^t}{\dot{m}_{R,D}}\right)^2\right] \quad 3.138$$

$$\dot{m}_R^t = \frac{\dot{m}_{IN}^t \sqrt{T_{IN}^t}}{p_{IN}^t} \quad 3.139$$

The electric power extracted from the component is obtained by introducing the electric generator efficiency η_{GEN}.

$$P_{el}^{t} = P_{mec}^{t}\,\eta_{GEN} \qquad 3.140$$

Quasi-steady state model has been used, so no state-variable are necessary to perform the model. Output variables can thus be determinate directly from input variables by mean of algebraic equations.

- *N° of equations*: 12
- *N° of fixed parameters:* 4
- *N° variables*: 15
- *N° of independent variables:* 3
- *N° of input variables*: 3
- *N° of state variables:* 0

Variables and parameters involved in the system are listed in table 3.5:

Table 3.5 Variables and Parameters involved in turbine dynamic model

Variables and Parameters of simulation at instant t			
Fixed parameters	***Input variables***	***State variables***	***Output variables***
K	H_{IN}^{t}		$\dot{m}_{IN}^{t}$
$\dot{m}_{R,D}$	p_{IN}^{t}		$\dot{m}_{OUT}^{t}$
$\eta_{is,D}$	p_{OUT}^{t}		H_{OUT}^{t}
η_{GEN}			P_{el}^{t}

Turbine model is not modelled by mean of differential equation, as a quasi-steady state model is used; nevertheless the chosen characteristic laws chosen leads to define input and output signals of the turbine model:

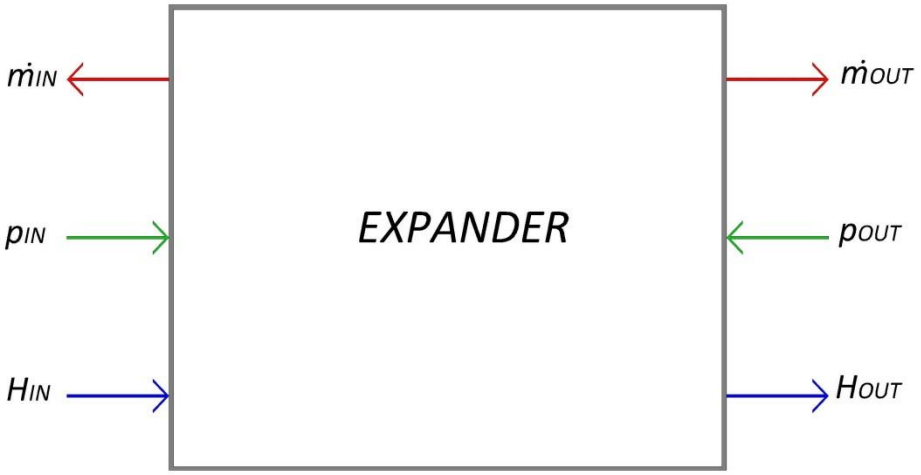

***Figure 3.9* Causality diagram of vapor expander dynamic model.**

3.7 Dynamic model of Pump

Pump model is here presented. This model is really similar to previous model configuration; nevertheless a tuning variable that allows controlling the component behavior is introduced. A variable rotational speed pump has been chosen for the model; allowing changing the characteristic curve in function of the rotational speed w^t.

Mass Balance equations

$$\dot{m}_{IN}^t = \dot{m}_{OUT}^t \qquad 3.141$$

Energy balance equations

$$\dot{m}_{IN}^t (H_{OUT}^t - H_{IN}^t) = P_{mec}^t \qquad 3.142$$

State equations

$$[\rho_{IN}^t, s_{IN}^t] = f(p_{IN}^t, H_{IN}^t) \qquad 3.143$$

$$[\rho_{OUT}^t] = f(p_{OUT}^t, H_{OUT}^t) \qquad 3.144$$

$$H_{OUT,is}^t = f(p_{OUT}^t, s_{IN}^t) \qquad 3.145$$

Other Correlations

The characteristic curve leads to calculate the process flow rate in off-design conditions. The curve is determinate by parameters ${y'}^t_D$, ${y'}^t_{0,D}$, ${\dot{V}'}^t_D$; which are function of design parameters y_D, y_0, $\dot{V}_D$ and the rotational speed.

$$y^t = \frac{{y'}^t_D - {y'}^t_{0,D}}{{\dot{V}'}^{t\,2}_D}\,\dot{V}^{t\,2} + {y'}^t_{0,D} \qquad 3.146$$

$$y^t = \frac{p^t_{OUT} - p^t_{IN}}{\rho^t_{IN}} \qquad 3.147$$

$$\dot{V}^t = \frac{\dot{m}^t_{IN}}{\rho^t_{IN}} \qquad 3.148$$

$${y'}^t_D = y_D \left(\frac{w^t}{w_D}\right)^2 \qquad 3.149$$

$${y'}^t_0 = y_0 \left(\frac{w^t}{w_D}\right)^2 \qquad 3.150$$

$${\dot{V}'}^t_D = \dot{V}_D \left(\frac{w^t}{w_D}\right) \qquad 3.151$$

$$\eta^t_{is,P} = \frac{H^t_{OUT,is} - H^t_{IN}}{H^t_{OUT} - H^t_{IN}} \qquad 3.152$$

The isentropic efficiency $\eta^t_{is,P}$ in off design conditions is computed assuming second degree dependence from processed flow rate.

$$\eta^t_{is,P} = 2\frac{\eta_{is,P,D}}{{\dot{V}'}^t_D}\dot{V}^t - \frac{\eta_{is,P,D}}{{\dot{V}'}^{t\,2}_D}\dot{V}^{t\,2} \qquad 3.153$$

$$P^t_{el} = P^t_{mec}\,\eta_{GEN} \qquad 3.154$$

- *N° of equations*: 15
- *N° of fixed parameters:* 6
- *N° variables*: 19

- *N° of independent variables:* 4
- *N° of input variables*: 4
- *N° of state variables:* 0

Table 3.6 Variables and Parameters involved in pump dynamic model

Variables and Parameters of simulation at instant t			
Fixed parameters	***Input variables***	***State variables***	***Output variables***
$\dot{V}_D$	H_{IN}^t		$\dot{m}_{IN}^t$
y_D	p_{IN}^t		$\dot{m}_{OUT}^t$
y_0	p_{OUT}^t		H_{OUT}^t
w_D	w^t		P_{el}^t
$\eta_{is,P,D}$			
η_{GEN}			

Differently for previous models here also a tuning variable is considered, the pump rotational speed *w*. The tuning variable in the diagram is marked with grey arrow and inlet direction:

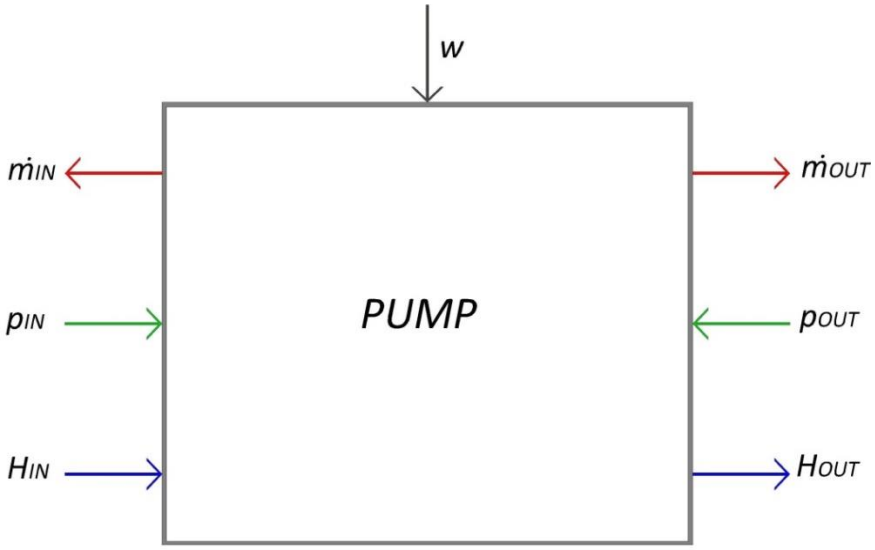

Figure 3.10 Causality diagram of pump dynamic model.

3.8 Dynamic model of Three Way Valve

Other two components are considered in off-design model: three way valve and mixer valve. These two components are not directly involved in the ORC system but they are used for system control. The three way valve split up the inlet fluid flow into two separates flows. Outlet flows has the same pressure and enthalpy of inlet fluid; only mass flow rate is split up and controlled by the parameter *k*; which defines valve opening:

$$\dot{m}_{1,OUT}^{t} = k^{t}\, \dot{m}_{IN}^{t} \qquad 3.155$$

$$\dot{m}_{2,OUT}^{t} = (1 - k^{t})\, \dot{m}_{IN}^{t} \qquad 3.156$$

As in previous model also for this component pressure losses are neglected, so pressure and temperature of both outlet flows are equal to inlet flow pressure and temperature.

$$p_{1,OUT}^{t} = p_{IN}^{t} \qquad 3.157$$

$$p_{2,OUT}^{t} = p_{IN}^{t} \qquad 3.158$$

$$T_{1,OUT}^{t} = T_{IN}^{t} \qquad 3.159$$

$$T_{2,OUT}^{t} = T_{IN}^{t} \qquad 3.160$$

As for pump model in this component a tuning variable is introduced, the *k* parameter of valve opening:

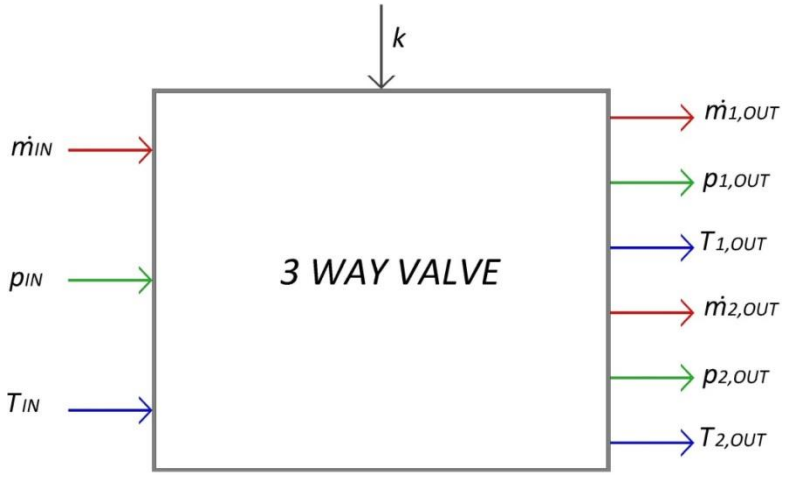

Figure 3.11 **Causality diagram of 3 way valve dynamic model.**

3.9 Dynamic model of Mixer Valve

In mixer valve, two inlet flows are mixed together into a unique outlet flow. This component is usually used in combination with a three way valve; performing a bypass system.

Outlet mass flow rate is the sum of the two inlet mass flow rates $\dot{m}_{1,IN}^{t}$ and $\dot{m}_{2,IN}^{t}$:

$$\dot{m}_{OUT}^{t} = \dot{m}_{1,IN}^{t} + \dot{m}_{2,IN}^{t} \qquad 3.161$$

The outlet pressure is the lower of the two inlet pressures:

$$p_{OUT}^{t} = min\,(p_{1,IN}^{t}, p_{2,IN}^{t}) \qquad 3.162$$

Outlet temperature (or enthalpy) is calculated by imposing the energy balance to the valve component:

$$\dot{m}_{1,IN}^{t}\,\bar{c}_{p,1}\left(T_{1,IN}^{t} - T_{OUT}^{t}\right) = \dot{m}_{2,IN}^{t}\,\bar{c}_{p,2}\left(T_{OUT}^{t} - T_{2,IN}^{t}\right) \qquad 3.163$$

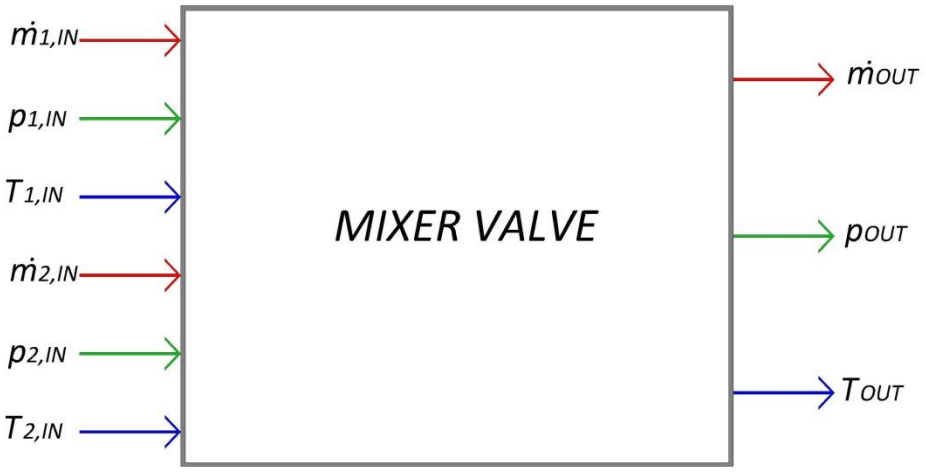

Figure 3.12 Causality diagram of mixer valve dynamic model.

Conclusions

In this chapter design model of components involved in an ORC system have been presented. The aim was to create general models of each component, which could be used also for studying different systems configurations or different applications. For each component fixed parameter and independent variables of the proposed dynamic model have been highlighted and listed. Causality diagrams of different components leads to understand how components can be connected together to create an organic Rankine cycle system model.

4. CASE STUDY

Introduction

In this chapter a realistic application of the dynamic model proposed in chapter 3 is presented. The aim of the chapter is to create an organic Rankine cycle dynamic model by mean of component models presented in chapter 3. In the first part the design of all components involved in the model is presented. In the second part the dynamic model of ORC system is tested for different simulations, in order to understand cycle behavior after variation of both hot and cold source.

4.1 ORC system design

The ORC dynamic model is applied to a realistic case. The studied case refers to a glass industry application, which is a typical application for Organic Rankine Cycle systems. The exhausted gasses are cooled down by mean of a recovery heat exchanger where thermal oil is heated up until a temperature of 300°C. The ORC receives the hot oil and cool it down until a temperature of 150°C. This temperature is the lowest temperature that the thermal oil can reach in order to avoid acid condensation risk in heat recovery exchanger. Nevertheless the oil temperature has not be higher than 150°C otherwise the thermal oil would not recover all design heat flow from exhausted gases; since the heat recovery exchanger is considered designed for the specified temperature drop (300°C – 150°C). The considered cold source is a cooling tower system, which provides to cool down the outlet water from the ORC condenser. Heat recovery exchanger and cooling tower are not considered in the model, only ORC system is modelled.
The first step is to design the ORC cycle; the chosen operating fluid is cyclopenthane, as suggested by Pierobon at al. [4] for a waste heat recovery system having similar characteristics.
Design specifications of both hot and cold source for the case study are presented in table 4.1.

Table 4.1 Hot and cold source design specifications

HOT SOURCE		
Fluid		Thermal_Oil
Mass Flow Rate	[kg/s]	58.80
Pressure	[bar]	5
Inlet Temperature	[°C]	300.0
Outlet Temperature	[°C]	150.0

COLD SOURCE		
Fluid		Water
Mass Flow Rate	[kg/s]	281.10
Pressure	[bar]	3
Inlet Temperature	[°C]	20.0
Outlet Temperature	[°C]	33.0

Thermodynamic cycle design model presented in chapter 2 is applied; results are presented in table 4.2.

Table 4.2 Thermodynamic cycle design; including intensive variables of each state point.

ORC		
Mass Flow Rate	[kg/s]	34.26
Turbine Isentropic Efficiency	#	0.85
Pump Isentropic Efficiency	#	0.70
Regenerator Efficiency	#	0.60
Generator Efficiency	#	0.96
ΔTap	[°C]	55
ΔTpp1	[°C]	23
ΔTpp2	[°C]	10
State point 1		
Pressure	[bar]	28.0
Temperature	[°C]	245.0
Enthalpy	[kJ/kg]	688.3
Entropy	[kJ/kg-K]	1.57
State point 2		
Pressure	[bar]	0.8
Temperature	[°C]	144.2
Enthalpy	[kJ/kg]	537.8
Entropy	[kJ/kg-K]	1.64
State point 3		
Pressure	[bar]	0.8
Temperature	[°C]	77.8
Enthalpy	[kJ/kg]	430.1
Entropy	[kJ/kg-K]	1.36
State point 4		
Pressure	[bar]	0.8
Temperature	[°C]	41.5
Enthalpy	[kJ/kg]	-14.8
Entropy	[kJ/kg-K]	-0.05
State point 5		
Pressure	[bar]	28.0
Temperature	[°C]	43.2
Enthalpy	[kJ/kg]	-9.4
Entropy	[kJ/kg-K]	-0.04
State point 6		
Pressure	[bar]	28.0
Temperature	[°C]	96.3
Enthalpy	[kJ/kg]	98.3
Entropy	[kJ/kg-K]	0.27
State point 7		

Pressure	[bar]	28.0
Temperature	[°C]	203.4
Enthalpy	[kJ/kg]	380.5
Entropy	[kJ/kg-K]	0.94
State point 8		
Pressure	[bar]	28.0
Temperature	[°C]	203.4
Enthalpy	[kJ/kg]	575.2
Entropy	[kJ/kg-K]	1.35

ORC PERFORMANCE		
Net Power Producton	[kW]	4767
Recover Efficiency	#	1.000
ORC efficiency	#	0.236
χ	#	0.236

The thermodynamic cycle can is represented in entropy-temperature diagram in figure 4.1. Hot and cold source are added in order to show thermal coupling between organic fluid and the two heat sources:

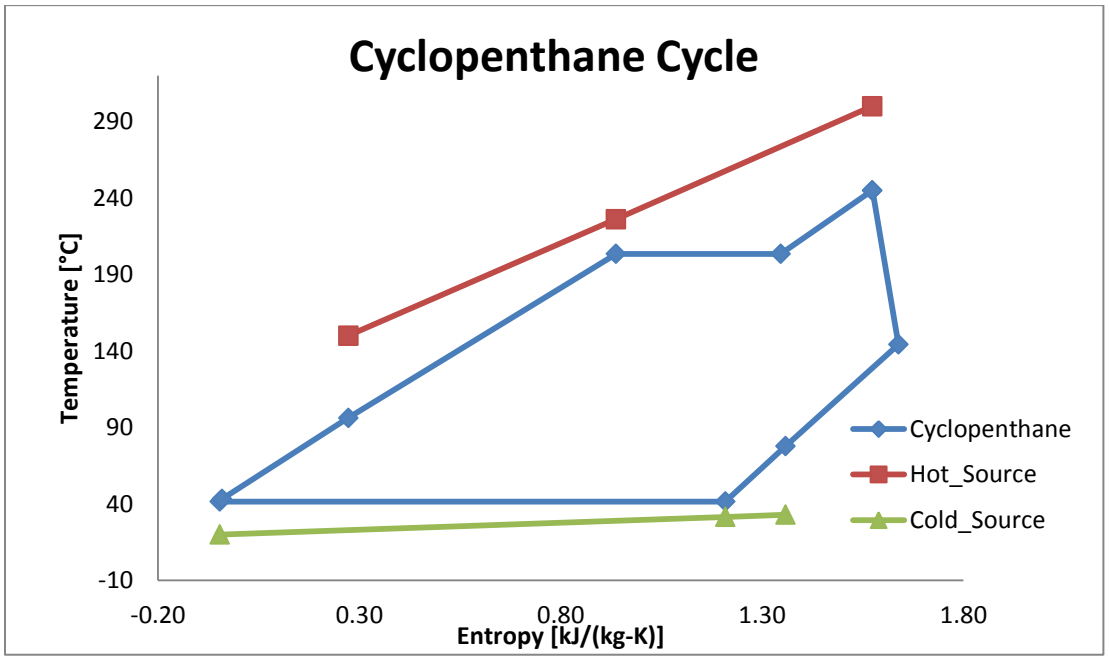

Figure 4.1 **Cyclopenthane thermodynamic cycle at design conditions.**

4.2 Components design

In this section the design of components involved in the system is presented. In thermodynamic cycle the economizer is considered heating the organic fluid received from regenerator until liquid saturation conditions; before entering the evaporator. In real application vapor creation inside the economizer in off-design conditions is to avoid; so the organic fluid comes out the component in condition of subcooled liquid.

Fluid velocity is limited up to 2 m/s for liquids, in fact over this value pressure losses become too relevant even if they are neglected in the proposed heat exchanger model.

In economizer and superheater thermal oil flows on tube side, even if its pressure is lower than cyclopenthane pressure. This choice has been done only for a modelling purpose. In evaporator thermal oil flows through the tube bundle and in order to simplifying Simulink model implementation the same choice has been done also for other the two exchangers with whom evaporator is connected.

For regenerator exchanger the high pressure liquid phase cyclopenthane flows on tube side and vapor phase cyclopenthane on shell side; respecting typical exchanger design guidelines.

For economizer and regenerator exchanger a 2 shell side passes – 4 tube side passes (2-4n) configuration has been chosen in order to ensure a perfect turbulent flow for tube side fluid and a sufficient high temperature factor (F_t>0.7) [29]. Superheater exchanger is designed with a 1-2n configuration.

Excel datasheet have been created implementing components design models proposed in chapter 2. In "*Process*" inlet and outlet design conditions of both fluids are shown; they represent the input variables for design model. In "*Configuration*" table the choice of exchanger configuration and temperature factor are displayed. "*Tube Geometry*" and "*Shell Geometry*" shows all geometric parameters that lead to configure the component in the Simulink heat exchanger model. "*Heat transfer coefficient*" table shows the value of heat transfer coefficients for both tube and shell sides and the global heat transfer coefficient.

Heat transfer coefficients are calculated for the average fluid temperature inside exchanger. Nevertheless for Evaporator component, where boiling heat transfer coefficient is very sensitive to pipe temperature, a more complex calculation is performed. The exchanger is split up into 5 parts, considering the average tube-side fluid temperature for each part, and the boiling heat transfer coefficient is calculated for all 5 parts. The boiling heat transfer coefficient shown is the arithmetic mean of the 5 computed coefficients.

Table 4.3 Economizer design datasheet

PROCESS		
Tube Side		
Fluid	HOT	Thermal Oil
Mass Flow Rate	[kg/s]	58.5
Inlet Pressure	[bar]	5
Inlet Temperature	[°C]	217.9
Outlet Temperature (estimation)	[°C]	149.1
Shell Side		
Fluid	COLD	Cyclopen
Inlet Pressure	[bar]	28
Mass Flow Rate	[kg/s]	34.26
Inlet Temperature	[°C]	96.3
Outlet Temperature	[°C]	194.0

CONFIGURATION		
Configuration Choice	#	2-4n
Temperature Factor - Ft	#	0.73
Tube-Side Reynolds number	#	13110
Tube side average velocity	[m/s]	1.29

TUBE GEOMETRY		
External Tube Diameter (OD)	[mm]	15.875
Internal Tube Diameter (ID)	[mm]	12.57
Tube Length	[m]	7
Pitch Distance	[mm]	19.84
Layout	[°]	30.00
Number of Tubes	#	1624

SHELL GEOMETRY		
Baffle Inlet Spacing	[mm]	500
Baffle Outlet Spacing	[mm]	500
Baffle Spacing	[mm]	546
Baffle Cut (%)	#	23
Inside Shell diameter	[mm]	883
No of pairs of sealing strips	#	1

HEAT TRANSFER COEFFICIENT		
Internal Exchange Surface	[m2]	449
External Exchange Surface	[m2]	567
Shell-Side Heat Transfer Coefficient	[kW/m2-K]	2.09

Tube-Side Heat Transfer Coefficient	[kW/m2-K]	1.33
Shell-side Fouling Resistance	[m2*K/kW]	0.10
Tube-side Fouling Resistance	[m2*K/kW]	0.10
Global Heat Transfer Coefficient - K	[kW/m2*K]	0.61
Target Heat Flux	[kW]	8594
Effective Heat Flux	[kW]	9135
Over Design (%)	%	6.28%

Table 4.4 Superheater design datasheet

PROCESS		
Tube Side		
Fluid	HOT	Thermal Oil
Mass Flow Rate	[kg/s]	58.8
Inlet Pressure	[bar]	5
Inlet Temperature	[°C]	300.0
Outlet Temperature (estimation)	[°C]	273.9
Shell Side		
Fluid	COLD	Cyclopen
Inlet Pressure	[bar]	28
Mass Flow Rate	[kg/s]	34.26
Inlet Temperature	[°C]	203.4
Outlet Temperature	[°C]	245.0

CONFIGURATION		
Configuration Choice	#	1-2n
Temperature Factor - Ft	#	0.95
Tube-Side Reynolds number	#	27487
Tube side average velocity	[m/s]	1.20

TUBE GEOMETRY		
External Tube Diameter (OD)	[mm]	15.875
Internal Tube Diameter (ID)	[mm]	12.57
Tube Length	[m]	2
Pitch Distance	[mm]	19.84
Layout	[°]	30.00
Number of Tubes	#	963

SHELL GEOMETRY		
Baffle Inlet Spacing	[mm]	500

Baffle Outlet Spacing	[mm]	500
Baffle Spacing	[mm]	500
Baffle Cut (%)	#	23.00
Inside Shell diameter	[mm]	687.00
No of pairs of sealing strips	#	1.00

HEAT TRANSFER COEFFICIENT		
Internal Exchange Surface	[m2]	76
External Exchange Surface	[m2]	96
Shell-Side Heat Transfer Coefficient	[kW/m2-K]	2.22
Tube-Side Heat Transfer Coefficient	[kW/m2-K]	1.89
Shell-side Fouling Resistance	[m2*K/kW]	0.10
Tube-side Fouling Resistance	[m2*K/kW]	0.10
Global Heat Transfer Coefficient - K	[kW/m2*K]	0.74
Target Heat Flux	[kW]	3875
Effective Heat Flux	[kW]	4242
Over Design (%)	%	9.46%

Table 4.5 Regenerator design datasheet

PROCESS		
Tube Side		
Fluid	COLD	Cyclopen
Mass Flow Rate	[kg/s]	34.26
Inlet Pressure	[bar]	28
Inlet Temperature	[°C]	43.2
Outlet Temperature (estimation)	[°C]	96.1
Shell Side		
Fluid	HOT	Cyclopen
Inlet Pressure	[bar]	0.78
Mass Flow Rate	[kg/s]	34.26
Inlet Temperature	[°C]	144.2
Outlet Temperature	[°C]	77.8

CONFIGURATION		
Configuration Choice	#	2-4n
Temperature Factor - Ft	#	0.91
Tube-Side Reynolds number	#	60028
Tube side average velocity	[m/s]	1.91

TUBE GEOMETRY

External Tube Diameter (OD)	[mm]	15.875
Internal Tube Diameter (ID)	[mm]	12.57
Tube Lenght	[m]	8
Pitch Distance	[mm]	47.63
Layout	[°]	30.00
Number of Tubes	#	831

SHELL GEOMETRY		
Buffle Inlet Spacing	[mm]	2000
Buffle Outlet Spacing	[mm]	2000
Buffle Spacing	[mm]	2000
Buffle Cut (%)	#	23
Inside Shell diameter	[mm]	662
No of pairs of sealing strips	#	1

HEAT TRANSFER COEFFICIENT		
Internal Exchange Surface	[m2]	394
External Exchange Surface	[m2]	497
Shell-Side Heat Transfer Coefficient	[kW/m2-K]	0.50
Tube-Side Heat Transfer Coefficient	[kW/m2-K]	3.01
Shell-side Fouling Resistance	[m2*K/kW]	0.10
Tube-side Fouling Resistance	[m2*K/kW]	0.10
Global Heat Transfer Coefficient - K	[kW/m2*K]	0.38
Target Heat Flux	[kW]	3688
Effective Heat Flux	[kW]	4627
Over Design (%)	%	25.47%

Table 4.6 Evaporator design datasheet

PROCESS		
Tube Side		
Fluid	HOT	Thermal Oil
Mass Flow Rate	[kg/s]	58.5
Inlet Pressure	[bar]	5
Inlet Temperature	[°C]	273.86
Outlet Temperature (Estimation)	[°C]	217.91
Shell Side		
Fluid	COLD	Cyclopen
Mass Flow Rate	[kg/s]	34.26
Pressure	[bar]	28

Inlet Temperature	[°C]	194.00
Outlet Temperature	[°C]	203.43
Outlet Quality	#	1

TUBE GEOMETRY		
Tube External Diameter OD	[mm]	15.88
Tube Internal Diameter ID	[mm]	12.57
Tube Lenght	[m]	6.0
Pitch Distance	[mm]	19.84
Layout	[°]	30
Number of Tubes	#	769
Number of Passes	#	2.00
Reynolds Number	#	25578
Tube side average velocity	[m/s]	1.44

SHELL GEOMETRY		
Shell Volume	[m3]	2.20
Shell Internal Diameter Ds	[m]	0.68

GLOBAL HEAT TRANSFER COEFFICIENT		
External Exchange Surface	[m2]	230.11
Internal Exchange Surface	[m2]	182.25
Shell-Side Heat Transfer Coefficient	[kW/m2-K]	16.5
Tube-Side Heat Transfer Coefficient	[kW/m2-K]	1.92
Shell-side Fouling Resistance	[m2*K/kW]	0.10
Tube-side Fouling Resistance	[m2*K/kW]	0.10
Global Heat Transfer Coefficient - K	[kW/m2*K]	1.06
Target Heat Flux	[kW]	7742
Effective Heat Flux	[kW]	8630
Over_Design	[%]	0.11

Table 4.7 Condenser design datasheet

PROCESS		
Tube Side		
Fluid	#	Water
Mass Flow Rate	[kg/s]	280.37
Inlet Pressure	[bar]	3
Inlet Temperature	[°C]	20.0
Outlet Temperature	[°C]	33.0

Shell Side		
Fluid	#	Cyclopen
Mass Flow Rate	[kg/s]	34.26
Inlet Pressure	[bar]	0.78
Inlet Temperature	[°C]	77.8
Outlet Temperature	[°C]	41.5
Outlet Quality	#	0

FINNED TUBE GEOMETRY		
Tube External Diameter OD	[mm]	25.4
Root Diameter OD	[mm]	22.9
Tube Internal Diameter ID	[mm]	18.7
Fin Height	[mm]	1.25
Fin Thickness	[mm]	0.3
Number of Fins per inch	[fpi]	26
Tube Lenght	[m]	6.0
Pitch Distance	[mm]	31.75
Layout	[°]	30.00
Number of Fins per Tube	#	6141
Number of Tubes	#	1330
Fin Efficiency	#	0.83
Wall Efficiency	#	0.86
Number of Passes	#	2
Reynolds Number	#	32811
Tube side average velocity	[m/s]	1.54

SHELL GEOMETRY		
Shell Volume	[m3]	5
Shell Internal Diameter Ds	[m]	1.03

GLOBAL HEAT TRANSFER COEFFICIENT		
External Exchange Surface	[m2]	1842
Internal Exchange Surface	[m2]	469
Shell-Side Heat Transfer Coefficient	[kW/m2-K]	2.44
Tube-Side Heat Transfer Coefficient	[kW/m2-K]	6.88
Shell-side Fouling Resistance	[m2*K/kW]	0.10
Tube-side Fouling Resistance	[m2*K/kW]	0.10
Global Heat Transfer Coefficient - K	[kW/m2*K]	0.68
Target Heat Flux	[kW]	15240
Effective Heat Flux	[kW]	17516
Overdesign	%	0.15

Turbine and pump design models only provides the parameters necessary to Simulink model, as a complete design procedure is not considered for such components.

Table 4.8 Turbine design datasheet

PROCESS		
Fluid		Cyclopen
Mass Flow Rate	[kg/s]	34.26
Inlet Pressure	[bar]	28.00
Inlet Temperature	[°C]	245.0
Outlet Pressure	[bar]	0.78
DESIGN PARAMETERS		
Stodola equation coefficient - K	[m2]	0.00262
Reduced mass flow rate	[m s K^0.5]	0.00028
Isentropic Efficiency	#	0.85
Generator Efficiency	#	0.96

Table 4.9 Pump design datasheet

PROCESS		
Fluid		Cyclopen
Mass Flow Rate	[kg/s]	34.26
Inlet Pressure	[bar]	0.78
Inlet Enthalpy	[kJ/kg]	-15.0
Outlet Pressure	[kg/m3]	28.00
DESIGN PARAMETERS		
Inlet Flow Rate	[m3/s]	0.055
y	[kJ/kg]	4.37
y_0	[kJ/kg]	5.5
Rotational Speed (w)	[giri/min]	1500
Isentropic Efficiency	#	0.7
Electric Motor Efficiency	#	0.96

4.3 ORC dynamic model

After having defined the design of the single components the ORC dynamic model can be built. In chapter 3 the dynamic model of all components has been defined, providing also the causality diagram for each component. The causality diagram of the whole system can be realized by connecting causality diagrams of different components. When two components are connected together output signals of a component are input signals for the other component and vice-versa.
Moreover the number of tuning variables involved in the system determines the number of variables that can be controlled during simulation.
For the proposed ORC dynamic model three variables are controlled:

- Liquid level in kettle evaporator; the aim of this control is to maintain constant the liquid level in evaporator in order to avoid risk of completely empty the component.
- Turbine inlet temperature; in order to control superheating level.
- Thermal oil outlet temperature; control of this parameter is imposed by design specification.

Since three variables need to be controlled; three components that include tuning variables shall be involved in the system:

- Pump; the rotational speed of pump component leads to control liquid level in evaporator;
- Three way valve; a bypass of thermal oil mass flow rate flowing in superheter exchanger allows controlling turbine inlet temperature;
- Three way valve; a bypass of thermal oil mass flow rate flowing in economizer exchanger allows controlling thermal oil outlet temperature.

The control is performed by mean of PID controllers, which are already included in Simulink Library.
The causality diagram of the whole system is represented in figure 4.2:

- Red lines: mass flow rate;
- Green lines: pressure;
- Blue lines: temperature or enthalpy;
- Dashed line: tuning variable control.

Arrows direction defines input and output signals:

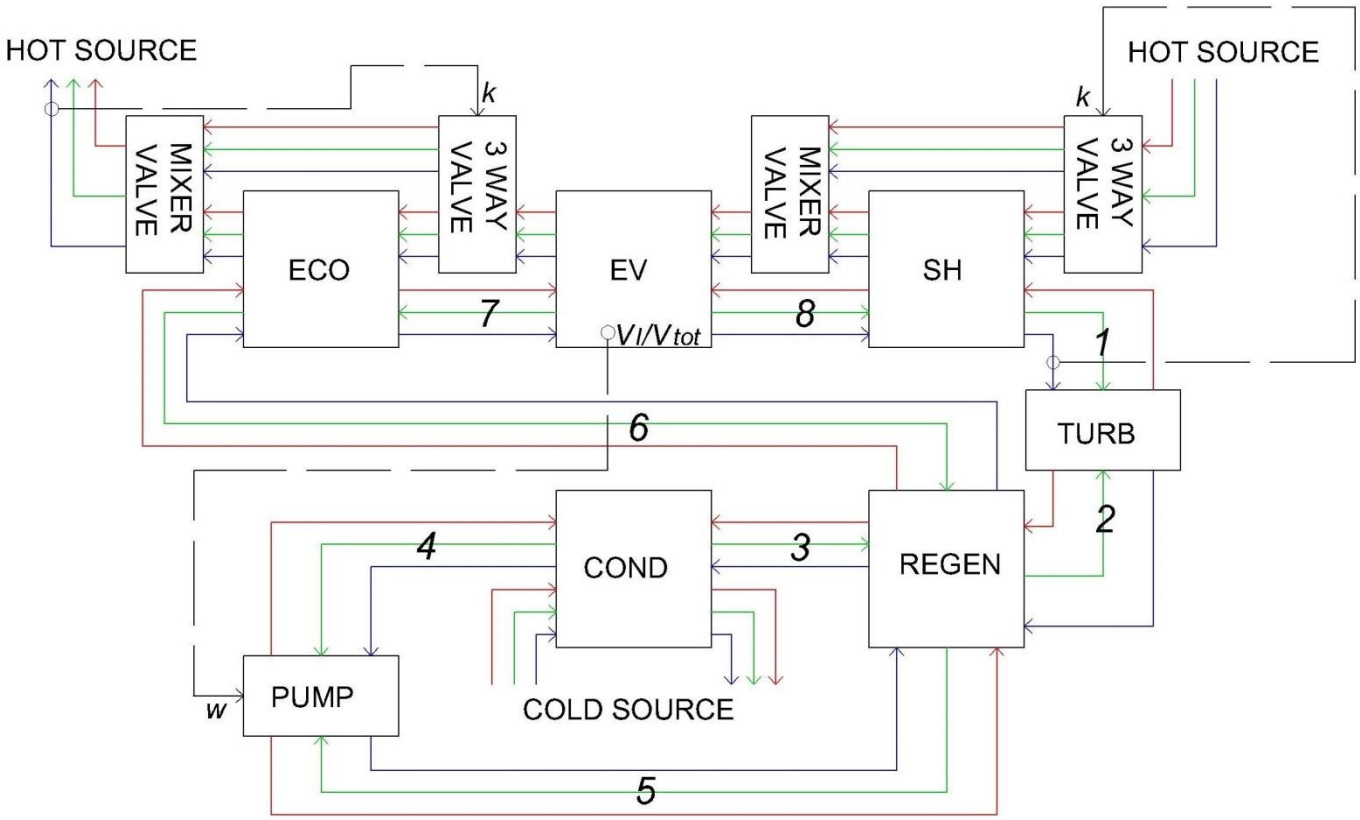

Figure 4.2 **Causality diagram of a regenerative superheated organic Rankine cycle, including control system**

In figure 4.2 the organic fluid flows are marked with a number, in accordance with cycle scheme of figure 2.1.

Two simulation tests have been performed in order to analyze how the system reacts to:

- Variation of hot source inlet mass flow rate;
- Variation of hot source cold source inlet temperature.

Both simulations have been performed considering:

- Time discretization Δt of 0.02 s;
- Axial discretization *nx* of 20 for Economizer, Regenerator and Superheater and 10 for Condenser and Evaporator.

4.4 Variation of hot source inlet mass flow rate

In this simulation only variation of hot source inlet mass flow rate is considered. At start time of simulation an initial solution of all state-variable involved in the model is provided so the model needs around 100 seconds to find the equilibrium of the whole system.

The evolution in time of the most important variables that describes the system is displayed:

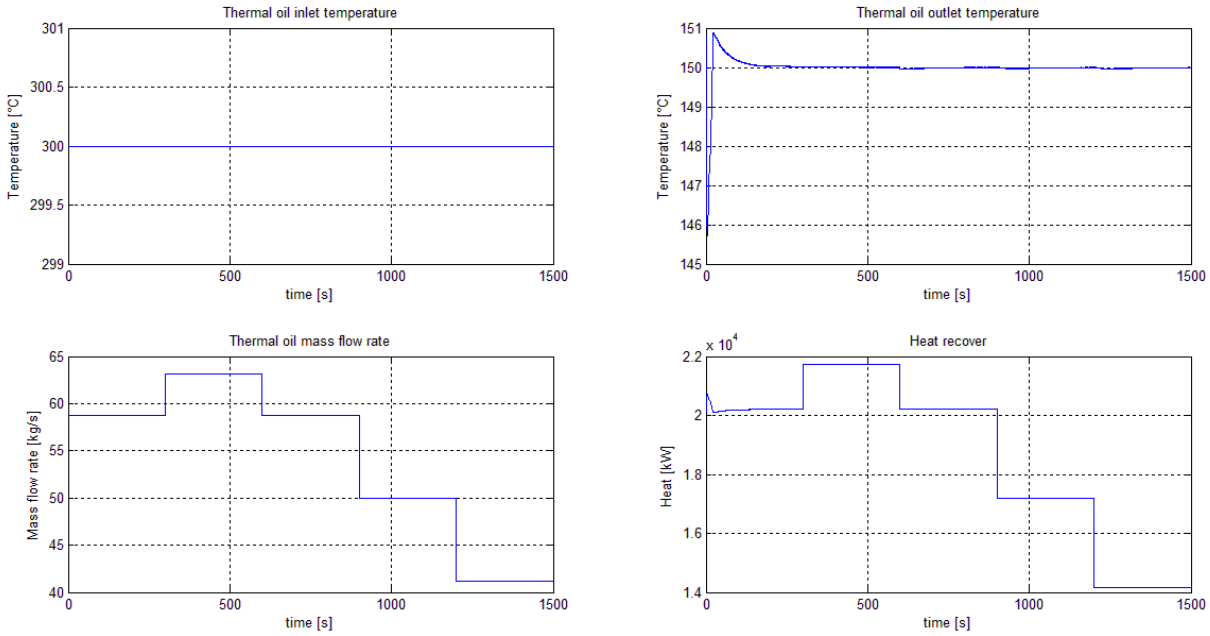

Figure 4.3 Hot source mass flow rate, inlet and outlet temperatures evolution in time

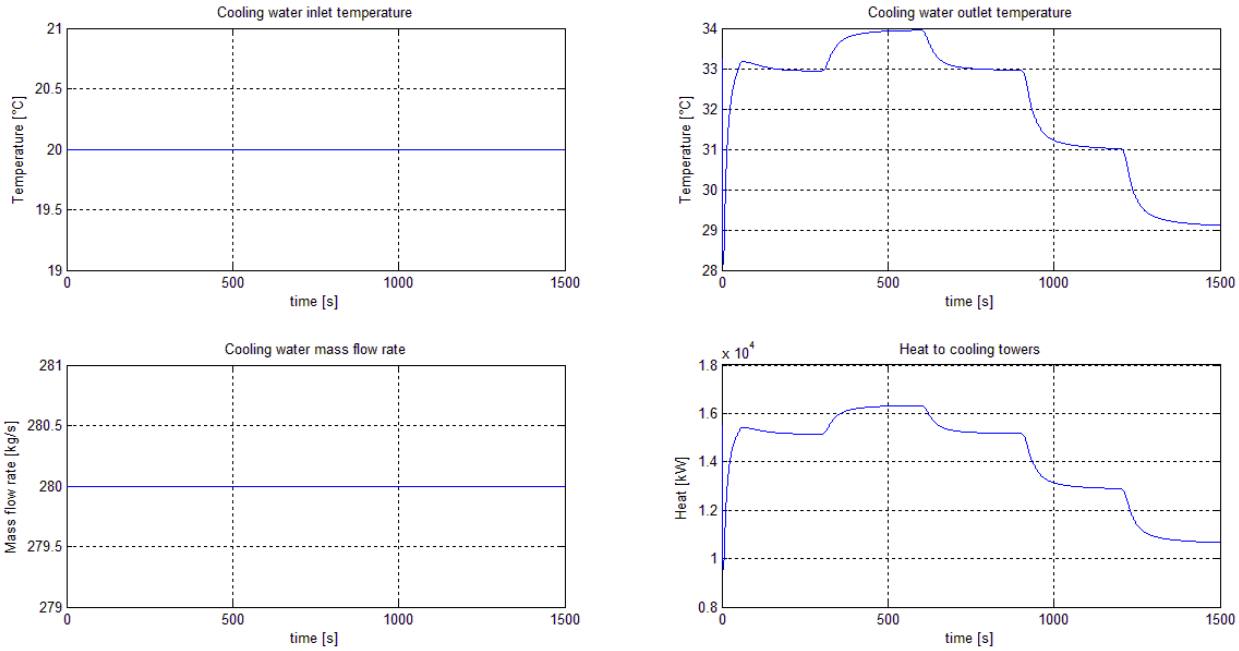

Figure 4.4 Cold source mass flow rate, inlet and outlet temperatures evolution in time

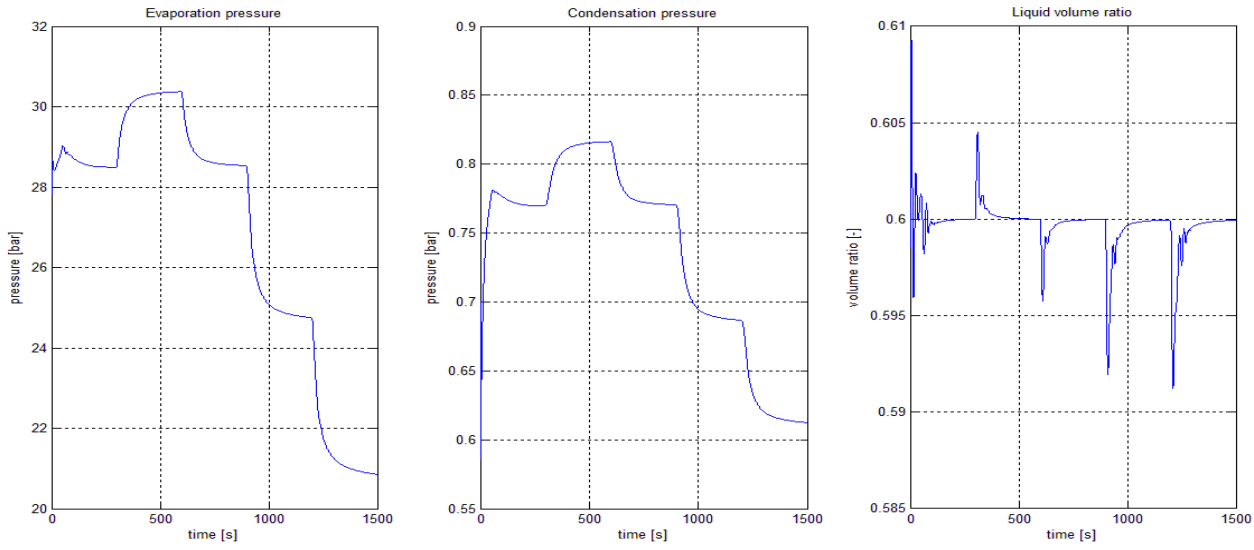

Figure 4.5 Evaporating pressure, condensing pressure and liquid volume ratio in evaporator evolution in time

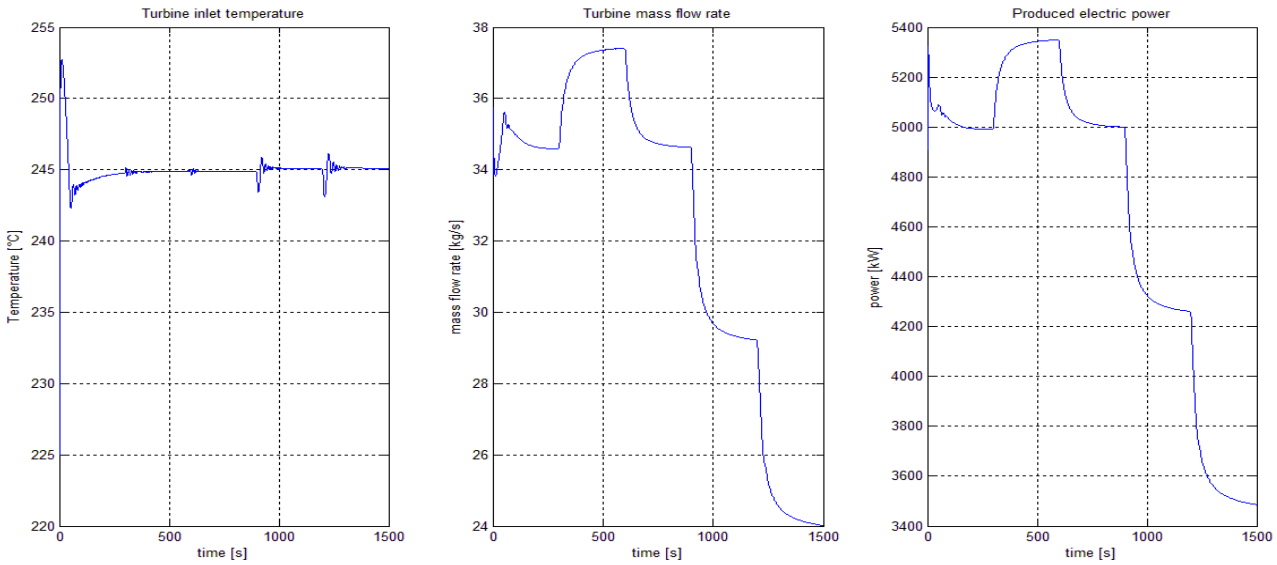

Figure 4.6 Turbine inlet temperature, mass flow rate and produced electric power evolution in time

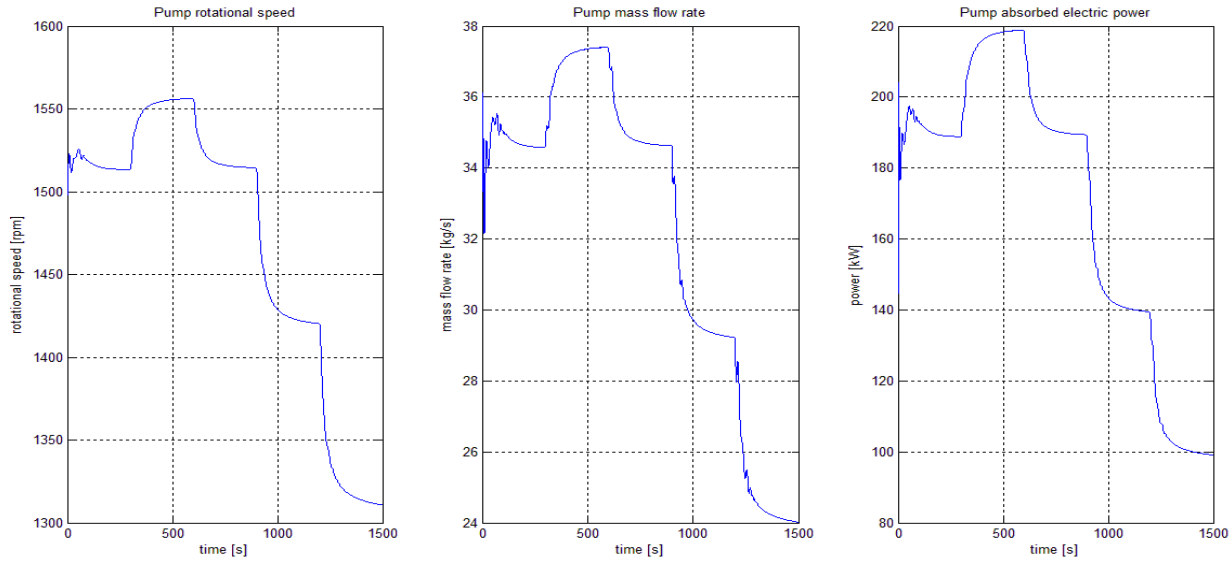

Figure 4.7 Pump rotational speed, mass flow rate and absorbed electric power evolution in time

The system is well controlled by mean of the three involved tuning variable.
When the hot source thermal input changes, the system finds the new equilibrium for a different evaporation pressure and so a lower mass flow rate processed by the turbine.
In evaporator component the liquid level is controlled by mean of pump component and the energy balance is performed by equation:

$$m_{2,l}^{t+\Delta t} u_{2,l}^{t+\Delta t} + m_{2,v}^{t+\Delta t} u_{2,v}^{t+\Delta t} = m_{2,l}^{t} u_{2,l}^{t} + m_{2,v}^{t} u_{2,v}^{t} + \left(\dot{m}_{2,IN}^{t} H_{2,IN}^{t} - \dot{m}_{2,OUT}^{t} H_{2,OUT}^{t} - \sum_{i=1}^{nx} \dot{q}_{CONV,2,i}^{t} \right) \Delta t$$

When the thermal oil mass flow rate increases also the term $\sum_{i=1}^{nx} \dot{q}_{CONV,2,i}^{t}$ is modified, and the new equilibrium is reached for an higher evaporating pressure value p_2^t and higher value of term $H_{2,OUT}^t$, since they are directly linked. Nevertheless a variation of p_2^t influences also $\dot{m}_{2,OUT}^t$, which is turbine processed mass flow rate, that varies in accordance with Stodola correlation.
Condensation pressure, when the cyclopenthane mass flow rate is increased/reduced, increases/decreases too. When the heat to dissipate is reduced, due to cold source modelling, the Condenser mean log temperature difference increases (water outlet temperature decreases) and the equilibrium condition is obtained for a lower cyclopenthane condensation pressure.
The dynamic model allows understanding the modification of the thermodynamic cycle during transient operation conditions. In figure 4.8 thermodynamic cycle modification during transient operation from 900s to 1100s at different time steps is presented. When the hot source mass flow rate decreases evaporating pressure decreases meanwhile inlet turbine temperature remains around of design value to control system. Condensing pressure is reduced, since cold source inlet temperature and mass flow rate are constant and heat to dissipate decreases.

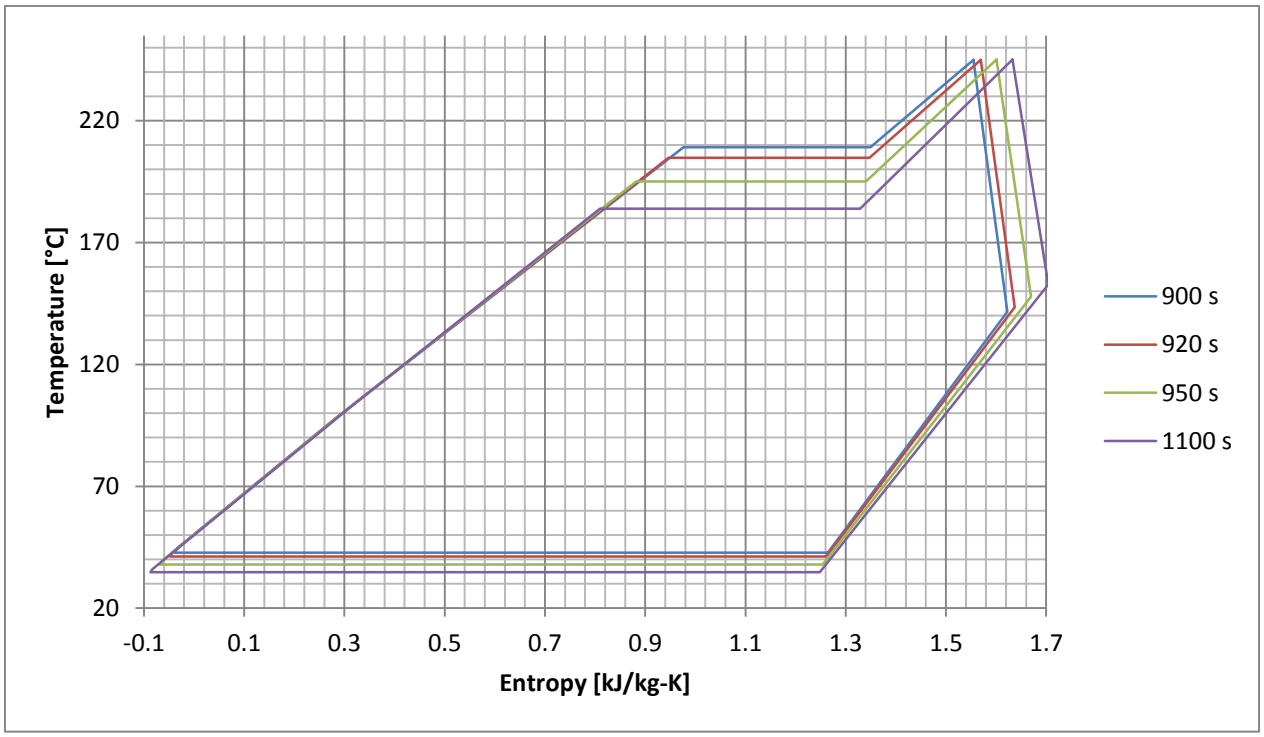

Figure 4.8 Thermodynamic cycle modification in transient operating conditions

In figure 4.9 thermodynamic cycles at different stable operating point conditions are represented.

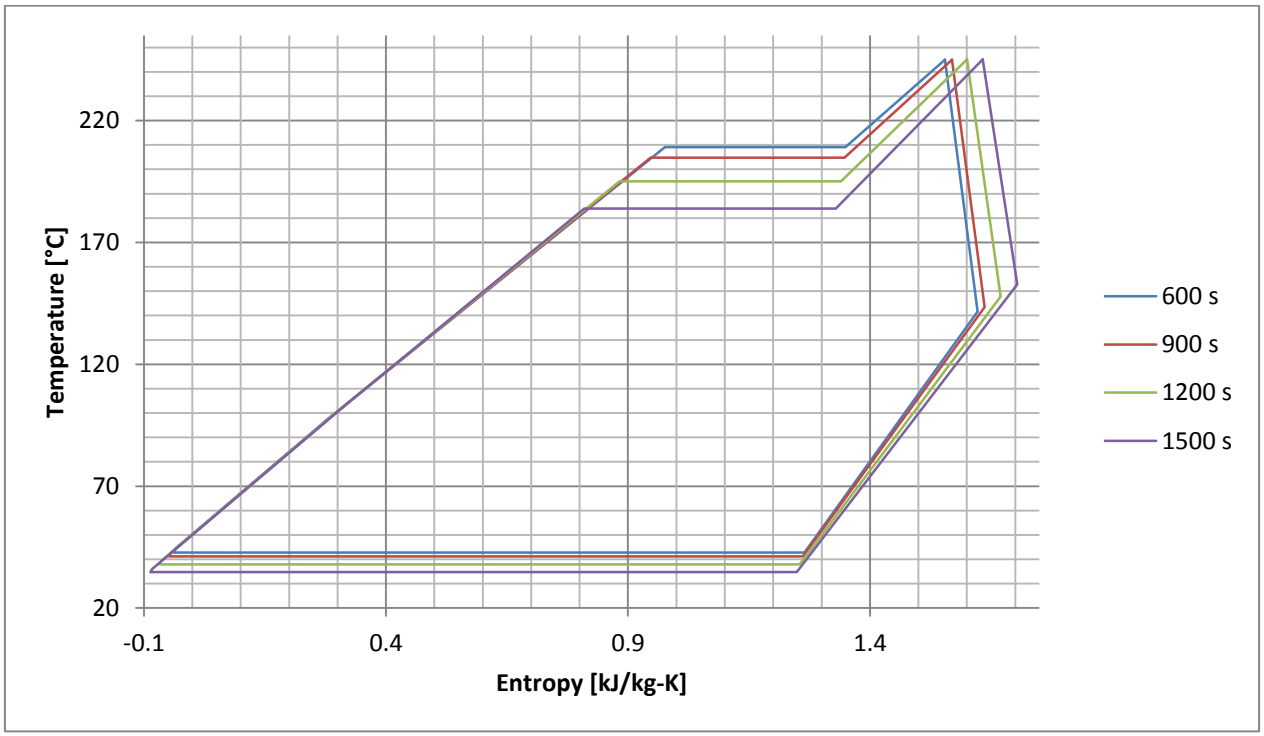

Figure 4.9 Thermodynamic cycle for different operating point

4.5 Variation of cold source inlet temperature

In this simulation only variation of could source inlet temperatures are considered.

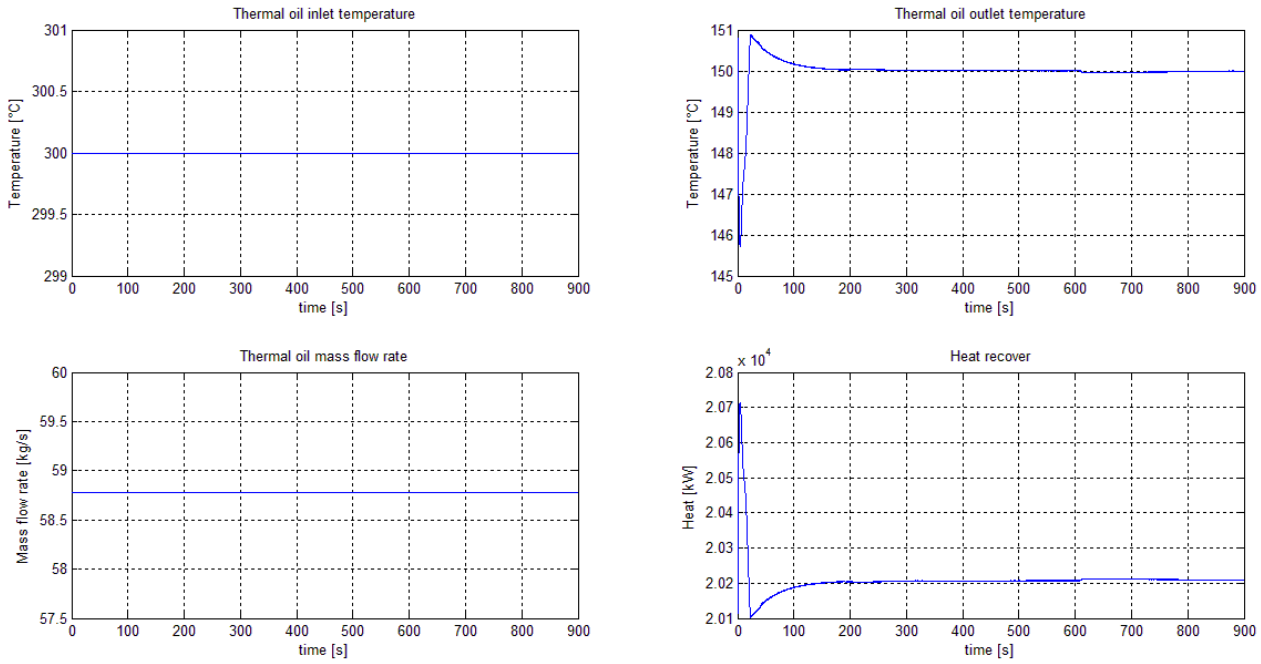

Figure 4.10 Hot source mass flow rate, inlet and outlet temperatures evolution in time

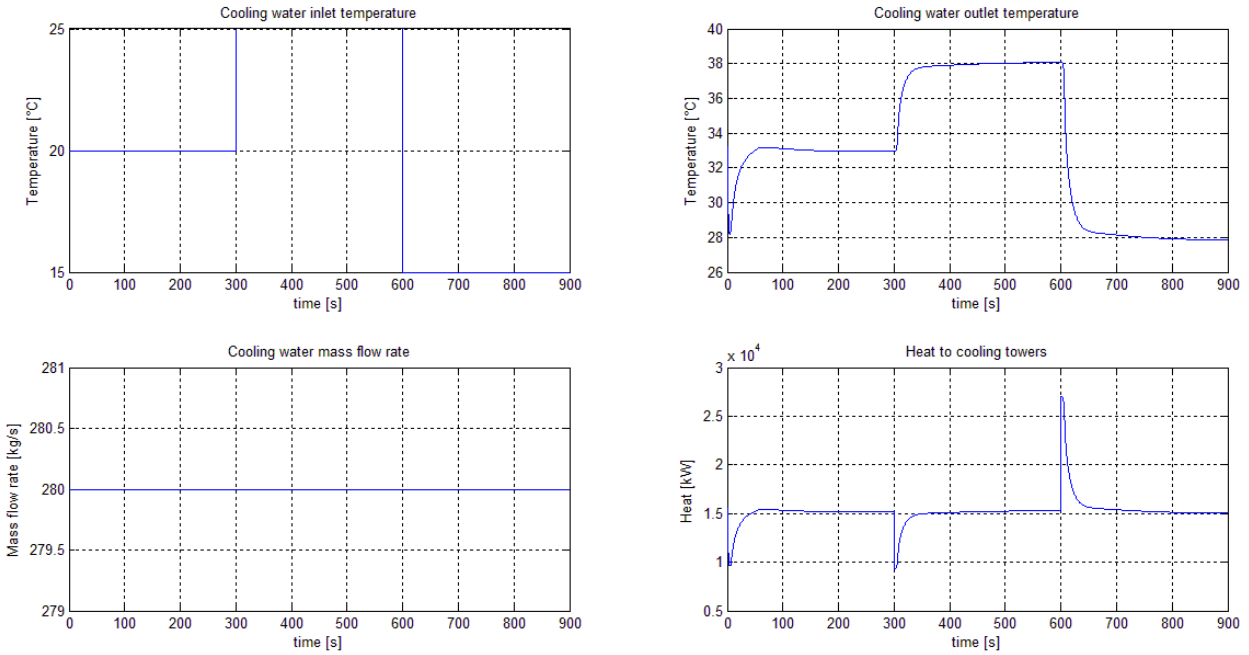

Figure 4.11 Cold source mass flow rate, inlet and outlet temperatures evolution in time

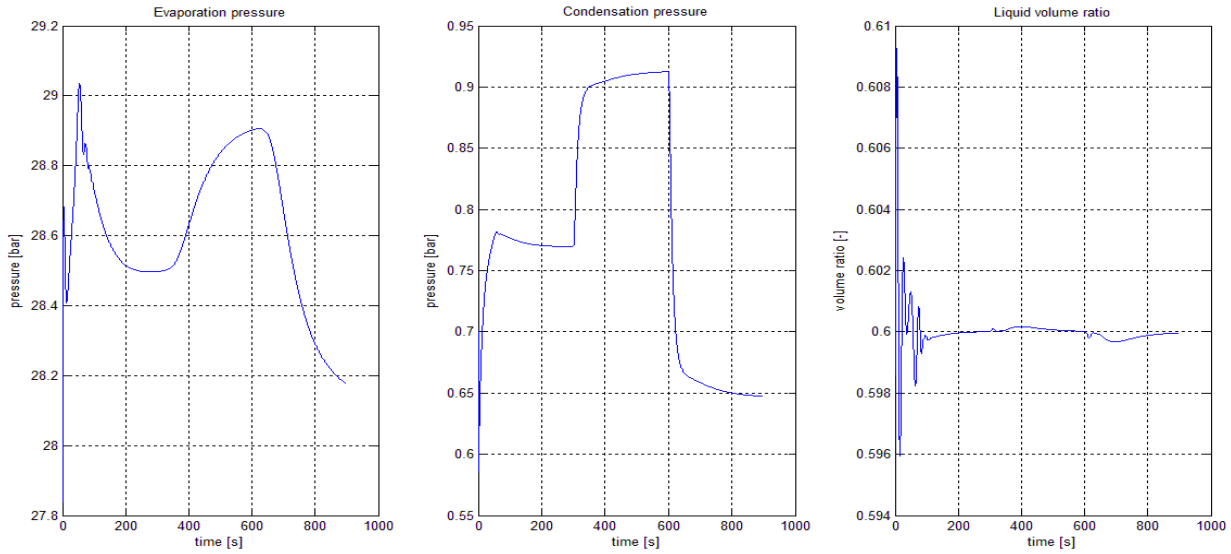

Figure 4.12 Evaporating pressure, condensing pressure and liquid volume ratio in evaporator evolution in time

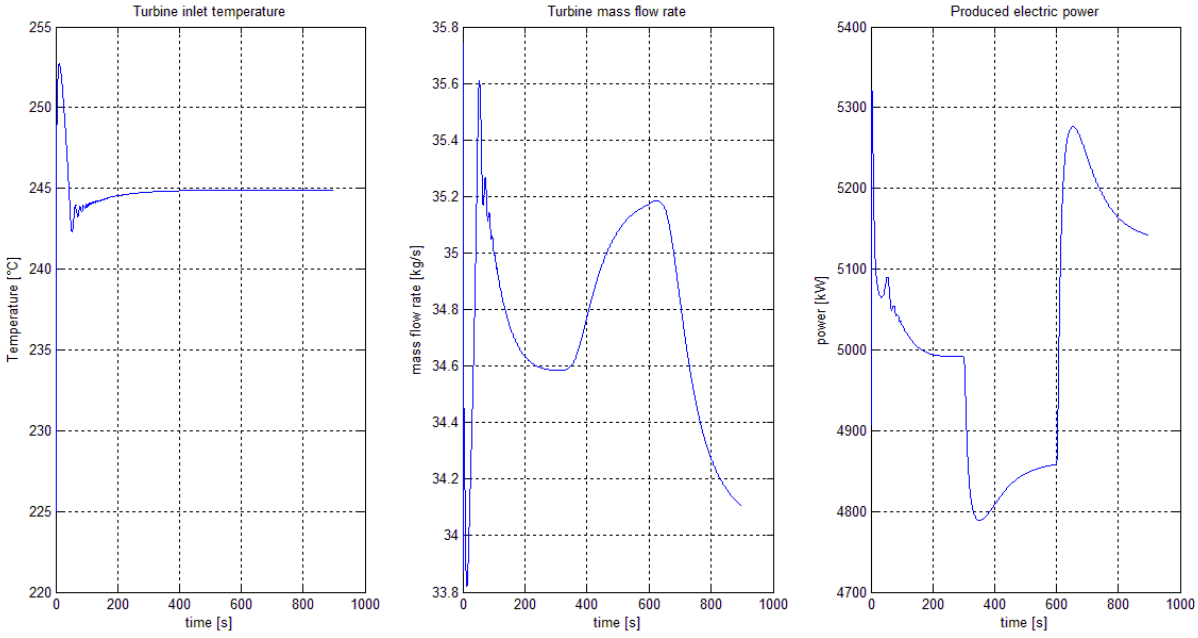

Figure 4.13 Turbine inlet temperature, mass flow rate and produced electric power evolution in time

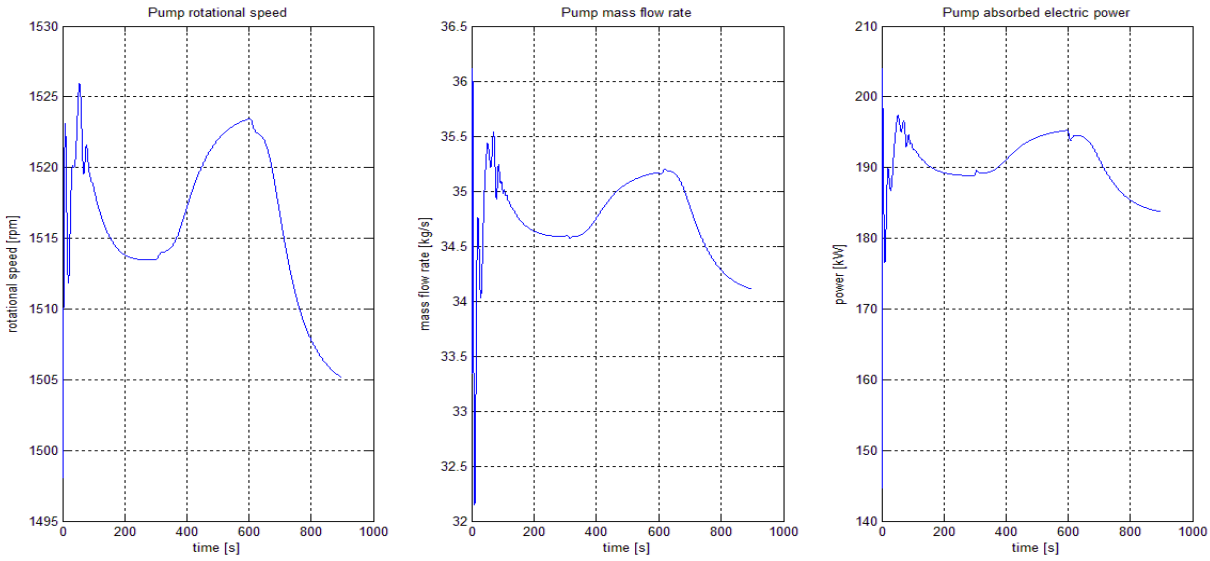

Figure 4.14 Pump rotational speed, mass flow rate and absorbed electric power evolution in time

In figure 4.15 thermodynamic cycles at different stable operating point conditions are represented.

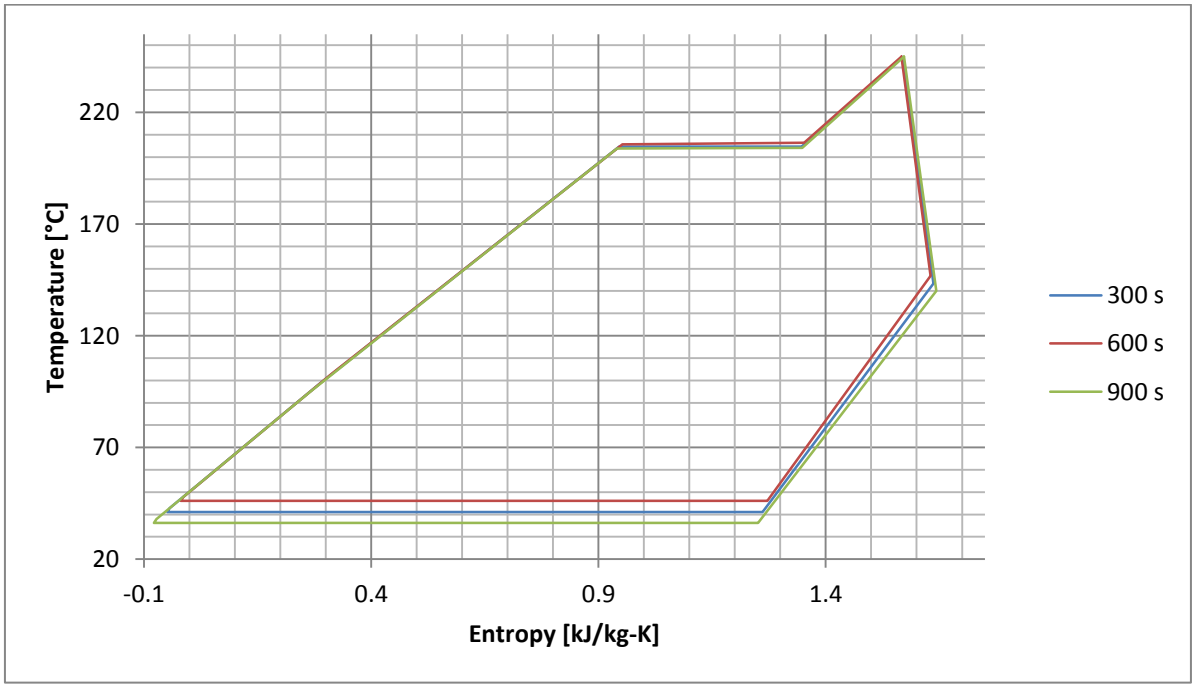

Figure 4.15 Thermodynamic cycle for different operating point

When cold source temperature increase or decrease, influnces mainly condensing pressure evolution in time. Evaporating pressure is not much influenced since hot source remains unchanged.

Conclusions

In this chapter a realistic application of the ORC dynamic model has been presented. Different simulations have been performed, analyzing the evolution in time of such variables that allow defining system performances. The gross electric power produced in five different steady state conditions has been compared with data available from a plant with the same characteristics of the case study; obtaining a difference lower than 1,3% in four cases and of around 5% in one case. A PID control system has been implemented, resulting suitable for the purpose.

CONCLUSIONS

In this work the off-design dynamic model of an organic Rankine cycle systems has been presented. Usually in off-design model of power cycles only fluid machines behavior is considered, by mean of characteristic curves. In this model also off-design model of shell-and-tube heat exchangers has been consider in order to evaluate realistic mass and thermal inertias of the system. A PID control system has been implemented, resulting suitable for the purpose. The proposed model can be tested for different control systems in order to evaluate the optimal control strategy for the ORC system.

REFERENCES

1- Toffolo A., Lazzaretto A., Manente G., Paci M., *A multi-criteria approach for the optimal selection of working fluid and design parameters in Organic Rankine Cycle systems*, Applied Energy (2014) 219-232.

2- Guo T., Wang H.X., Zhang S.J., *Selection of working fluids for a novel low-temperature geothermally-powered ORC based cogeneration system*, Energy Conversion and Management 52 (2011) 2384-2391.

3- Wang E.H., Zhang H.G., Fan B.Y., Ouyang M.G., Zhao Y., Mu Q.H., *Study of working fluid selection of organic Rankine cycle (ORC) for engine waste heat recovery*, Energy 36 (2011) 3406-3418).

4- Pierobon L., Nguyen T., Larsen U., Haglind F., Elmegaard, *Multi-objective optimization of organic Rankine cycles for waste heat recovery: Application in an offshore plant*, Energy 58 (2013) 538-549.

5- Branchini L., De Pascale A., Peretto A., *Systematic comparison of ORC configurations by means of comprehensive performance index,* Applied Thermal Engineering 61 (2013) 129-140.

6- Wang J., Yan Z., Wang M., Ma S., Dai Y., *Thermodynamic analysis and optimization of an (organic Rankine cycle) ORC using low grade heat source*, Energy 49 (2013), 356-365.

7- Sun J., Li W., *Operation optimization of an organic rankine cycle (ORC) heat recovery power plant*, Applied Thermal Engineering 31 (2011) 2032-2041.

8- Calise F., Capuozzo C., Carotenuto A., Vanoli L., *Thermoeconomic analysis and off-design performance of an organic Rankine cycle powered by medium temperature heat sources*, Solar Energy (2013)

9- Quolin S., Aumann R., Grill A., Schuster A., Lemort V., Spliethoff H., *Dynamic modeling and optimal control strategy of waste heat recovery Organic Rankine Cycles*, Applied Energy 88 (2011) 2183-2190

10- Xie H., Yang C., *Dynamic behavior of Rankine cycle system for waste heat recovery of heavy duty diesel engines under driving cycle*, Applied Energy 112 (2013) 130-141

11- Zhang J., Zhang W., Hou G., Fang F., *Dynamic modeling and multivariable control of organic Rankine cycles in waste heat untilizing processes*, Computers and Mathematics with Application 64 (2012), 908-921

12- Vaja J, *Definition of an object oriented library for the dynamic simulation of advanced energy systems: methodologies, tools and application to combined ICE-ORC power plant*, phD thsesis, Industrial engineering department, Università degli Studi di Parma, Italy, 2009.

13- Quolin S., Van Den Broek M., Declaye S., Dewallef P., Lemort V., *Techno-economic survey of Organic Rankine Cycle (ORC) systems*, Renewable and Sustainable Energy Reviews 22 (2013) 168-186.

14- Vélez F., Segovia J., Martìn M., Antolìn G., Chejne F., Quijano A., *A techical, economical and market review of organic Rankine cycles for the conversion of low-grade heat for power generation*, Renewable and Sustainable Energy Reviews 16 (2012) 4175-4189.

15- Campana F., Bianchi M., Branchini L., De Pascale A., Peretto A., Baresi M., Fermi A., Rossetti N., Vescovo R., *ORC waste heat recovery in European energy intensive industries, Energy and GHG savings*, Energy Conversion and Management 76 (2013) 244-252.

16- Chen Q., Xu J., Chen H., *A new design method for Otganic Rankine Cycles with constrain of inlet and outlet heat carrier fluid temperatures coupling with the heat source*, Applied Energy 98 (2012) 562-573.

17- Hajabdollahi Z., Hajadbollahi F., Tehrani M., Hajadbollahi H.*; Thermo-economic environmental optimization of Organic Rankine Cycle for diesel waste heat recovery*, Energy 63 (2013) 142-151

18- Fernàndez F.J., Prieto M.M., Suàrez I., *Thermodynamic analysis of high-temperature regenerative organic Rankine cycles using siloxanes as working fluids*, Energy 36 (2011) 5239-5249

19- Vélez F., Segovia J., Martìn M., Antolìn G., Chejne F., Quijano A., *Comparative study of working fluids for Rankine cycle operating at low temperature*, Fuel Processing Technology 103 (2012) 71-77.

20- Kang S.H., *Design and experimental study of ORC (organic Rankine cycle) and radial turbine using R245fa working fluid*, Energy 41 (2012) 514-524.

21- Algieri A., Morrone P., *Comparative energetic analysys of high-temperature subcritical and transcritical Organic Rankine Cycle (ORC). A biomass application in the Sibari district*, Applied Thermal Engineering 36 (2012) 236-244.

22- Manente G., Toffolo A., Lazzaretto A., Paci M., *An Organic Rankine Cycle off-design model for search the optimal control strategy*, Energy 58 (2013) 97-106.

23- Casella F., Mathijssen T., Colonna P., *Dynamic Modeling of Organic Rankine Cycle Power Systems*, Journal of Engineering for Gas Turbines and Power 135 (2013).

24- Kim E., Yoshida T., Yashiki T., *Dynamic Heat-Exchanger Model for Any Combination of Water and Steam States*, Journal of Engineering for Gas Turbines and Power 135 (2013).

25- Jia X., Tso C.P., Chia P.K., *A distributed model for prediction of the transient response of an evaporator*, Int. J. Refrig. 18 (1995) 336-342.

26- Cooke D.H., *On Prediction of Off-Design Multistage Turbine Pressures by Stodola's Ellipse*, Journal of Engineering for Gas Turbines and Power 107 (1985) 596-601

27- Gyarmathy G., Ortmann P., *The off-design of single-and dual pressure steam cycles in CC plants*, Asme Cogen-Turbo IGTI 6 (1991) 271-279.

28- Wei D., Lu X., Lu Z., Gu J.,*Performance analysis and optimization of organic Rankine cycle (ORC) for waste heat recovery*, Energy Conversion and Management 48 (2007) 1113-1119.

29- Serth R., *Process Heat Transfer, principles and applications*, Elsevier, 2007

30- Stoecker W.F., *Design of Thermal Systems*, McGraw-Hill,1989.

31- Burmeister L.C., *Elements of Thermal-Fluid System Design*, Prentice Hall, 1988.

APPENDIX 1

Temperature factor correlations

Temperature factor is a key parameter in heat exchangers design.

Temperature factor leads to calculate the effective log mean temperature difference ΔT_{ml}, introducing the deviation from perfect countercurrent log mean temperature difference $\Delta T_{ml,cc}$.

Temperature factor is defined as the ratio between ΔT_{ml} and the equivalent ΔT_{ml} for a perfect countercurrent exchanger process with the same value of input and output temperatures of the two fluids involved in the process ($\Delta T_{ml,CC}$):

$$F_t = \frac{\Delta T_{ml}}{\Delta T_{ml,CC}} \qquad \text{A. 1}$$

Log mean temperature difference is very easy to calculate for a perfect countercurrent configuration:

$$\Delta T_{ml,CC} = \frac{\left(T_{IN}^{hot} - T_{OUT}^{cold}\right) - \left(T_{OUT}^{hot} - T_{IN}^{cold}\right)}{log\left[\left(T_{IN}^{hot} - T_{OUT}^{cold}\right)/\left(T_{OUT}^{hot} - T_{IN}^{cold}\right)\right]} \qquad \text{A. 2}$$

$\Delta T_{ml,cc}$ represents the maximum driving force temperature for this process.

Empirical correlations lead to calculate the value of F_t by knowing inlet and outlet design temperatures of both shell-side and tube-side fluid. In particular, in literature, charts and correlations are available for several different configurations; allowing the calculation of F_t as function of parameters *R* and *S*, defined by equations A.3 and A.4:

$$R = \frac{T_{IN}^{shell} - T_{OUT}^{shell}}{T_{OUT}^{tube} - T_{IN}^{tube}} \qquad \text{A. 3}$$

$$S = \frac{T_{OUT}^{tube} - T_{IN}^{tube}}{T_{IN}^{shell} - T_{IN}^{tube}} \qquad \text{A. 4}$$

In exchanger model presented in chapter 2, only three possible configurations are considered; so F_t correlations are presented only for these configurations.
For perfect countercurrent configuration, F_t assumes unitary value, by definition.

For one shell-side pass, two tube-side passes configuration the empirical correlation for temperature factor is [29]:

$$F_{t,1,2} = \frac{\frac{\sqrt{R^2+1}}{R-1} \cdot log_{10}\left(\frac{1-S}{1-SR}\right)}{log_{10}\left(\frac{\left(\frac{2}{P}\right)-1-R+\sqrt{R^2+1}}{\left(\frac{2}{P}\right)-1-R-\sqrt{R^2+1}}\right)} \qquad A.\ 5$$

In the figure here below the value of $F_{t,1,2}$ is shown for discretized value of R parameter.

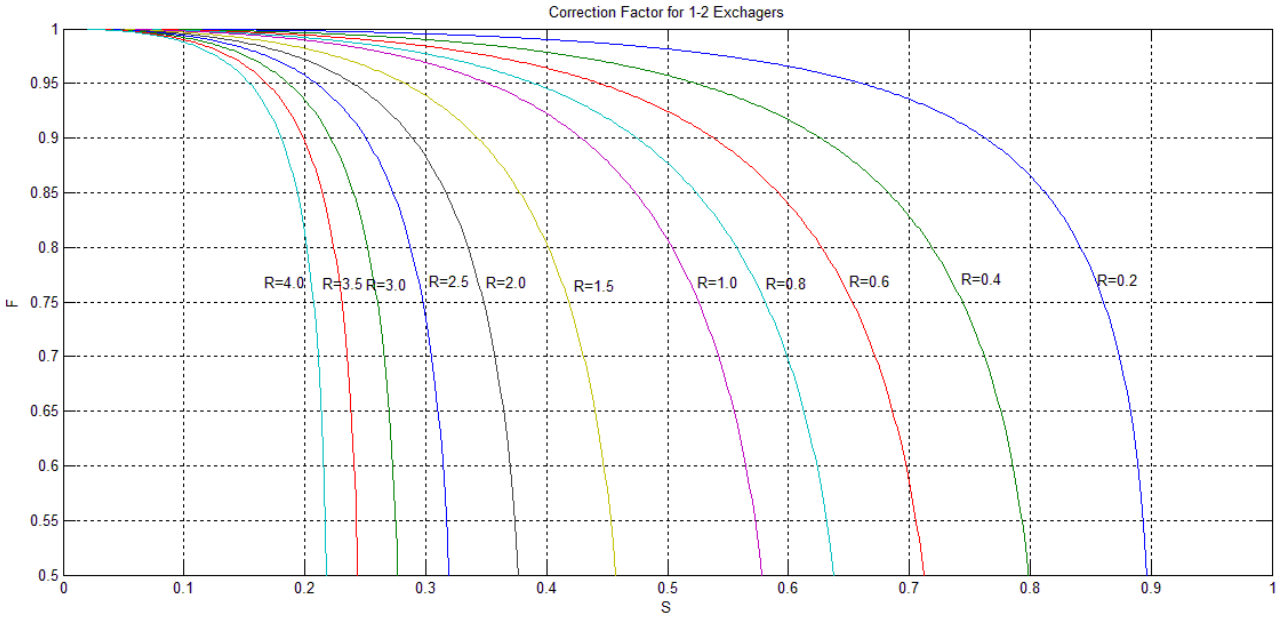

Figure A. 1 Temperature factor for 1-2 heat exchanger for discretized value of R parameter.

For two shell-side passes, four tube-side passes configuration the empirical correlation for temperature factor is [ASME]:

$$F_{2,4} = \frac{\frac{\sqrt{R^2+1}}{2(R-1)}\log_{10}\left(\frac{1-P}{1-RP}\right)}{\log_{10}\frac{(2/P)-1-R+\frac{2}{P}\sqrt{(1-P)(1-RP)}+\sqrt{R^2+1}}{(2/P)-1-R+\frac{2}{P}\sqrt{(1-P)(1-RP)}-\sqrt{R^2+1}}} \qquad A.\ 6$$

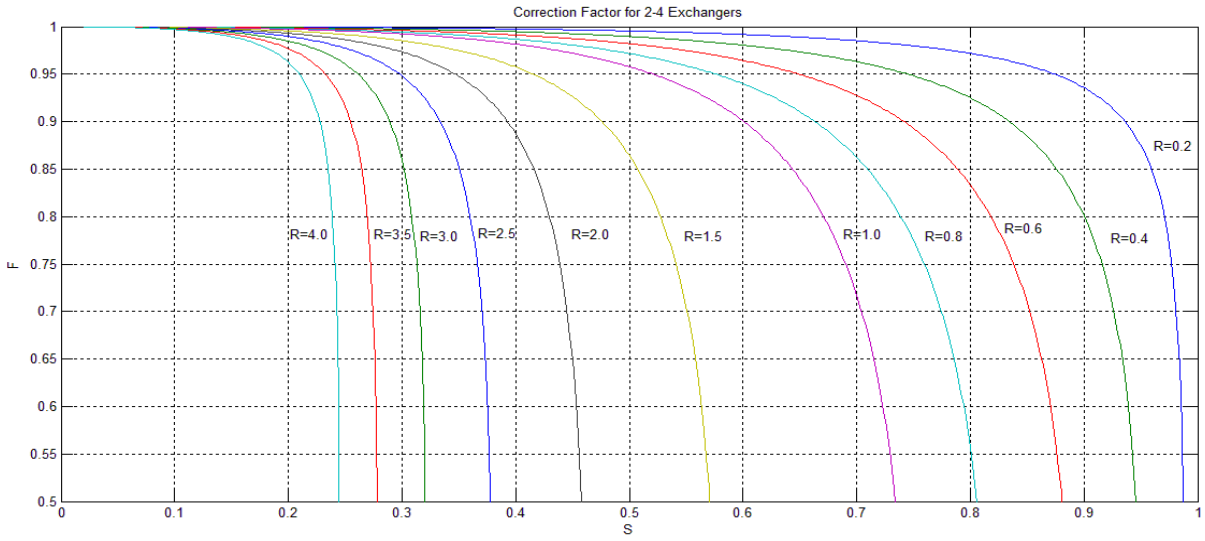

Figure A. 2 Temperature factor for 2-4 heat exchanger for discretized value of R parameter.

Heat Flux Correlation

In this section heat flux correlations used in this work are presented. In equation systems of chapter 2 and 3 the value of heat transfer coefficients is only defined as a generic function of variables and parameters involved in the system. The aim of this section is to define these generic functions.

The section is subdivided in:

- *Tube-side heat transfer coefficients*
- *Shell-side heat transfer coefficients*
- *Nucleate boiling heat transfer coefficients*

- *Condensation heat transfer coefficients*

Tube-side heat transfer coefficients

Forced convection heat transfer correlations for fluids flowing inside pipes are presented. The generic function used in chapter 2 and 3 for heat transfer coefficient calculation is:

$$\alpha_{tube} = f(\dot{m}, T, p, ID, L, N_{tt}, conf)$$

Glielinsky correlation well approximate heat transfer coefficient for fluid in transition and turbulent regime [29], 2100<Re<10^6 and 0.6<Pr<2000:

$$v = \frac{\dot{m}\, N_{pass}}{\rho\, \pi\, ID\, N_{tt}} \quad \text{A. 7}$$

$$[\rho, \mu, \lambda, c_p] = f(T, p) \quad \text{A. 8}$$

$$N_{pass} = \begin{cases} 1 \text{ if } conf = CC \\ 2 \text{ if } conf = 1\text{-}2 \\ 4 \text{ if } conf = 2\text{-}4 \end{cases} \quad \text{A. 9}$$

$$Re = \frac{\rho \cdot v \cdot ID}{\mu} \quad \text{A. 10}$$

$$Pr = \frac{c_p \mu}{\lambda} \quad \text{A. 11}$$

$$f = [0.782 \cdot ln(Re) - 1.51]^{-2} \quad \text{A. 12}$$

$$Nu = \frac{(f/8) \cdot (Re - 1000) \cdot Pr}{1 + 12.7 \cdot \sqrt{f/8} \cdot (Pr^{2/3} - 1)} \cdot \left[1 + \left(\frac{ID}{L}\right)^{2/3}\right] \quad \text{A. 13}$$

$$\alpha_{tube} = \frac{Nu \cdot \lambda}{ID} \quad \text{A. 14}$$

Shell side heat transfer coefficient

Shell-side heat-transfer coefficients are computed by means of Delaware-method correlations [29]. It utilizes empirical correlations referred to ideal bank tube correlations and a set of empirical correlations to introduce corrections factors.

Ideal Tube Bank Correlations

$$j = \frac{h \cdot Pr^{2/3}}{c_p \cdot G \cdot \varphi} \qquad \text{A. 15}$$

$$j = a_1 \cdot \left(\frac{1.33}{P_T/OD}\right)^{a} \cdot Re^{a_2} \qquad \text{A. 16}$$

$$a = \frac{a_3}{1 + 0.14 \cdot Re^{a_4}} \qquad \text{A. 17}$$

Tab A. 1 Set of coefficients used in ideal heat transfer coefficient correlation

Layout angle	***Re***	***a1***	***a2***	***a3***	***a4***
30°	$10^5 \div 10^4$	0.321	-0.388	1.450	0.519
	$10^4 \div 10^3$	0.321	-0.388		
	$10^3 \div 10^2$	0.593	-0.477		
	$10^2 \div 10$	1.360	-0.657		
	< 10	1.400	-0.667		
45°	$10^5 \div 10^4$	0.370	-0.396	1.930	0.500
	$10^4 \div 10^3$	0.370	-0.396		
	$10^3 \div 10^2$	0.730	-0.500		
	$10^2 \div 10$	1.498	-0.656		
	< 10	1.550	-0.667		
90°	$10^5 \div 10^4$	0.370	-0.395	1.187	0.370
	$10^4 \div 10^3$	0.107	-0.266		
	$10^3 \div 10^2$	0.408	-0.460		
	$10^2 \div 10$	0.900	-0.631		
	< 10	0.970	-0.667		

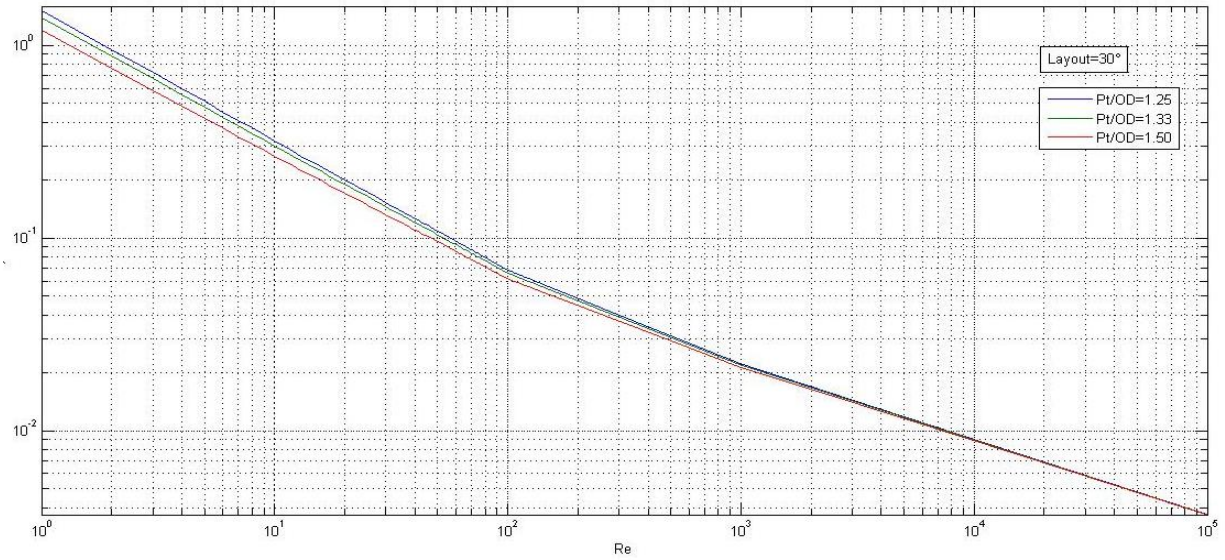

Figure A. 3 j factor for tube layout of 30°

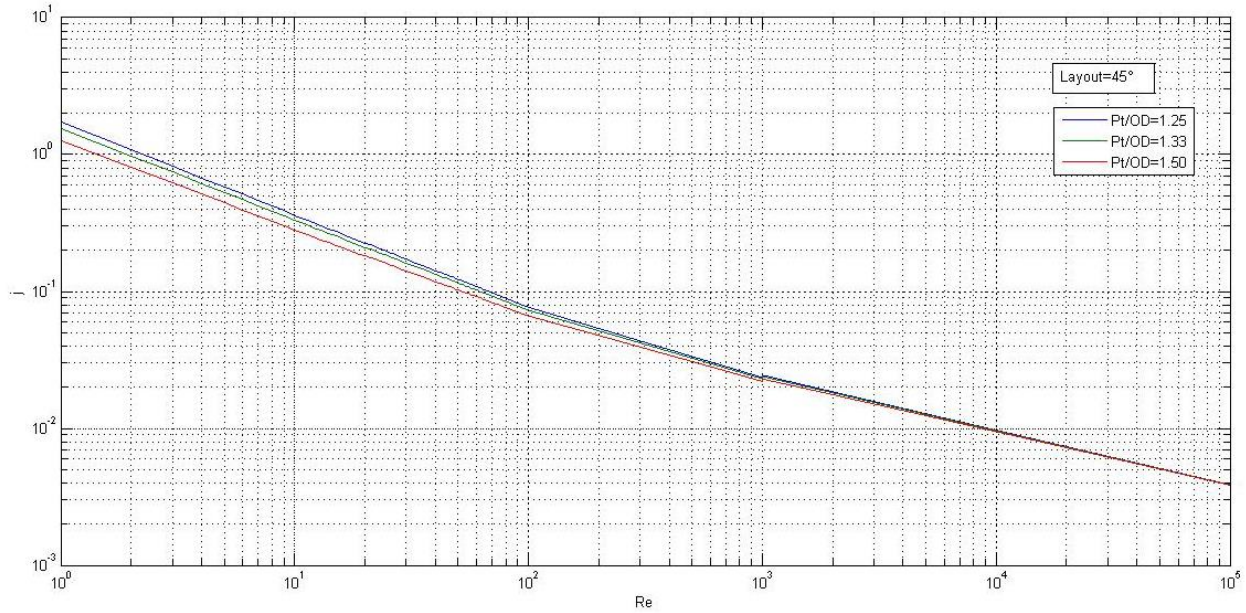

Figure A. 4 j factor for tube layout of 45°

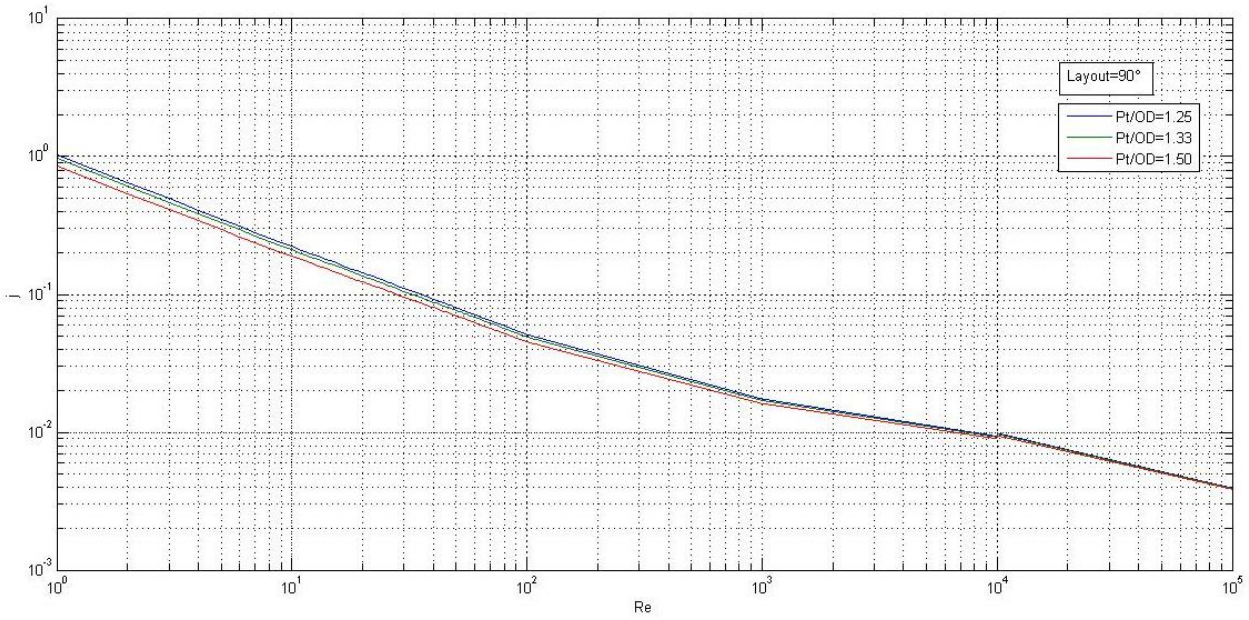

Figure A. 5 j factor for tube layout of 90°

Shell side heat transfer coefficient is evaluated by introducing 5 corrections factor which depend on exchanger geometry:

$$h_0 = h_{ideal} \cdot (J_C \cdot J_L \cdot J_B \cdot J_R \cdot J_S) \qquad \text{A. 18}$$

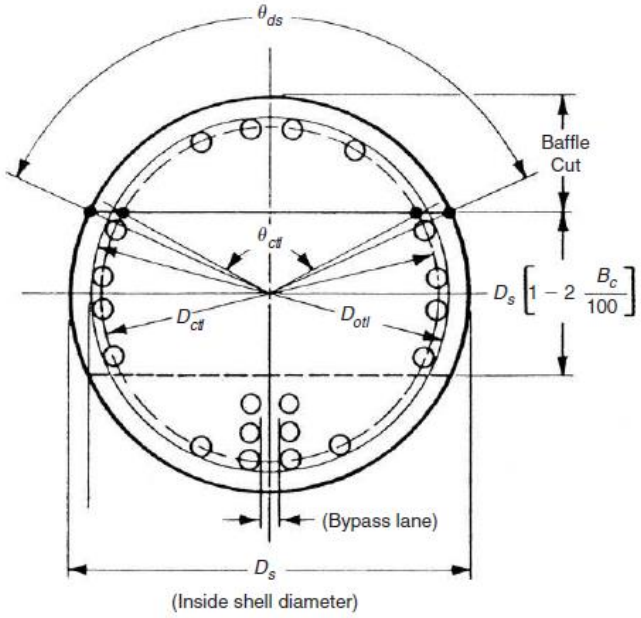

Figure A.6 Shell and tube exchanger geometrical parameters [29]

Correlations for the correction factors

Correction factor for baffle windows flow

The factor J_C expresses the effect on heat transfer coefficient of the flow in the baffle windows. It is linked to tubes number in a windows and the number of tubes in cross flow between baffle tips. It ranges from 0.65, for very large baffle cuts to 1.15 for small baffle cuts.

$$\theta_{ctl} = cos^{-1}\left[\frac{D_s(1-2B_c)}{D_{ctl}}\right] \quad \text{A. 19}$$

$$F_c = 1 + \frac{1}{\pi}(sin\,\theta_{ctl} - \theta_{ctl}) \quad \text{A. 20}$$

$$J_C = 0.55 + 0.72F_c \quad \text{A. 21}$$

The linear correlation used for J_C is valid for practical range of baffle cuts (15% ÷ 45%).

Correction factor for baffle leakage effects

The factor J_L expresses the effect on heat transfer coefficient of the tube-to-baffle and shell-to-baffle leakage streams. These streams flow from one baffle space to the next through gaps between tubes and baffle and gaps between the shell and the baffle. Practical range of J_L is from 0.2 to 1.0, with typical values of 0.7-0.8.

$$\delta_{sb} = 0.0008 + 0.002D_s \quad \text{A. 22}$$

$$\theta_{ds} = 2\,cos^{-1}(1-2B_c) \quad \text{A. 23}$$

$$S_{sb} = D_s\delta_{sb}(\pi - 0.5\theta_{ds}) \quad \text{A. 24}$$

$$\delta_{tb} = \begin{cases} 0.4\ mm\ for\ L < 1m \\ 0.2\ mm\ for\ L > 1m \end{cases} \quad \text{A. 25}$$

$$S_{tb} = 0.5\pi D_0 \delta_{tb} n_t (1 + F_c) \quad \text{A. 26}$$

$$r_s = \frac{S_{sb}}{S_{sb} + S_{tb}} \quad \text{A. 27}$$

$$r_l = \frac{S_{sb} + S_{tb}}{S_m} \quad \text{A. 28}$$

$$J_L = 0.44(1 - r_s) + [1 - 0.44(1 - r_s)]exp(-2.2r_l) \quad \text{A. 29}$$

Correction factor for bundle bypass effects

The correction factor J_B expresses the effects of the bundle bypass flow on heat transfer. Typical values for J_B are in the range of 0.7-0.9.

$$P_T' = \begin{cases} P_T & if\ \theta_{tp} = 90 \\ P_T \cos\theta_{tp} & if\ \theta_{tp} = 30° \text{ or } 45° \end{cases} \quad \text{A. 30}$$

$$N_c = \frac{D_s(1 - 2B_c)}{P_T'} \quad \text{A. 31}$$

$$r_{ss} = \frac{N_{ss}}{N_c} \quad \text{A. 32}$$

$$S_b = B(D_s - D_{otl}) \quad \text{A. 33}$$

$$C_J = \begin{cases} 1.35\ if\ Re < 100 \\ 1.25\ if\ Re \geq 100 \end{cases} \quad \text{A. 34}$$

$$J_B = \begin{cases} exp\left[-C_J(S_b/S_m)\left(1 - \sqrt[3]{2r_{ss}}\right)\right] for\ r_{ss} < 0.5 \\ 1.0 \qquad\qquad\qquad\qquad\qquad for\ r_{ss} \geq 0.5 \end{cases} \quad \text{A. 35}$$

Correction factor for unequal baffle spacing

The correction factor J_S depends on the inlet baffle spacing, the outlet baffle spacing and the central baffle spacing. Typical values for J_S are in the range of 0.85-1.0.

$$n_1 = \begin{cases} 1/3 \ for\ Re < 100 \\ 0.6 \ \ for\ Re \geq 100 \end{cases} \quad \text{A. 36}$$

$$J_S = \frac{(n_b - 1) + (B_{in}/B)^{(1-n_1)} + (B_{out}/B)^{(1-n_1)}}{(n_b - 1) + (B_{in}/B) + (B_{out}/B)} \quad \text{A. 37}$$

Laminar flow correction factor

The correction factor J_R accounts for the fact that in laminar flow the heat-transfer coefficient decreases with downstream distance, which is interpreted as the number of tube rows crossed. The range of J_R is from 0.4 to 1.0 (1.0 for Re>100).

$$N_{cw} = \frac{0.8 B_c D_s}{P_T'} \quad \text{A. 38}$$

$$N_{ct} = (n_b + 1)(N_c + N_{cw}) \quad \text{A. 39}$$

$$J_R = \begin{cases} (10/N_{ct})^{0.18} \ for\ Re \leq 20 \\ 1.0 \qquad\quad for\ Re \geq 100 \end{cases} \quad \text{A. 40}$$

For 20<Re<100, J_R is calculated by linear interpolation.

Nucleate boiling heat transfer coefficient

Several correlations are presented in literature for nucleate boiling.
In that model evaporation outside a bundle of tubes is considered, so also natural convection phenomena are considered.

$$h_b = h_{nb} F_b + h_{nc} \quad \text{A. 41}$$

Mostinski correlation is used to express h_{nb} [29]:

$$h_{nb} = 1.167 \cdot 10^{-8} \, P_C^{2.3} \, \Delta T_e^{2.333} F_P^{3.333} \quad \text{A. 42}$$

F_p is the pressure correction factor, given by the equation A.43:

$$F_P = 2.1P_r^{0.27} + [9 + (1 - P_r^2)^{-1}]P_r^2 \quad \text{A. 43}$$

Fb coefficient depends on the bundle geometry and it can be expressed by empirical equation A.44:

$$F_b = 1 + 0.1\left[\frac{0.785D_b}{C_1(P_T/OD)^2 OD} - 1\right]^{0.75} \quad \text{A. 44}$$

$$C_1 = \begin{matrix} 1.0\ if\ layout = 45° \text{ or } 90° \\ 0.866\ if\ layout = 30° \end{matrix} \quad \text{A. 45}$$

$$h_{nc} = \frac{Nu_{nc}\,\lambda}{L} \quad \text{A. 46}$$

$$Nu_{nc} = \left\{0.60 + \frac{0.387\ (Gr\ Pr)^{1/6}}{[1 + (0.559/Pr)^{9/16}]^{8/27}}\right\}^2 \quad \text{A. 47}$$

Condensation Heat transfer coefficients

In shell & tube exchangers usually takes places outside a bundle of tubes where cooling water flows. That situation is well described by Kern equation [29]:

$$h_{cond} = 1.52\left[\frac{k_l^3 \rho_l(\rho_l - \rho_v)g}{4\mu_l \Gamma^*}\right]^{1/3} \quad \text{A. 48}$$

$$\Gamma^* = \frac{\dot{m}_{cond}}{L\, n_t^{2/3}} \quad \text{A. 49}$$

All fluid properties are evaluated at T_f ($T_f = 0.75T_{wall}+0.25T_{sat}$).

In organic Rankine cycles the vapor at condenser inlet is usually superheated and not saturated as in traditional steam cycles. The condensation heat transfer coefficient should take account of sensible heat released by the superheated vapor.

The total heat *q* detracted from the condensing flow is:

$$q = \dot{m}_{cond}\lambda + \dot{m}_{cond}\, c_{p,v}(T_{in} - T_{cond}) = \dot{m}_{cond}\lambda' \quad \text{A. 50}$$

$$\lambda' = \lambda + c_{p,v}(T_{in} - T_{cond}) \quad \text{A. 51}$$

λ' is the equivalent latent heat, which accounts the desuperheating effect.

The heat transfer coefficient becomes:

$$h'_{cond} = h_{cond}\left(\frac{\lambda'}{\lambda}\right)^{1/4} \quad \text{A. 52}$$

If the tube bundle is composed by finned tubes, heat transfer coefficient equation is modified in order to account fins presence:

$$h_{cond} = 0.609\left[\frac{k_l^3\,\rho_l\,(\rho_l - \rho_v)\,g\,\eta_w\,(A_{tot}/L)}{\mu_l\,D_e\,\Gamma^*}\right]^{1/3} \quad \text{A. 53}$$

$$D_e = \left(\frac{1.30\,\eta_f\,A_{fins}\,E^{-0.25} + A_{prime}\,D_r^{-0.25}}{\eta_{wall}\,A_{tot}}\right) \quad \text{A. 54}$$

APPENDIX 2

The aim of this appendix is to show and explain how the Simulink model of *Components* has been created. For each Component involved in the ORC process a specific Simulink model has been designed in order to create a library of components that could be used in future also for different simulations.

Simulink is a graphical editor for building and managing block diagrams. Simulink provide a wide set of predefined blocks that allow creating detailed block diagram. In addition customized functions by incorporating hand-written Matlab code can be introduced into the model; by mean of s-function block. Signal lines (continuous lines) establish mathematical relationship between systems blocks or components. An interesting task Simulink is the possibility of creating hierarchy in model visualization; encapsulating groups of blocks and signals into subsystems visualized as a single block. Several level of hierarchy can be introduced, creating custom interface to a subsystem. A mask can be used to hide subsystem content allows interacting with it by mean of a parameter dialog block.

The created libraries of components include:

- *Exchanger (without change of phase).*
- *Kettle (Evaporator)*
- *Condenser*
- *Pump*
- *Turbine*

Heat Exchanger Simulink model

In this section the Simulink model of Exchanger with no change phase is presented. Three different configurations are considered, in accordance with assumptions presented in chapter 2:

- Single pass shell-side, single pass tube-side (perfect countercurrent)
- Single pass shell-side, two passes tube-side (1-2)
- Two passes shell-side, four passes tube-side (2-4)

Single pass shell-side, single pass tube-side

One pass shell-side, one pass tube-side model is here presented. It is the easiest configuration to model, due to the fact that shell-side fluid, tube-side fluid and pipe are all discretized in *nx* control volumes.

Component description will follow a top-down approach. Four level of hierarchy are introduced in order clear how model is organized and how different parts interact. At higher level (level 1) heat exchanger component is visualized as a single block, where only input and output signals are displayed. Component mask is presented in Fig. A2.1:

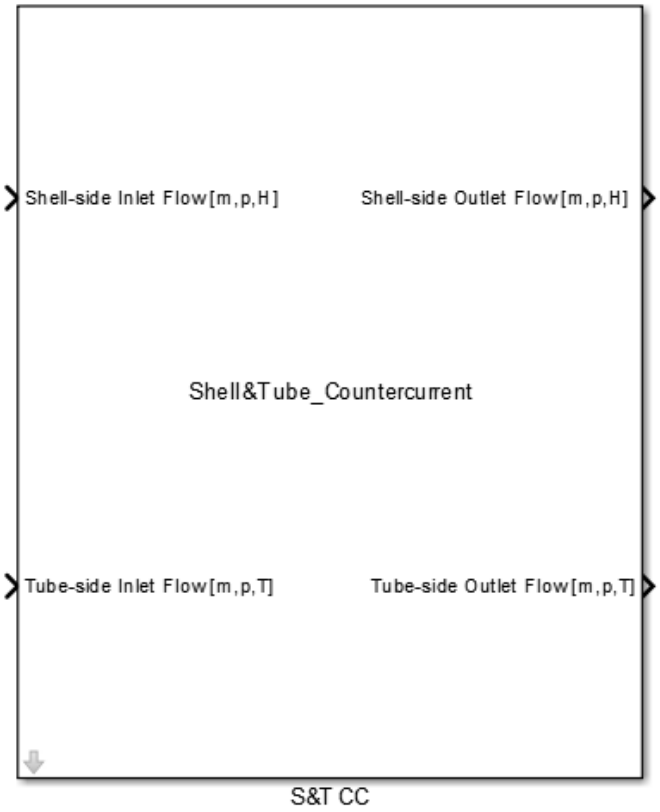

Fig. A2. 1 Simulink block of Countercurrent Shell&Tube heat exchanger (*level 1 of hierarchy*)

Both input and input signals are vectors composed by 3 elements: mass flow rate, pressure and temperature (or enthalpy) of operating flud: $[\dot{m}, p, T]$ or $[\dot{m}, p, H]$.
The user can interact with heat exchanger block by mean of parameter dialog block, presented in figure Fig. A2.2.

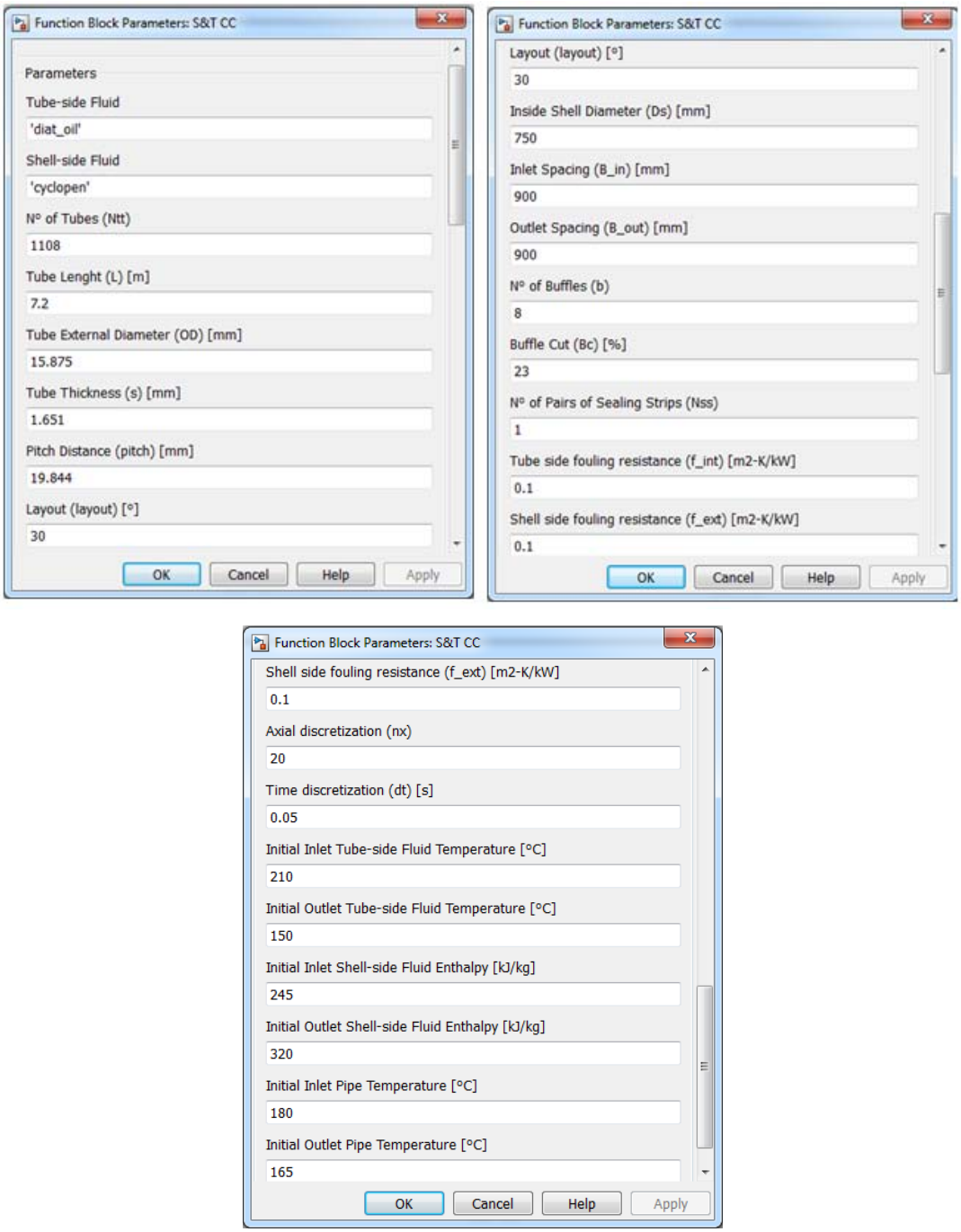

Fig. A2. 2 Parameter dialog block of Countercurrent Shell&Tube heat exchanger

The dialog block asks to define geometrical parameters in order to characterize the component. All these parameters are provided by Shell-and-tube design model presented in chapter 2.

Axial discretization of the component, which defines simulation degree of accuracy, can be imposed by the user. Above mentioned "*s-function*" blocks allows working with no fixed dimension vectors; in fact *Matlab* is very performing in operating with vectors and matrix

signals. Furthermore "*s-function*" block also allows integration of Simulink model with Refprop database by mean of *refpropm.m* function.

Initialization section of mask editor allows writing a Matlab algorithm executed by the model before starting simulation. This algorithm evaluates all fixed parameters, which cannot vary during simulation; such as exchange area, volume, etc.

By providing the inlet and outlet value of temperature or enthalpy of both fluids and pipe the initialization algorithm creates the starting value of shell-side fluid enthalpy, tube-side fluid and pipe temperature vectors; state-variables of heat exchanger model.

Going down to a lower level of hierarchy (level 2), system is subdivided into three different subsystems that can be described separately: Shell-side fluid, Tube-side fluid and Pipe.

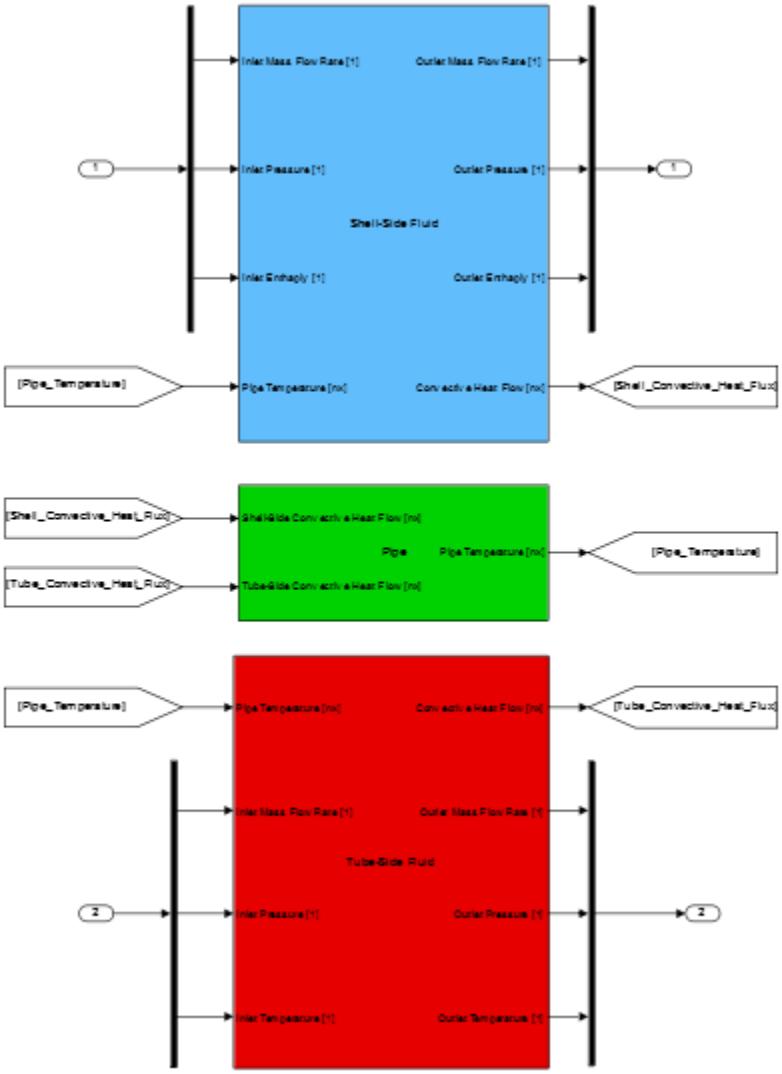

Fig. A2. 3 Block diagram of Countercurrent Shell&Tube heat exchanger *(level 2 of hierarchy)*

Shell-side fluid subsystem

Input and output of Shell-side fluid subsystem are shown in fig A2. 4:

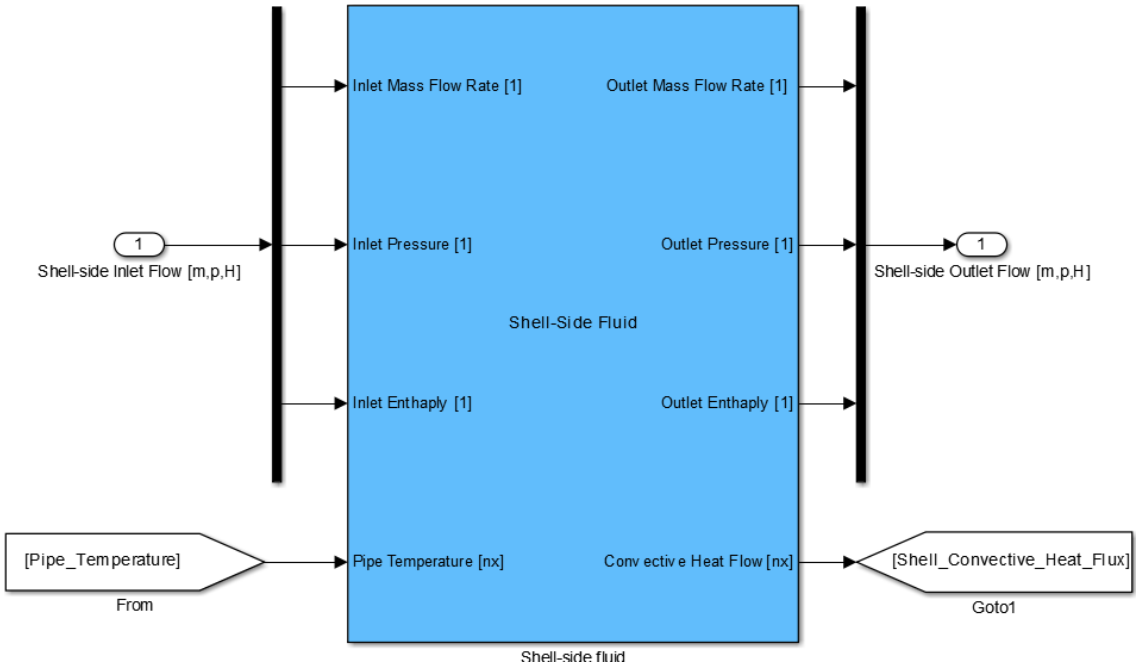

Fig. A2. 4 Shell-side fluid subsystem block, Countercurrent Shell&Tube heat exchanger *(level 2 of hierarchy)*

Inlet and Outlet mass flow rate, pressure and enthalpy are respectively input and output signals of the global component.

Differently *Pipe Temperature* and *Convective Heat Exchanged* signals are vector of *nx* dimension providing respectively the value of *nx Pipe* temperatures and *nx* convective heat fluxes exchanged between fluid and pipe units at time *t* of simulation.

The block diagram of *Shell-Side Fluid* subsystem is presented in Fig. A2.5:

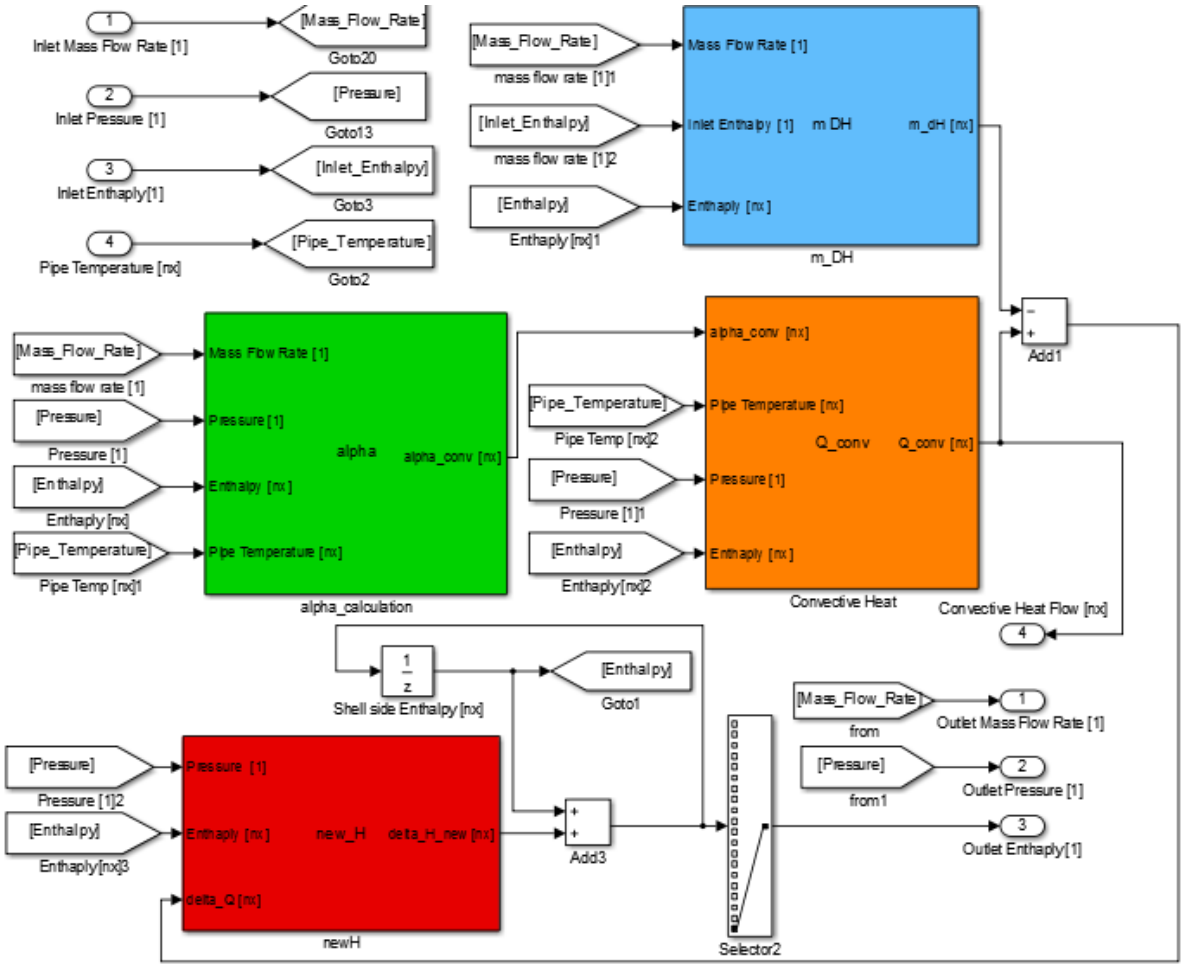

Fig. A2. 5 Block diagram of Shell-side fluid subsystem, Countercurrent Shell&Tube heat exchanger, (*level 3 of hierarchy*)

Input signals are all connected to "*from*" block. In combination with "*to*" block it allows linking two or more blocks avoiding usage of continuous connection lines; simplifying diagram comprehension.

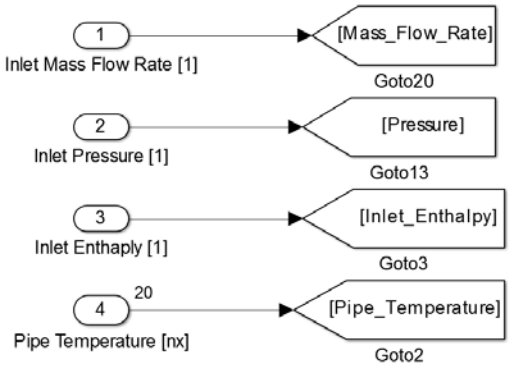

Fig. A2. 6 Input signals of Shell-side fluid subsystem, Countercurrent Shell&Tube heat exchanger, (*level 3 of hierarchy*)

"*alpha*" subsystem (green) evaluates the *nx* dimension vector of convective heat transfer coefficients:

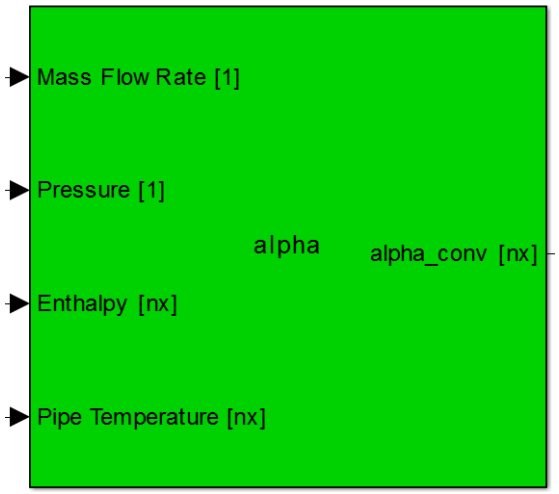

Fig. A2. 7 "alpha" subsystem block, Shell-side fluid subsystem, Countercurrent Shell&Tube heat exchanger, (*level 3 of hierarchy*)

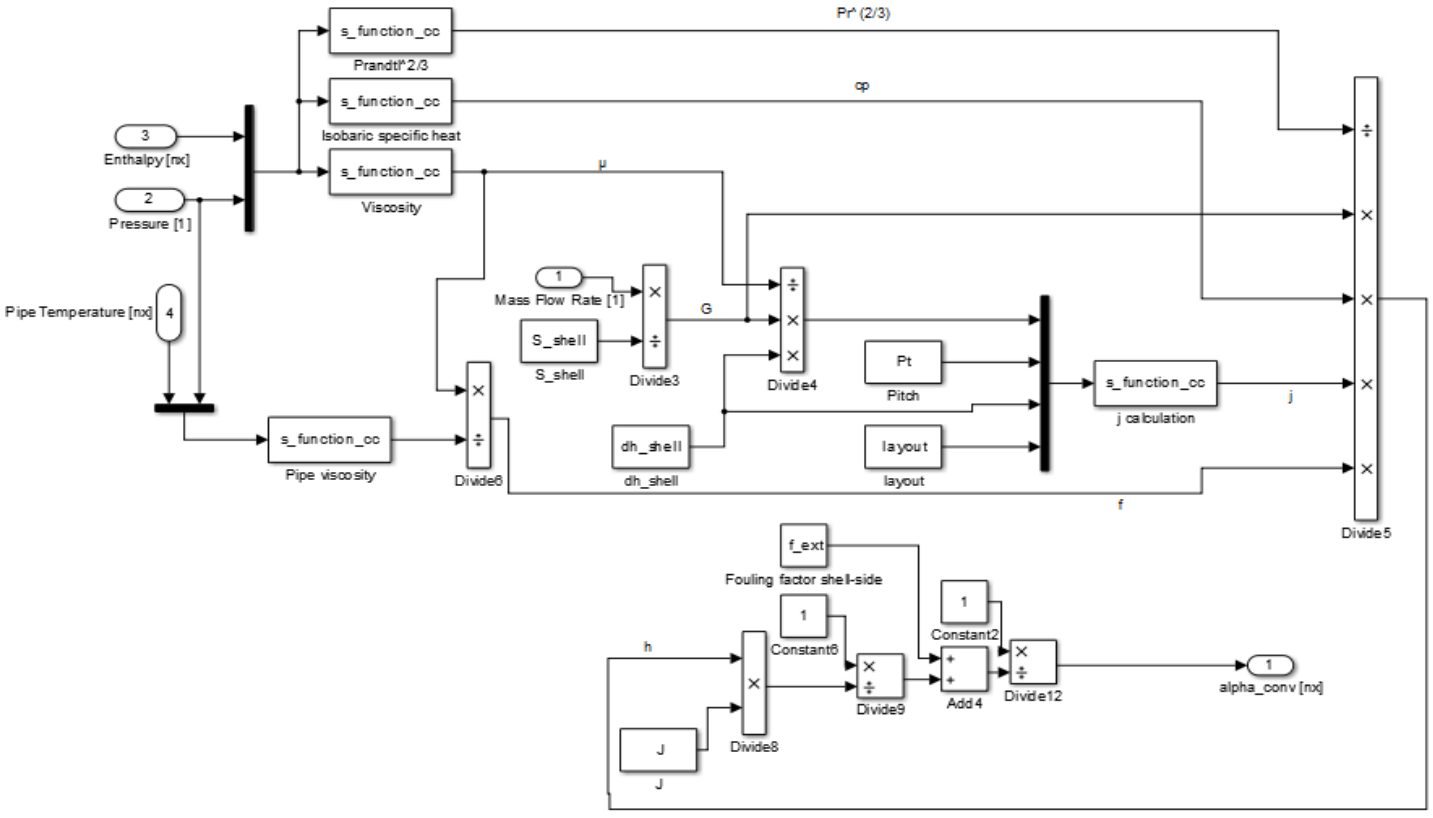

Fig. A2. 8 "alpha" subsystem block, Shell-side fluid subsystem, Countercurrent Shell&Tube heat exchanger, (*level 4 of hierarchy*)

The presented block scheme implements equations:

$$h|_{nx}^{t} = \frac{c_p\big|_{nx}^{t}\ G^t\ \varphi|_{nx}^{t}\ \ j|_{nx}^{t}}{(Pr|_{nx}^{t})^{2/3}}\ J$$

$$\alpha_{conv}|_{nx}^{t} = \frac{1}{\frac{1}{h|_{nx}^{t}} + f_{ext}}$$

The fluid heat transfer resistance is considered in series with internal fouling resistance, obtaining global shell-side heat transfer coefficients vector $\alpha_{conv}|_{nx}^{t}$.

The three s-function "*Prantdl^2/3*", "*Isobaric specific heat*" and "*Viscosity*" allows calculating Prandtl number, isobaric specific heat and dynamic viscosity of fluid units at time step of simulation, by knowing enthalpy vector $H_1|_{nx}^{t}$ and pressure p_1^t .
S-function block needs definition of inputs and outputs number before simulation starting; for clearness they are expressed near subroutine name:

```
%Prandtl^2/3 (in=nx+1, out=nx);
  for i=1:nx
    Output(i)=(refpropm('^','P',u(nx+1)*100,'H',u(i)*1000,specie))^2/3;
  end

%Isobaric specific heat (in=nx+1, out=nx);
  for i=1:nx
    Output(i)=refpropm('C','P',u(nx+1)*100,'H',u(i)*1000,specie)*10^-3;
  end

%Viscosity (in=nx+1, out=nx);
  for i=1:nx
    Output(i)=refpropm('V','P',u(nx+1)*100,'H',u(i)*1000,specie);
  end
```

In *s-function* subroutines *u(i)* and *Output(i)* refer respectively to input and output vector.
The s-function "*Pipe Viscosity*" evaluates fluid dynamic viscosity at pipe temperature:

```
%Pipe Viscosity (in=nx+1, out=nx);
  for i=1:nx
    Output(i)=refpropm('V','T',u(i)+273.15,'P',u(nx+1)*100,specie);
  end
```

"*j calculation*" calculates *j* parameter of Shell-side fluid heat transfer correlations by knowing Reynolds number, pitch distance and external diameter:

```
%j calculation (in=nx+1, out=nx);
  for i=1:nx
    if u(nx+3)==30
      if u(i)<10^2
        A=[1.36 -0.657 1.45 0.519];
      elseif u(i)<10^3
        A=[0.593 -0.477 1.45 0.519];
      elseif u(i)<10^4
        A=[0.321 -0.388 1.45 0.519];
      else
        A=[0.321 -0.388 1.45 0.519];
      end
    elseif unx+3==45
       if u(i)<10^2
        A=[0.498 -0.656 1.93 0.5];
       elseif u(i)<10^3
        A=[0.73 -0.5 1.93 0.5];
       elseif u(i)<10^4
        A=[0.37 -0.396 1.93 0.5];
       else
        A=[0.37 -0.396 1.93 0.5];
       end
    else
       if u(i)<10^2
        A=[0.900 -0.631 1.187 0.37];
       elseif u(i)<10^3
        A=[0.408 -0.46 1.187 0.37];
       elseif u(i)<10^4
        A=[0.107 -0.266 1.187 0.37];
       else
        A=[0.370 -0.395 1.187 0.37];
       end
    end
    a=A(3)/(1+0.14*u(i)^A(4));
    Output(i)=A(1)*(1.33/(u(nx+1)/u(nx+2)))^a*u(i)^A(2);
  end
```

Second subsystem analyzed is "*Q_conv*", the orange depicted one. It leads to calculate convective heat fluxes vector, exchanged by fluid and pipe.

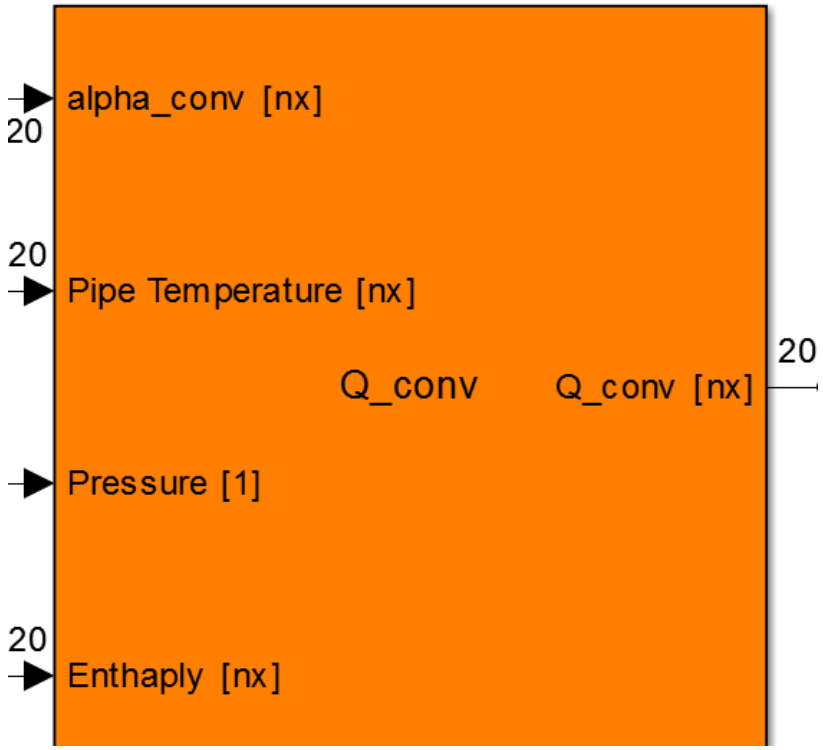

Fig. A2. 9 "Q_conv" subsystem block, Shell-side fluid subsystem, Countercurrent Shell&Tube heat exchanger, (*level 3 of hierarchy*)

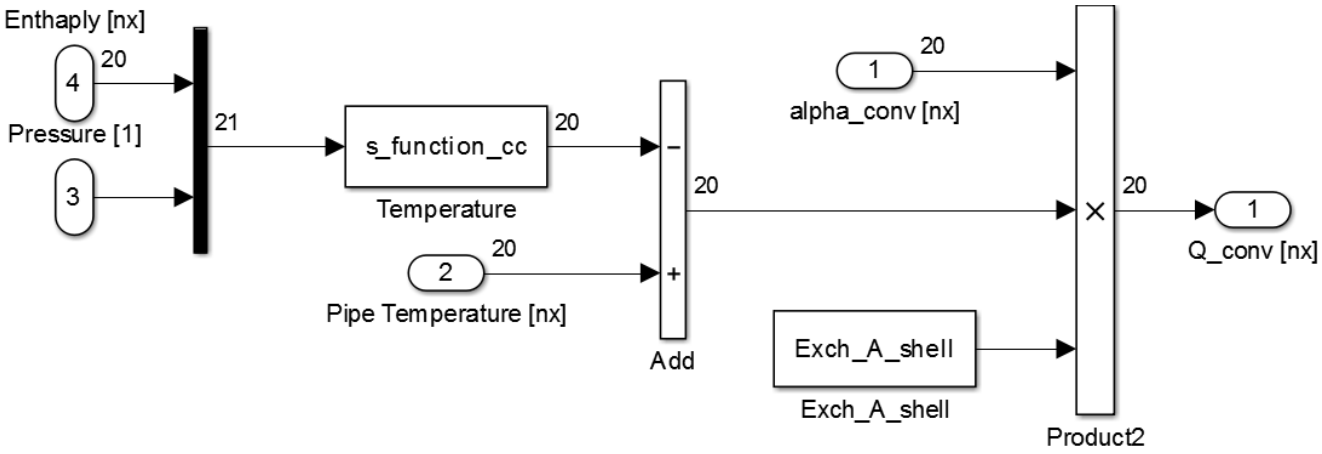

Fig. A2. 10 "Q_conv" subsystem block, Shell-side fluid subsystem, Countercurrent Shell&Tube heat exchanger, (*level 4 of hierarchy*)

The presented block diagram performs following equation:

$$\dot{q}_{conv}|_{nx}^{t} = \alpha_{conv}|_{nx}^{t} \cdot A \cdot \left(T_{pipe}|_{nx}^{t} - T|_{nx}^{t}\right)$$

"*Temperature*" block evaluates fluid temperatures vector at time *t* by fluid enthalpy vector $H_1|_{nx}^t$ and pressure p_1^t .

```
%Temperature (in=nx+1, out=nx);
  for i=1:nx
    [T]=refpropm('T','P',u(nx+1)*100,'H',u(i)*1000,specie);
    Output(i)=T-273.15;
  end
```

The output signal of "*Q_conv*" subsystem is the convective heat fluxes vector: $\dot{q}_{1,conv}\Big|_{nx}^{t}$.

The next subsystem to be analyzed is "*M DH*", the light blue one. The output of such subsystem is the heat transferred between two subsequent units of fluid $\dot{m}(H_i - H_{i-1})|_{nx}^t$:

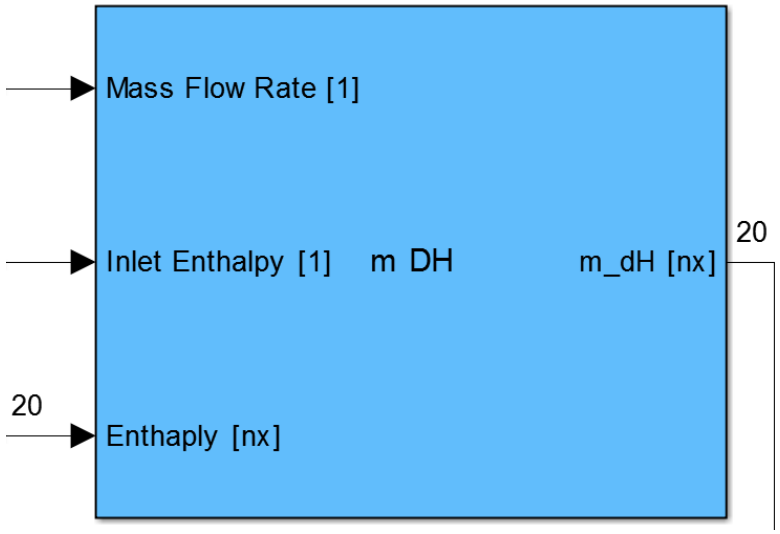

Fig. A2. 11 "m DH" subsystem block, Shell-side fluid subsystem, Countercurrent Shell&Tube heat exchanger, (*level 3 of hierarchy*)

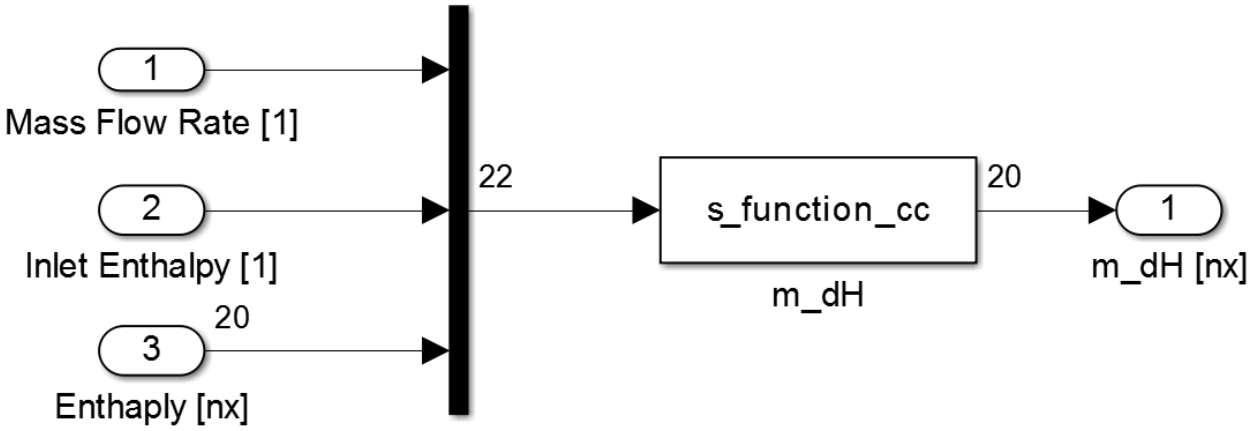

Fig. A2. 12 "m DH" subsystem block, Shell-side fluid subsystem, Countercurrent Shell&Tube heat exchanger, (*level 4 of hierarchy*)

"*m_dH*" s-function computes following algorithm:

```
%m_dH (in=nx+2, out=nx)
  for i=1:nx
    Output(i)=u(1)*(u(2+i)-u(1+i));
  end
```

"*NewH*" subsystem provides the variation of "*Shell side Enthalpy"* vector from instant *t* to *t+Δt* $[H|_{nx}^{t+\Delta t} - H|_{nx}^{t}]$ applying energy conservation equation for shell-side fluid.

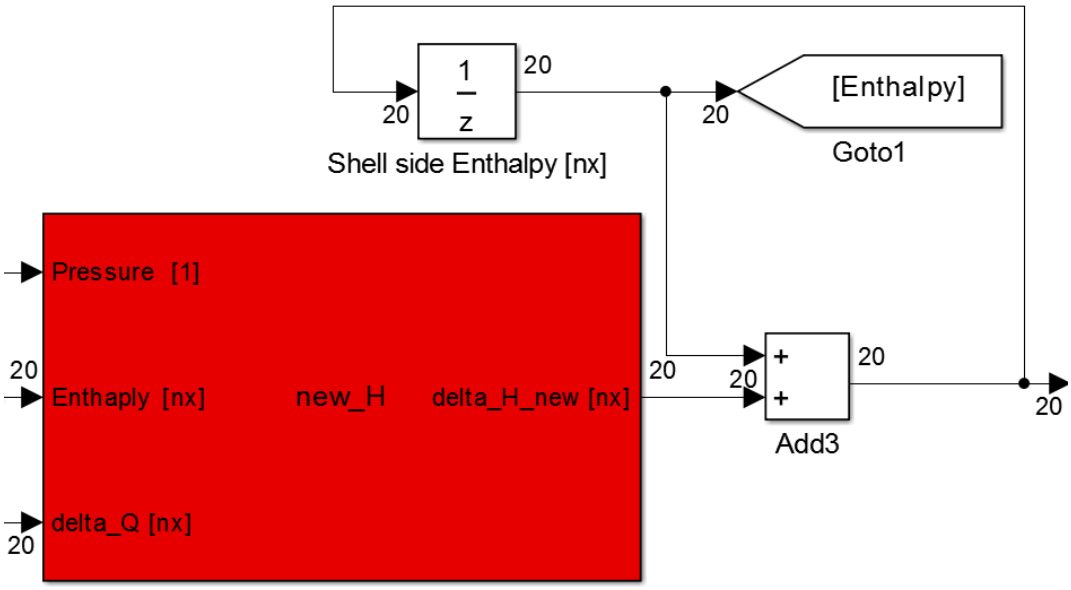

Fig. A2. 13 "new_H" subsystem block, Shell-side fluid subsystem, Countercurrent Shell&Tube heat exchanger, (*level 3 of hierarchy*)

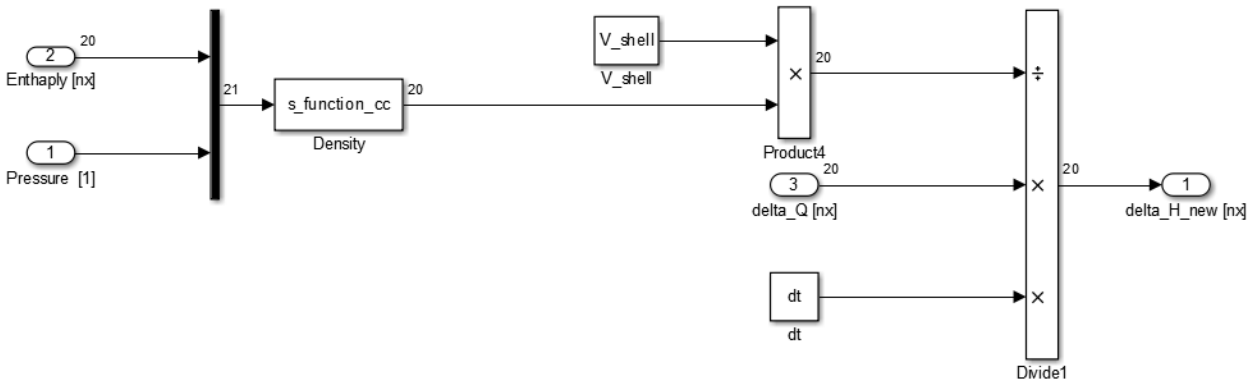

Fig. A2. 14 "new_H" subsystem block, Shell-side fluid subsystem, Countercurrent Shell&Tube heat exchanger, (*level 4 of hierarchy*)

Energy conservation equation balance is performed by mean of:

$$[H|_{nx}^{t+\Delta t} - H|_{nx}^{t}] = \frac{(\dot{q}_{conv}|_{nx}^{t} - \dot{m}(\Delta H)|_{nx}^{t})\,\Delta t}{\rho\, V}$$

"*Density*" s-function computes fluid density vector at time *t*:

```
%Density (in=nx+1, out=nx);
  for i=1:nx
    Output(i)=refpropm('D','P',u(nx+1)*100,'H',u(i)*1000,specie);
  end
```

Loop shown in Fig A2.13 evaluates shell-side fluid enthalpy vector at time $t+\Delta t$:

$$H|_{nx}^{t+\Delta t} = H|_{nx}^{t} + [H|_{nx}^{t+\Delta t} - H|_{nx}^{t}]$$

The simulation can restart with state-variable vectors provided by simulation at time *t*.

State-variable vectors are modelled using "*unit-delay*" block. It allows fixing the initial value of the block that changes at each time step of simulation, with the new provided value.

By mean of a selector block the last element of shell-side fluid enthalpy vector is extracted and sent as output signal of the component.

In accordance with model assumptions, outlet pressure and outlet mass flow rate of shell side fluid are equal to the inlet value.

Tube-side fluid subsystem

Input and output vectors of "*Tube-side fluid*" subsystem are shown in figure:

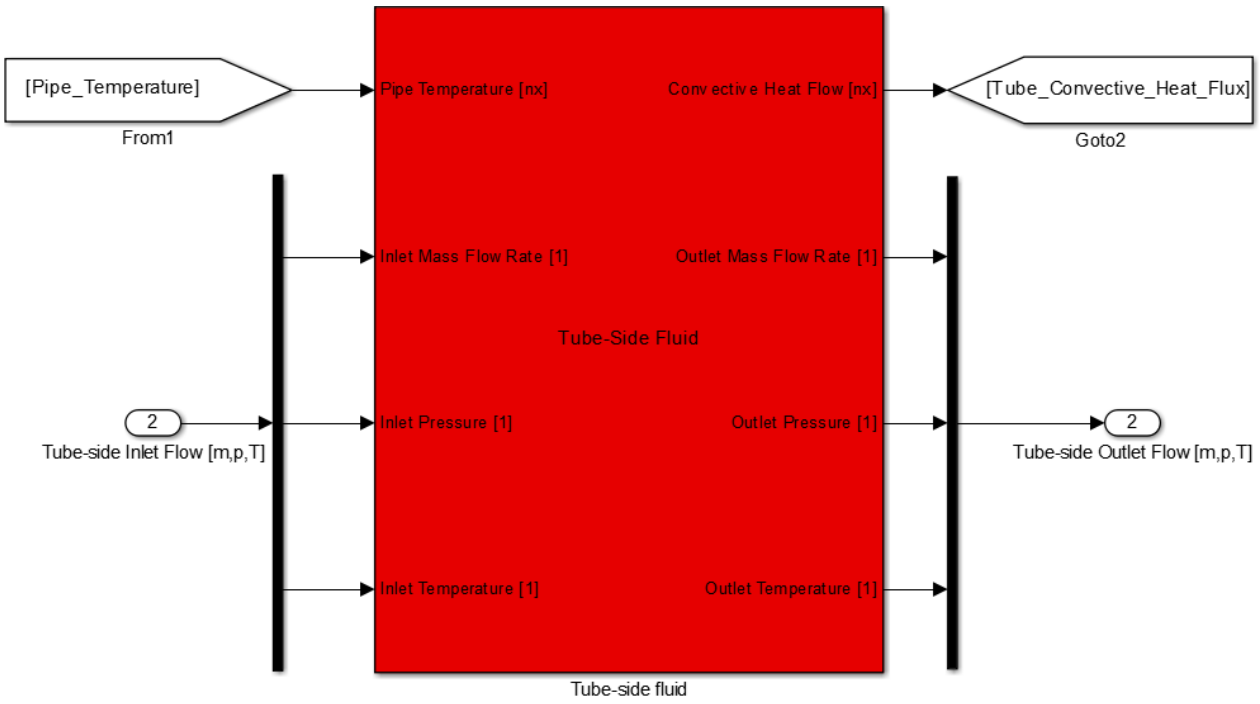

Fig. A2. 15 Tube-side fluid subsystem block, Countercurrent Shell&Tube heat exchanger (*level 2 of hierarchy*)

The presented subsystem is very similar to the previous one; nevertheless here state-variable vector is *Temperature* vector.

The scheme block of such subsystem is here shown:

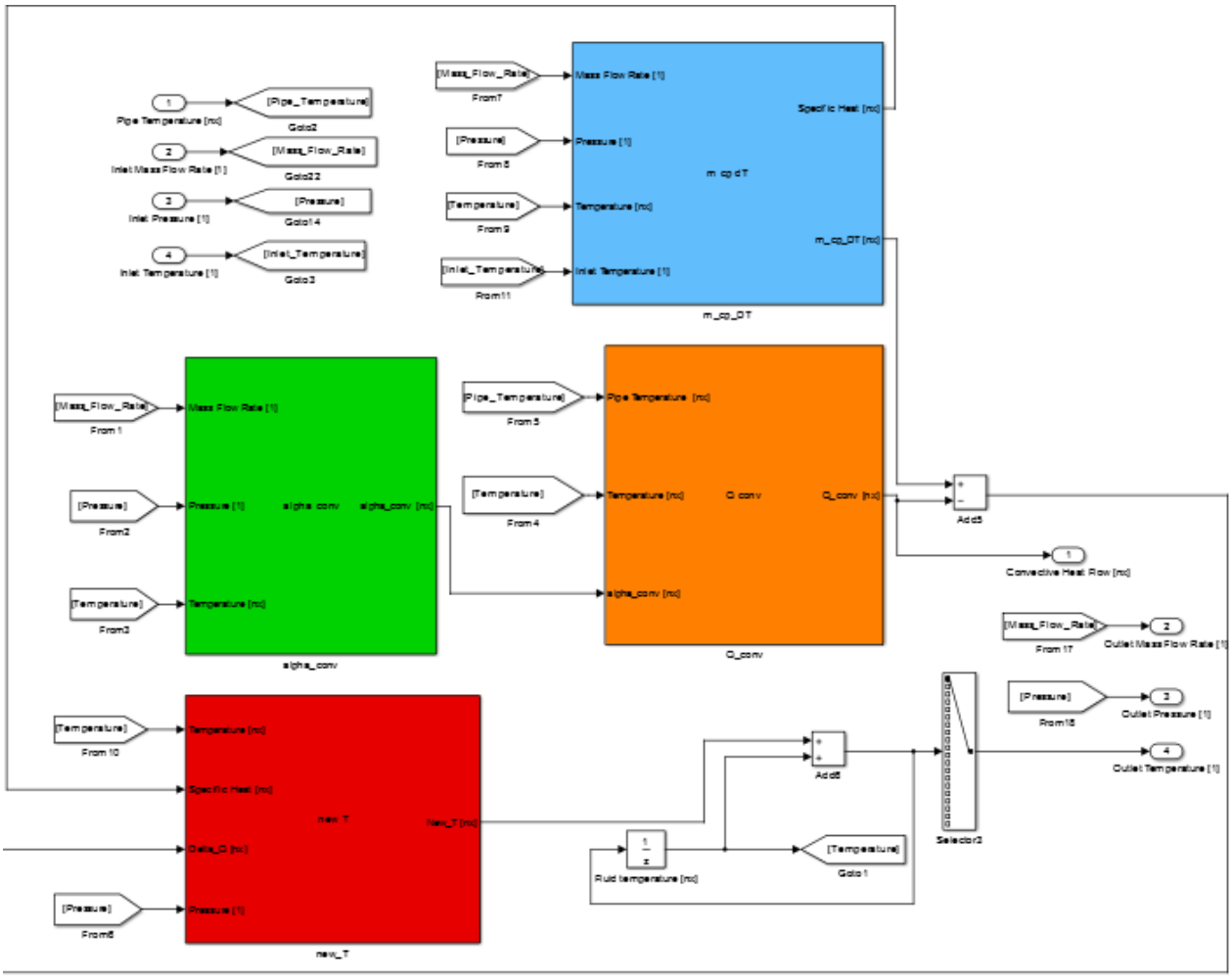

Fig. A2. 16 Block diagram of Tube-side fluid subsystem, Countercurrent Shell&Tube heat exchanger, (level 3 of hierarchy)

"alpha_conv" subsystem provides tube-side convective heat transfer coefficients for each fluid unit:

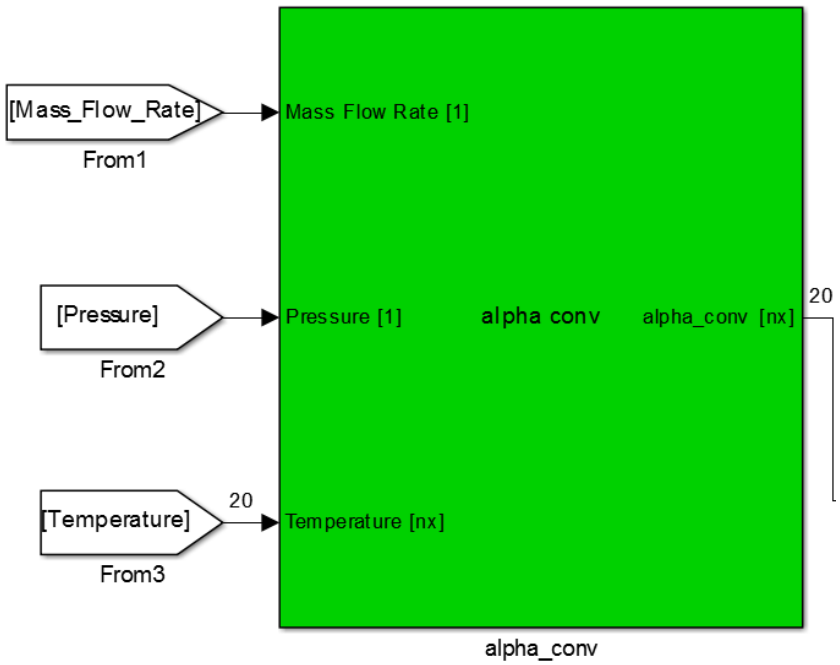

Fig. A2. 17 "alpha conv" subsystem block, Tube-side fluid subsystem, Countercurrent Shell&Tube heat exchanger, (*level 3 of hierarchy*)

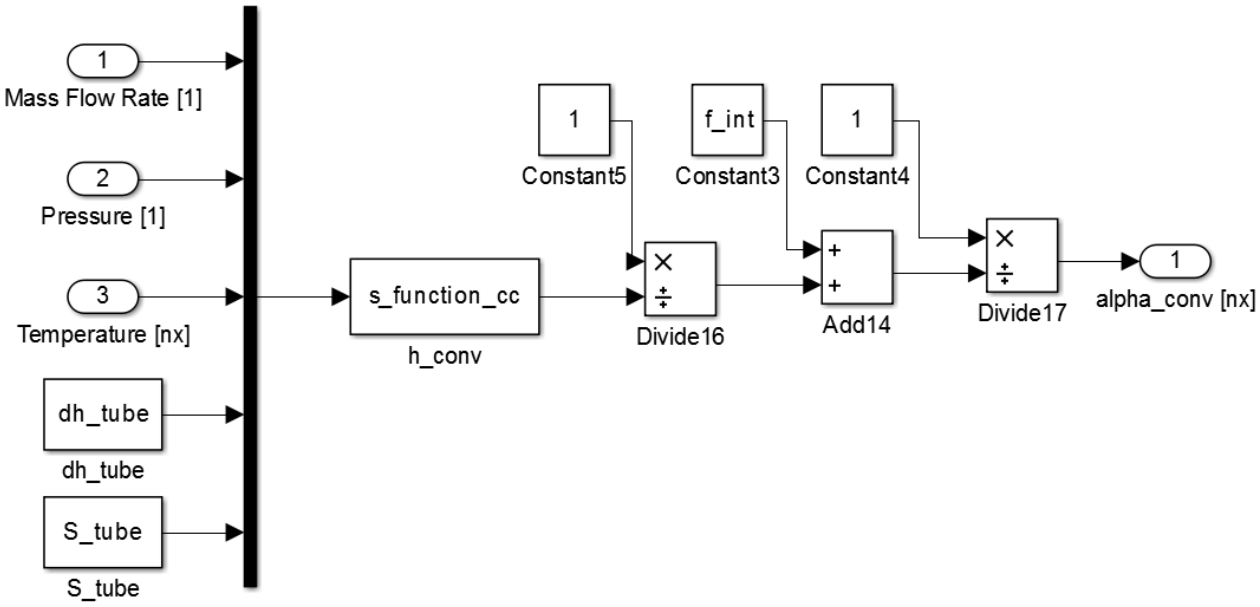

Fig. A2. 18 "alpha conv" subsystem block, Tube-side fluid subsystem, Countercurrent Shell&Tube heat exchanger, (*level 4 of hierarchy*)

S-function "*h_conv*" computes tube-side fluid convective heat transfer coefficients:

```
%h_conv (in=nx+4, out=nx)
   m=u(1);
   p=u(2);
   d_h=u(nx+3);
   Sez=u(nx+4);
   for i=1:nx
      %calcolo alpha in ingresso
      Output(i)= calcolo_alpha_conv (u(i+2),p,m,d_h,Sez,specie);
   end
```

The s-function "*h_conv*" utilizes Matlab function "*calcolo_alpha_conv*"; where heat transfer correlations are implemented:

```
function [h_conv]= calcolo_alpha_conv (T,p,m,d_h,Sez,specie)

%T   [°C] Temperature
%p   [bar] Pressure
%m   [kg/s] Mass Flow Rate
%d_h [m] Hydraulic Diameter
%Sez [m2] Flow Area

k=strcmp(specie,'diat_oil');
if k>0
   L=prop_therminol('L',T);
   L=L/1000;
   mi=prop_therminol('V',T);
   Pr=prop_therminol('Pr',T);

   Re=m*d_h/(Sez*mi);
   f=(0.79*log(Re)-1.64)^(-2);
   Nu=(f/8)*(Re-1000)*Pr/(1+12.7*(f/8)^0.5*(Pr^(2/3)-1));

   h_conv=Nu*L/d_h;
else

   [l, mi, Pr]=refpropm('LV^','T',T+273.15,'P',p*100,specie);

   L=l/1000;

   Re=m*d_h/(Sez*mi);
   f=(0.79*log(Re)-1.64)^(-2);
   Nu=(f/8)*(Re-1000)*Pr/(1+12.7*(f/8)^0.5*(Pr^(2/3)-1));

   h_conv=Nu*L/d_h;
end
```

Function "*prop_therminol*" leads to calculate thermodynamic properties of thermal oil considered in this model:

```
function [prop]=prop_therminol(P,T)

%T [°C] Temperature

%provide P (Propertiy)
%'D'-> density              [kg/m3]
%'C'-> specific heat       [kJ/kg*K]
%'L'-> thermal conductivity [W/mK]
%'V'-> dynamic viscosity    [Pa*s]
%'Pr'-> Prandtl Number

k=strcmp(P,'D'); %density [kg/m3]
if k>0
   prop=-0.614254*T-0.000321*T^2+1020.62;
end
k=strcmp(P,'C'); %specific heat [kJ/kg*K]
if k>0
   prop=0.003313*T+0.0000008970785*T^2+1.496005;
end
k=strcmp(P,'L'); %thermal conductivity [W/mK]
if k>0
   prop=-0.000033*T-0.00000015*T^2+0.118294;
end
k=strcmp(P,'V'); %dynamic viscosity [Pa*s]
if k>0
   kv=exp(586.375/(T+62.5)-2.2809);
   d=-0.614254*T-0.000321*T^2+1020.62;
   prop=kv*d*10^-6;
end
k=strcmp(P,'Pr'); %Prandtl Number
if k>0
   kv=exp(586.375/(T+62.5)-2.2809);
   d=-0.614254*T-0.000321*T^2+1020.62;
   m=kv*d*10^-6;
   cp=0.003313*T+0.0000008970785*T^2+1.496005;
   l=-0.000033*T-0.00000015*T^2+0.118294;
   prop=m*cp*10^3/l;
end
```

This function allows treating thermal oil as Refprop fluids, so calculating thermodynamic properties from pressure and temperature.

Fouling factor resistance is considered in order to evaluate effective heat transfer coefficient $\alpha_{conv}|_{nx}^{t}$ for tube-side fluid.

$\alpha_{conv}|_{nx}^{t}$ is input signal of "*Q_conv*" subsystem; which calculates convective heat transferred between fluid and pipe $\dot{q}_{conv}|_{nx}^{t}$. In order to evaluate $\dot{q}_{conv}|_{nx}^{t}$ also pipe temperature vector $T_{pipe}\big|_{nx}^{t}$ is needed.

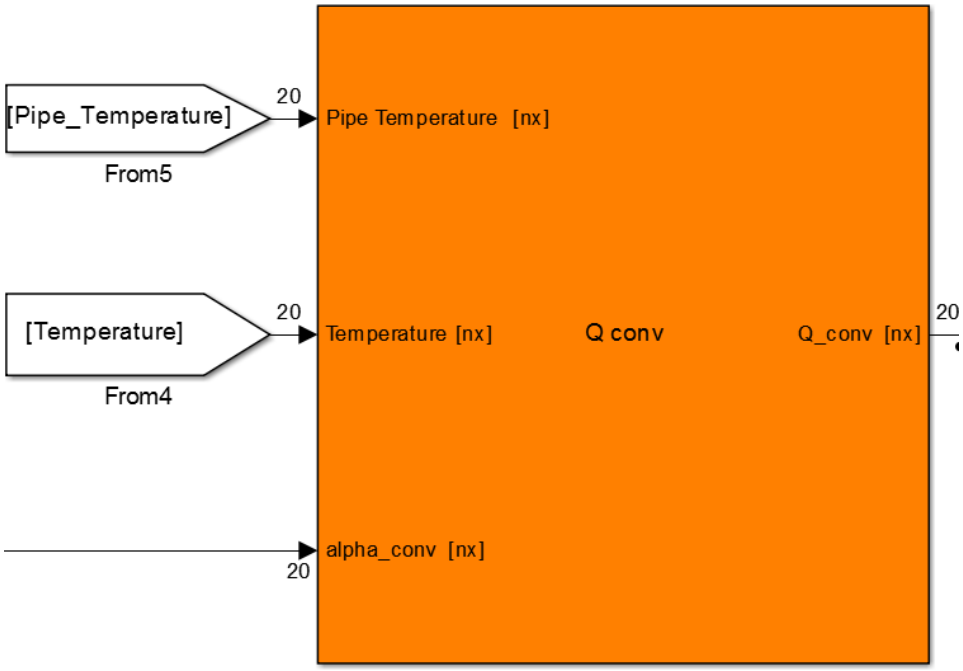

Fig. A2. 19 "Q conv" subsystem block, Tube-side fluid subsystem, Countercurrent Shell&Tube heat exchanger, (*level 3 of hierarchy*)

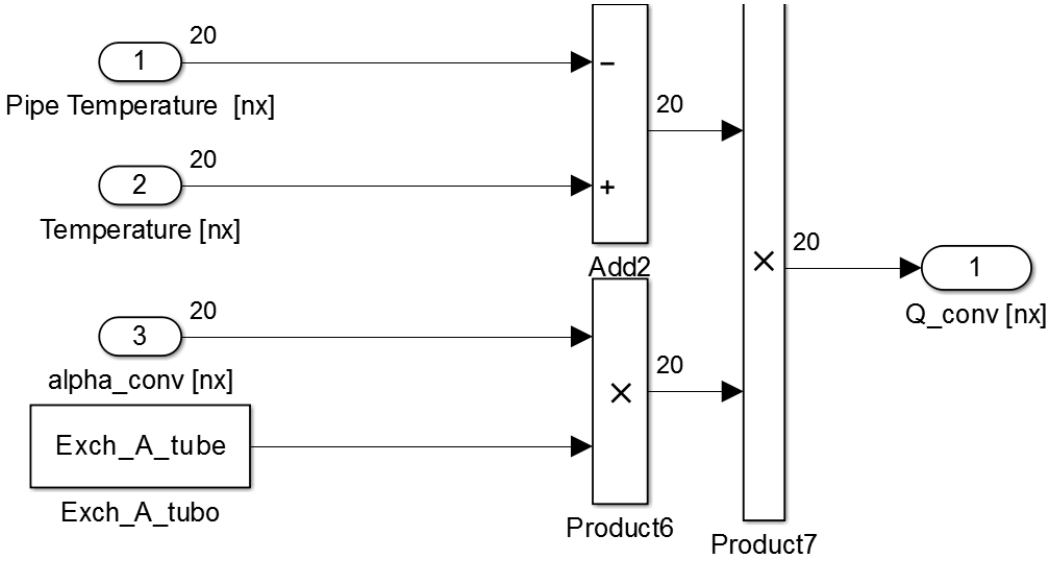

Fig. A2. 20 "Q conv" subsystem block, Tube-side fluid subsystem, Countercurrent Shell&Tube heat exchanger, (*level 4 of hierarchy*)

Block diagram in Fig A2. 20 performs following equation:

$$\dot{q}_{conv}|_{nx}^{t} = \alpha_{conv}|_{nx}^{t} \cdot A \cdot \left(T|_{nx}^{t} - T_{pipe}|_{nx}^{t}\right)$$

"*m cp dT*" subsystem provides specific heat coefficients vector $c_p|_{nx}^{t}$ and vector of heat transferred between two subsequent fluid units $\left[\dot{m}\, c_p(T_i - T_{i-1})\right]|_{nx}^{t}$.

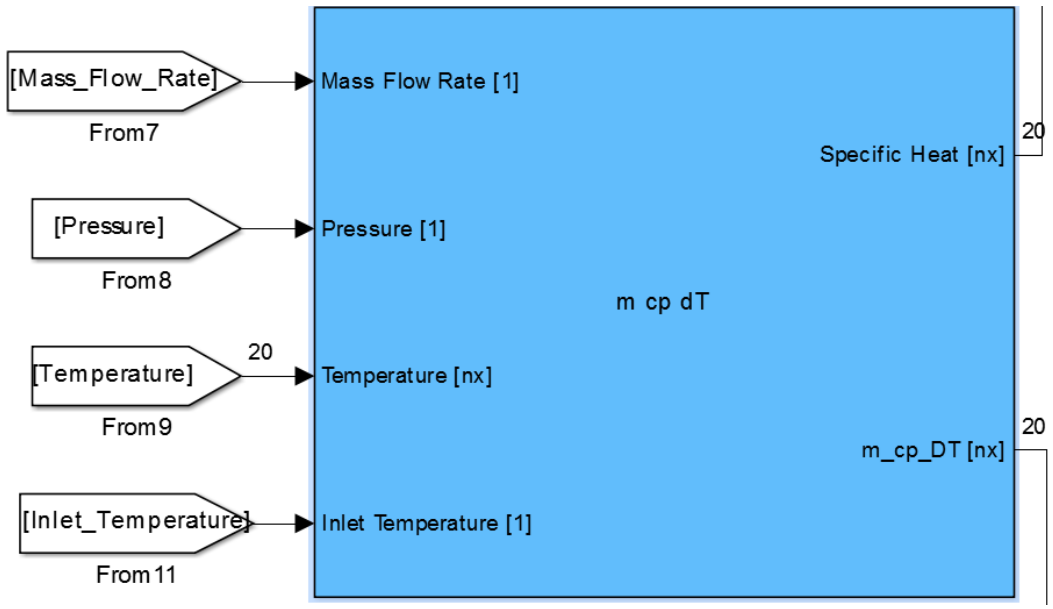

Fig. A2. 21 "m cp DT" subsystem block, Tube-side fluid subsystem, Countercurrent Shell&Tube heat exchanger, (*level 3 of hierarchy*)

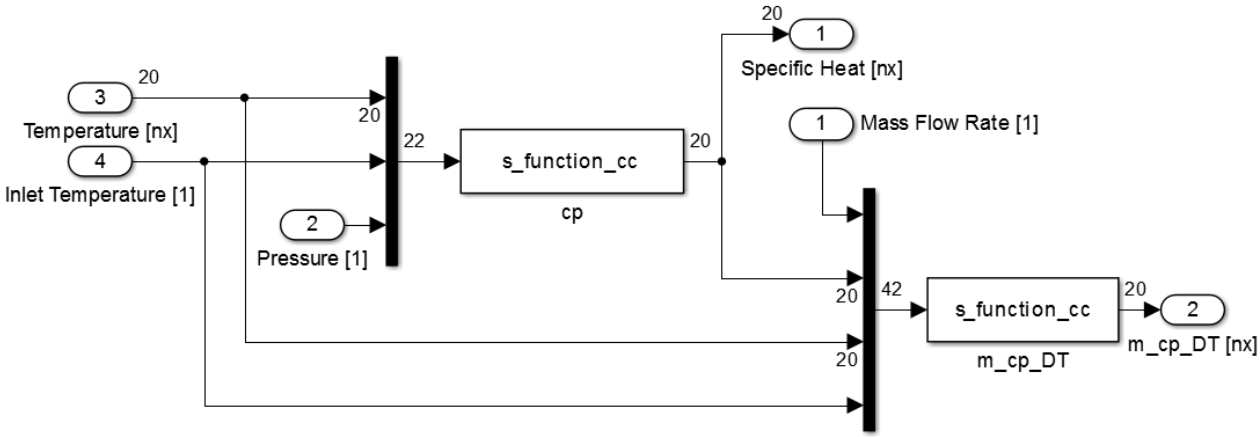

Fig. A2. 22 "m cp dT" subsystem block, Tube-side fluid subsystem, Countercurrent Shell&Tube heat exchanger, (*level 4 of hierarchy*)

"*cp*" and "*m_cp_DT*" s-function are presented:

```
%cp (in=nx+2, out=nx)
```

```
p=u(nx+2)*100;
for i= 1:nx
   T=(u(i)+u(i+1))/2;
   k=strcmp(specie,'diat_oil');
   if k>0
      cp=prop_therminol('C',T);
   else
      [cp]=refpropm('C','T',T+273.15,'P',p,specie);
      cp=cp/1000;
   end
   Output(1,i)=cp;
end

%m_cp_DT (in=2*nx+2, out=nx)
   for i=1:nx
     Output(i)=u(1)*u(i+1)*(u(nx+2+i)-u(nx+1+i));
end
```

Output vectors of "*Q conv*" and "*m cp DT*" are sent to "*new T*" subsystem, which evaluates the variation of Tube-side fluid temperature vector from time *t* to time *t+Δt*: $[T|_{nx}^{t+\Delta t} - T|_{nx}^{t}]$.

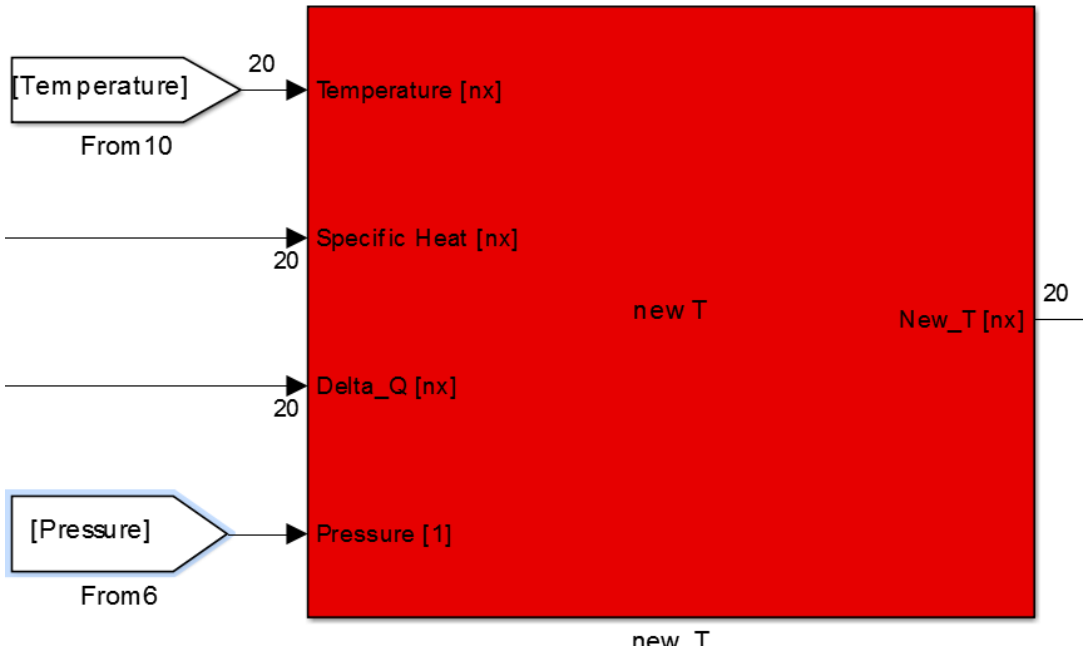

Fig. A2. 23 "new T" subsystem block, Tube-side fluid subsystem, Countercurrent Shell&Tube heat exchanger, (*level 3 of hierarchy*)

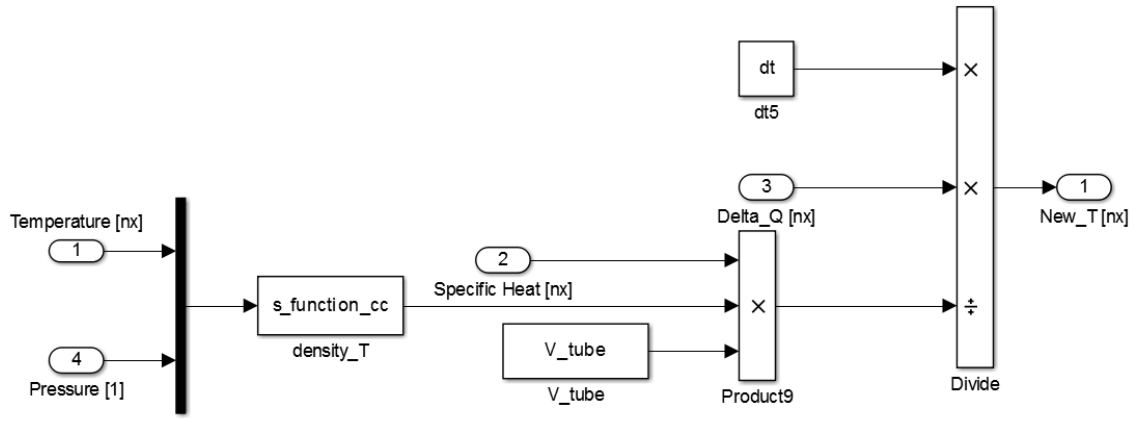

Fig. A2. 24 "new T" subsystem block, Tube-side fluid subsystem, Countercurrent Shell&Tube heat exchanger, (*level 4 of hierarchy*)

Energy conservation is guaranteed applying equation:

$$[H|_{nx}^{t+\Delta t} - H|_{nx}^{t}] = \frac{\left(\dot{q}_{conv}|_{nx}^{t} - \dot{m}\, c_p(\Delta T)\big|_{nx}^{t}\right)\, \Delta t}{\rho\, V\, c_p}$$

S-function "*density_T*" provides the fluid density vector:

```
%density_T (in=nx+1, out=nx);
  p=u(nx+1)*100;
  for i=1:nx
    T=u(i);
    k=strcmp(specie,'diat_oil');
    if k>0
      rho=prop_therminol('D',T);
    else
      rho=refpropm('D','T',T+273.14,'P',p,specie);
    end
    Output(i)=rho;
  end
```

"*new_T*" output vector is state-variables the loop cycle in Fig A2. 24:

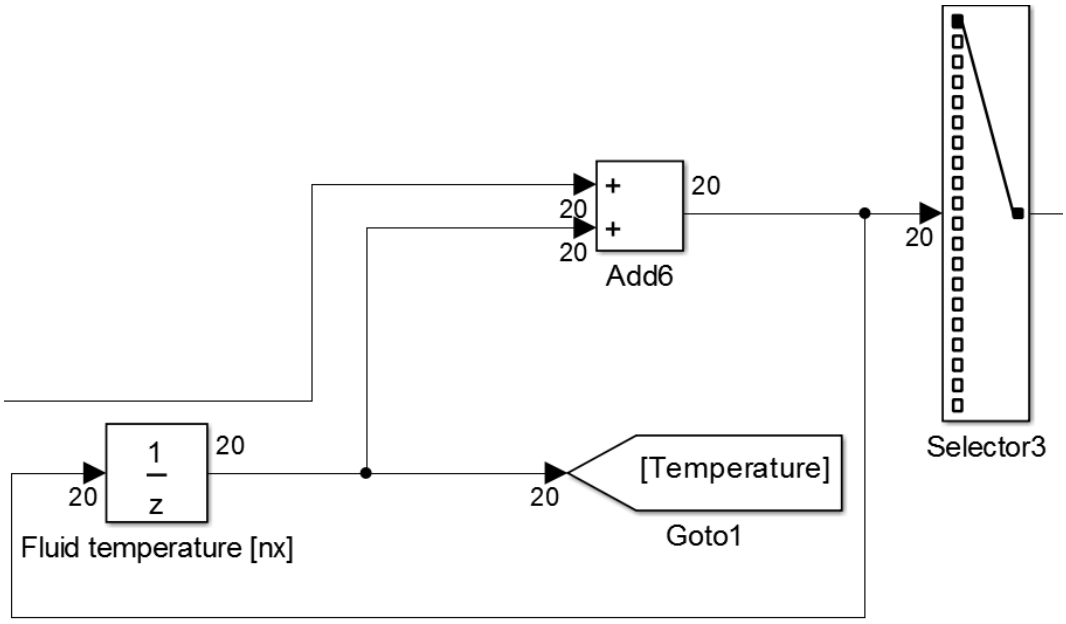

Fig. A2. 25 Fluid temperature loop of Tube-side fluid subsystem, Countercurrent Shell&Tube heat exchanger, (*level 3 of hierarchy*)

The selector block extracts the first element of Temperature vector and sends it as output signal of the component.

In accordance with model assumptions, tube side fluid outlet pressure and mass flow rate are equal to their inlet value.

Pipe subsystem

Input and output vectors of "*Pipe*" subsystem are shown in Fig. A2. 26:

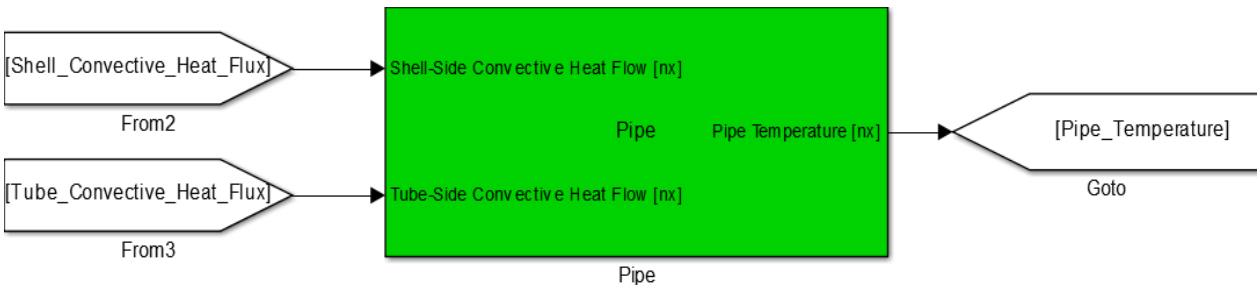

Fig. A2. 26 Tube-side fluid subsystem block, Countercurrent Shell&Tube heat exchanger (*level 2 of hierarchy*)

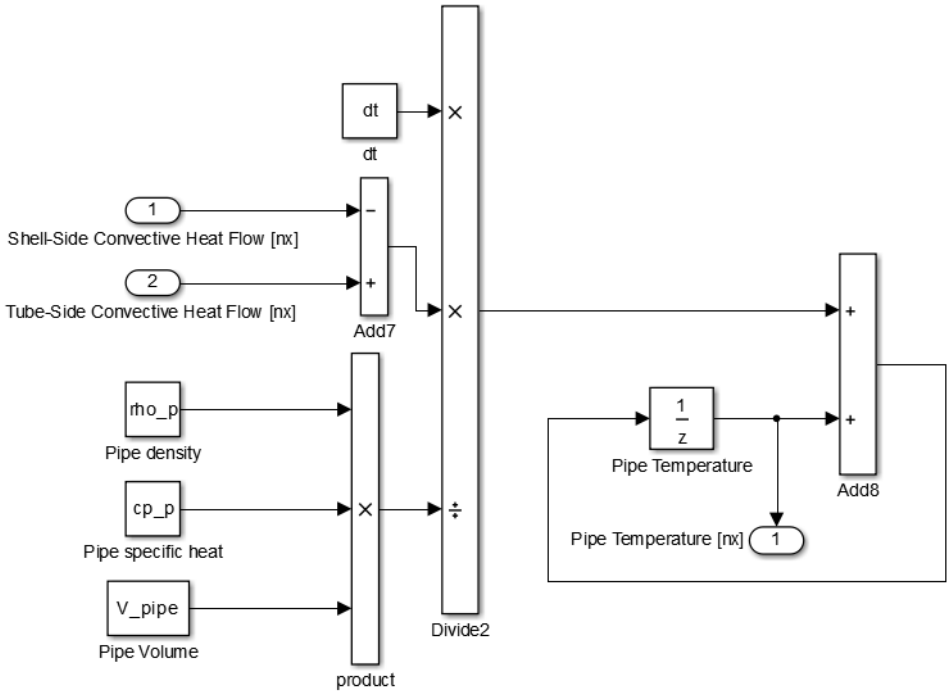

Fig. A2. 27 Block diagram of Pipe subsystem, Countercurrent Shell&Tube heat exchanger, (*level 3 of hierarchy*)

"Pipe" subsystem receives from "*Shell-side Fluid*" and "*Tube-side Fluid*" subsystems signals of convective heat fluxes vectors.

Energy conservation is applied by mean of equation:

$$\left[T_{pipe}\big|_{nx}^{t+\Delta t} - T_{pipe}\big|_{nx}^{t}\right] = \frac{\left(\dot{q}_{tube}\big|_{nx}^{t} - \dot{q}_{shell}\big|_{nx}^{t}{}_{nx}^{t}\right)\Delta t}{\rho_{pipe}\, V_{pipe}\, c_{p,pipe}}$$

Loop shown in Fig. A2. 26 allows calculating pipe temperature vector at following step time, subsequently sent to "*Shell-side Fluid*" and "*Tube-side Fluid*" subsystems.

One pass shell-side, two pass tube-side

One pass shell-side, two pass tube-side heat exchanger model is here presented. To model the two passes of tube-side fluid, both fluid and pipe are discretized in 2*nx* units, while shell-side fluid still in *nx* units as previous model.

"*Shell-side Fluid*" subsystem needs to modified in order to take account of new exchanger configuration. Since the two other subsystems are discretized in 2*nx* control volumes, also "*Shell-side Fluid*" subsystem will be discretized into 2*nx* fictitious units, in order to can be connected with them. Each unit of shell-side fluid volume is split up into two fictitious units; having same temperature and properties of starting unit, but linked with different pipe units. The heat transferred by each couple of fictitious units are subsequently summed together in order to calculate the temperature (or enthalpy) of the *nx* starting unit at following time step.

"Tube-side Fluid" and *"Pipe"* subsystem are modelled exactly as Countercurrent heat exchanger model, only discretized into 2*nx* parts. Only "*Shell-side Fluid"* subsystem is analyzed in this section, in order to highlight differences from previous model.

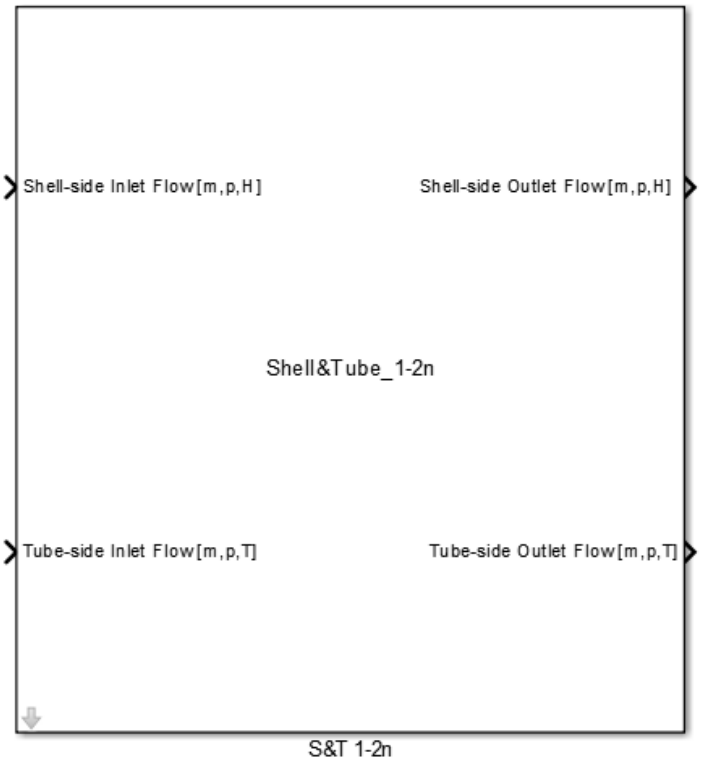

Fig. A2. 28 Simulink block of 1-2n Shell&Tube heat exchanger (level 1 of hierarchy)

Going down to a lower level of hierarchy (level 2), system is subdivided into three different subsystems as previous model; the only difference is that dimension of interconnection signal vectors is 2*nx* instead of *nx*.

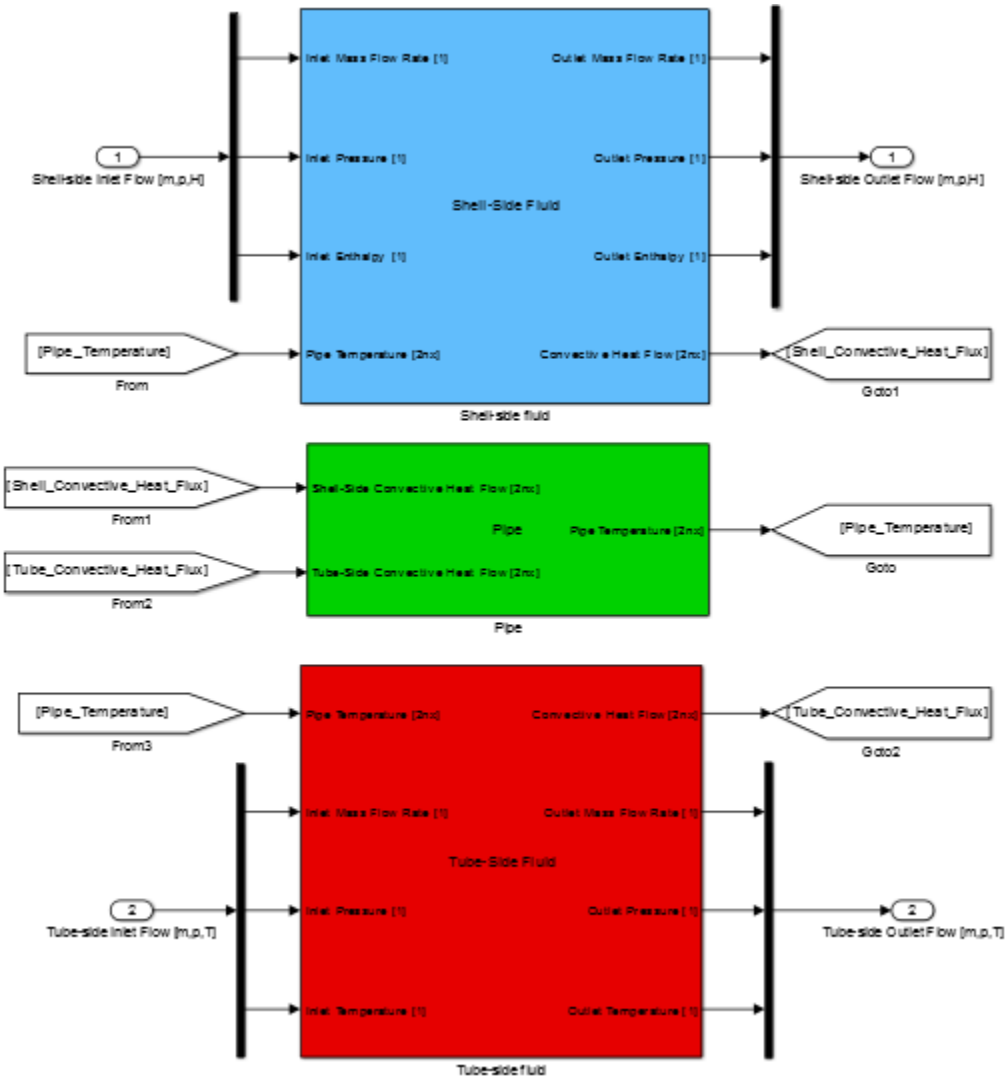

Fig. A2. 29 Block diagram of 1-2n Shell&Tube heat exchanger (level 2 of hierarchy)

Shell-side fluid subsystem

Input and output of such subsystem are shown in Fig. A2. 30:

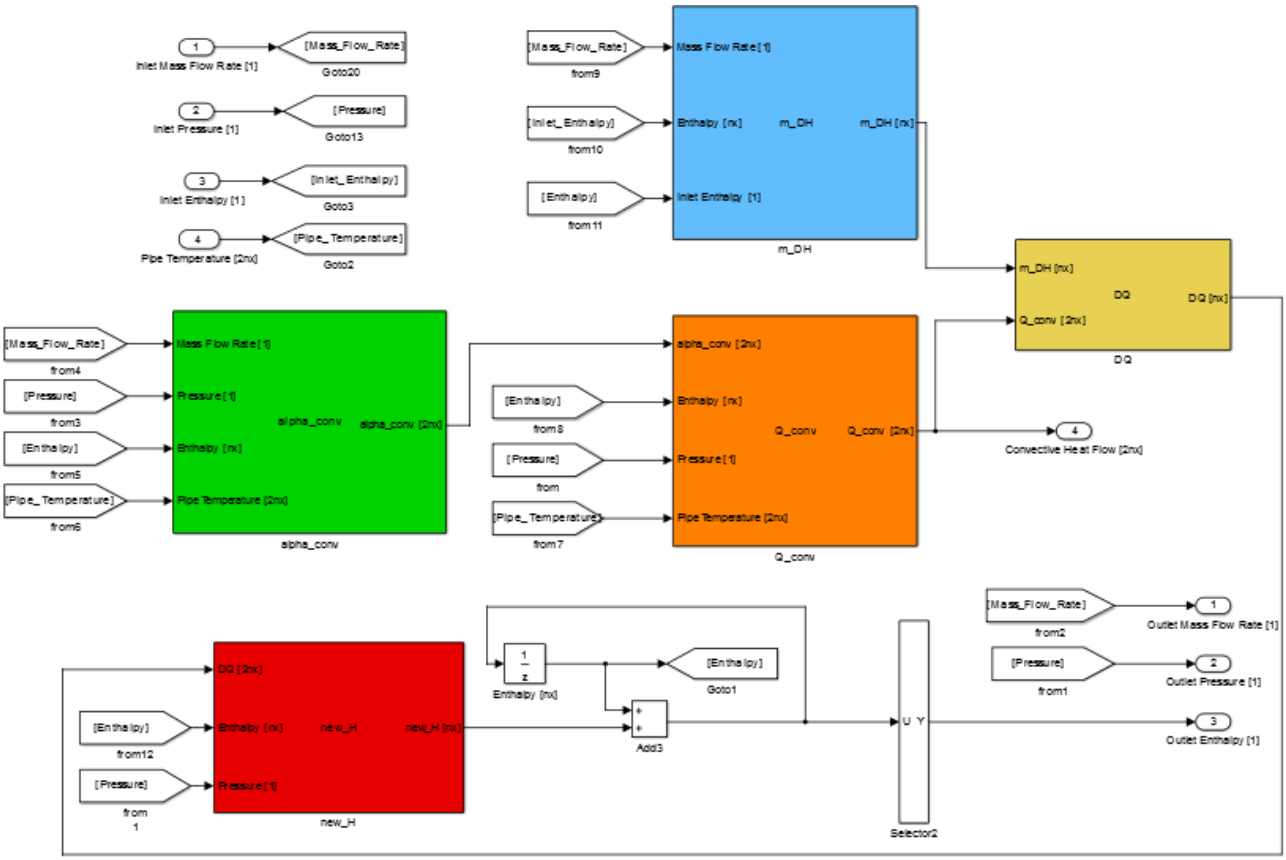

Fig. A2. 30 Block diagram of Shell-side fluid subsystem1-2n Shell&Tube heat exchanger, (level 3 of hierarchy)

Subsystem configuration is the same of countercurrent exchanger model, only an additional subsystem is added.

Output vector of "*alpha_conv*" subsystem is now composed by 2*nx* elements instead of *nx* as previous model. "*alpha_conv*" subsystem bock diagram is presented in Fig. A2. 31:

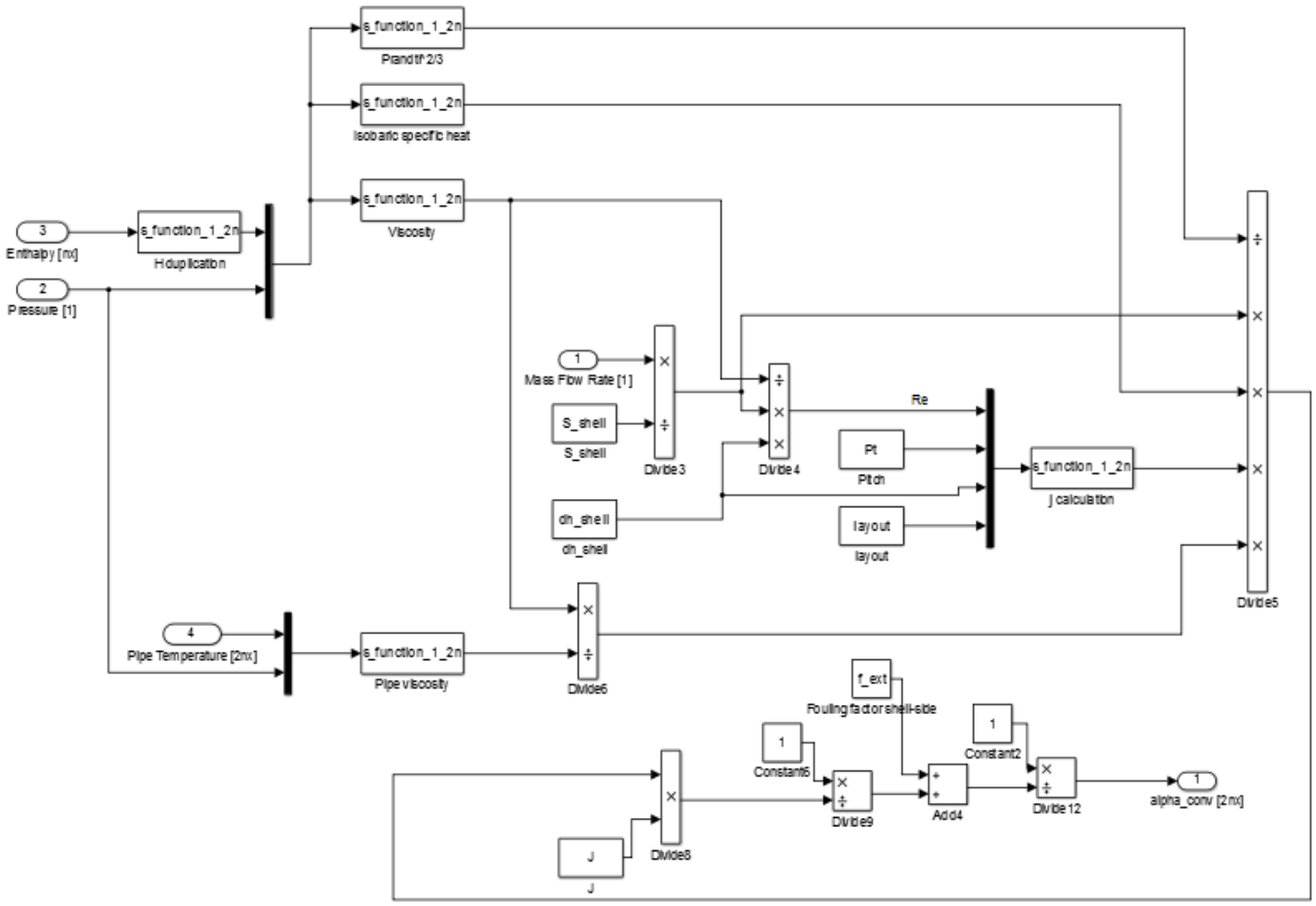

Fig. A2. 31 "alpha" subsystem block, Shell-side fluid subsystem, 1-2n Shell&Tube heat exchanger, (level 4 of hierarchy)

An additional s-function is introduced: "*H_duplication*". It creates an enthalpy vector of dimension 2*nx* splitting up each fluid unit::

```
%H_duplication (in=nx, out=2*nx);
  for i=1:nx
    Output(i)=u(i);
    Output(2*nx+1-i)=u(i);
  End
```

The output signal is convective heat transfer coefficients vector at time *t:* $\alpha_{conv}|_{2nx}^{t}$.

"*Q_conv*" and "*m_DH*" subsystems are not changed; the only difference is that "*Q_conv*" operates with vectors of 2*nx* dimensions. The output signals of such subsystems are respectively $\dot{q}_{conv}|_{2nx}^{t}$ and $\dot{m}(\Delta H)|_{nx}^{t}$. The two vectors are not of same dimension and cannot be directly subtracted. For that purpose "*DQ*" subsystem is introduced:

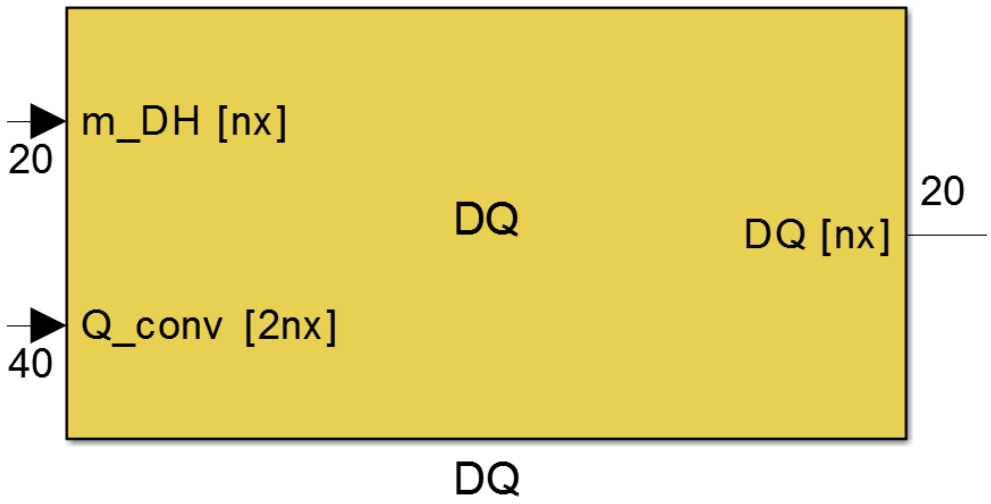

Fig. A2. 32 "alpha" subsystem block, Shell-side fluid subsystem, Countercurrent Shell&Tube heat exchanger, (*level 3 of hierarchy*)

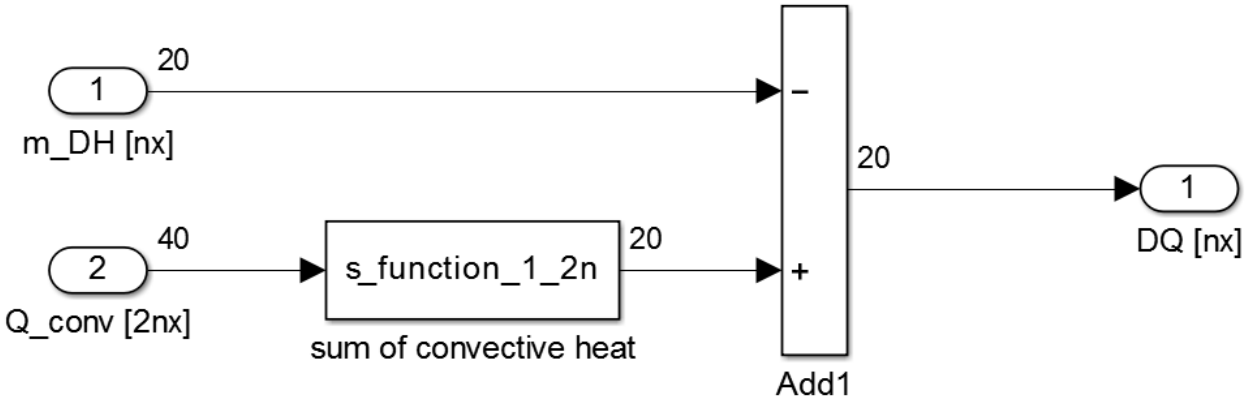

Fig. A2. 33 "alpha" subsystem block, Shell-side fluid subsystem, Countercurrent Shell&Tube heat exchanger, (*level 4 of hierarchy*)

"*sum of convective heat*" s-function provides summing together heat fluxes of fictitious units couple:

```
%sum of convective heat (in=2*nx, out=nx);
  for i=1:nx
    Output(i)=(u(i)+u(2*nx+1-i));
  end
```

Two pass shell-side, four pass tube-side

Two pass shell-side, four pass tube-side model is here presented. This exchanger is modelled by combining two "*signle pass shell-side, two pass tube-side*" heat exchanger models. Component mask is presented in Fig. A2. 34:

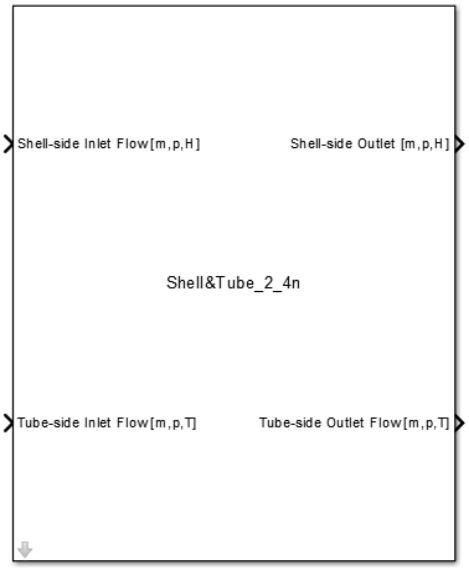

Fig. A2. 34 Simulink block of 2-4n Shell&Tube heat exchanger (*level 1 of hierarchy*)

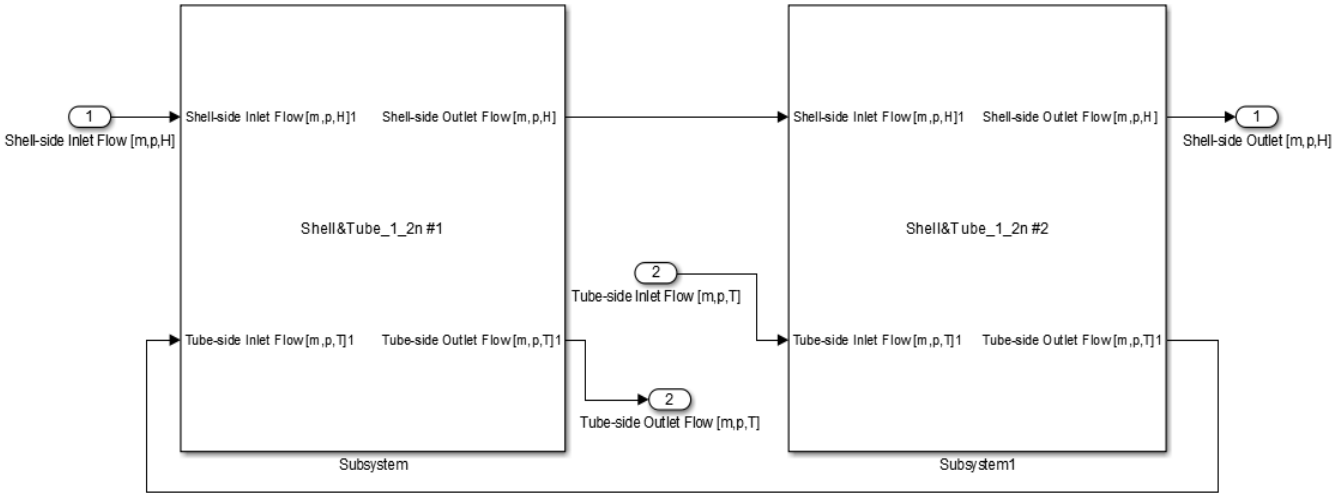

Fig. A2. 35 Block diagram of Countercurrent Shell&Tube heat exchanger (*level 2 of hierarchy*)

Shell side fluid flows before in "*Shell&Tube_1_2n #1*" and then in "*Shell&Tube_1_2n #2*" while tube side fluid flows throughout exchangers in opposite direction; thus creating the desired arrangement.

Exchanger with change phase

In this section the Simulink model of Exchangers with change phase are presented. Two modelled components are included in this category:

- Evaporator
- Condenser

These two components are modelled with the same approach. Tube side fluid and Pipe subsystems are modelled as "*Exchanger with no-change phase*" model.

Shell side fluid is not discretized into units as previous model; but it is considered a unique unit in perfect equilibrium concerning liquid and vapor phase. In accordance with this assumption, only pressure value is sufficient to calculate all fluid properties for both liquid and vapor phase. For Shell-side fluid energy and mass balance equations are applied. For Shell-side fluid in fact also mass storage is considered.

Kettle Evaporator Simulink model

The considered evaporator is a shell&tube kettle evaporator. Tube-side fluid and Pipe subsystems are modelled as presented for "*Exchanger with no-change phase*"; therefore they are not analyzed again.

Shell-side fluid total mass is composed by both liquid and vapor mass, in accordance with perfect bi-phase equilibrium assumption. Kettle is considered filled with a liquid flow, close to saturation point; while the outlet flow is saturated vapor. A tube bundle where hot fluid circulates is submerged into liquid mass; supposed in boiling conditions.

Kettle evaporator block mask is presented in Fig. A2. 34:

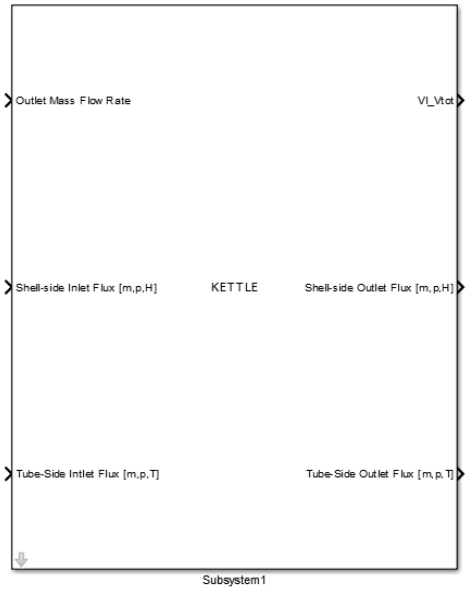

Fig. A2. 36 Simulink block of Kettle evaporator (level 1 of hierarchy)

For shell-side fluid initial pressure and initial liquid level (ratio between volume occupied by liquid phase and global volume) are to be provided for simulation starting. They represent the state-variables of the component, in addition to tube-side fluid and pipe temperature vector.

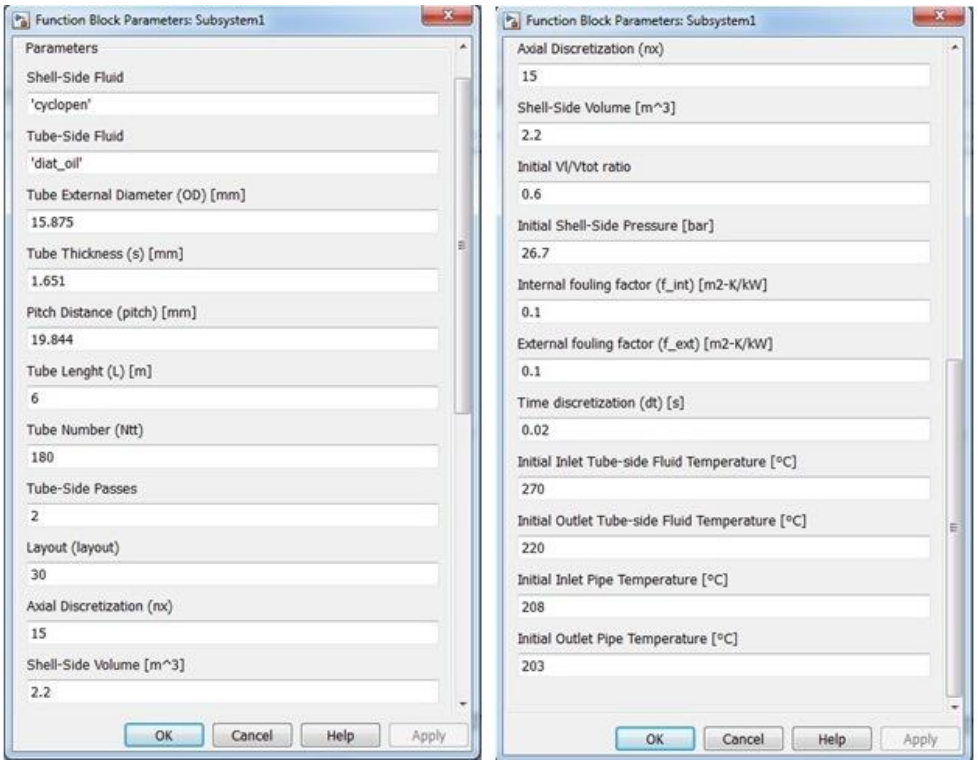

Fig. A2. 37 Parameter dialog block of Kettle evaporator

Going down to a lower level of hierarchy (level 2), system is again subdivided into three different subsystems: Shell-side fluid, Tube-side fluid and Pipe.

"*Shell-side fluid*" subsystem is presented in Fig. A2. 38:

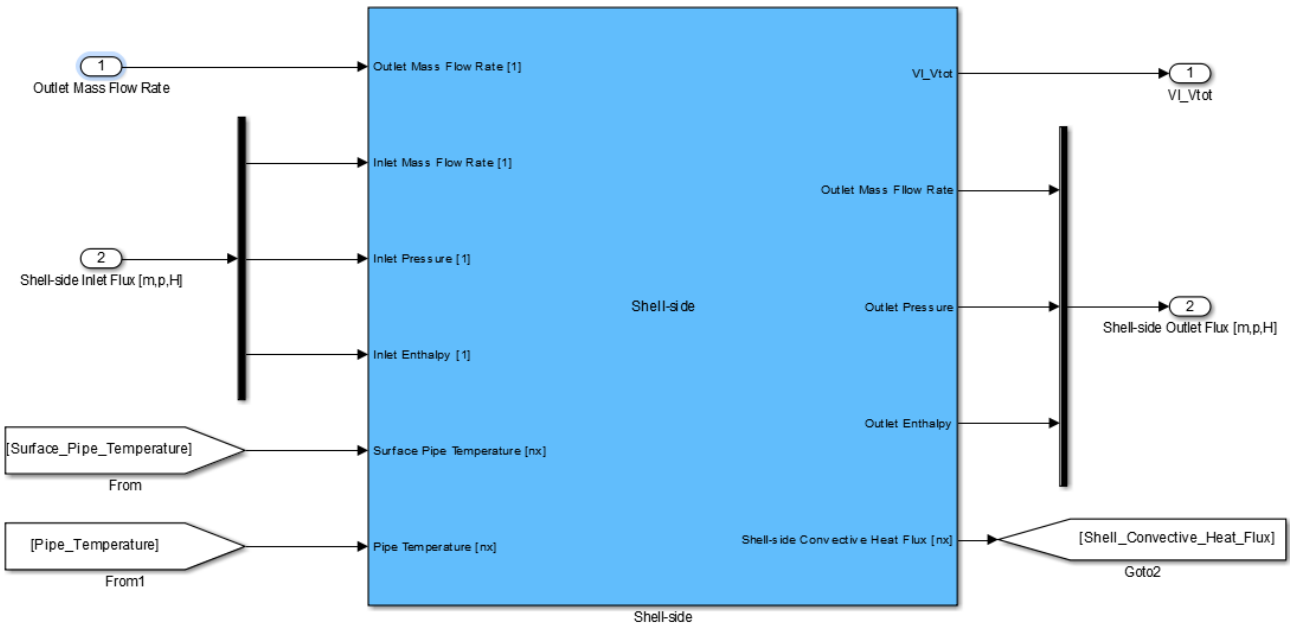

Fig. A2. 38 Shell-side fluid subsystem block, Kettle evaporator (*level 2 of hierarchy*)

Compared to "*Exchanger with no-change phase*" models, two additional input signals are considered: "*Outlet Mass Flow Rate*" and "*Surface_Pipe_Temperature*".

"*Outlet Mass Flow Rate*" refers to mass flow rate that outs the component.

"*Surface_Pipe_Temperature*" is pipe surface temperature vector. Boiling heat transfer coefficients are very sensitive to wall temperature, so a more accurate calculation of external surface temperature is necessary, instead of average pipe temperature.

Internal pressure is not real input signal of the component model; nevertheless it is presented as input signal only in order to simulate effective inlet flow. Inlet pressure shell be greater than shell pressure, otherwise inlet fluid cannot flows into the kettle. In ORC system model this is achieved by imposing pump outlet pressure equal to evaporator pressure and neglecting pressure losses.

Shell-side block scheme is here presented:

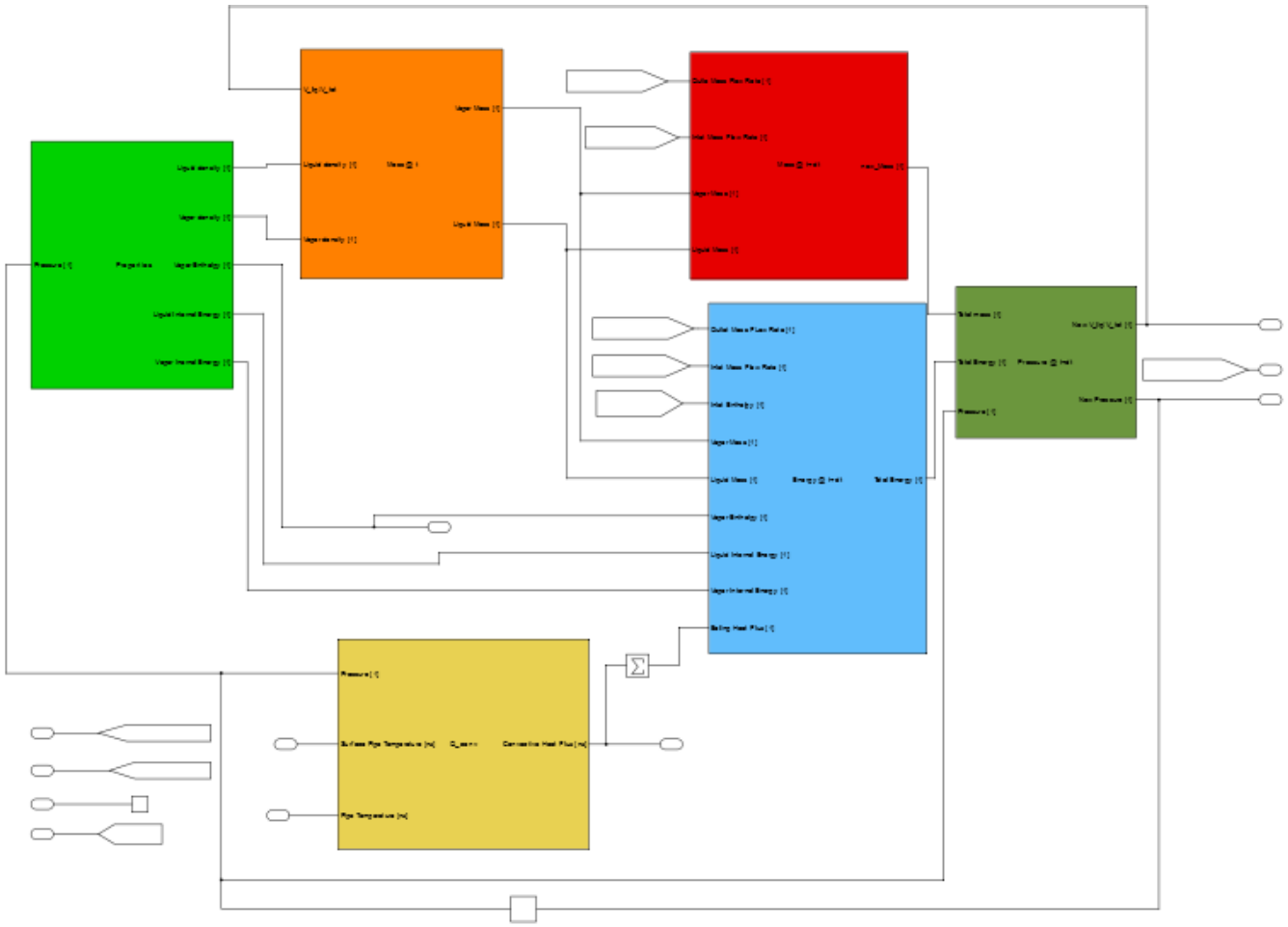

Fig. A2. 39 Block diagram of Shell-side fluid subsystem, Kettle evaporator, (*level 3 of hierarchy)*

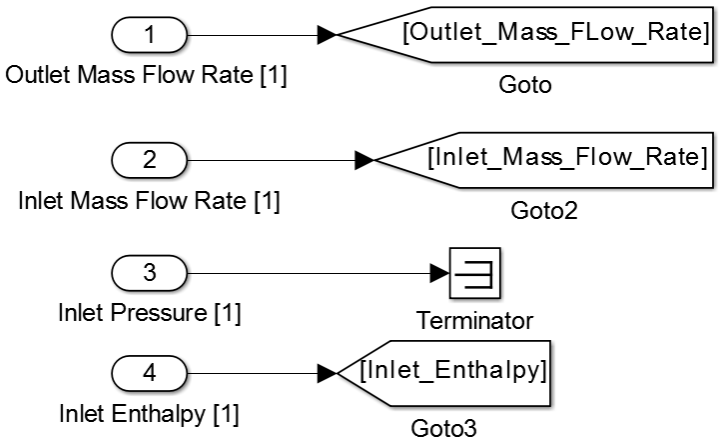

Fig. A2. 40 Input signals of Shell-side fluid subsystem, Kettle evaporator, (*level 3 of hierarchy*)

As inlet pressure is not an input signal, it directly linked to a terminator block.

The first subsystem analyzed is “properties” subsystem (light-green), presented in Fig.A2 41 and Fig. A2 42:

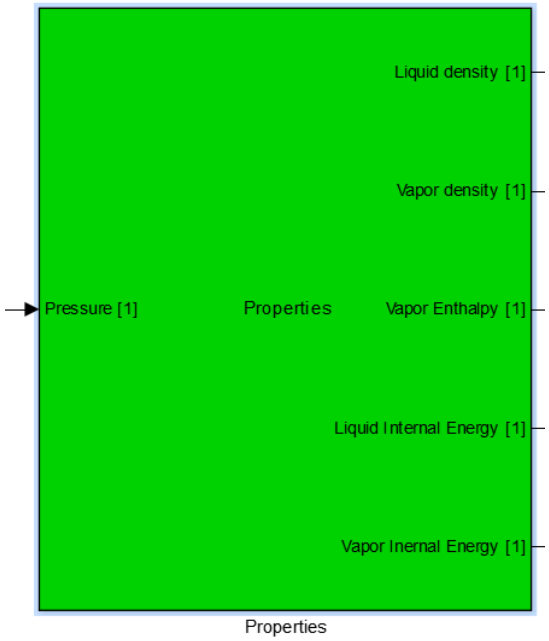

Fig. A2. 41 “Properties” subsystem block, Shell-side fluid subsystem, Kettle evaporator, (*level 3 of hierarchy*)

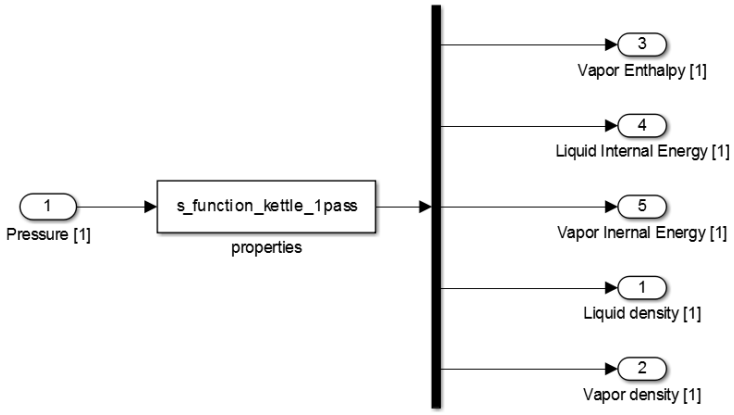

Fig. A2. 42 “Properties” subsystem block, Shell-side fluid subsystem, Kettle evaporator, (*level 4 of hierarchy*)

“*properties*” s-function evaluates liquid and vapor thermodynamic properties such as enthalpy, density and internal energy at time *t*; They can be obtained by knowing fluid pressure at rime *t* p^t

```
%properties (in=1,out=5)

p=u(1)*100;
[ul, dl]=refpropm('UD','P',p,'Q',0,specie);
[hv, uv, dv]=refpropm('HUD','P',p,'Q',1,specie);
Output=[hv/1000 ul/1000 uv/1000 dl dv];
```

Liquid and vapor density at time *t* (ρ_l^t, ρ_v^t) are input signals of "*Mass @ t*" block, which evaluates shell side fluid total mass at time t by knowing liquid level in kettle evaporator $\frac{V_l^t}{V_{tot}}$.

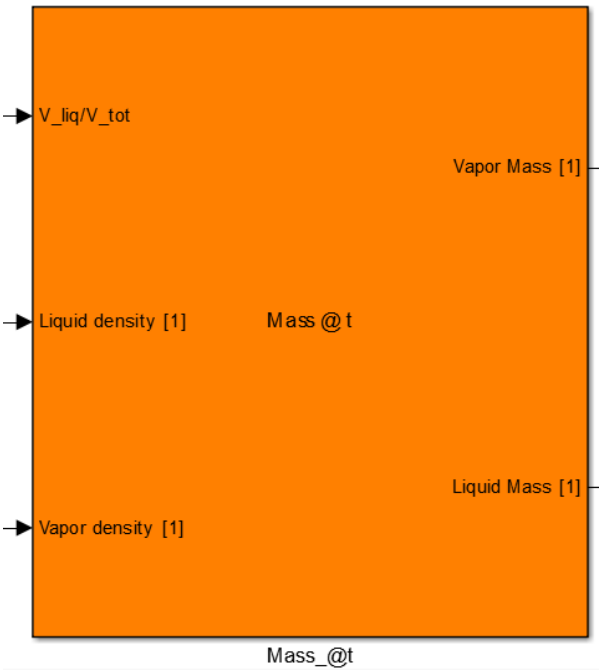

Fig. A2. 43 "Mass @ t" subsystem block, Shell-side fluid subsystem, Kettle evaporator, (*level 3 of hierarchy*)

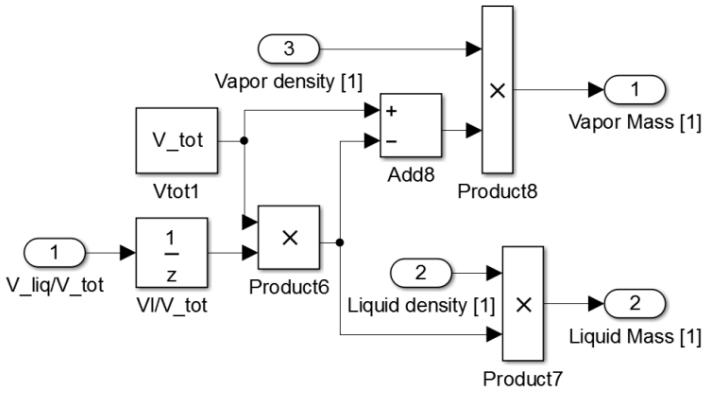

Fig. A2. 44 "Mass @ t" subsystem block, Shell-side fluid subsystem, Kettle evaporator, (*level 4 of hierarchy*)

"Mass @ t" subsystem performs following two equations:

$$m_l^t = \rho_l^t \, V_l^t$$

$$m_v^t = \rho_v^t (V_{tot} - V_l^t)$$

The two output signals m_l^t and m_v^t, in addition to inlet and outlet mass flow rate ($\dot{m}_{in}^t$, $\dot{m}_{out}^t$), are sent by "*Mass @ t+dt*" subsystem to evaluate total fluid mass at following step of simulation $m_{tot}^{t+\Delta t}$ by mean of equation:

$$m_{tot}^{t+\Delta t} = m_l^t + m_v^t + (\dot{m}_{in}^t - \dot{m}_{out}^t)\,\Delta t$$

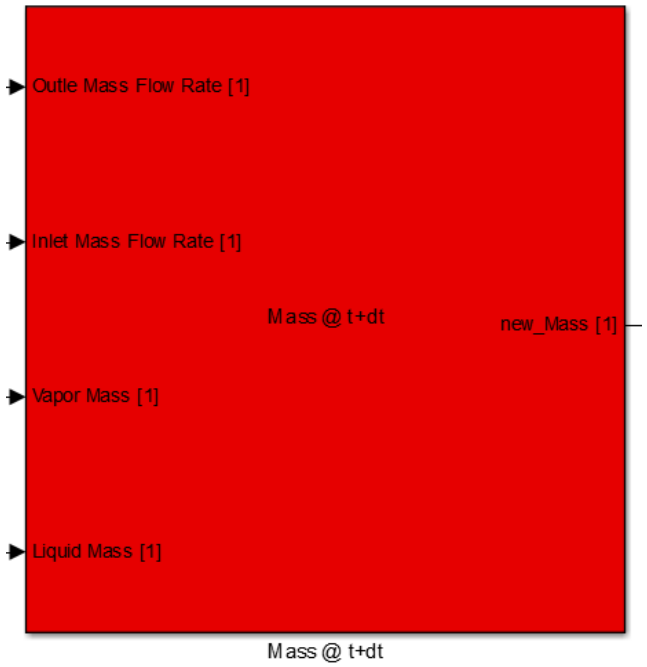

Fig. A2. 45 "Mass @ t+dt" subsystem block, Shell-side fluid subsystem, Kettle evaporator, (*level 3 of hierarchy*)

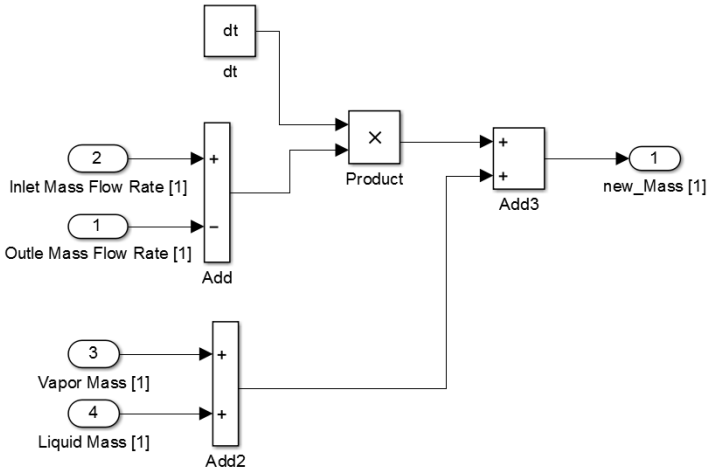

Fig. A2. 46 "Mass @ t+dt" subsystem block, Shell-side fluid subsystem, Kettle evaporator, (*level 4 of hierarchy*)

"*Q_conv*" subsystem provides heat flux transferred from pipe to shell-side fluid, considered in nucleate boiling conditions. Since pipe is discretized in *nx* units; also *nx* fictitious units of shell-side fluid temperature $T^t = f(p^t, x = 0)$ are introduced. Fluid and pipe can be interconnected, obtaining the *nx* dimension vector of transferred heat fluxes. The *nx* dimension vector is sent to "*Pipe*" subsystem in order to apply energy conservation equations to pipe. As the *nx* units are fictitious, all elements of such vector are summed together; obtaining total transferred heat flux, sent to "*Energy @ t+dt*" subsystem.

"*Q_conv*" is presented in Fig. A2. 47:

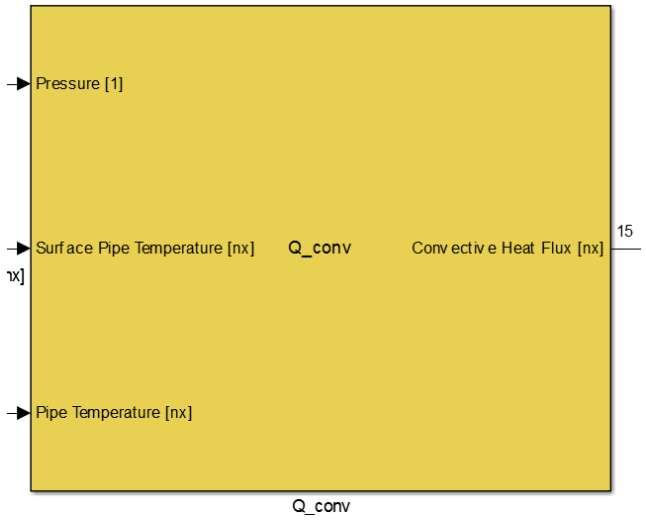

Fig. A2. 47 "Q conv" subsystem block, Shell-side fluid subsystem, Kettle evaporator, (*level 3 of hierarchy*)

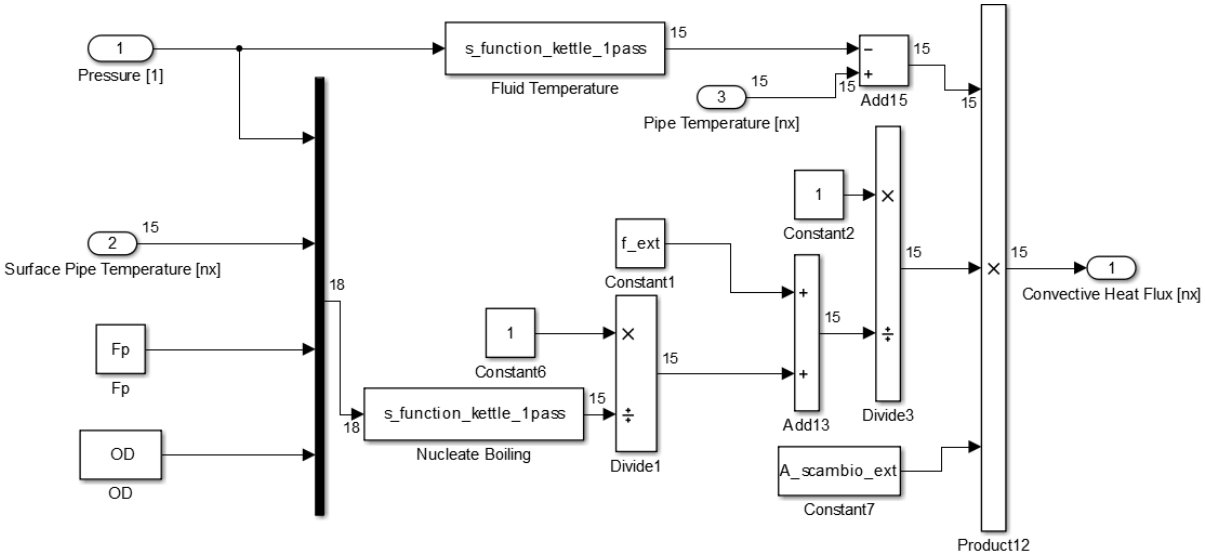

Fig. A2. 48 "Q conv" subsystem block, Shell-side fluid subsystem, Kettle evaporator, (*level 4 of hierarchy*)

"Fluid Temperature" s-function introduces the *nx* dimension vector of shell-side fluid temperature $T|_{nx}^{t}$:

```
%Fluid Temperature (in=1, out=nx)
   T_ev=refpropm('T','P',u(1)*100,'Q',0,specie);
   for i=1:nx
      Output(i)=T_ev-273.15;
   end
```

"*Nucleate Boiling*" s-function estimates the *nx* dimension vector of boiling heat transfer coefficients $h_{nb}|_{nx}^{t}$ by mean of "*N_Boiling*" Matlab function:

```
%Nucleate Boiling (in=nx+3, out=nx)
   for i=1:nx
      Output(i)=N_Boiling(u(1),u(i+1),u(nx+2),u(nx+3)/1000,specie);
   end


function [h_b]= N_Boiling (p,Tp,Fp,de,specie)

%Nucleate boiling heat transfer coefficient

%provide
%p - Pressure  [bar]
%Tp - Pipe Surface Temperature  [°C]
%Fp - Fp factor
%de - External tube diameter [m]


   [Pr_l, lamba_l, T_ev, M, a_l,b]=refpropm('^LTM$B','p',p*100,'Q',0,specie);
   a_l=a_l/(100^2);
   [p_cr]=refpropm('P','C',0,' ',0,specie);
   Pr=(p*100/p_cr);

   T_ev=T_ev-273.15;

   h_nb=(55*(Tp-T_ev)^0.67*Pr^0.12*(-log10(Pr))^(-0.55)*M^(-0.5))^(1/0.33);


   Gr=9.81*b*abs(Tp-T_ev)*de^3/a_l;
   Nu=(0.6+0.387*(Gr*Pr_l)^(1/6)/(1+(0.559/Pr_l)^(9/16))^(8/27))^2;
   h_nc=Nu*(lamba_l)/(de);

   h_b=(h_nc+Fp*h_nb)/1000;
end
```

Total transferred heat flux ($\dot{q}_{nb}^{t} = \sum \dot{q}_{nb}|_{nx}^{t}$) is sent to "*Energy @ t+dt*" subsystem which imposes energy conservation equation to shell control volume:

$$E_{tot}^{t+\Delta t} = m_l^t u_l^t + m_v^t u_v^t + (\dot{m}_{in}^t h_{in}^t - \dot{m}_{out}^t h_{out}^t + \dot{q}_{nb}^t)\,\Delta t$$

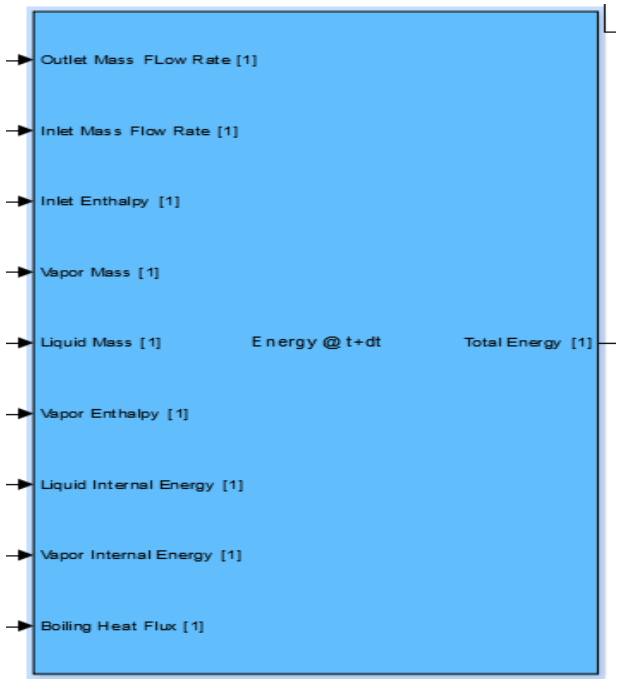

Fig. A2. 49 "Energy @t+dt" subsystem block, Shell-side fluid subsystem, Kettle evaporator, (*level 3 of hierarchy*)

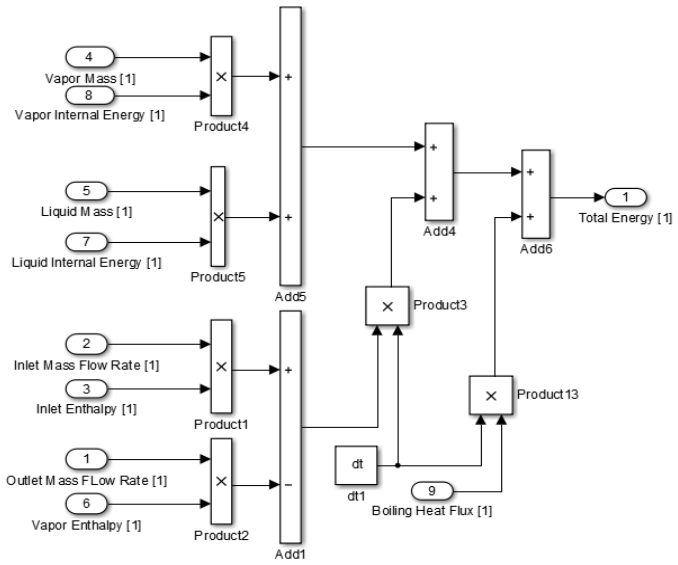

Fig. A2. 50 "Energy @t+dt" subsystem block, Shell-side fluid subsystem, Kettle evaporator, (*level 4 of hierarchy*)

Output signals of "*Energy @t+dt*" and "*Mass @ t+dt*" subsystems are sent to "*Pressure @t+dt*" subsystem which evaluates independent variables $p^{t+\Delta t}$, $\frac{V_l^{t+\Delta t}}{V_{tot}}$ at next step time..

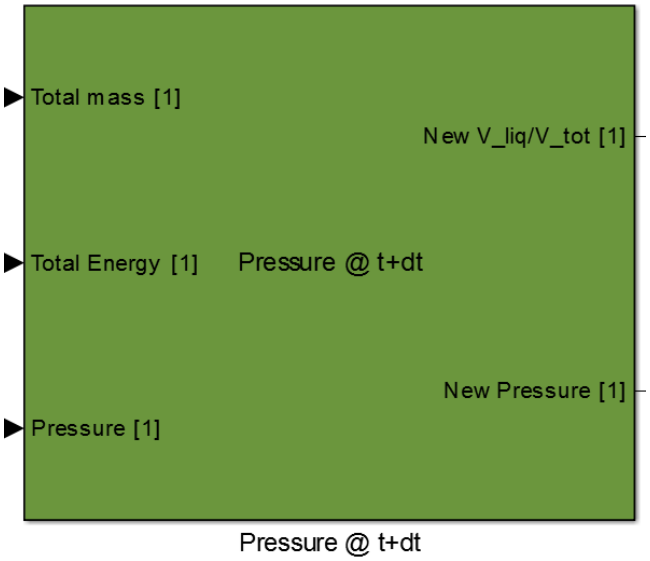

Fig. A2. 51 "Energy @t+dt" subsystem block, Shell-side fluid subsystem, Kettle evaporator, (*level 3 of hierarchy*)

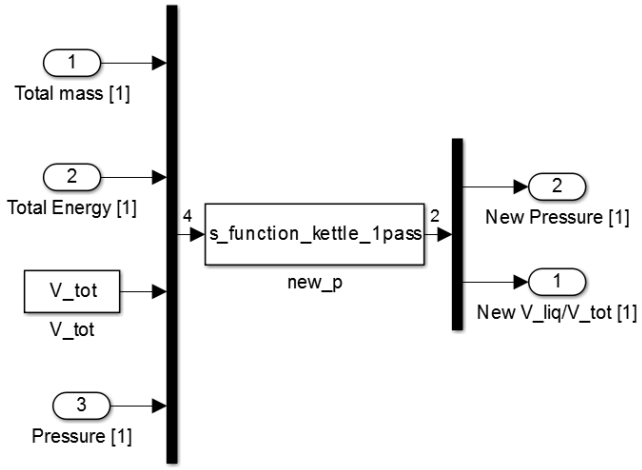

Fig. A2. 52 "Energy @t+dt" subsystem block, Shell-side fluid subsystem, Kettle evaporator, (*level 4 of hierarchy*)

"*new_p*" provides the value of pressure and liquid volume imposing mass, energy and volume conservation equations. It solves the following non-linear equation at step of simulation:

$$V_{tot} - \frac{E_{tot}^{t+\Delta t} - m_{tot}^{t+\Delta t}\, u_v^{t+\Delta t}}{\rho_l^{t+\Delta t}\left(u_l^{t+\Delta t} - u_v^{t+\Delta t}\right)} - \frac{m_{tot}^{t+\Delta t}\, u_l^{t+\Delta t} - E_{tot}^{t+\Delta t}}{\rho_v^{t+\Delta t}\left(u_l^{t+\Delta t} - u_v^{t+\Delta t}\right)} = 0$$

```
%new_p (in=4;out=2)
   m_tot=u(1);
   E_tot=u(2);
   V_tot=u(3);
   p=u(4)*100;

   f_p=@(p) V_tot-(E_tot-
m_tot*refpropm('U','P',p,'Q',1,specie)/1000)/(refpropm('D','P',p,'Q',0,specie)*(refpropm('U','P',p,'Q',0,sp
ecie)/1000-refpropm('U','P',p,'Q',1,specie)/1000))+(m_tot*refpropm('U','P',p,'Q',0,specie)/1000-
E_tot)/(refpropm('D','P',p,'Q',1,specie)
*(refpropm('U','P',p,'Q',0,specie)/1000-refpropm('U','P',p,'Q',1,specie)/1000))

p_new=fzero(f_p,p);

   dl=refpropm('UD','P',p_new,'Q',0,specie);
   dv=refpropm('UD','P',p_new,'Q',1,specie);

   m_vap=(V_tot-m_tot/dl)/(1/dv-1/dl);
   m_liq=m_tot-m_vap;

   V_liq=m_liq/dl;
   Vl_Vtot=V_liq/V_tot;

   Output=[p_new/100 Vl_Vtot];
```

Matlab "*fzero*" function allows solving the nonlinear equation "*f_p*"; function of *p* variable, starting from the initial value which corresponds to pressure at precedent step time.

"*Pipe*" and "*Tube-side fluid*" Simulink models are only shown and not analyzed:

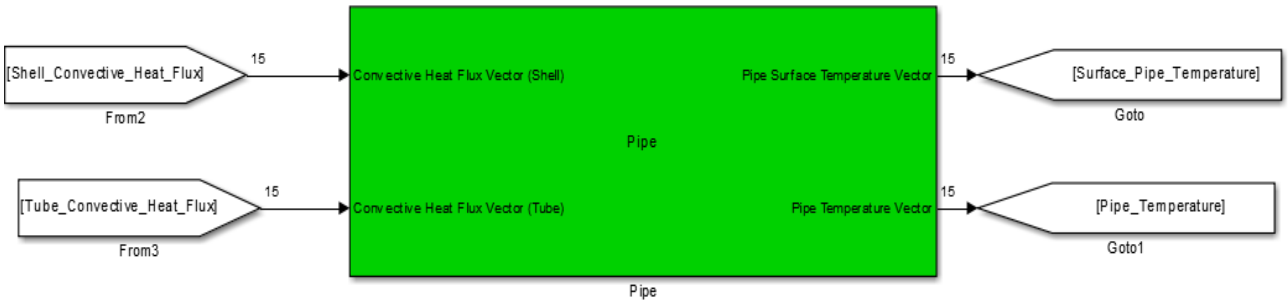

Fig. A2. 53 Pipe subsystem block, Kettle evaporator (*level 2 of hierarchy*)

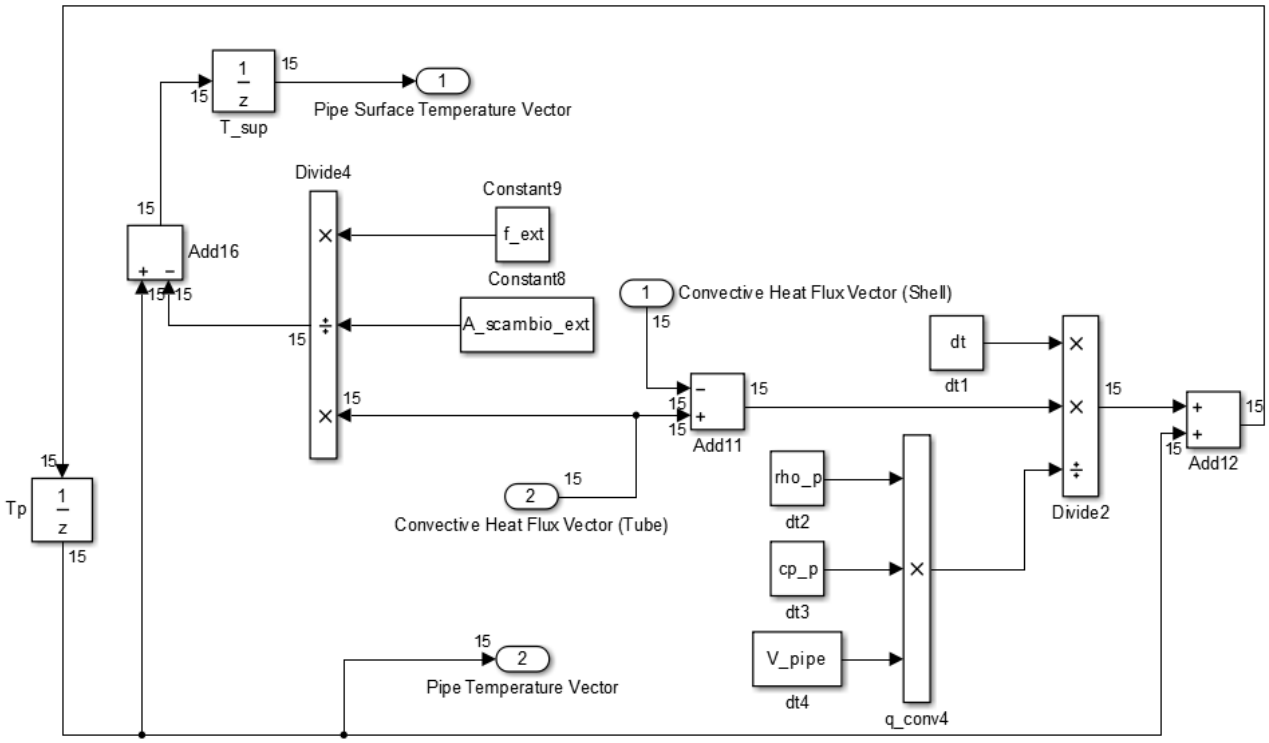

Fig. A2. 54 Block diagram of Pipe subsystem, Kettle evaporator, (*level 3 of hierarchy*)

Fig. A2. 55 Block diagram of Tube side fluid subsystem, Kettle evaporator, (*level 3 of hierarchy*)

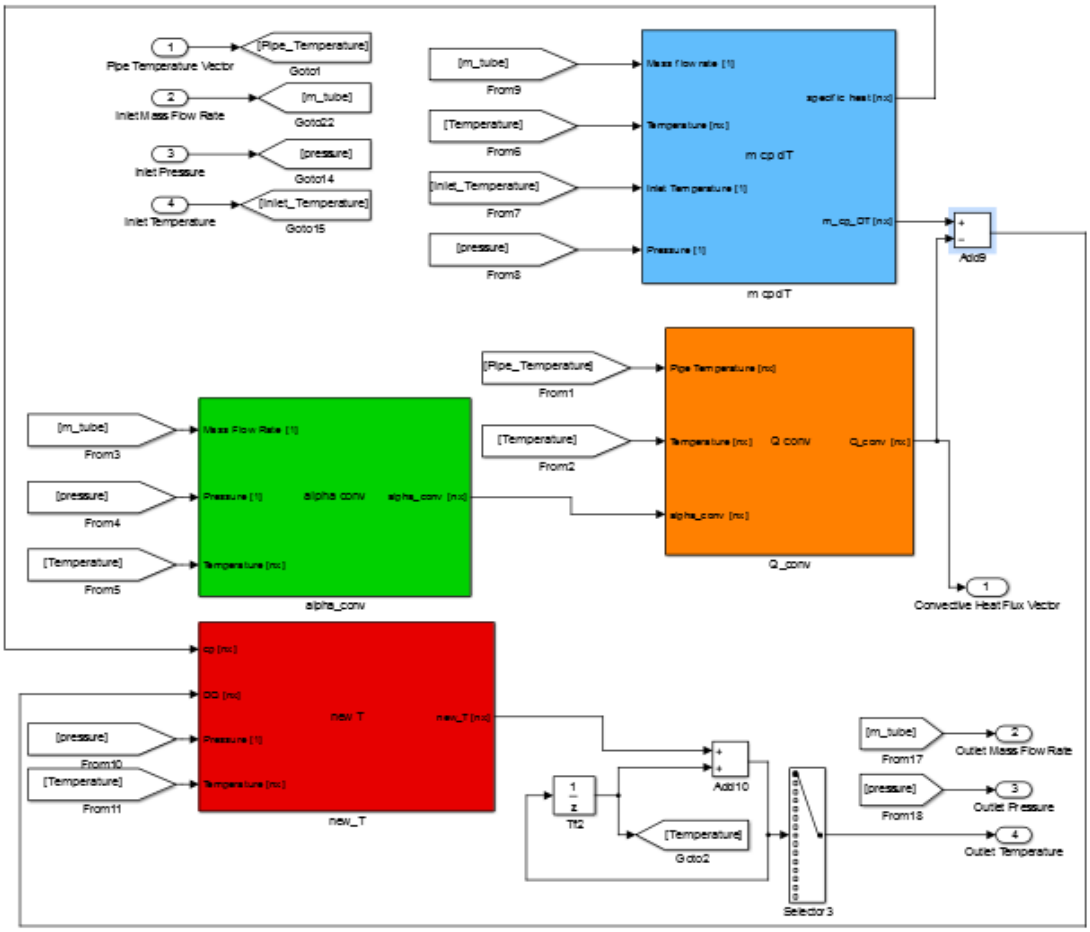

Fig. A2. 56 Block diagram of Tube side fluid subsystem, Kettle evaporator, (*level 3 of hierarchy*)

Condenser Simulink model

The condenser considered in that model is shell&tube condenser. The component is modelled as evaporator component; only few differences are introduced. Condenser is filled with superheated vapor and the outlet flow is saturated liquid.

Contrary to precedent model here finned tubes are used to enhance exchanger performances. Only subsystems that finned tubes performances are presented.

"*Fin efficiency*" subsystem, included in "*Shell-side Fluid*", leads to evaluate wall efficiency η_{wall} and *De* parameter both necessary to calculate condensation heat transfer coefficients for finned tubing. To evaluate η_{wall} average condensing heat transfer coefficient is necessary, in addition to geometric parameters provided in component parameter dialog.

The block diagram is shown in :

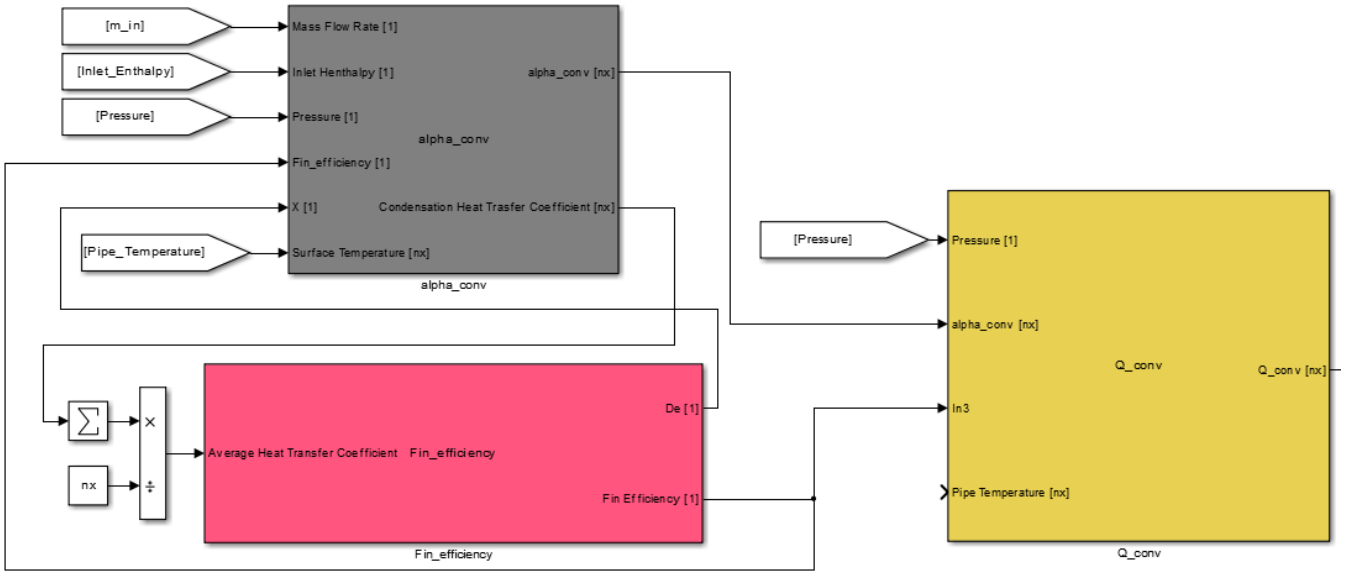

Fig. A2. 57 Block diagram of Shell side fluid subsystem, Condenser, (*level 3 of hierarchy*)

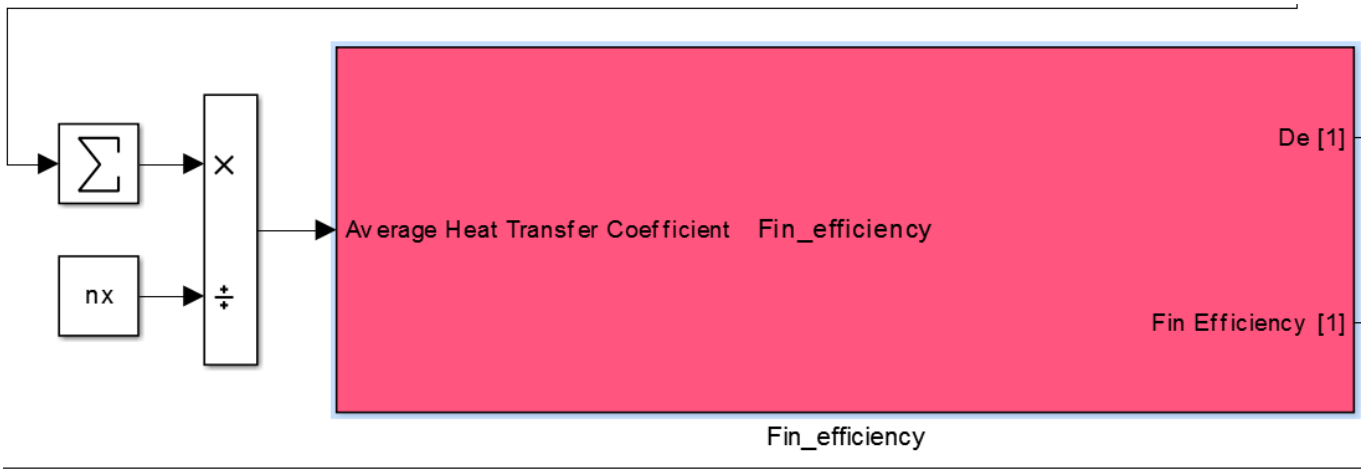

Fig. A2. 58 "Fin_efficiency" subsystem block, Shell-side fluid subsystem, Condenser, (*level 3 of hierarchy*)

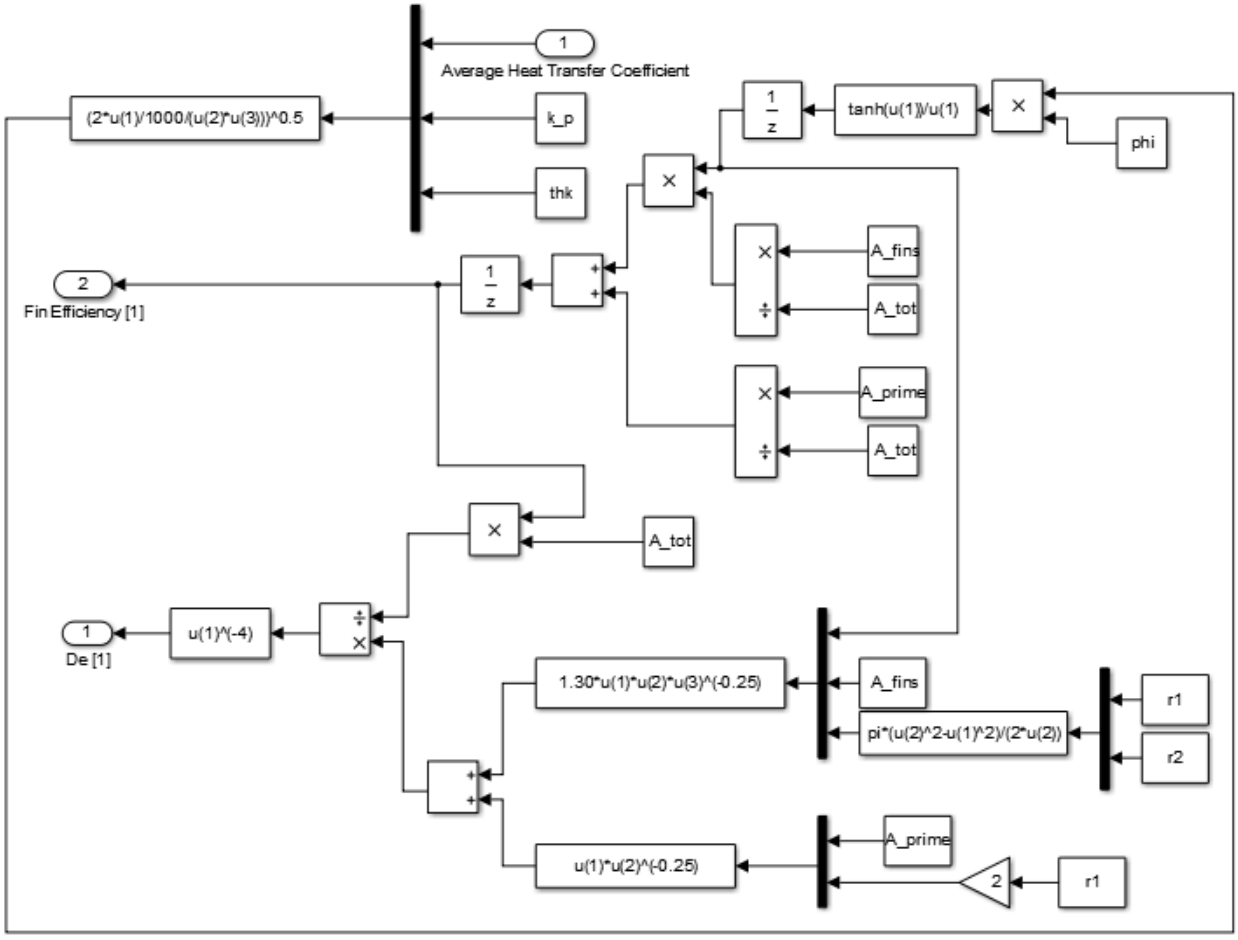

Fig. A2. 59 "Fin_efficiency" subsystem block, Shell-side fluid subsystem, Condenser, (*level 4 of hierarchy*)

Output signals of "*Fin efficiency"* subsystem are sent to "*alpha_conv*" subsystem which leads to calculate condensing heat transfer coefficients for finned tubing:

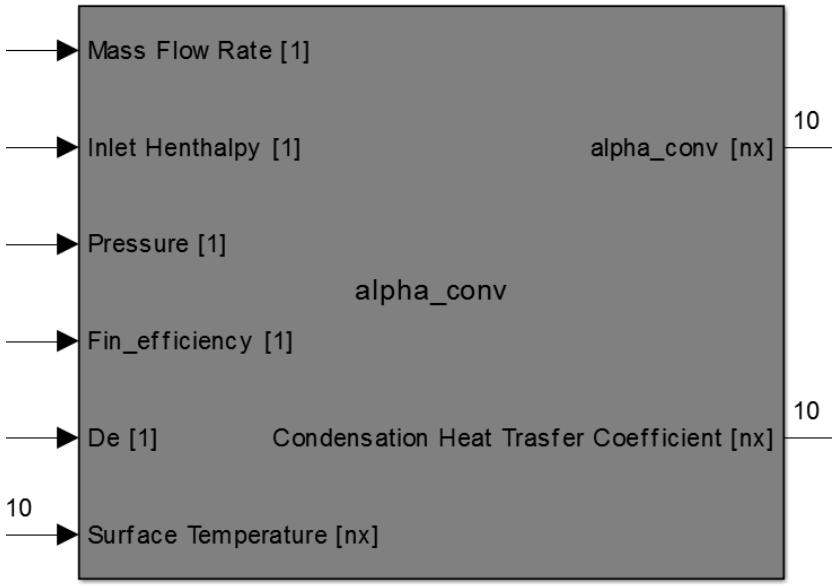

Fig. A2. 60 "alpha_conv" subsystem block, Shell-side fluid subsystem, Condenser, (*level 3 of hierarchy*)

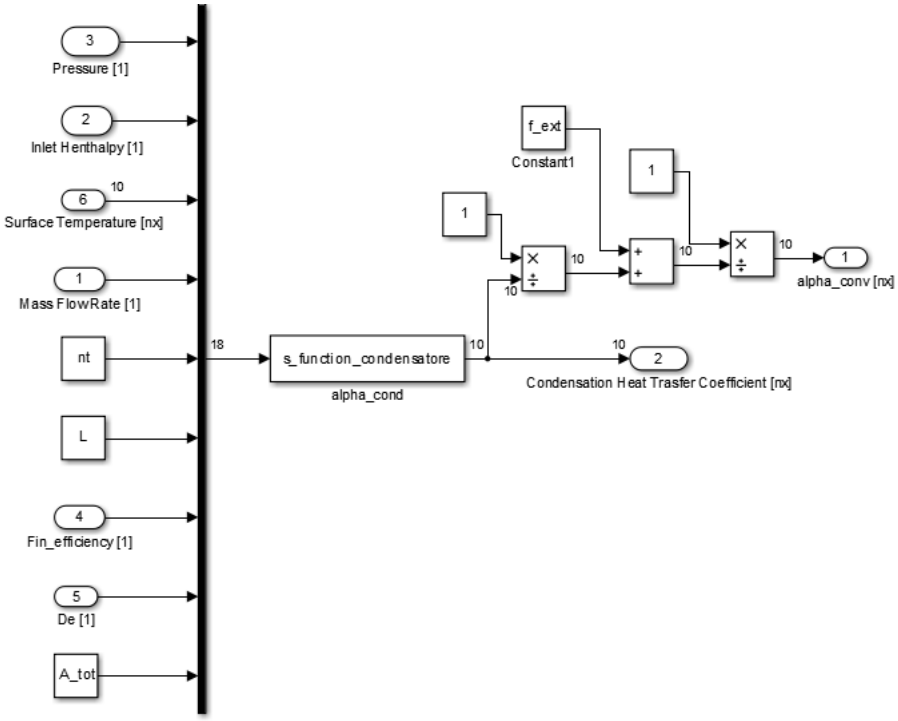

Fig. A2. 61 "alpha_conv" subsystem block, Shell-side fluid subsystem, Condenser, (*level 4 of hierarchy*)

"alpha_cond" s-function evaluates condensing heat transfer coefficients:.

```
%alpha_cond (in=nx+8, out=nx)
   for i=1:nx

Output(i)=alpha_condensation(u(1),u(2),u(i+2),u(nx+3),u(nx+4),u(nx+8),u(nx+5),u(nx+6),u(nx+7),spec
ie);
   end
```

Where "*alpha_condensation*" Matlab function is:

```
function [h_cond]= alpha_condensation (p,h_in,Tp,m,nt,A_tot,L,eta_w,De,specie)

[h_l]=refpropm('H','P',p*100,'Q',0,specie)/1000;
[h_v]=refpropm('H','P',p*100,'Q',1,specie)/1000;

T_c=refpropm('T','P',p*100,'Q',0,specie)-273.15;
T=0.75*Tp+0.25*T_c;

[k_l, rho_l, mi_l]=refpropm('LDV','T',T+273.15,'Q',0,specie);
[rho_v]=refpropm('D','T',T+273.15,'Q',1,specie);

h=0.609*(k_l^3*rho_l*(rho_l-rho_v)*9.81*eta_w*(A_tot/L)/(mi_l*De*(m/(L*nt^(2/3)))))^(1/3);
h_cond=h*(((h_in-h_l)/(h_v-h_l))^(1/4))/1000;
end
```

"Q_conv" subsystem leads to calculate heat transfer flux vector transferred from condensing fluid to pipe:

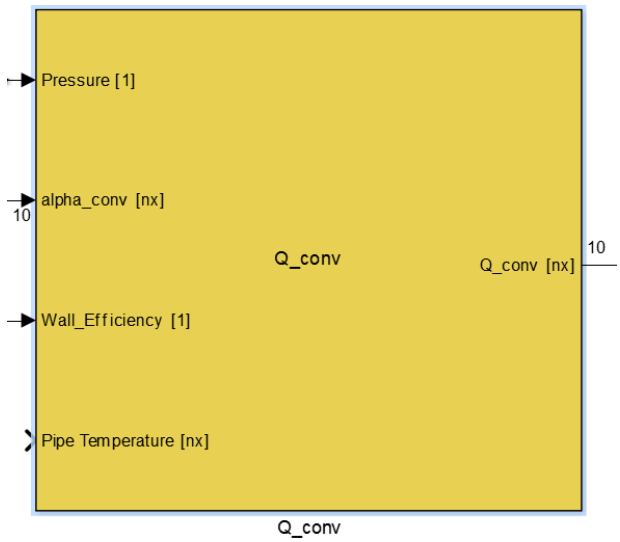

Fig. A2. 62 "Q_conv" subsystem block, Shell-side fluid subsystem, Condenser, (*level 3 of hierarchy*)

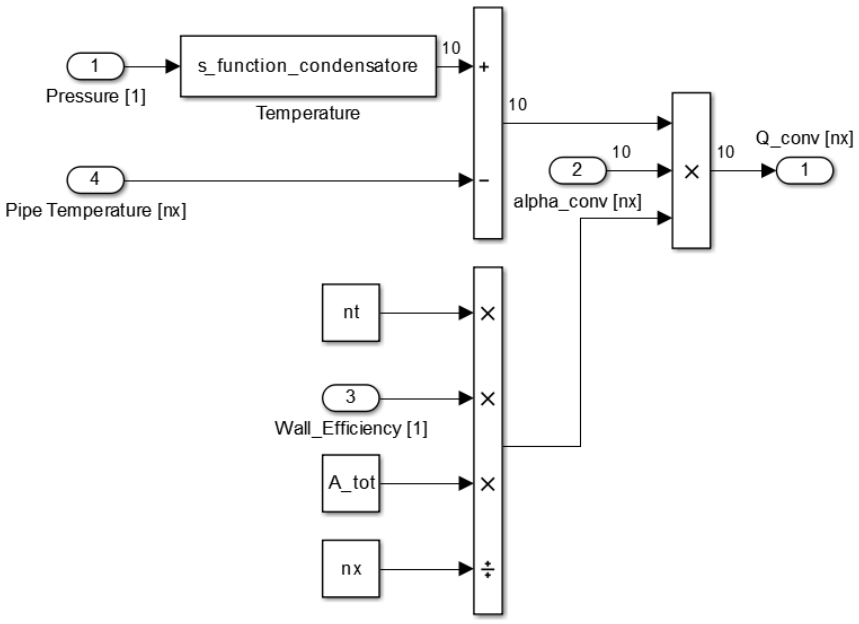

Fig. A2. 63 "Q_conv" subsystem block, Shell-side fluid subsystem, Condenser, (*level 4 of hierarchy*)

Pump Simulink model

Pump model is presented in this section. *Pump* and *Turbine* components are modelled with a different approach compared to heat exchangers. In machine components no mass or energy storage is considered, simplifying model implementation. In accordance with that, no state-variable are considered in following models. The modelled pump is a variable rotational speed pump. A change in rotational speed produces a variation in component characteristic curve and consequently component behavior. Rotational speed is considered a tuning variable for the ORC system, allowing controlling liquid level in kettle evaporator or evaporating pressure by mean of a PID control system.

Component block and parameter dialog are presented in Fig. A2. 64 and 65:

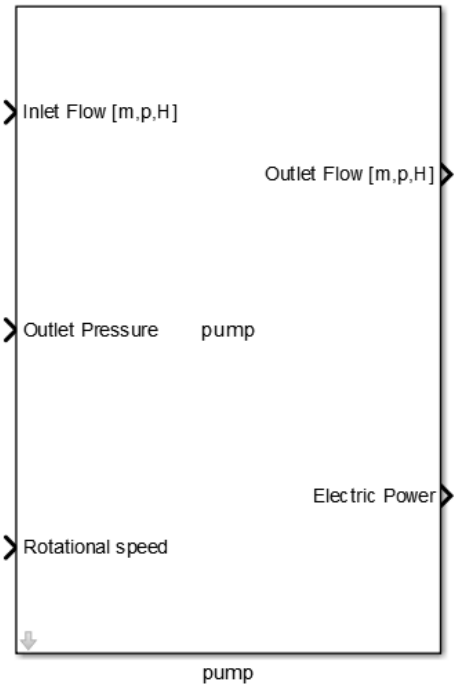

Fig. A2. 64 Simulink block of Pump (*level 1 of hierarchy*)

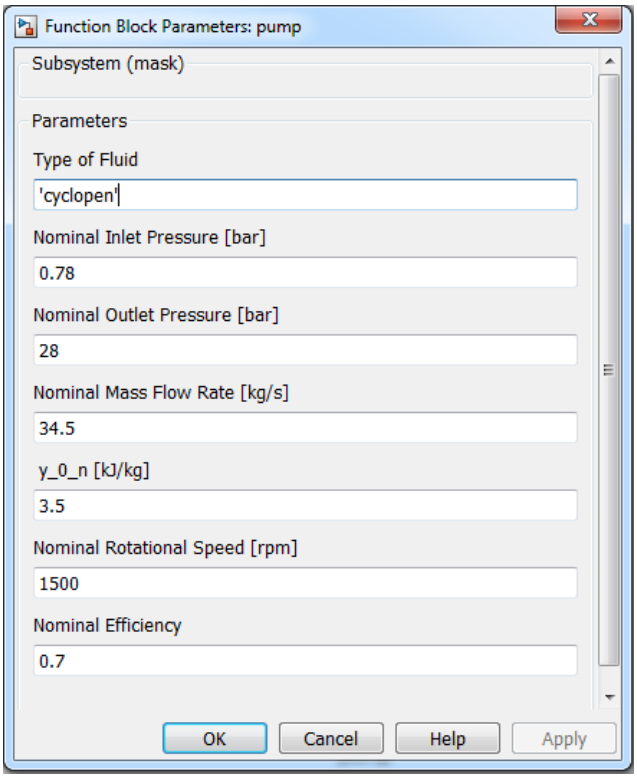

Fig. A2. 65 Parameter dialog block of Pump

Parameter dialog block allows defining nominal parameters of component; provided by design model of pump component presented in chapter 2.

Going down to a lower level of hierarchy (level 2), system block diagram arrargement is present in Fig. A2. 66

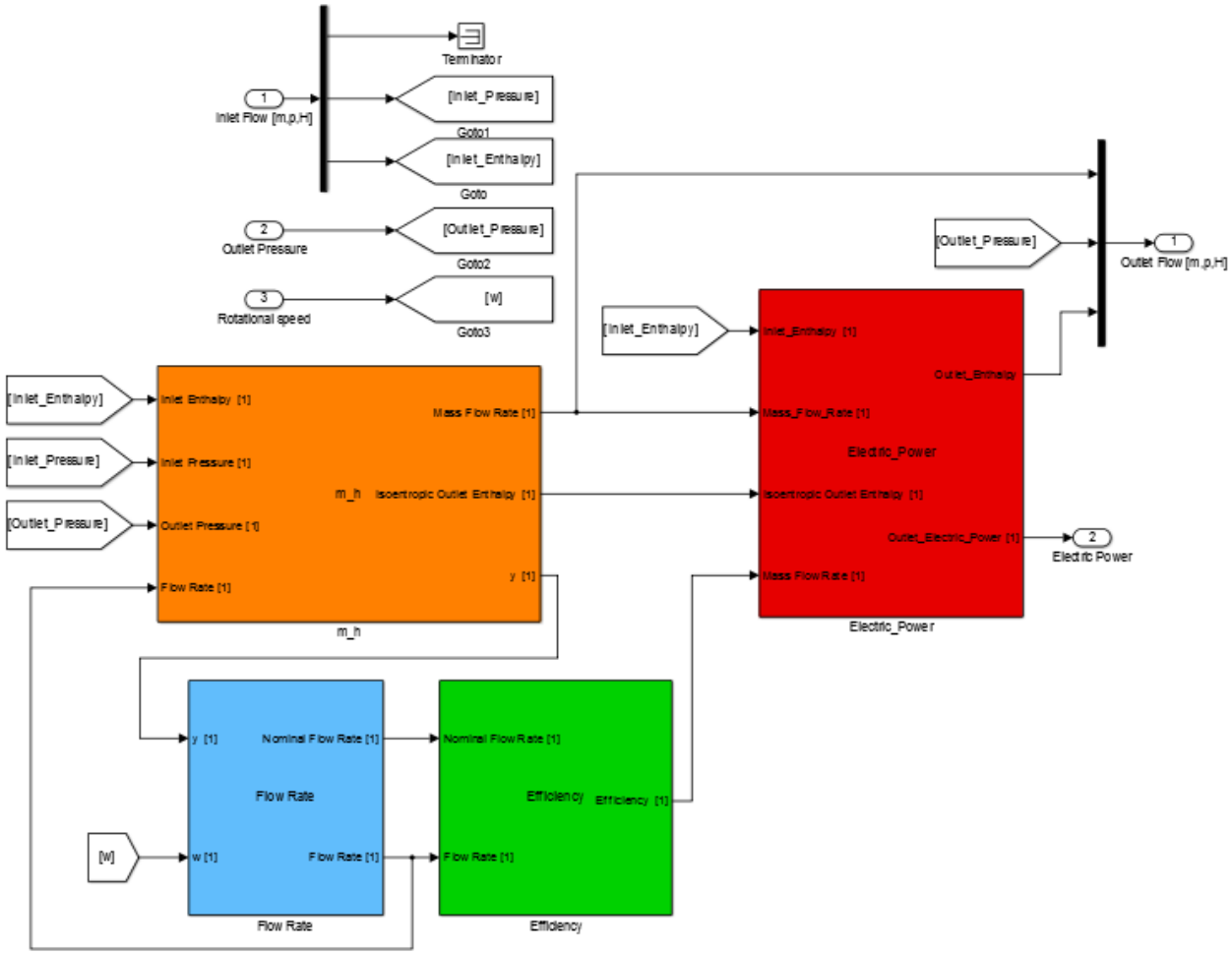

Fig. A2. 66 Block diagram of Pump *(level 2 of hierarchy)*

"Flow Rate" subsystem evaluates flow rate processed by the pump component. It depends on inlet and outlet pressure levels and rotation speed. Following equations are used to calculate processed flow rate:

$$y_D^t = \frac{p_{OUT,D}^t - p_{IN,D}^t}{\rho_{IN,D}^t}$$

$$y'^t_D = y_D \left(\frac{w^t}{w_D}\right)^2$$

$$y'^{t}_{0,D} = y_{0,D}\left(\frac{w^t}{w_D}\right)^2$$

$$\dot{V}^t = \dot{V}'^{t}_{D}\sqrt{\frac{y^t - y'^{t}_{0,D}}{y'^{t}_{D} - y'^{t}_{0,D}}}$$

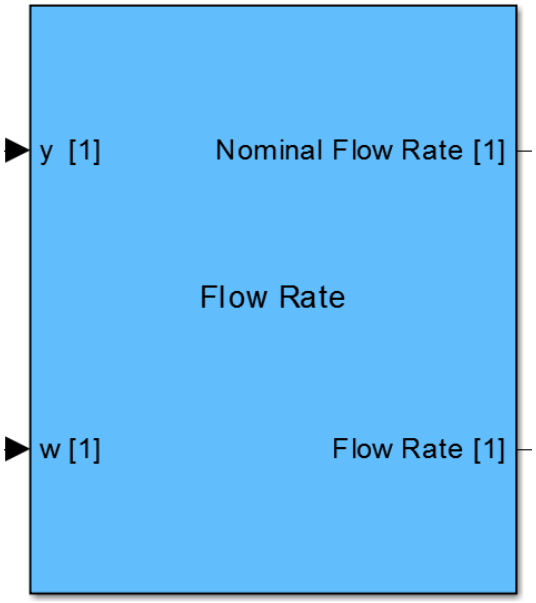

Fig. A2. 67 "Flow Rate" subsystem block, Pump, (*level 2 of hierarchy*)

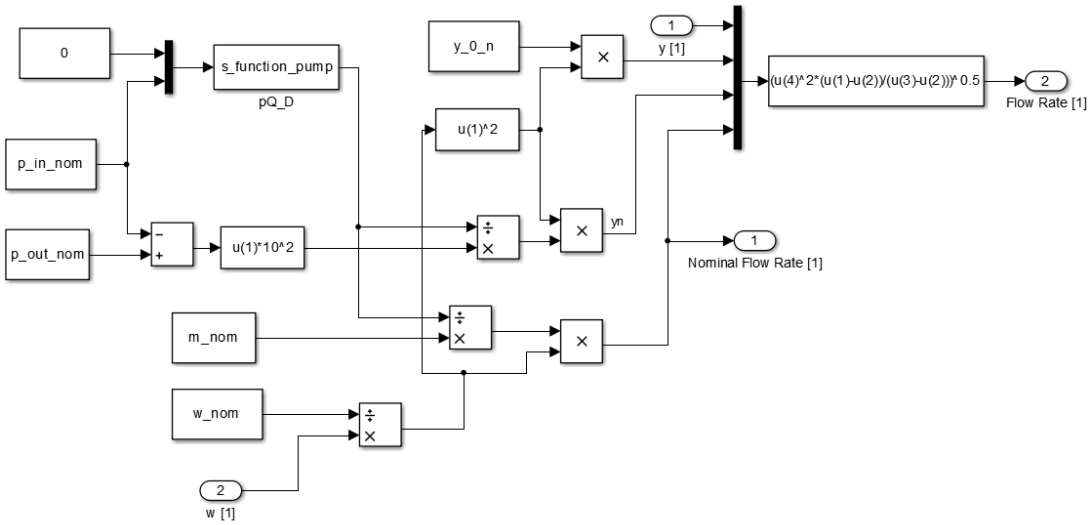

Fig. A2. 68 "Flow Rate" subsystem block, Pump, (*level 3 of hierarchy*)

"*y*" input signal of "*Flow Rate*" subsystem is computed by mean of "*m_h*" subsystem; using equation:

$$y^t = \frac{p_{OUT}^t - p_{IN}^t}{\rho_{IN}^t}$$

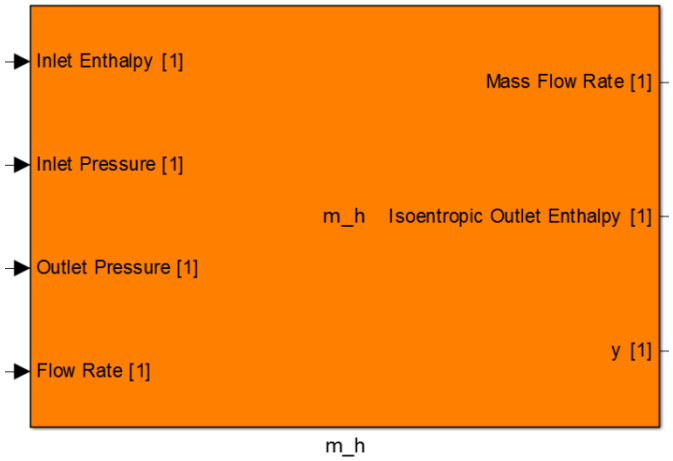

Fig. A2. 69 "m_h" subsystem block, Pump, (*level 2 of hierarchy*)

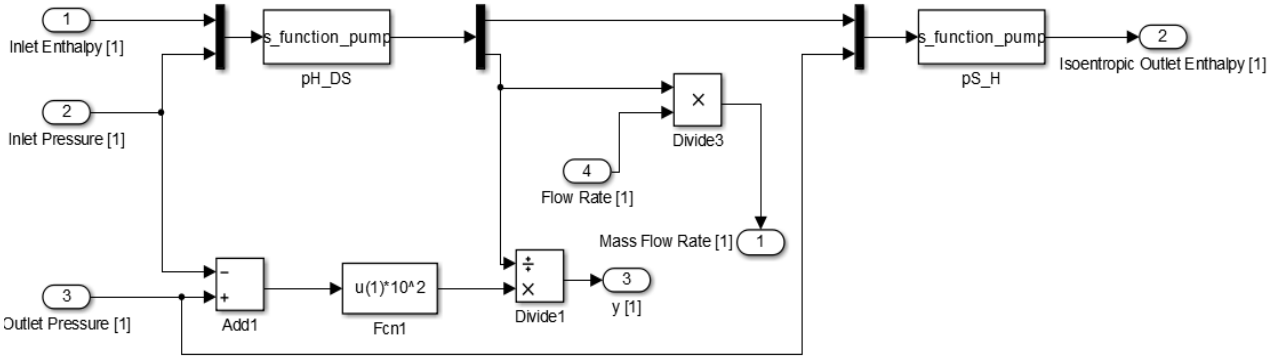

Fig. A2. 70 "m_h" subsystem block, Pump, (*level 3 of hierarchy*)

"*pH_DS*" and "*pS_H*" s-function:

```
%prop_pH_DS (in=2,out=2)
   p=u(1)*100;
   h=u(2)*1000;
   [d, s]=refpropm('DS','p',p,'H',h,specie);
   Output= [d s];

%prop_pS_H (in=2,out=1)
```

```
p=u(1)*100;
s=u(2);
Output=(refpropm('H','p',p,'S',s,specie))/1000;
```

"*m_h*" subsystem evaluates outlet isentropic enthalpy and processed mass flow rate applying equations:

$$H^t_{OUT,is} = f(p^t_{OUT}, s^t_{IN})$$
$$\dot{m}^t = \dot{V}^t \rho^t_{IN}$$

Isentropic efficient of the pump is calculated by "*Efficiency*" subsystem by mean of equation:

$$\eta^t_{is,P} = 2\frac{\eta_{is,P,D}}{\dot{V}'^t_D}\dot{V}^t - \frac{\eta_{is,P,D}}{\dot{V}'^{t\,2}_D}\dot{V}^{t\,2}$$

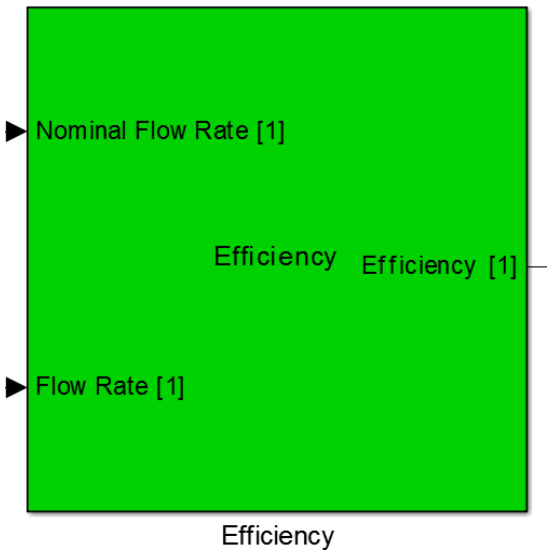

Fig. A2. 71 "Efficiency" subsystem block, Pump, (*level 2 of hierarchy*)

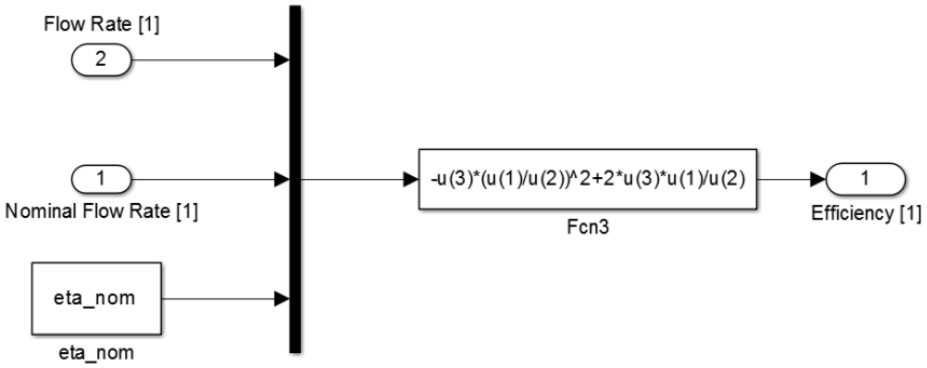

Fig. A2. 72 "Efficiency" subsystem block, Pump, (*level 3 of hierarchy*)

"*Power*" provides outlet fluid enthalpy and electric power absorbed by the component:

$$H_{OUT}^{t} = H_{IN}^{t} + \frac{\left(H_{OUT,is}^{t} - H_{IN}^{t}\right)}{\eta_{is,P}^{t}}$$

$$P_{mec}^{t} = \dot{m}_{IN}^{t}\left(H_{OUT}^{t} - H_{IN}^{t}\right)$$

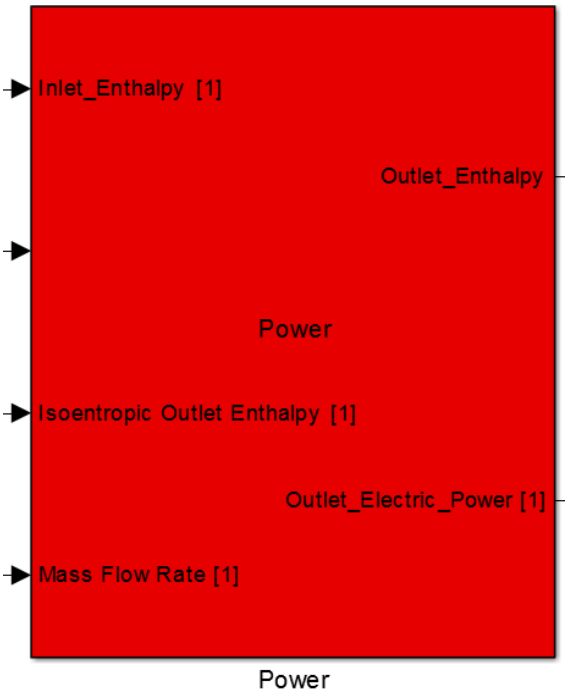

Fig. A2. 73 "Power" subsystem block, Pump, (*level 2 of hierarchy*)

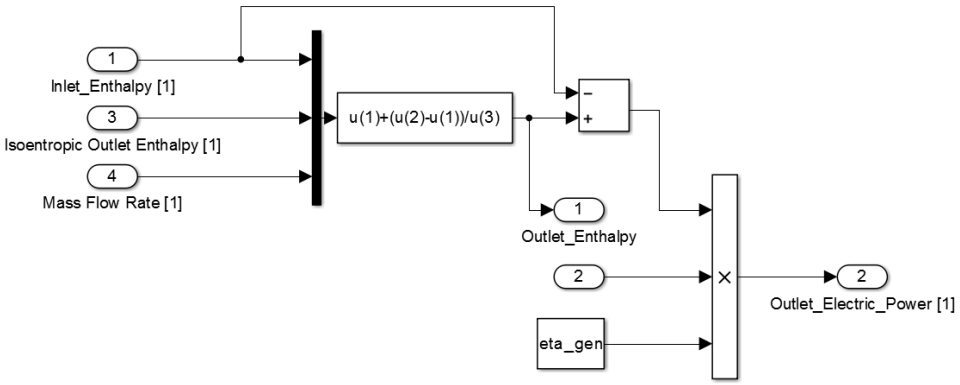

Fig. A2. 74 "Power" subsystem block, Pump, (*level 3 of hierarchy*)

Turbine Simulink model

Turbine component Simulink model is presented in this section. Turbine model is similar to precedent pump model, since same assumptions are considered for both fluid machine components. As in pump model mass flow rate processed is evaluated by knowing inlet and outlet pressure level. Component block and parameter dialog are presented in Fig. A2. 75 and 76:

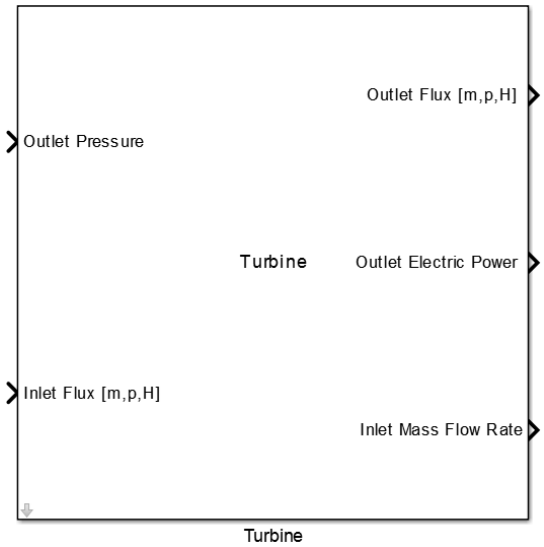

Fig. A2. 75 Simulink block of Turbine (*level 1 of hierarchy*)

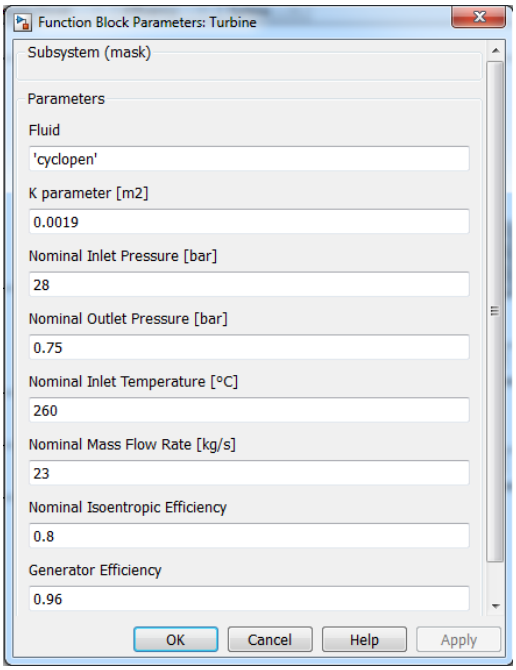

Fig. A2. 76 Parameter dialog block of Turbine

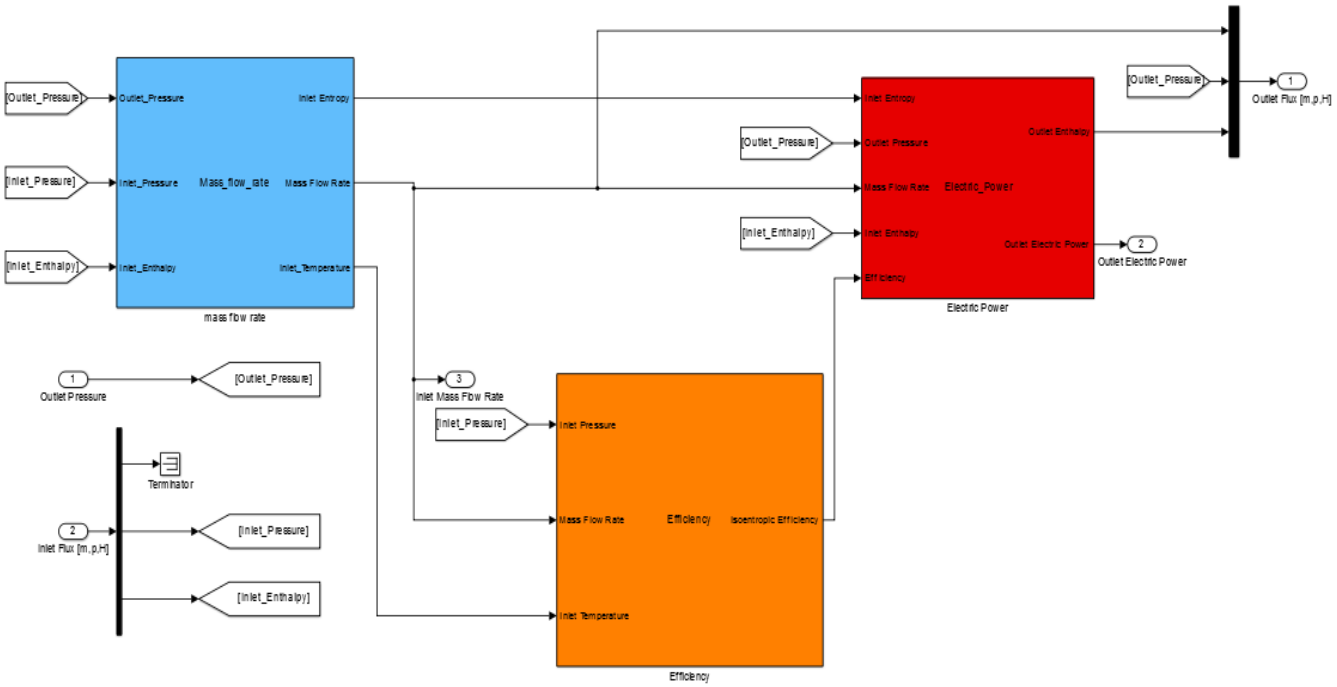

Fig. A2. 77 Block diagram of Turbine *(level 2 of hierarchy)*

"*Mass_flow_rate*" subsystem evaluates processed mass flow rate by knowing inlet and outlet pressure and inlet temperature of operating fluid. Stodola equation is applied to perform this estimation:

$$\dot{m}_{IN}^{t} = K\sqrt{\rho_{IN}^{t}\, p_{IN}^{t}\left[1-\left(\frac{1}{\varepsilon^{t}}\right)^{2}\right]}$$

$$\varepsilon^{t} = \frac{p_{IN}^{t}}{p_{OUT}^{t}}$$

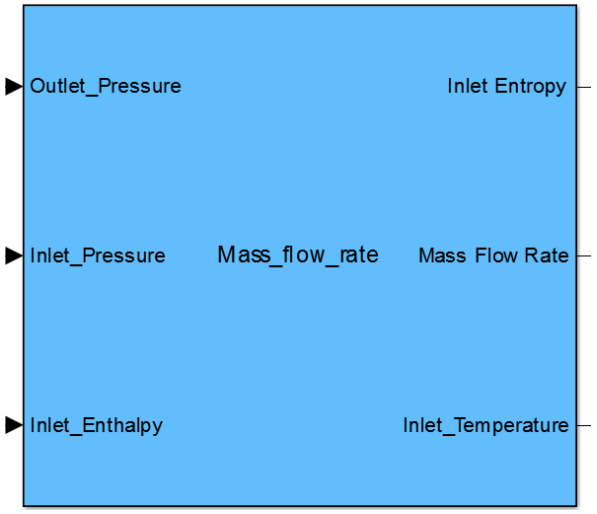

Fig. A2. 78 "Mass_flow_rate" subsystem block, Turbine, (*level 2 of hierarchy*)

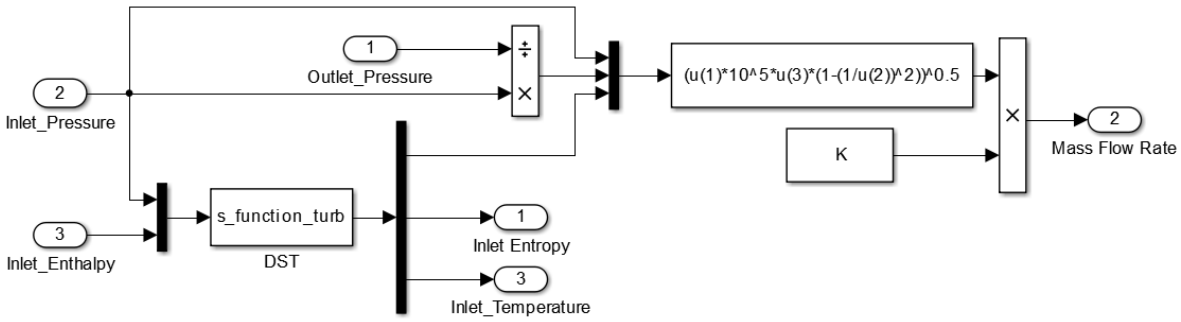

Fig. A2. 79 "Mass_flow_rate" subsystem block, Turbine, (*level 3 of hierarchy*)

"*DST*" s-function calculates density, entropy and temperature of inlet flow:

```
%DST (in=2,out=3)
   p=u(1)*100;
   h=u(2)*1000;
   [d, s, T]=refpropm('DST','p',p,'H',h,specie);
   Output= [d s/1000 T];
```

"*Efficiency*" subsystem evaluates isentropic expansion efficiency, which is assumed to vary depending on reduced inlet mass flow rate:

$$\dot{m}_R^t = \frac{\dot{m}_{IN}^t \sqrt{T_{IN}^t}}{p_{IN}^t}$$

$$\eta_{is,T}^t = \eta_{is,T,D} \left[2\frac{\dot{m}_R^t}{\dot{m}_{R,D}} - \left(\frac{\dot{m}_R^t}{\dot{m}_{R,D}} \right)^2 \right]$$

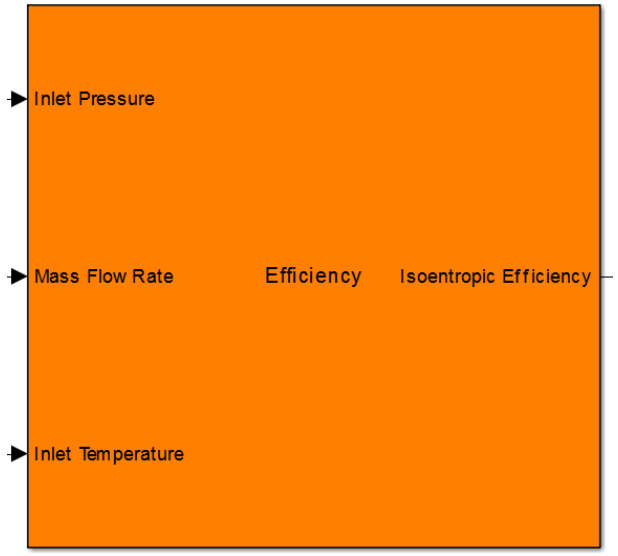

Fig. A2. 80 "Efficiency" subsystem block, Turbine, (*level 2 of hierarchy*)

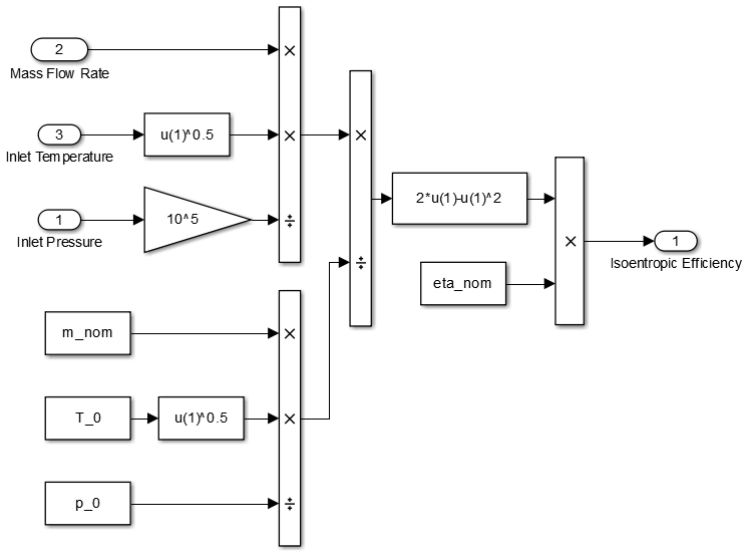

Fig. A2. 81 "Efficiency" subsystem block, Turbine, (*level 3 of hierarchy*)

"*Electric_Power*" calculates vapor outlet enthalpy and electric power produced by turbine component:

$$H_{OUT}^{t} = H_{IN}^{t} - \eta_{is,T}^{t}\left(H_{IN}^{t} - H_{OUT,is}^{t}\right)$$

$$P_{el}^{t} = \dot{m}_{IN}^{t}(H_{IN}^{t} - H_{OUT}^{t})\,\eta_{GEN}$$

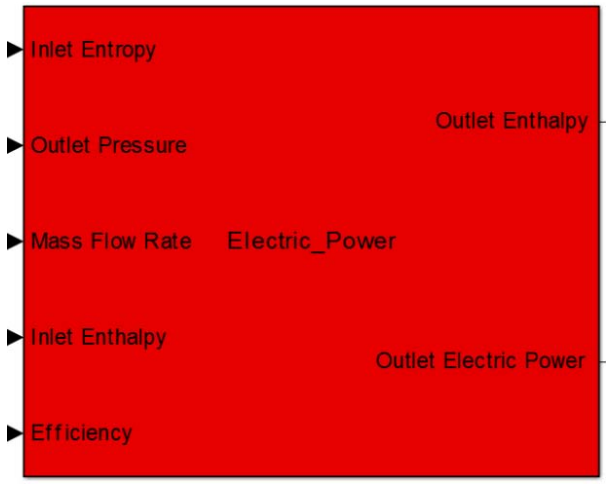

Fig. A2. 82 "Electric_Power" subsystem block, Turbine, (*level 2 of hierarchy*)

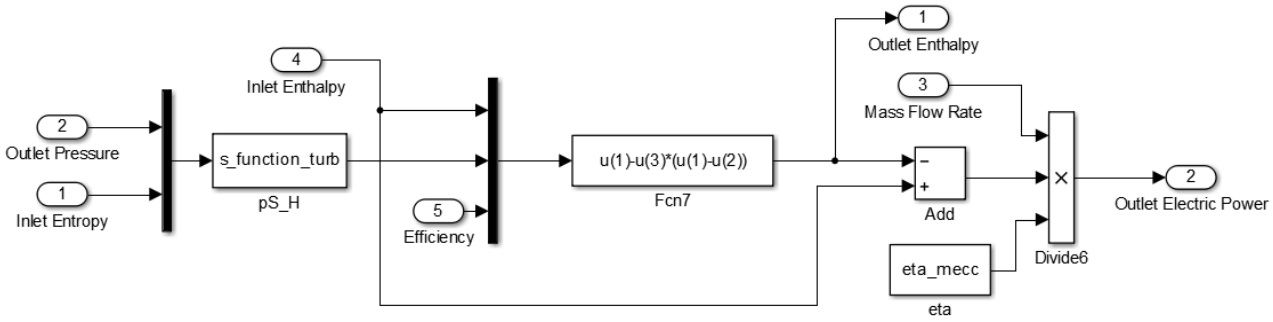

Fig. A2. 83 "Electric_Power" subsystem block, Turbine, (*level 3 of hierarchy*)